12-1997

Modeling the Uptake and Transpiration of TCE Using Phreatophytic Trees

Douglas P. Wise

MODELING THE UPTAKE AND TRANSPIRATON OF TCE USING PHREATOPHYTIC TREES

THESIS

Douglas P. Wise

AFIT/GEE/ENV/97D

DEPARTMENT OF THE AIR FORCE
AIR UNIVERSITY
AIR FORCE INSTITUTE OF TECHNOLOGY

Wright-Patterson Air Force Base, Ohio

AFIT/GEE/ENV/97D-22

MODELING THE UPTAKE AND TRANSPIRATON OF TCE USING PHREATOPHYTIC TREES

THESIS

Douglas P. Wise

AFIT/GEE/ENV/97D

Disclaimer Statement

The views expressed in this thesis are those of the author and do not reflect the official policy or position of the Department of Defense or the United States Government.

AFIT/GEE/ENV/97D-22

MODELING THE UPTAKE AND TRANSPIRATION OF TCE USING PHREATOPHYTIC TREES

THESIS

Douglas P. Wise, B.S., P.E.
Captain, USAF

Presented to the Faculty of the School of Engineering

of the Air Force Institute of Technology

In Partial Fulfillment of the Requirements for the Degree of

Master of Science

Member

Member

Advisor

AFIT/GEE/ENV/97D-22

MODELING THE UPTAKE AND TRANSPIRATION OF TCE USING PHREATOPHYTIC TREES

THESIS

Presented to the Faculty of the

School of Engineering

of the Air Force Institute of Technology

Air University

In Partial Fulfillment of the Requirements for the

Degree of Master of Science

Douglas P. Wise, B.S., P.E.

Captain, USAF

December 1997

Preface

This thesis would not have been possible without the support and guidance of numerous people. I would first like to thank my parents, for the wonderful guidance they gave me growing up and for instilling a strong sense of values and a healthy work ethic. To my wife, for her patience throughout the past year and just for putting up with me in general. You are a beautiful lady and make my life complete. Also, to our cats, especially Blackie, who kept me company as I spent countless hours in front of my computer working on this thesis.

Professionally, I would like to thank Dr. Shelley, an incredibly insightful individual who helped insurmountably in seeing my model to completion. Also, to my other committee members, Dr. Bleckmann and Mr. Harvey, who provided invaluable input and guidance throughout my research. I would also like to thank the numerous professors and professionals in the phytoremediation, silviculture, and plant biology fields who supported me in this thesis effort with invaluable expert advice. This includes Dr. Lee Newman, Dr. Joel Burken, Dr. Milton Gordon, Dr. Don Dickmann, Dr. Ron Hendrick, Dr. Lawrence Davis, Dr. Ed Gatliff, and Dr. Ray Hinchman. Last, I would like to thank my friends who provided me with diversions from the rigors of school, in particular: "Crazy" Nancy and Kyle, Robert and Jennie, Wade and Landa, and Pat and Lisa.

Douglas P. Wise

Table of Contents

	Page
Preface	ii
List of Figures	iii
List of Tables	xi
Abstract	xii
I. Introduction	1
Problem Background	1
Purpose Statement	6
Research Objective	7
Project Scope	7
II. Literature Review	10
TCE History	10
Physical and Chemical Properties of TCE	13
TCE Soil Contamination	13
TCE Uptake by Plants	14
Phytoremediation	20
Advantages of Phytoremediation	22
Disadvantages of Phytoremediation	22
Rhizosphere	25
Plant Physiology	34
Root	35
Stem	44
Leaf	48
Photosynthesis and Transpiration	50
Poplars	52
Rhizosphere Cometabolism of TCE	55
Plant Metabolism of TCE	59
Growth of Poplars	61
Models	67
Site Conditions	72
III. Methodology	75
Overview	75

Page

Conceptualization 77
Reference Mode 77
Boundary 78
Influence Diagram 79
Formulation 85
Assumptions 85
Detailed Structure and Parameters . . . 86
TCE Uptake 86
Cometabolism 89
Rhizosphere 90
Vascular Flow 91
Plant Growth 92
Vascular Volume 99
Flow/Gradient Equations 101
Plant Metabolism 103
Selection of Parameters 104
Testing and Implementation 107
Reference Mode Comparison 107
Parameters Requiring Testing and Sensitivity Analysis 109
Validation Tests 110
Tests of Model Structure 111
Structure Verification . . . 111
Parameter Verification . . . 111
Extreme Conditions 112
Boundary Adequacy . . . 113
Dimensional Consistency . . 113
Tests of Model Behavior 113
Behavior Anomaly 113
Behavior Sensitivity 114
Soft Parameter Sensitivity . . 115
Changed-Behavior Prediction . . 115
Additional Validity Tests 117
Test of Site Parameters . . . 117
Comparison to Real World Data . . 117

IV. Results and Discussion 119

Testing and Implementation 119
Validation Tests 119
Tests of Model Structure 119
Structural Verification . . . 119
Parameter Verification . . . 120

Page

Extreme Conditions 120
Boundary Adequacy . . 128
Dimensional Consistency . . . 128
Tests of Model Behavior 129
Behavior Anomaly 129
Behavior Sensitivity 136
Soft Parameter Sensitivity . . . 161
Changed-Behavior Prediction . . 173
Other Validation Tests 174
Test of Site Parameters . . . 174
Comparison to Real World Data . . 178
Summary 180

V. Conclusions and Recommendations 181

Conclusions 181
Recommendations 184

Appendix 1: Stella Model 186

Appendix 2: Stella Equations and Documentation . . . 208

Appendix 3: Saturable Uptake Approximation 272

Appendix 4: Rhizosphere Volume Approximation . . . 276

Appendix 5: Xylem and Phloem Flow Rates 278

Appendix 6: Leaf, Stem, and Root Growth Volumes . . . 280

Appendix 7: Root Vascular Volumes 285

Appendix 8: Stem Vascular Volumes 294

Appendix 9: Partition Coefficients 297

Bibliography 299

Vita 317

List of Figures

Figure	Page
1.1 Air Force Plant 4 TCE Phytoremediation Site Plan	5
2.1 The Phytoremediation Process.	24
2.2 Zones of a Woody Dicotyledon Root	37
2.3 Diagram of a Root Tip.	38
2.4 Fine Root Cross-Section	40
2.5 Mature Root Zone Cross-Section	44
2.6 Longitudinal Stem Cross-Section	46
2.7 Leaf Cross-Section	49
2.8 World Map of Poplar Distribution	55
2.9 Reductive Dechlorination Pathways of TCE Under Anaerobic Conditions	57
2.10 Reductive Dechlorination Pathways of TCE Under Aerobic Conditions	58
2.11 Degradative Pathways of TCE in Plant Tissue	61
2.12 *Populus* Root Diagram	66
3.1 Hypothesized Reference Mode	78
3.2 High Level Influence Diagram	80
3.3 Typical Saturable Uptake Curve	88
3.4 Rhizosphere Volume	91
3.5 Leaf Volume	93
3.6 Stem Volume	94

Figure Page

3.7 Root Volume 96

3.8 Leaf Area 98

3.9 Stem Vascular Volume 100

3.10 Root Vascular Volume 101

3.11 Reference Mode Comparison 108

4.1 TCE Uptake and Transpiration at a TCE Ground Water Concentration of 0 ppm 121

4.2 TCE Uptake and Transpiration at a TCE Ground Water Concentration of 100 ppm 122

4.3 TCE Uptake and Transpiration at an Unsaturated Depth of 0 Meters 123

4.4 TCE Uptake and Transpiration at an Unsaturated Depth of 10 Meters 124

4.5 TCE Uptake and Transpiration Over 18 Years . . . 125

4.6 TCE Uptake with Extremes of V_{max} 126

4.7 TCE Uptake with Extremes of K_m 127

4.8 TCE Leaf Mass Anomaly 129

4.9 TCE Leaf Mass Anomaly with Total Flows 130

4.10 TCE Concentration in Leaf Anomaly 132

4.11 Leaf Air Transfer Rate Coefficient Behavior Anomaly Test . 134

4.12 Fine Root Tissue Volume Coefficient Behavior Anomaly Test . 135

4.13 Secondary Growth Root Tissue Volume Coefficient Behavior Anomaly Test 135

Figure Page

4.14 TCE Uptake Sensitivity to the Rhizosphere TCE Half Life . 137

4.15 TCE Uptake Sensitivity to the Rhizosphere TCE Half Life at a TCE Ground Water Concentration of 50 ppm . . 138

4.16 TCE Transpiration Sensitivity to the Leaf Air Partition Coefficient 139

4.17 TCE Transpiration Sensitivity to the TCE Air Background Concentration 140

4.18 TCE Transpiration Sensitivity to the Leaf Partition Coefficient 141

4.19 TCE Uptake Sensitivity to the Xylem Flow Rate per Leaf Area 142

4.20 TCE Transpiration Sensitivity to the Xylem Flow Rate per Leaf Area 143

4.21 TCE Transpiration Sensitivity to the Phloem Flow Rate per Leaf Area 144

4.22 TCE Uptake Sensitivity to the Phreatophytic Tree Densities . 145

4.23 TCE Transpiration Sensitivity to the Phreatophytic Tree Densities 147

4.24 TCE Transpiration Sensitivity to the Stem and Root Partition Coefficients 148

4.25 TCE Uptake Sensitivity to the Secondary Growth Root to Fine Root Ratio 149

4.26 TCE Transpiration Sensitivity to the Secondary Growth to Fine Root Ratio 150

4.27 TCE Uptake Sensitivity to the Fine Root Flow Weight . . 151

4.28 TCE Transpiration Sensitivity to the Fine Root Flow Weight . 152

4.29 TCE Uptake Sensitivity to Rhizosphere Thickness . . 153

Figure Page

4.30 TCE Uptake Sensitivity to V_{max} at a Ground Water TCE Concentration of 605 ppb 155

4.31 TCE Uptake Sensitivity to V_{max} at a Ground Water TCE Concentration of 50 ppm 156

4.32 TCE Uptake Sensitivity to K_m. 157

4.33 TCE Uptake Sensitivity to TCE Ground Water Concentration . 158

4.34 TCE Uptake Sensitivity to Ground Water Depth . . . 159

4.35 TCE Uptake Sensitivity to Unsaturated/Capillary Fringe Soil Depth 160

4.36 TCE Transpiration Sensitivity to the Leaf Vascular Ratio. . 163

4.37 TCE Transpiration Sensitivity to the Leaf Air Transfer Rate Coefficient 164

4.38 TCE Transpiration Sensitivity to the Leaf TCE Half Life. . 165

4.39 TCE Transpiration Sensitivity to the Stem and Root TCE Half Lives 166

4.40 TCE Transpiration Sensitivity to the Stem, Phloem, and Root Transfer Rate Coefficients 168

4.41 TCE Transpiration Sensitivity to the Fine Root and Secondary Root Tissue Volume Coefficients . . . 169

4.42 TCE Transpiration Sensitivity to the Fine Root to Fine Root Xylem Ratio 170

4.43 TCE Uptake Sensitivity to the Rhizosphere Diffusion Coefficient 170

4.44 TCE Uptake Sensitivity to the Capillary Fringe Thickness at AF Plant 4 175

Figure Page

4.45 TCE Uptake Sensitivity to the TCE Ground Water Concentration at AF Plant 4. 176

4.46 TCE Uptake Sensitivity to the Depth to Ground Water at AF Plant 4 177

4.47 Comparison to Real World Data 179

List of Tables

Table	Page
2.1 Properties of TCE	13
2.2 Chemicals Susceptible to Phytoremediation	16
2.3 TCE and Metabolic Products in Tissue of Poplars.	18
2.4 Major Taxonomic Groups of Microorganisms	30
2.5 Genus of *Populus deltoides*	54
3.1 Literature Parameters	105
3.2 Soft Parameters	106
4.1 Sensitivity of Literature Parameters	172
4.2 Sensitivity of Soft Parameters	173
4.3 Sensitivity of Air Force Plant 4 Parameters.	179

Abstract

Phytoremediation is a recent addition to the numerous methods used today to remediate ground water contaminants. It is proving more effective and efficient compared to existing remediation techniques.

The use of phreatophytes, or water seeking trees, has great potential for phytoremediation. These trees are fast growing, long lived, grow their roots down to the ground water table, transpire large amounts of water, and are proven to actively remove contaminants from the soil horizon.

The purpose of this research is to develop quantitative concepts for understanding the dynamics of TCE uptake and transpiration by phreatophytic trees over a short rotation crop time frame. This will be done by constructing a system dynamics model of this process and running it over a wide range of conditions. This research will offer managers a tool to simulate long-term uptake and transpiration of TCE at potential sites.

The results of this study indicate that TCE is actively removed from the soil horizon by phreatophytic trees and a significant proportion of this TCE is then transpired. Changes in soil horizon parameters, xylem flow rates, and variables in the uptake equation greatly influence TCE uptake rate as well as transpiration. Also, parameters used in equations representing flows in and out of the leaf greatly influence transpiration. Better understanding of these

processes is essential for managers to accurately predict the amount of TCE removed and transpired during potential phytoremediation projects.

MODELING THE UPTAKE AND TRANSPIRATION OF TCE USING PHREATOPHYTIC TREES

I. Introduction

Problem Background

Trichloroethylene (TCE) is a suspected carcinogen in humans and, due to its former extensive use as a degreasing agent, is now a widespread contaminant in groundwater [Strand and others, 1995:605]. This can particularly be seen at military and government installations, where extensive past use of TCE has led to numerous contaminated sites [Duba and others, 1996:1982; Steinberg and DeSesso, 1993:146]. Since TCE is a dense nonaqueous phase liquid (DNAPL), it tends to sink to the bottom of an aquifer. As these DNAPLs then dissolve into the groundwater, they provide a persistent source of contamination which may take numerous years to remediate [Travis and Doty, 1990:1465]. The typical remediation process today, pump and treat, is based on groundwater extraction by wells or drains, which is then sometimes accompanied by treatment of extracted water before disposal [Mackay and Cherry, 1989:630]. Since the dissolved contaminant is taken up with the extracted water, this technique results in an initial marked decrease of groundwater contaminant concentrations. The remaining contaminant is removed at a much slower rate. This is because most contaminants show a higher affinity to soil particles than

water and strongly adsorb to soil particles [Atlas, 1992:430]. Depending upon the type of contaminant and soil classification, reaching standards through this approach may take decades to centuries, at a very high cost [Newman, 1997:1062]. Several studies comparing pump and treat costs to the use of plants to remediate contaminants, or phytoremediation, show great promise for the latter. In similar scenarios using computer cost programming and site comparisons the cost of phytoremediation is estimated as 10% to 37% of the typical cost of pump and treat technology [Black, 1995:1106; Nyer and Gatliff, 1996:61; Strand and others, 1995:611]. In comparison to other existing soil remediation techniques, phytoremediation once again comes out as the economic choice. The cost of phytoremediation is estimated as 12.5% to 25% and 33% to 75% of the cost of microbial remediation and in situ microbial remediation respectively [Cunningham and others, 1996:67]. A recent study estimates the total resource requirements for clean up of Superfund, RCRA, UST, Department of Defense, Department of Energy, state, and private sites under existing regulatory policy and existing clean up technology to be approximately $750 billion [Russell and others, 1991:1]. Today, this value is estimated as $1.7 trillion [Gurdarshan, 1997]. Given the cost and realization that mechanical systems do not remove up to 70% of the soil solution trapped in micropores, other systems with this polishing capability are needed [Matso, 1995:48]. Phytoremediation fills this gap; it works over time at the micropore level, removing contaminants with a slow consistent seasonal uptake of soil

solution. When one considers that up to 80% of groundwater contaminants are within 20 meters of the soil surface, it further strengthens the potential of phytoremediation [Newman, 1997:1062]. Phytoremediation is also much less expensive, aesthetically pleasing to the eye, and environmentally acceptable through its natural attenuation processes. This does not mean phytoremediation is the panacea to all groundwater remediation problems though. Phytoremediation is only viable if certain parameters are met.

- The dissolved TCE plume or groundwater needs to be within reach of the roots of the phreatophyte in question (phreatophyte means "well plant" or a plant that extends its roots into the aerobic portion of the groundwater system [Meinzer, 1927:1])

- Concentrations of TCE can't exceed 100,000 gm/m^3, higher concentrations are deadly to poplars [Strand and others, 1995:605]

- Area soils must tend towards a sandy classification, this improves plant uptake and decreases soil adsorption of contaminant as compared to silty and especially clayey type soils [Cunningham and others, 1996:70]

- There is no immediate human threat due to the groundwater contamination

- Time is not of the essence; phytoremediation may take 50 years or more

- The contaminant has a moderate hydrophobicity (K_{ow} from .5 to 3) [Schnoor and others, 1995:2]

One such site which meets these requirements is at Air Force Plant 4 near Fort Worth, TX. The ASC Environmental Management Directorate Restoration Division is conducting a study of phytoremediation at this site using trees to mitigate a TCE plume over the next two years. The water table is at 10-12 feet, soil TCE concentrations vary from 240 - 970 mg/L, the aquifer is in a sandy gravel soil layer, human exposure is minimal, and the plume is not threatening any water sources now or in the near future. Also, the contaminant, TCE, has an octanol-water coefficient (K_{ow}) of 2.29 [Biernacki and others, 1995:762]. To test the benefits of phytoremediation, *Populus deltoides*, or eastern cottonwood, were planted in the spring of 1996 at Air Force Plant 4 perpendicular to the plume flow (Figure 1). By the summer of 1997 the trees are expected to extend their roots to the water table and start the phytoremediation process.

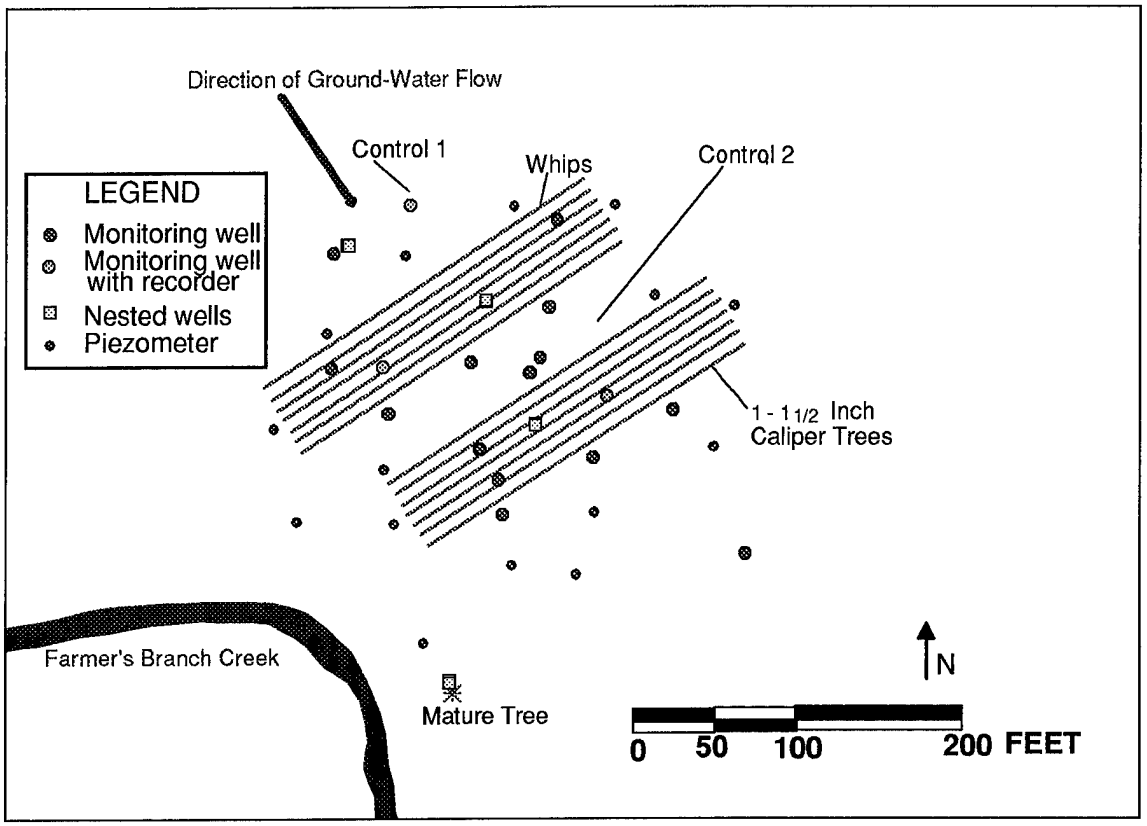

Figure 1.1 Air Force Plant 4 TCE Phytoremediation Site Plan

Populus deltoides was selected for the study at Air Force Plant 4 due to its natural widespread prevalence and extraordinary physical characteristics. The eastern cottonwood is distributed throughout the eastern half of the United States and Canada and phreatophytes are found throughout the world. Furthermore, *Populus deltoides* is usually associated with bottom lands, alluviums, and riparian areas, but can actually grow almost anywhere due to its drought resistant physiology [Dickmann and Stuart, 1983:16]. Coupled with this attribute is their amazing growth rate, up to 3.6 meters in a growing season, the fastest of any tree in North America [Dickmann and Stuart, 1983:118,122].

Since these trees are phreatophytes, water uptake of a mature tree during the summer months can exceed 300 GPD [Nyer and Gatliff, 1996:59]. Also, considering their longevity of 50 years or more, these trees provide a viable alternative to existing pump and treat or bioremediation technologies.

With the many advances in scientific research and plant physiology, there is now a better understanding of the intricate processes between plants and their ecosystems. Still, some processes are not well understood, limiting our ability to fully comprehend the complex internal and external interactions taking place within and around an autotrophic organism. Using powerful computers, mathematical expressions, and an understanding of the important causal relationships, we can now represent these dynamic interactions using simulation models. One method of simulating system behavior, even beyond the range of the actual observed system, is called system dynamics modeling. System dynamics modeling allows us to gain insight into the dynamics and structure of the actual system, including only the necessary influences to give an accurate representation of the real world behavior. This mechanistic modeling technique is the primary backdrop for this thesis.

Purpose Statement

The purpose of this thesis is to develop quantitative concepts to trace the uptake, cometabolism, translocation, storage, metabolism, and transpiration of TCE in the rhizosphere and the phreatophytic tree over a woody crop rotation time frame. It will also show how the physiological function of this process

influences the removal of TCE from contaminated groundwater and its transpiration from a phreatophytic tree. These concepts will allow environmental managers the ability to determine more realistic rates of removal and transpiration on an individual tree basis, how these rates vary with time, optimal rates of uptake and transpiration, and the expected time frame for phytoremediation.

Research Objective

The objectives of this research are as follows:

1. Determine how the following parameters affect the removal of TCE from contaminated groundwater and the amount transpired by a phreatophytic tree over time:

    a. TCE soil concentration

    b. site hydrogeological and environmental characteristics

    c. plant physicochemical properties and physiological characteristics

    d. rhizosphere characteristics, and

    e. time frame of study

Project Scope

Previous research on uptake and transpiration of TCE by phreatophytic trees has been limited to greenhouse studies and laboratory experiments of young trees over a single growing season [Gordon, 1997; Newman, 1997; Burke, 1996]. Field research is just starting using saplings [Chappell, 1997;

Tech Demo Plan, 1996] and will not provide significant cumulative uptake and transpiration data for years to come. This thesis research project will accomplish two tasks towards a better understanding of the phytoremediation process. First, through a system dynamics model, the uptake, translocation, cometabolism, storage, metabolism, and transpiration of TCE by a growing phreatophytic tree will be realized. Second, over a 10 year time frame an estimation will be made of the total amount of TCE removed from ground water and then transpired by a phreatophytic tree. Short rotation woody crops are harvested at approximately 7 years, so a 10 year time frame was selected to adequately cover this period.

To best represent phytoremediation by phreatophytes, this thesis project will focus on modeling relevant processes within the plant tissue and rhizosphere. In the soil an investigation will take place of the different soil horizons (ground water, capillary fringe, and unsaturated zone) and how they affect the growth of the phreatophyte and its uptake of TCE. In the rhizosphere research will include how the root soil interface affects plant uptake and the effect of cometabolism. In the plant the following will be investigated: the growth of the phreatophyte over time including the leaf, stem, and root compartments, the uptake process of contaminants into the tree; plant storage and metabolism of TCE, vascular flow and growth over time, transport of TCE by the vascular flow system, and the manner by which TCE transpires out of the tree itself. All these factors are necessary to represent the uptake and transpiration of TCE by

a phreatophytic tree. The research will seek to simulate reasonable behavior in comparison to empirically observed or intuitively understood realistic uptake and transpiration and to establish confidence in the model structure through validation testing.

II. Literature Review

TCE History

TCE is a colorless, nonflammable, volatile liquid with a characteristic ethereal odor similar to chloroform, was first synthesized in 1864, and has been in commercial use for over 80 years [Merck Index, 1989:1378; Steinberg and DeSesso, 1993:138]. TCE and other chlorinated aliphatics fall into a class of chemically stable compounds commonly known as "safety solvents" [Schnabel and others, 1997:1]. Some of the properties of "safety solvents" include [Schaumberg, 1990:18];

- a high solvency for oils, greases, waxes, tars, resins, lubricants, and coolants
- noncorrosive towards steel, copper, zinc, or other metals
- highly stable in the presence of common chemical stabilizers
- a low boiling point (87.1 ^{o} C); this permits low heat input and facilitates handling of work following degreasing operations
- nonflammable and nonexplosive at ordinary temperatures, and
- a high vapor density (4.5 that of air); this results in maintenance of a distinct vapor level near condensing coils in degreasing tanks and prevents excessive vapor losses to the surrounding atmosphere

Due to the aforementioned reasons, these chlorinated aliphatics saw widespread use for a majority of the twentieth century. This included applications as a degreasing agent, a dry cleaning solvent, an extraction agent

in decaffeinated coffee, a general anesthetic in medicine and dentistry, a dye solvent, as a heat exchange liquid in refrigerant and heat systems, in the manufacture of plastics, and as a fumigant [Verschueren, 1996:1783; Ensley, 1991:283; Schaumberg, 1990:17; Merck Index, 1989:1378].

Though TCE served well in many industrial situations, after extended exposure, workers started showing chronic affects. This included cell apoptosis, which is cell suicide due to overproduction of an enzyme, or necrosis, which is cell death due to a "running down" of the metabolic activity of the cell, as well as fatty liver [Plaa, 1986:288]. In animal bioassays, chlorinated hydrocarbons are cytotoxic after a single dose or upon chronic uptake, mainly in the liver and kidney of rodents [Williams and Weisburg, 1986:135]. Further studies by the National Cancer Center show that TCE induces hepatocellular carcinomas in mice [Williams and Weisburg, 1986:136]. It is now believed, through data and research, that TCE is metabolized by cytochrome P-450 in tissues and forms a reactive intermediate capable of binding to the catalytic enzyme, to other cellular proteins, and to DNA or RNA causing or resulting in mutagenicity [Ensley, 1991:288]. However, the extensive literature on the toxicology of TCE is at times conflicting, and substantial arguments exist that TCE is not a human carcinogen [ACGIH, 1986:63]. Taking a conservative stance, the EPA currently classifies TCE as a probable human carcinogen [USEPA, 1987:3]. This classification results from sufficient evidence of the carcinogenic effect in animal bioassays suggesting that it is very likely a human carcinogen [Cohrssen and

Covello, 1989:49]. Vinyl chloride, an intermediate product in the reductive dechlorination of TCE, is a proven carcinogen in humans [Creech and Johnson, 1974:150]. Some authors argue that only vinyl chloride gives a clear indication of genotoxicity in short-term tests and besides this evidence, that there is no indicative proof of a hazard to man by chloroethylenes [Green, 1990:77].

Because of its adverse attributes, in 1976 TCE was added to the ever-expanding list of hazardous substances [Schaumberg, 1990:17]. Since 1976, the production and use of TCE has been on the decline due to the increasing regulation of its use and substitution of new safer solvents, such as methyl chloroform and methylene chloride [USEPA, 1985:3-5].

Despite increased regulation and substitution of noncarcinogenic solvents, TCE was listed in 1991 as one of the "Top 50 Chemicals for Largest Releases" with a total of over 35 million pounds of the chemical released to the environment from industrial sources alone [USEPA, 1991:36]. Today, TCE is one of the most prevalent groundwater contaminants in the United States [Westrick, 1984:52]. There is no indication though that TCE is persistent or that it bioaccumulates in the food chain [USEPA, 1992:10-1].

Due to its former widespread use, accidental spills, leaking storage tanks, and improper disposal practices, TCE is now the object of soil and groundwater remediation efforts throughout the United States, especially at military installations. The EPA has set the minimum potable water standards for TCE at 2.7 to 5 micrograms of TCE per liter of solution [CFR,1994:354; Vogel,

1987:723]. This low standard has driven much of the remediation efforts we see today.

Physical and Chemical Properties of TCE

The properties of a contaminant influence its effect on and fate in the environment. Some important properties of TCE are shown in Table 2.1.

Property	Value
Molecular Formula	$Cl_2C=CHCl$[1]
Molecular Weight	131.4 gm/mole[2]
Vapor Pressure	20 mm Hg @ 0° C[4]
Henry's Law Constant	0.2 @ 10° C, 0.6 @ 35° C[4]
Boiling Point	87° C[1,4]
Vapor Specific Gravity	4.55 @ boiling point[5]
Solubility in Water	1.1 gm/L @ 25° C[1]
Density	1.46 gm/mL @ 20° C[1,4]
Organic Carbon Water Partition Coefficient	1.08×10^2 cm^3/gm^3
Octanol-Water Partition Coefficient (Log Kow)	2.29 - 2.42[1,4,6]
Air-Water Partition Coefficient (Log Kaw)	2.74[6]

Sources: [1]Anderson and others, 1993: 6; [2]Lenhard and others, 1995:50; [3]Narayanan and others, 1996:6; [4]Verschueren, 1996:1783; [5]USEPA, 1979:52-2; [6]Biernacki, 1995:761

Table 2.1 Properties of TCE

TCE Soil Contamination

TCE partitions into the soil in four distinct ways; it can be found in a vapor phase, sorbed to soil particles, dissolved in groundwater, or as a dense nonaqueous phase liquid (DNAPL) [Mackay and Cherry, 1989:632]. A DNAPL is at or near saturation, having displaced a majority of the pore water. Due to its

high density, TCE moves preferentially downward until it reaches bedrock, making extraction difficult [Lenhard and others, 1995:65]. These DNAPLs slowly bleed off contaminant, resulting in a persistent contaminant that is extremely difficult to remove at the source.

TCE is considered a highly volatile compound and partitions to air over water [Schaumberg, 1990:17]. Typically, at the soil surface, TCE concentration are insignificant. At a depth as little as 10 cm, the TCE soil concentration increases markedly. This of course depends on the soil moisture content, with wet and relatively saturated soils increasing much faster than dry and relatively unsaturated soils [Narayanan and others, 1996:5]. TCE concentrations are highest in ground water. TCE concentrations increase nearly three orders of magnitude between the top of the capillary fringe and the water table [McCarthy and Johnson, 1993:1682]. The maximum TCE concentration able to dissolve in water is 1,100 mg/L, so is the expected upper bound in the saturated zone [USGS, 1996:25].

In the unsaturated zone, mass transport is controlled by diffusion of gases as well as convection and dispersion. In the saturated and tension saturated zones, the transport of water is controlled by convection and dispersion only [Narayanan and others, 1996:2]. The dominant transport process between the saturated and unsaturated zones is through diffusion [McCarthy and Johnson, 1993:1682].

TCE Uptake by Plants

Lipophilicity is the most important property in determining if a chemical will move into and within a plant. Lipophilicity is the balance between the affinity of a chemical for aqueous phases and that for lipid phases and is related to K_{ow}, the octanol water partition coefficient [Cunningham and others, 1996:73]. Contaminants with an K_{ow} less than .5 are hydrophilic, and are not sufficiently sorbed to roots or actively transported through plant membranes while those with an K_{ow} greater than 3 are hydrophobic, and show poor translocation in plants due to lipid binding sites [Schnoor and others, 1995:2]. Chemicals susceptible to phytoremediation fall in between these two values and show good uptake by plant roots, translocate easily within the plant, and also show metabolic potential in all parts of plants [Cunningham and others, 1996:210] (Table 2.2).

Contaminant	K_{ow} Value
Chloroethene (Vinyl Chloride)	0.6
Dichloromethane	1.15
Methyl Isobutyl Ketone	1.25
Methylene Chloride	1.25
Phenol	1.46
1,2-Dichloroethane (DCA)	1.48
1,1-DCA	1.79
Trichloromethane (Chloroform)	1.93
m-, o-, p-cresols	~1.95
1,1,2-Trichloroethane	2.07
Benzene	2.13
1,1-DCE	2.13
1,1,2,2-Tetrachloroethane	2.39
TCE	2.42
1,1,1-Trichloroethane (TCA)	2.48
Carbon Tetrachloride	2.73
Toluene	2.73
Chlorobenzene	2.84
Tetrachloroethylene (PCE)	2.88
1,1,1,2-tetrachloroethane	3.03
Ethylbenzene	3.15
m-, o-, p-xylenes	~3.16

Source: Schnoor and Kurimiski, 1995; EPA, 1994

Table 2.2 Chemicals Susceptible to Phytoremediation

In the past, authors have felt root uptake of contaminants in most plants is minimal and that the rhizosphere, the soil root interface, was the primary location of organic contaminant degradation [Anderson and Walton, 1995:2046]. Other authors investigating agricultural plants found TCE uptake was primarily through foliar uptake [Schroll, 1994:203]. Foliar uptake occurs as plant leaves transpire, reaching an equilibrium with the background concentration of contaminant in the air. New research by scientists using poplar hybrids have found TCE is actively taken up by these trees, metabolized within various parts of the plant into

extractable metabolites, and fixed in tissue as non-extractable material [Gordon and others, 1997:3] (Table 2.3). These values are from greenhouse studies using poplar cuttings grown in soil columns exposed to 50 ppm of TCE over an eight month time frame. In field studies with sandy loam soil and ground water at a 4 feet depth, 97% of TCE in soil solution was taken up by poplars [Gordon, 1997]. In the same field studies, researchers did not see any increase of TCE concentrations in the rhizosphere [Newman, 1997]. Other research has substantiated the aforementioned results. TCE was found to concentrate in root tissues over leaves; a linear correlation with TCE concentrations in roots and adjacent soil suggested this as the primary uptake mechanism [Biernacki and others, 1995:761]. One scientist found approximately 10% of TCE is oxidized into carbon dioxide by plants [Matso, 1995:48]. Other scientists, investigating uptake of TCE by alfalfa, have revealed an uptake rate of 52% by plant material at 200 μL/L of TCE in ground water [Erickson and others, 1991:110]. Though no research of TCE uptake with changing soil classifications was found, it has been shown that uptake of atrazine by poplars varies with soil growth media. In silica sand the uptake of atrazine was 76-94% while in silty loam soil the uptake rate decreased to 20-29% [Burken and others, 1996:5]. In studies with tomatoes, 74-95% of ^{14}C labeled TCE was volatilized from plants, 5-25% was sorbed to soil, and very little was found in the plants [Schnabel and others, 1997:6]. Besides changes in soil texture, which may increase or decrease tortuosity of the flow path, pH may affect the bioavailability of the compound, especially those that are

charged or whose sorption is dependent on ionic binding sites [Cunningham and others, 1996:67].

Sample Type	Tissue	TCE	Chloral Hydrate	Trichloro ethanol	Dichloro acetic Acid	Trichloro acetic Acid
Control 1	leaves	ND	ND	ND	ND	ND
	stems	ND	ND	ND	ND	ND
Control 2	leaves	ND	ND	ND	ND	25
	stems	ND	ND	ND	ND	ND
Control 3	leaves	ND	ND	ND	ND	ND
	stems	15	ND	ND	ND	ND
TCE 1	leaves	13	ND	180	ND	1100
	stems	770	ND	140	ND	31
TCE 2	leaves	49	ND	19	180	7200
	stems	1900	ND	170	ND	22
TCE 3	leaves	27	ND	24	ND	2100
	stems	1300	ND	125	ND	100
TCE 4	Roots: upper	13	ND	200	320	44
	middle	150	ND	110	25	21
	lower	640	ND	31	270	44

Values shown are nanogram of contaminant per gram of sample
From: Newman and others, 1997:1067; Gordon and others, 1997

Table 2.3 TCE and Metabolic Products in Tissues of Poplars

The uptake of water by plants, especially trees, can substantially influence the local ground water table, thus controlling the flow of contaminant plumes. This uptake is similar to mechanical pump and treat systems, constantly flushing water upward through the soil column. Calculations of uptake in two 40' trees in southwestern Ohio during the midsummer months showed pumping rates from 50-300 gallons per day per tree [Nyer and Gatliff, 1996:59].

The path of uptake in a plant root varies greatly between authors. Most authors have only studied young roots, and therefore consider the root hair zone

the major area of water uptake [Curl and Truelove, 1986:45]. According to Dickmann and Stuart, Hofer, and Curl and Truelove - the root hair zone is the zone of major water uptake [1983:211, 1991:134, 1986:47]. When one considers the perennial plant root hair zone makes up only 1% of the root [Kolek, 1992:183; Curl and Truelove, 1986:47], regarding the root hair zone as a major source of uptake is questionable. Also, authors have investigated suberized roots in poplars and have found uptake rates that vary from 0 to 30,000 cubic millimeters of water per square centimeter of root per hour [Kolek, 1992:183]. The disparity in the authors' values is most likely due to differences in thickness, breaks, and structure of root bark. Other authors have found uptake rates at different locations of the root change with rate of uptake; at low uptake rates the apical root is the major zone of uptake, while at high rates of uptake the basal root is the major zone of uptake [Brouwer, 1953:135; 1954:78]. Researchers have found root hair zone uptake varies from 2 to 70% of total uptake; this variance is possibly due to changes in water availability; the more water readily available the less root hair and fine root uptake and also, the less root hairs and fine roots necessary [Gatliff, 24 Aug 1997]. Still other authors state the root hair zone performs no uptake function, basing this on the fact that the conductance of the root hairs is much lower than that of soil, making root hairs an unlikely media for water uptake [Weatherly, 1982:105].

Phytoremediation

In Latin, *phyto* means plant and *remedium* means to correct or remove an evil. Phytoremediation is defined as the engineered use of green plants to remove, contain, or render harmless, environmental contaminants such as heavy metals, trace elements, organic compounds, and radioactive compounds in soil or water [Hinchman and others, 1996:8]. This includes all plant-influenced biological, chemical, and physical processes that aid in the uptake, sequestration or storage, degradation, and metabolism of contaminants by either plants or the free-living organisms that constitute the plant's root soil interface or rhizosphere [Hinchman and others, 1996:9]. Phytoremediation is a biological, solar driven, pump and treat system with its own gravimetric self extending water seeking uptake media.

Phytoremediation is not a new technology by any means. Using vegetation to control contaminants has existed for many years, mostly in applications involving wastewater treatment [Matso, 1995:46]. In fact the first plant-based system was installed over 300 years ago in Germany for treatment of municipal sewage [Cunningham and others, 1996:61]. Only recently though, scientists have started experimenting with phytoremediation as an in situ remediation technique for contaminated soils and groundwater.

Phytoremediation takes place via two mechanisms: 1) direct uptake of contaminants and accumulation of nonphytotoxic metabolites into plant tissue or volatilization into the atmosphere; 2) release of exudates and enzymes that

stimulate microbial activity and biochemical transformations and enhance mineralization in the rhizosphere [Schnoor and others, 1995:1]. Subsets of phytoremediation include phytodecontamination and phytosequestering. The former deals with organic uptake, which includes; rhizosphere metabolism (rhizodegradation), plant metabolism (phytodegradation), binding to sites in the plant, and transpiration (phytovolatilization). The latter, phytosequestering, refers to the uptake of inorganics and their subsequent storage in plant compartments.

Plants, especially phreatophytes, transpire considerable amounts of water. This loss of water causes a draw down of water in the water table adjacent to a plant, similar to the draw down seen around wells. Not only does the plant take up water, but contaminants as well. The uptake of contaminants can reverse their downward migration, as seen with DNAPLs, as well as their horizontal movement with the ground water gradient flow [Schnoor and others, 1995:1].

There is currently some concern that contaminant uptake and volatilization will simply result in moving a contaminant from one habitat, soil, to another, the atmosphere, ultimately contaminating the food chain [Watanabe, 1997:185a]. Tests are being conducted on animals, such as birds and mice nesting in contaminated leaves and exposed to contaminant volatiles, as well as tests on aquatic organisms to verify the exposure and affect on the food chain [Watanabe, 1997:187a]. Conservative calculations of transpiration rates of TCE

from an aquifer contaminated with 100 mg/L of TCE show Occupational Exposure Limits an order of magnitude less than EPA requirements [Narayanan, unpublished article:2-5]. Therefore, volatilization is not considered as a significant problem to the application of phytoremediation, but is still a significant research issue.

Phytoremediation has numerous advantages and disadvantages, some giving it definite potential application possibilities and others restricting its utility.

Advantages of Phytoremediation. [Burken and others, 1996:1.23; Tech Demo Plan, 1996:3-4; Chappell, 1997:3-4]

- Able to withstand higher contaminant concentrations than bioremediation
- Plants serve as wind screens, stopping movement of toxic particulates
- Plants minimize wind and water erosion
- Lower maintenance than traditional pump and treat technology
- Lower cost than current remediation techniques
- Plants rebeautify an area, increasing the aesthetic value
- Harvested trees may be used as fuel or for income after phytoremediation is complete
- Creation of wildlife habitats
- Public acceptance
- Soils remain in place and are usable after treatment

Disadvantages of Phytoremediation. [Schnoor and others, 1995:6; Burken and others, 1996:1.23; Chappell, 1997:3-4]

- Only feasible in aquifers near the soil surface
- EPA does not currently recognize phytoremediation as an approved regulatory treatment, therefore it is limited to special EPA approved projects
- May take longer than current technologies
- Only works with contaminants of moderate hydrophobicity
- High contaminant concentrations are lethal to plants; phytoremediation may serve as a polishing step
- Uptake in clayey and silty soils is limited due to contaminant adsorption
- Due to EPA substantive limits on TCE contaminant in community water sources, phytoremediation is limited to areas where the ground water contamination will not potentially affect local drinking water
- Potential for contaminants to enter food chain

Phytoremediation is driven by ambient sunlight. Not only is it responsible for the rate of transpiration, it also is responsible for photosynthesis which has been shown to correlate to the amount of exudates released to plant roots. Typical exudates from plant roots are 10-20% that of the photosynthetic rate [Schnoor and others, 1995:2]. These exudates support microorganisms adjacent to the root in symbiotic, cometabolic, and commensal relationships, assisting greatly in the breakdown of organic chemical contaminants as seen in Figure 2.1.

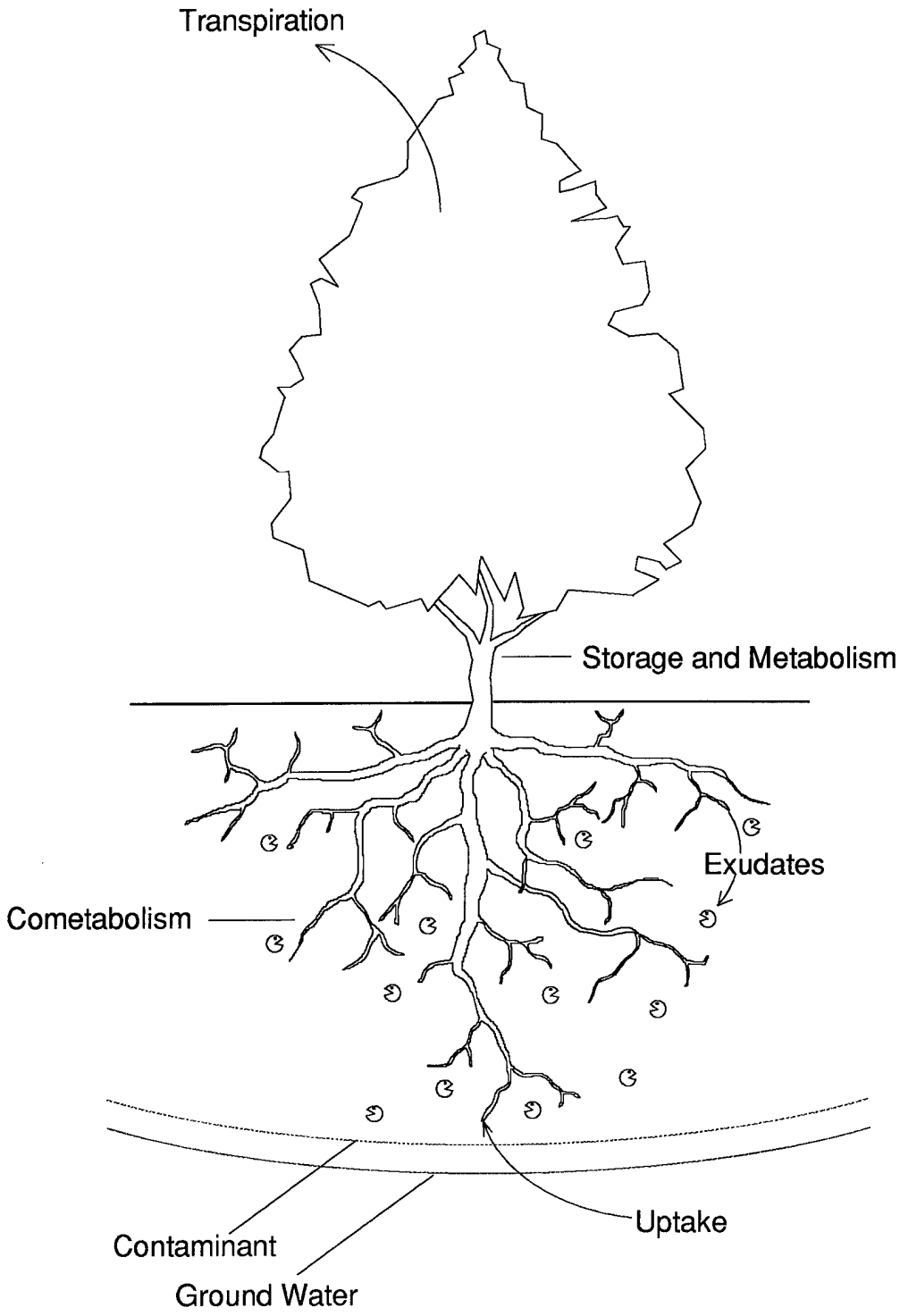

Adapted from Schnoor and others, 1995:321

Figure 2.1 The Phytoremediation Process

Rhizosphere

The rhizosphere is the region immediately surrounding the root of a plant and serves as an enrichment zone for increased growth of certain bacteria and fungi [Shimp and others, 1993:47]. This zone includes the root surface or rhizoplane, the apoplast or nonliving wall structure of the cortex cells, and surroundings of plant roots [Campbell, 1985:15]. It is usually assumed to extend a few millimeters, up to 5 millimeters, from the rhizoplane [Schmidt, 1991:82]. This does not mean all of the rhizosphere contains microorganisms; bacterial colonies may only cover 4-10% of the root surface [Shimp and others, 1993:47]. Electron micrographs have proven this is true; only 7 - 15% of the actual root surface in plants studied had microbial cells [Foster, 1983:194]. Still, large microbial populations are sustained in the rhizosphere in part through exudates and secretions from the plant root. These exudates and secretions are direct products of photosynthesis; from 10-20% of the total carbon photosynthesized by plants is released from the root to soil [Whipps and Lynch, 1985:65]. Other researchers put this value at 12-18% [Bowen, 1976:123]. These materials include sugars, such as glucose and fructose, some pentoses, di-, tri-, and oligosaccharides are also reported; common amino acid exudates are, alanine, serine, leucine, valine, glutamic and aspartic acids, glutamine, and asparagine [Bowen and Rovira, 1991:646-647; Campbell, 1977:74; Curl and Truelove, 1986:71]. Research so far has identified a minimum of 10 sugars and 25 amino acids as exudates from plant roots [Curl and Truelove, 1986:72]. These

materials are used by microorganisms as nutrient media for growth, along with other nutrients found naturally in the soil. There are currently five recognized origins of organic material for microbial growth [Bowen and Rovira, 1991:646-647; Rovira, 1979:1-3; Curl and Truelove, 1986:53]:

1) Exudates from roots to soil leaking passively from intact cells along a concentration gradient; may be chemicals or elaborate metabolites
2) Secretions of compounds of high or low molecular weight which are actively released by root tissue
3) Lysates or compounds released by autolysis of older epidermal cell walls when the plasmalemma fails, increasing with distance from the root apex
4) Plant mucilage, a material coating plant roots which acts as a soil lubricant for root penetration, expedites root growth; it is released from the root cap, as polysaccharide hydrolysates from the primary cell wall between epidermal cells and sloughed root cap cells, secreted by epidermal cells with primary walls, and produced by bacterial degradation of old dead epidermal cells, and
5) Mucigel, a product of the entire root-soil-microbial complex with its own distinct morphological and biochemical properties; a gelatinous material at surface of roots made of natural and modified mucilages, bacterial cells, metabolic products, colloidal minerals, and organic matter

Exudates and mucilage occur over the entire root surface, but the primary area of release is at the root tip [Shimp and others, 1993:49]. This is because the

root cap cells, which protect the root from abrasion, may be lost to the soil at a rate of 10,000 cells for a typical plant each day [Campbell, 1985:107]. In older regions of roots, mucilage and exudates disappear and more organics are released through death and decay of epidermal and cortical cells [Curl and Truelove, 1986:50]. Estimates of the annual amount of exudates, secretions, lysates, and mucilage released to the soil vary from 7% to 27% of the total plant mass [Shimp and others, 1993:50]. Other authors have determined by chemical methods that this figure ranges from 10 - 100 mg per gram of root for soluble exudates, 100 - 250 mg per gram of root for insoluble root material, and 20 - 50 mg per gram of root from the root cap and mucilage [Newman, 1985:110,114]. Roots of different and similar plants release different amounts of substances, depending on development of plant, soil factors, plant nutrition, microbial activity, temperature, light, and disease or injury [Curl and Truelove, 1986:79]. Together, exudates, secretions, mucilage, lysates, and mucigel, are collectively called rhizodeposition. Approximately 44% of rhizodeposition is exudates, secretions, and mucilage and 56% is lysates and mucigel [Fogel, 1991:93]. The largest source of rhizodeposition is from death of roots [Whipps, 1990:62]. All forms of rhizodeposition occur discontinuously along the root, with differing proportions of each controlling the type and structure of microorganisms present due to their specific substrate tendencies [Curl and Truelove, 1986:50]. Scientists currently believe microorganisms have an affect on the amount of

rhizodeposition, excluding lysates, which are programmed to die by the plant itself [Whipps, 1990:62].

The increased microbial activity and biomass in the rhizosphere increases the degradation rates compared to nonvegetated soils. The difference in microbial populations between these soil types may vary on an order of magnitude or higher [Cunningham and others, 1996:86]. Concentrations of microorganisms in the rhizosphere can reach values of 10^{10} - 10^{12} bacteria per gram of rhizosphere soil [Schmidt, 1991:82; Foster, 1983:194]. This rhizosphere effect is typically quantified as the ratio of microorganisms in the rhizosphere soil to the number of microorganisms in nonrhizosphere soil, known as the R/S ratio [Katznelson, 1946:345]. R/S ratios from 5 to 20 are common, and occasionally are as high as 100 or more [Katznelson, 1965:188]. A plant producing a large amount of exudate in sandy soils with very few microorganisms may have a rhizosphere extending several centimeters whereas a plant producing moderate or small amounts of exudate in an organic rich soil with higher rhizoplane populations may have a rhizosphere coincident with the rhizoplane [Campbell, 1977:82], the interface of the root and soil. Though organic material content in soils is the major driving force for microbial existence, growth, and type of organism found [Bowen and Rovira, 1991:645], there are other conditions influencing these factors. One of these is soil depth; as one extends further down into the soil horizon, microorganism presence usually decreases. Some studies indicate though that bacteria may be recovered to depths of many

meters in the rhizosphere; nitrogen fixing rhizobia have been recovered from root nodules of trees at depths of 3.9 to 4.5 meters [Waldon and others, 1989:3058]. Also, soil temperature and pH affect microorganism occurrence; as soil temperature decrease, so do microorganisms and as the pH drops below 5, the occurrence of fungi drops dramatically [Campbell, 1977:68-69]. The typical growth rates for mesophiles shows a rapid decline as the temperature of soil decreases below 15^{o} C, with optimum temperatures for growth in laboratory soils between 30 to 45^{o} C [Shimp and others, 1993:60]. Under grass cover at approximately 6', the ambient soil temperature is approximately equal to the groundwater temperature of 27^{o} C in Texas.

Microorganisms conversely affect the growth of the plant with which they have an association. They affect plant growth by influencing; 1) nutrient availability and uptake, 2) nitrogen fixation, 3) symbiotic relationships, 4) plant response to microbial metabolites, and 5) plant pathogens, their activity and coincident disease [Curl and Truelove, 1986:167].

The three major types of soil microorganisms are bacteria, fungi, and actinomycetes [Shimp and others, 1993:43]. Major taxonomic groups of microorganisms found in soil are shown in Table 2.4.

Microorganism	Number/gm Dry Weight in Rhizosphere	R:S Ratio
Bacteria	1200×10^6	240
Actinomycetes	46×10^6	6.6
Fungi	12×10^5	12
Protozoa	24×10^2	2.4
Algae	5×10^3	0.2

Source: Campbell, 1997:80

Table 2.4 Major Taxonomic Groups of Soil Microorganisms

Prokaryotic single-cell bacteria are the most numerous of the three, and are typically heterotrophs that feed on carbon in organic compounds. These bacteria are sometimes found in anaerobic environments, but are usually autocthonous to aerobic environments. In the rhizosphere, bacteria are found in microcolonies embedded in the mucigel surrounding the root, in the grooves between epidermal cells, and on the surface of the epidermal cells [Parke, 1991, 33-34].

Fungi, or mycorrhizae, have one of the most important symbiotic relationships with the plant root. With few exceptions, all plants develop mycorrhizae to various degrees [Schultz and others, 1983:17]. Mycorrhizae improve tree and plant growth through improved water and nutrient uptake and high temperature tolerance. Also, mycorrhizal roots live longer and are less susceptible to infection [Campbell, 1977:87]. It should also be noted that small diameter root hairs, .1 to .03 mm, are the primary strata for micorrhizal growth [Dickmann and Stuart, 1983:98]. The fungi benefit from this relationship in that

they generally do not have the ability to break down complex carbohydrates, which are presumed to come from the host [Campbell, 1990:134]. Five types of mycorrhizae are currently recognized, including ectomycorrhizae, endomycorrhizae, ericaceous mycorrhizae, ectoendomycorrhizae, and orchidaceous mycorrhizae [Reid, 1990:282-286]. The two types of mycorrhizae most frequently encountered are ectomycorrhizae and endomycorrhizae. Endomycorrhizae are commonly referred to as "vesicular-arbuscular" fungi and are the most widespread of the root symbionts [Schultz and others, 1983:18]. Endomycorrhizae form large, conspicuous, thick walled spores on the root surface, in the rhizosphere, and sometimes in feeder-root tissues. Endomycorrhizae penetrate the cell walls of the epidermis and grow into cortical cells of the root where they form vesicles and arbuscules, or nutrient exchanging structures [Schultz and others, 1983:18]. Ectomycorrhizae are common on forest trees, forming a sheath outside roots and penetrating between the cortical cells, forming what is called the Hartig net [Campbell, 1977:84]. This external mantle or sheath greatly improves the uptake of water and nutrients, not only increasing the movement of water to the root, but extending the influence of the root farther out into the soil. The Hartig net consists of hyphae which have developed intercellulary in the root cortex; this net may completely replace the middle lamellae between cortical cells [Schultz and others, 1983:17]. The Hartig net forms a fungal mantle which may vary from a few hyphae to a mass greater than the diameter of the root itself and typically is 20-40 μm thick [Reid,

1990:282,290]. The Hartig net may account for as much as 40% of the root weight and 6% of the total tree biomass [Campbell, 1990:132; Lynch and Whipps, 1991:19]. It should be noted that ectomycorrhizae never penetrate into the synplast of cortical cells although moribund root cap cells may be invaded [Reid, 1990, 282]. Another feature of ectomycorrhizal fungi is their hyphae which extend into the soil. The hyphae extend into the soil in a fan-shape pattern, increasing and branching into multiple strands with growth [Read, 1985:195]. These hyphae may extend 2 meters from their parent root, with more than 120 lateral branches, greatly improving the roots' area of influence [Fogel, 1991:95]. Ectomycorrhizal fungi also modify the root in which they come into contact. The epidermal cells and root hairs are nonexistent and the apical meristem is very small, resulting in a smaller root mass [Fogel, 1991:95]. These morphological alterations result in changes in the nutritional status of the root, increased photosynthetic rates, altered levels of growth-regulating substances, and altered patterns of root exudation due to changes in membrane permeability [Linderman, 1991:343]. It is difficult to quantify the effect of mycorrhizae, but data shows uptake rates increase up to six times [Dickmann and Stuart, 1983:211].

Actinomycetes are a group of prokaryotic soil bacteria that are superficially similar to fungi. They are single celled, but form filaments resembling mycelia and often produce spores. Actinomycetes are able to

degrade compounds resistant to decomposition by other bacterial and fungal species [Shimp and others, 1993:43].

The rhizosphere population is primarily made up of bacteria. Microbial population density is inversely related to the distance from the root, with highest populations usually occurring at the rhizoplane [Bazin and others, 1990:100]. Typically, the highest populations of microorganisms are found in the root hair zone, where exudation is the greatest [Parke, 1991:33]. Some experiments with grass roots have shown bacterial counts between young and old roots are not statistically different [Newman, 1974:209]. Though the meristem releases large amounts of exudates, it is generally sterile; this is due to the fact that the cap grows faster than microorganisms can move. Typical motile bacteria move at a rate of 20 - 80 μmeters per second, but are unable to maintain this rate for extended periods [Newman, 1985:116] while a maize root will extend at a rate of 40 mm per day from the meristem coupled with the zone of elongation rate of growth of 40 mm per day [Drew, 1990:36]. The few organisms that are found at the root cap are more than likely opportunistic organisms in soil colonies which the exploratory root came into contact with during its growth [Campbell, 1990:115]. Since the density of roots in forests are so high, 180 cm of root length per cubic centimeter of soil, bacteria do not require great motility and fungi do not need to spread far to get to new root sources [Newman, 1985:115].

Plant Physiology

Plants have mechanisms to detoxify biological contaminants. These mechanisms fall into two categories: 1) exclusion of the toxic material through immobilization, sequestration, or inhibition of uptake and, 2) detoxification through oxidative pathways [Tech Demo Plan, 1996:3-1]. Trees have both these capabilities, and through a better understanding of tree physiology, the processes involved are better understood.

"A tree is a shell of living tissue encasing an elaborate and massive chromatograph column of twigs, branches, trunk and roots" [Stomp and others, 1993:229]. Tree tissue, or wood, is composed of thousands of hollow tubes which function as a vast vascular network, moving water and nutrients throughout the plant. The vascular network which moves water and nutrients from the soil up into the plant is called the xylem. The opposite network which moves the sugars and other photosynthetic products from the leaves throughout the plant is called the phloem. Xylem tubes are actually dead cells, whose death is carefully programmed by the plant to produce a water-conducting tissue which also functions as mechanical support for the tree [Stomp and others, 1993:229]. Trees have three main growing parts - the root tip, the stem tips, and the cambium layer which is found between the bark and the wood throughout a tree [U.S. Dept of Agriculture, 1982:2].

Root

The root system performs several primary functions; one is the acquisition of water, dissolved ions, and nutrients, another is to furnish support for the stem and anchorage for the plant, and last, to serve as a food storage organ [Fitter, 1991:3; http, :8].

The root is divided up into five separate zones in woody dicotyledonous plants, including the 1) growing zone, 2) root hair zone, 3) maturation zone, 4) branching zone, and 5) moribund zone [Fogel, 1991:92-93; Kolek, 1992:32] (Fig 2.2). As mentioned before, the main growth in the root of a plant is at the root tip or growing zone. Figure 2.3 shows a typical root tip and its functional parts. The growing zone is made up of the apical meristem and elongation zones, with the apical meristem making up one third to one fourth the growing zone. The apical meristem, located at the root tip, manufactures new cells for growth. New cells are produced bidirectionally from the apical meristem, with new cells forming on the inside of the root continuing root growth and elongation, while the new cells forming out from the apical meristem form the root tip. The cells growing outward from the apical meristem are called the proximal meristem, while those growing towards the quiescent center are defined as the distal meristem [Sutton and Tinus, 1983:7,27]. The proximal meristem, or root tip, serves as protection for the apical meristem, protecting it from the abrasion of soil as the root pushes its way deeper into the soil. The root cap cells grow continuously outward from the apical meristem, programmed to die; before death

these statocyte cells are transformed into secretion cells, producing mucilage before being sloughed off [Sievers and Hensel, 1991:53]. The combination of mucigel and sloughed off cells together serve to protect the apical meristem [Howes, 1991:53]. In general, only a few days are necessary for this process to take place. This mucilage assists in reducing friction between the root tip and soil matrix, improving growth incursion. Some authors question the exact purpose of mucilage since it varies greatly, from profuse to nonexistent, between plant types in similar soils and even between the same plant located in separate geographic locations. A side benefit to mucilage is its use by soil microorganisms as a growth media.

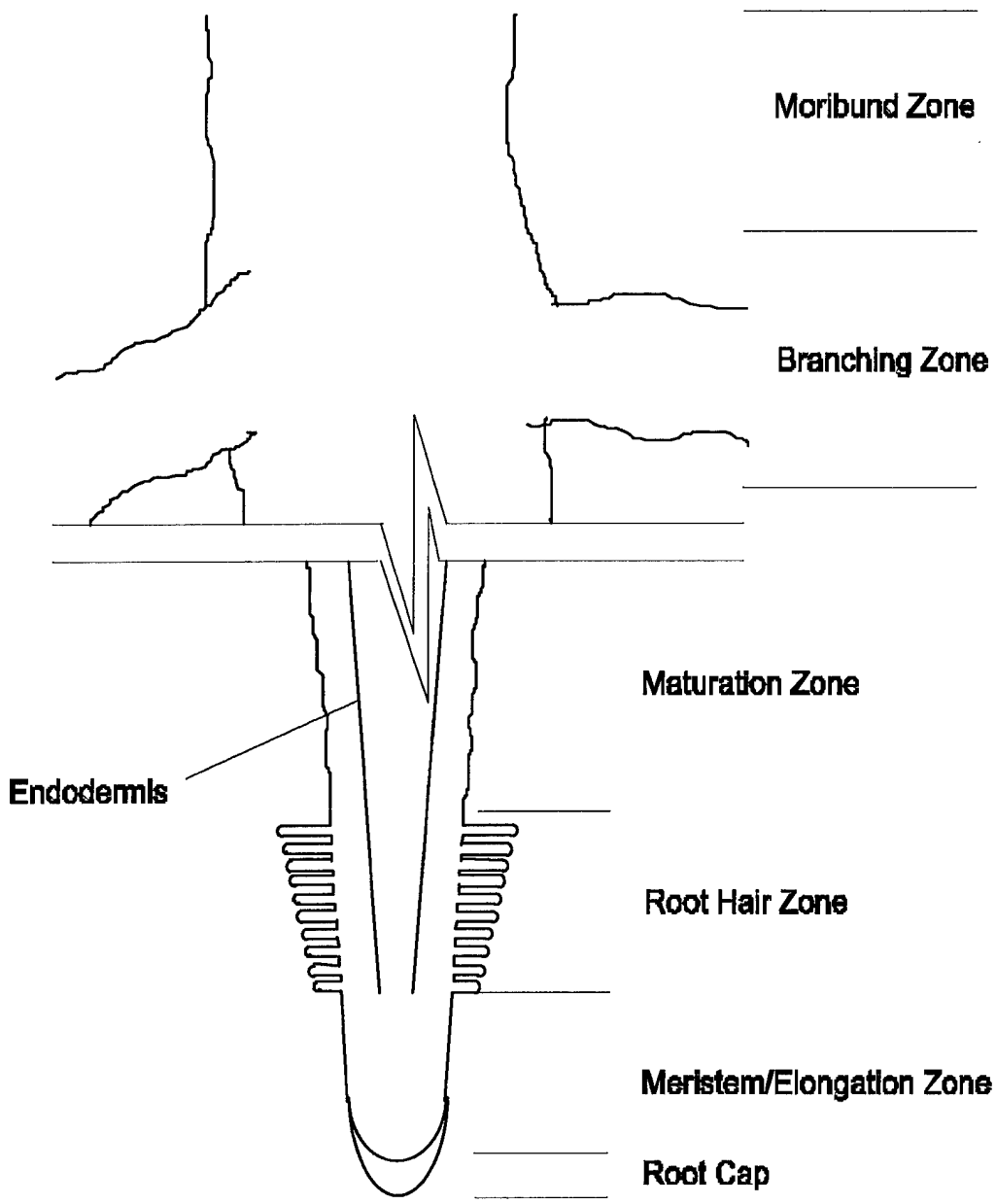

Adapted from Fogel, 1991:92-93; Fried and Broeshart, 1967:70

Figure 2.2 Zones of a Woody Dicotyledon Root

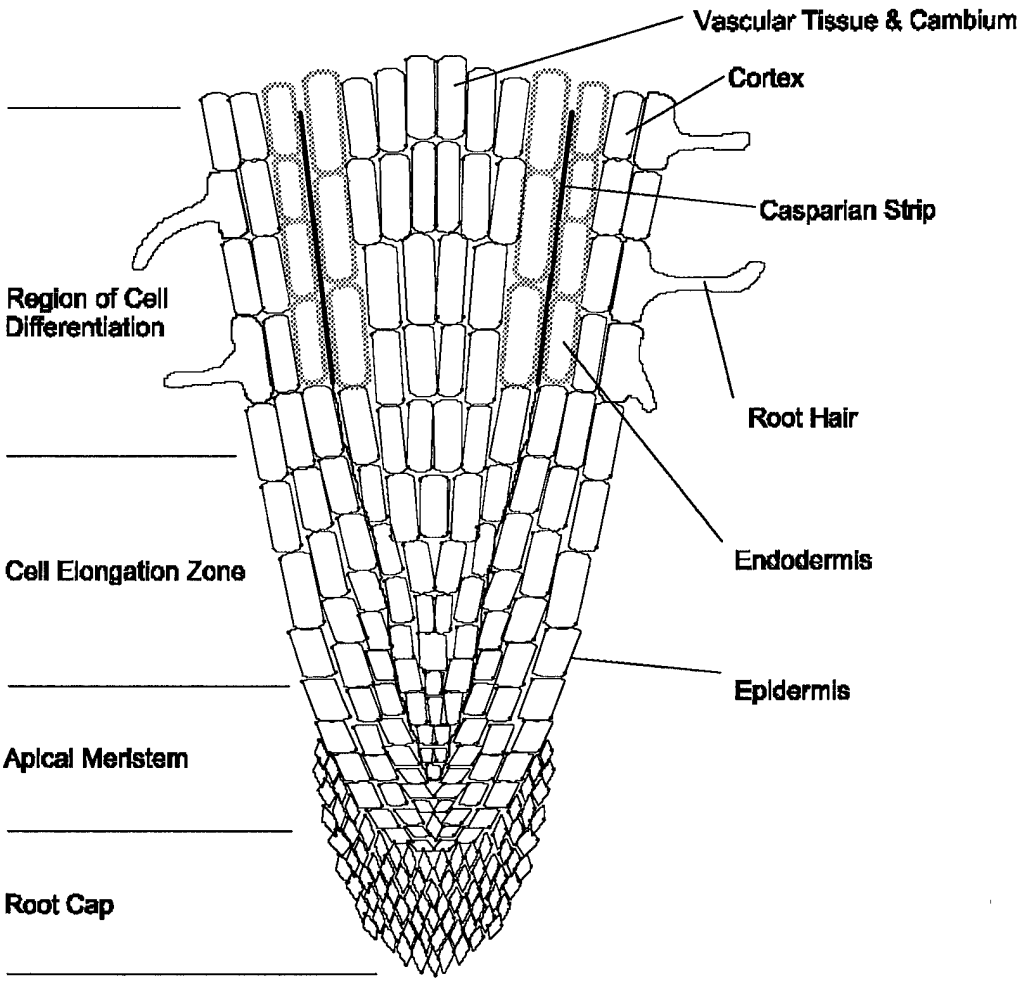

Adapted from Nobel, 1991:7

Figure 2.3 Diagram of a Root Tip

The distal meristem cells elongate through food and water absorption, pushing the apical and proximal meristem through the soil. This elongation zone is also the site or morphological differentiation of cells, where they become specific tissues, such as the epidermis, cortex, or vascular tissue [Kolek, 1992:48]. The primary phloem is the first to form, then the primary xylem.

The next zone in a root is the root hair zone or absorption zone. This zone exists for 2-3 days in most plants before maturation takes place. It is a

major site for mycorrhizal infection, exudation from the root, and water and nutrient uptake [Fogel, 1991:92]. As previously stated, differentiation of cells is complete in this zone.

One type of cell formed is the epidermis. The epidermis is the outermost portion of the plant root, separating plant tissue from the soil matrix (Fig 2.4). The epidermis includes root hairs, which have a cylindrical straight form with a dome-shaped tip often forming a right angle with the root surface. They are elongated epidermal cells that have changed their growth direction [Hofer, 1991:130]. Root hairs are short-lived cells, collapsing and being worn away after a few days or weeks, and vary in length from 80 to 1500 um [Hofer, 1991:130]. Conversely, root hairs in a symbiotic relationship with mycorrhizal fungi show a life span estimated from one to eight years, depending on size, species, and mycorrhizal status [Dickmann and Stuart, 1983:106; Reid, 1990:290]. As covered in the section "TCE Uptake by Plants," some authors feel root hairs are primarily water and nutrient uptake exchange media for plants and also serve as anchorage [Hofer, 1991:134]. Authors also state young white roots are thought to be most important for water and nutrient uptake, older suberized brown roots to a lesser extent [Dickmann and Stuart, 1983:211]. This is balanced with arguments for significant suberized root uptake and minimal to no uptake through the root hair zone [Kolek, 1992:183; Brouwer, 1953:135; 1954:78; Weatherly, 1982:105].

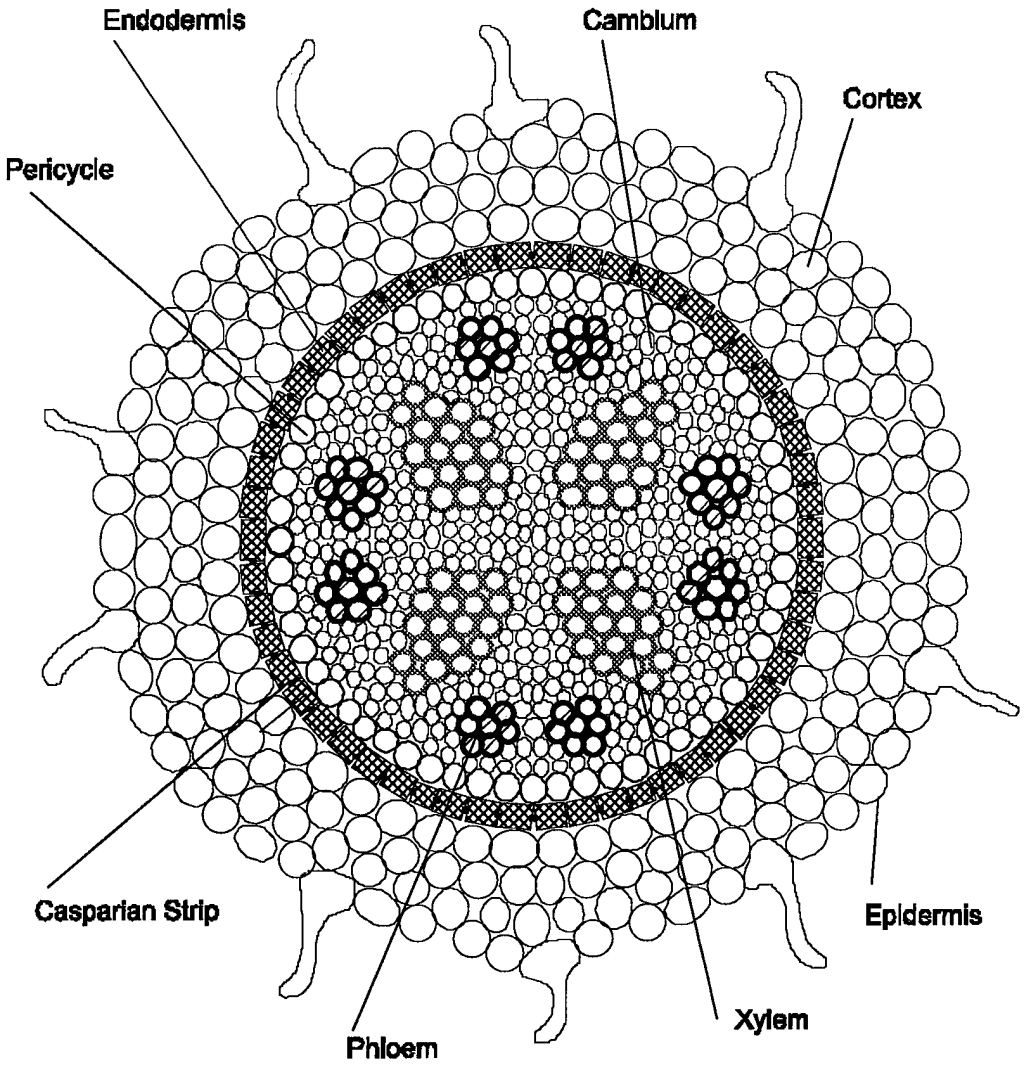

Adapted from Nobel, 1991:7; Moreshet, 1991:607

Figure 2.4 Fine Root Cross-Section

Immediately adjacent to the epidermis is the cortex, which functions as a water translocation network and as storage tissue. The cortex is made of symplastic and apoplastic tissue, allowing movement of water, nutrients, and even mycorrhizal fungi through its apoplast. The open pathway for water and solute movement between the cortex cells of the root has been termed the apparent free space, and is comprised of cellulose and open spaces that form a

sponge-like material that provides structural support while allowing free water and solute movement [Lindstrom and others, 1991:130]. The apparent free space is approximately 7% of the tissue volume, but because of its structure, accounts for most of the water and solute movement from the soil solution to the endodermis [Lindstrom and others, 1991:130].

Interior to the cortex is the endodermis, or casparian strip, which forms a continuous sheath of one-cell thickness around the vascular stele in the center of the root and is formed within a few millimeter of the root tip [Moreshet and Huck, 1991:608; Clarkson, 1991:424]. These cells are characterized by the presence of hydrophobic bands of lignin and suberin in their radial walls which completely circle each cell. This waxy barrier inhibits the movement of water into the interior of the root [Cunningham and others, 1996:74]. The casparian strip also serves as an exclusion mechanism for the plant, only allowing chemicals of a given hydrophobicity access to the root interior. The casparian strip therefore greatly reduces the porosity and permeability of the radial walls. The only way to pass from the cortical apoplast to the stele is through the endodermal protoplast, a journey that requires passage across the endodermal plasma membrane [Clarkson, 1991:424]. This means all water, solutes, and non-aqueous phase liquids must pass by mass transport through cell membranes at least two times to reach the vascular tissue [Cunningham and others, 1996:74]. The term mass transport is used to describe this movement of

chemicals into the root through diffusion, advection, and active uptake [Lindstrom and others, 1991:132].

After passing through the casparian strip, solutes enter the stele, where root vascular tissue is located. There are three ways for solutes to pass into the stele: 1) via cell wall apoplastic pathways, 2) via the cytoplasm symplastic pathway using the plasmadesmata as a bridge, and 3) by transcellular or vacuole to vacuole movement [Moreshet and Huck, 1991:610-611; Weatherly, 1982:90-91].

The stele consists of vascular tissue, including xylem and phloem and also nonvascular tissue, including the pericycle and parenchymal cells. In dicotyledons the xylem occupies the central part of the root, with extensions projecting outward from the center [Moreshet and Huck, 1991:608]. The xylem in the center of a root is the first to form, called the protoxylem, with later xylem formed in bundles around the center, called metaxylem [Sutton and Tinus, 1983:49-50, 67]. The first phloem to form in the elongation zone, or protophloem, develops toward the center of the stele and the later phloem, or metaphloem, forms adjacent and inside of the pericycle [Kolek, 1992:65]. The metaphloem have a larger diameter and are more numerous than the protophloem. Parenchyma tissue is composed of brick shaped cells, and is concerned with storage and distribution of food materials while the pericycle is commonly one layer of cells, interior and adjacent to the casparian strip [Sutton

and Tinus, 1983:57]. The pericycle is made of parenchymal tissue, and is the location from which lateral roots originate [Moreshet and Huck, 1991:608].

Above the root hair zone is the maturation zone. In this zone, primary growth slows, secondary growth begins, and the root becomes suberized. Secondary growth is typical in woody dicotyledons. Secondary growth starts with parenchymal tissue differentiating into a vascular cambium between the protophloem and the protoxylem, forcing the two apart [Curl and Truelove, 1986:29; Kolek, 1992:76-77]. From this vascular cambium the metaxylem and metaphloem form, forcing the protophloem and protoxylem further apart. Rings similar to stem rings are formed during secondary growth, but are more irregular and thicken eccentrically [Kolek, 1992:76-77]. The increased diameter of the root causes disruption of the endodermis, cortex and epidermis, resulting in this tissue being sloughed off [Curl and Truelove, 1986:29] (Fig 2.5). Suberin, a complex material made of ω-hydroxy fatty acids of 16-24 carbon chains, corresponding dicarboxylic acids, long chain alcohols, and waxes is deposited in cells during secondary growth [Drew, 1990:37]. This strengthens the root, but at the same time inhibits radial movement of water within the root. In perennials, the suberized portion of a root makes up to 99% of the total root [Kolek, 1992:183, Curl, 1986:47].

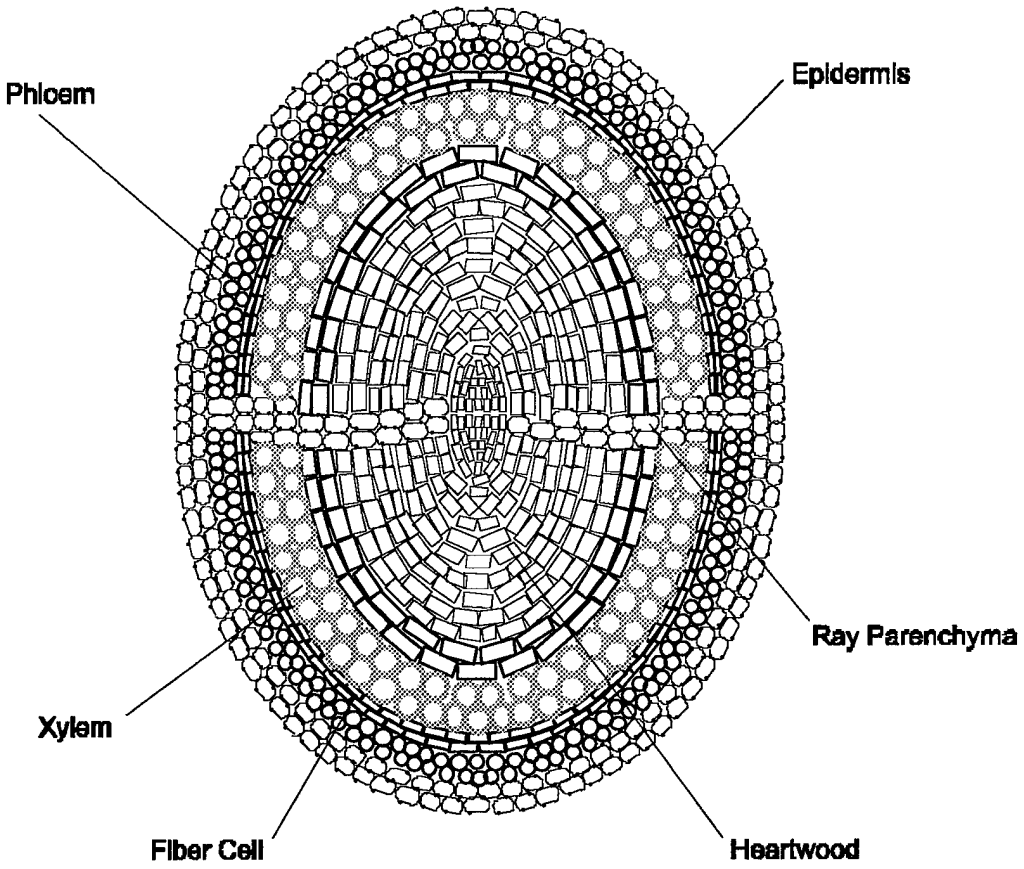

Adapted from Salisbury and Ross, 1991:97

Figure 2.5 Mature Root Zone Cross-Section

Adjacent to the maturation zone is the branching zone. Branches form from the pericycle, the outermost portion of the parenchymal tissue. Little is known or published on this zone.

Finally, the moribund zone is reached. Little activity is seen in this zone except for the release of carbon into the soil [Fogel, 1991:93].

Stem

The stem is the structure which supports the buds and leaves and serves as a conduit for carrying water, minerals, and sugars [http, 1996:1]. The three

major components of the stem are the xylem, phloem, and the cambium (Fig 2.7). The cambium is a meristem, which is a site of cell division and active growth, producing xylem, or wood, to its interior, and phloem, or bark, to its exterior (Fig 2.6) [http, 1996:1; Nobel, 1991:6]. The cambium layer is generally a single cell layer in width, found throughout the stem of a tree. The phloem is a living part of a plant, and consists mainly of cellulose and suberin, a waxy fatty substance which protects the living cells in the cambium from drying out and dying [U.S. Dept of Agriculture, 1982:2]. The phloem is made up of several types of cells; there are sieve cells and sieve-tube members, and though these cells may contain no nuclei at maturity, they remain metabolically active [Nobel, 1991:7]. The phloem mostly transports sugars, but also amino acids and amides through the sieve tube elements [Shimp and others, 1993:65]. Transport in the phloem is generally from the leaf to the root, but may be bidirectional, depending on hydrostatic pressure gradients [Shimp and others, 1991:65; Nobel, 1991:516]. Connections between the phloem and xylem occur in both the leaf and the root. These connections allow water to pass from the phloem to the xylem and vice versa, by mass flow [Lindstrom and others, 1991:131]. The xylem constitutes almost all of the wood in a tree and is only functional after the xylem cell has died. In *Populus deltoides*, xylem elements are abundant and crowded, in clusters or radial chains of 2-6 [Cutler and others, 1987:150].

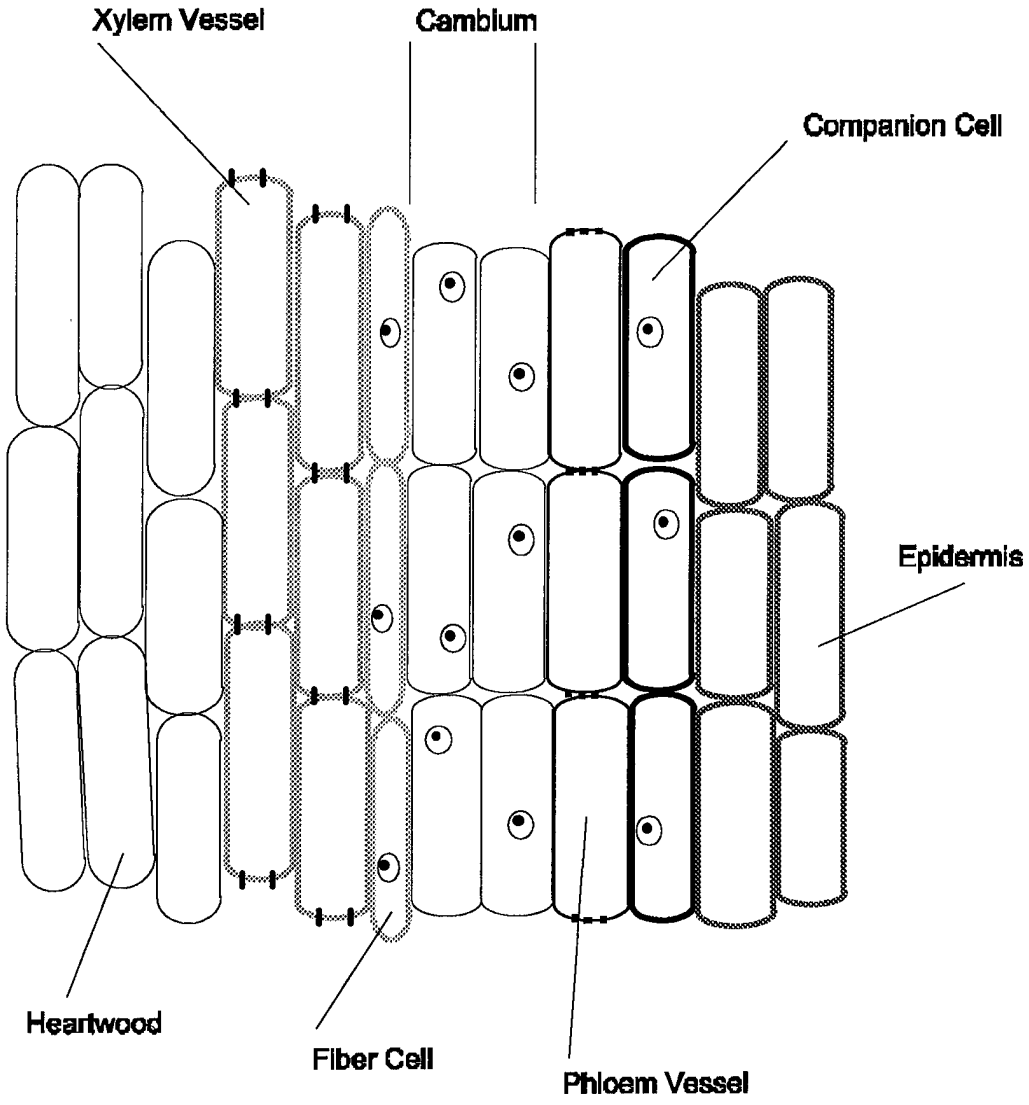

Adapted from Nobel, 1991:5

Figure 2.6 Longitudinal Stem Cross-Section

The transfer of water through a tree is explained by the cohesion-tension theory, which states leaves of trees act like sponges on top of a tube. As the water evaporates from the sponge, or leaves, cohesive forces of water maintain the water column, pulling additional water up into the sponge, or leaf [Shimp and others, 1993:65]. Water conduction in the xylem of a tree often occurs only in

the outermost annual ring, adjacent to the cambium [Altman, 1966:66]. This active portion of the xylem is referred to as the hydroactive xylem and the inactive portion, or heartwood, is referred to as the hydropassive xylem [Cermak and others, 1973:172]. Xylem tissue is made of various cell types, specifically tracheids and vessel members. Tracheids are conducting cells which lose their protoplasts, with the remaining cell walls forming a low-resistant channel for the passage of solution [Nobel, 1991:6]. The vessel members are shorter and wider than tracheids, and are joined end-to-end in long linear files, forming a long tube called a xylem vessel, also serving as a transportation media [Nobel, 1991:507]. Other types of cells in the xylem are parenchymal cells and fibers which contribute to the structural support of a plant as well as serving as storage sites for starches, fat, and proteins. Softwood xylem is made of approximately 90-94% tracheids and vessel members by volume, with the remaining cells storage parenchyma [Gartner, 1995:126]. The storage parenchyma of poplar wood is primarily made of ray parenchyma; axial parenchyma are almost nonexistent [Sauter, 1994:298-299]. Plant xylem consists mainly of cellulose fibers and lignin, a dark-colored chemical hydrophobic substance which gives wood extra hardness and strength [U.S. Dept of Agriculture, 1982:2].

Contaminant transport in the xylem is much more rapid than transport in the phloem. This is because the plasmalemma is readily permeable to chemicals which penetrate into the symplast, or phloem, but display an apoplastic transport pattern; the symplast can't retain these compounds, and

consequently they leach into the apoplast and are carried with the transpiration stream, or xylem [Jachetta and others, 1986:1000]. Estimates of xylem and phloem flow for trees are 3.6-12.6 meters per hour and .10-2 meters per hour, respectively [Nobel, 1991:511,515; Hinckley and others, 1994:1015; Shimp and others, 1993:65].

Leaf

The principle function of leaves is to absorb sunlight for the manufacture of sugars through photosynthesis. It is therefore not surprising that the physiological makeup of the leaf is primarily to serve this process (Fig 2.8). Like the root, the leaf is covered with an epidermis, usually one cell layer in thickness. Epidermal cells have a relatively thick waterproof cuticle on their exterior surface containing cutin, which prevents water loss as well as inhibiting invasion by pathogens [http, 1996:4]. On the underside of phreatophyte trees are stomatal openings in the leaf. Stomata are each regulated by two specialized epidermal cells, or guard cells, which, when under turgor, open the stomata, and conversely, when flaccid, close the stomatal openings. This allows for flow of carbon dioxide and other atmospheric gases into the plant that are necessary for photosynthesis and at the same time regulates the loss of water from the plant [Nobel, 1991:4; Paterson and others, 1990:301].

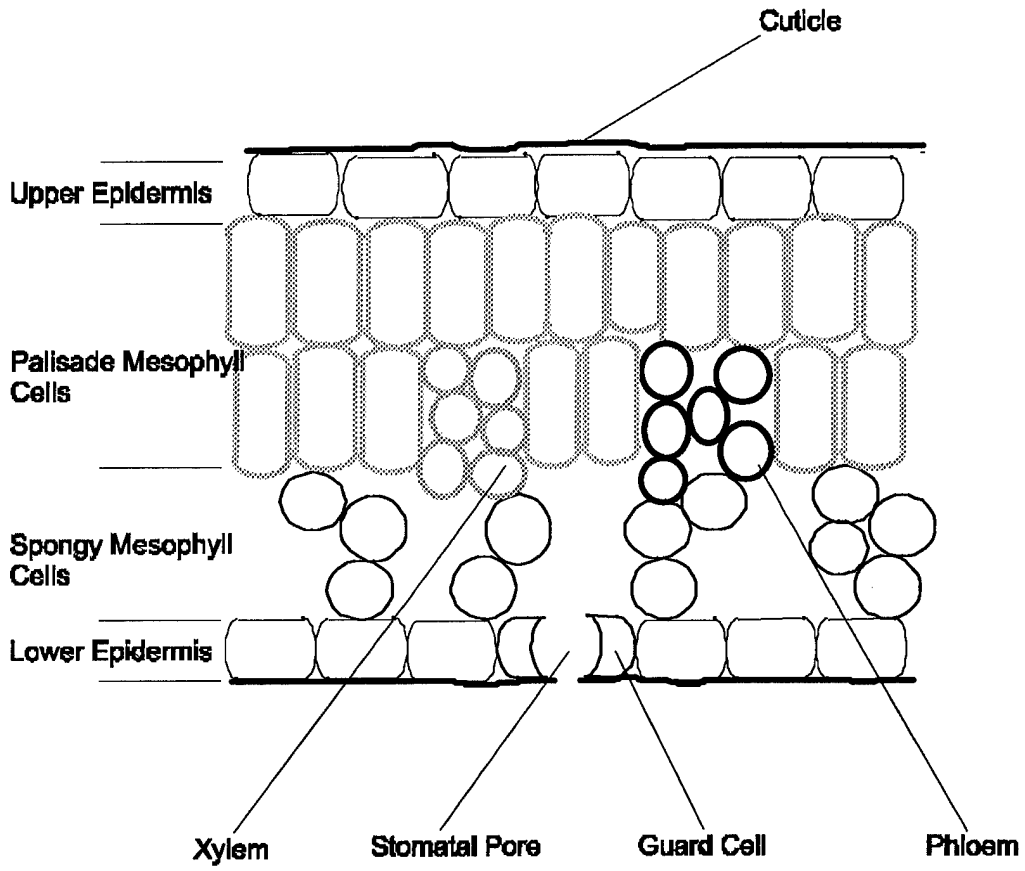

Adapted from Nobel, 1991:3

Figure 2.7 Leaf Cross-Section

Immediately interior to the epidermis, on the upper side of a leaf, are the palisade mesophyll cells, which contain chloroplast cells for photosynthesis. The xylem and phloem elements are found in this layer. Below this is the spongy mesophyll cell layer. This area is made of loosely packed cells with conspicuous intercellular air spaces, allowing for diffusion of carbon dioxide, oxygen, and other chemicals in and out of the leaf through the stomatal openings [Nobel, 1991:4].

The leaf also serves as a temperature regulation device. Gradual uptake by the roots, translocation through the stem, and transpiration from the leaves aid in stabilizing plant temperatures, especially in the leaves [http, 1996:16]. Relative humidity in a leaf can approach 100%. When stomata are open, the humidity is released, forming a cloud of high humidity around the leaf, slowing transpiration and cooling the leaf [http, 1996:17]. As wind blows this vapor away from the leaf, transpiration increases to balance the humidity. On a hot summer day the volume of water lost may exceed the total water content of the plant [Tech Demo Plan, 1996:3-2]. To survive then, plants must have an adequate water supply moving from root to canopy to balance this transpiration loss. Transpiration is based on plant density, leaf area, radiant solar flux, depth to ground water, maximum daily temperatures, relative humidity, and wind speed [Nichols, 1994: (Tech Demo Plan)].

Photosynthesis and Transpiration

Photosynthesis and respiration for trees follow a seasonal pattern, reaching a maximum during the hottest and longest summer days. In the fall, as the temperature drops and the days become shorter, the photosynthetic and respiration rate drops to 1-10% of summer rates [Foote and Schaedle, 1976:652]. Only a small amount of the water respired by plants, much less than 1% of the transpiration stream, is required by the plant for growth and other processes [Oertli and Eth, 1991:559]. The remainder of the water is used by the plant to maintain leaf temperature and turgor. Photosynthesis is related to leaf

area, with 19 µmol of photosynthate produced per square meter of leaf per second in August [Ceulemans, 1991:71].

The transpiration flow rate is estimated as 2-10 µg transpirate per square centimeter of foliage per second while the symplastic flow rate is estimated as .05 ug per second per square centimeter of foliage [McFarlane and others, 1981:93; Crank and others, 1981:32]. In the top exterior leaves of *Populus* trees the stomatal conductance can exceed .48 moles per square meter of leaf per second; in lower interior leaves, the stomatal conductance falls to .074 moles per square meter of leaf per second, and on average is .723 moles per square meter of leaf per second [Hinckley and others, 1994:1014]. Under optimal conditions, a poplar tree occupying 4 square meters of ground can cycle 100 liters of groundwater in a single day or .1 m^3/day [Stomp and others, 1993:229]. A .2 m diameter tree, 10 m in height at 4 square meter spacing transpires .06 m^3/day [Nobel, 1991:529]. Other studies of transpiration rates in trees show a midday loss rate of 100 g/hr or .0001 m^3/hr and an average loss at night of 5-8 g/hr or .000005-.000008 m^3/hr [Steinberg and others, 1989:468]. Other studies show five-year-old trees transpire 100-200 L/day or .1-.2 m^3/day [Newman and others, 1997:1062]. In studies, leaves transpired approximately 1.0 µgm TCE per leaf per hour at a TCE concentration of 50 mg/L; this varied from undetectable levels to 1.6 µgm TCE per leaf per hour [Gordon and others, 1997:3].

Researchers have also found that of the TCE taken up into phreatophytes, generally 75% is volatilized and in mass balance studies it accumulated in leaves 1.2% [Burken, 1996:40,63-65]. Greenhouse studies support this evidence, with approximately 66% of TCE taken up by *Populus* hybrids volatilized into the atmosphere [Gordon, 1997]. Field trials by the same scientist are inconclusive; the amount of TCE volatilized varies a great deal from one tree to another, with an average of only 10% of TCE taken up by plants being volatilized.

Poplars

Eastern cottonwood, or *Populus deltoides* are of the genus *Populus*, a complex amalgam of tree species which are typically found in or near wetlands, lowlands, and areas of periodic flooding [Dickmann and Stuart, 1983:2]. The genus is a member of the willow family and is comprised of five sections, consisting of 30 species of wide distribution throughout the Northern Hemisphere (Table 2.5, Figure 2.9). *Aigeiros*, under which *Populus deltoides* falls, is the most important section of *Populus* due to their great commercial importance, and typically grows on moist silty or sandy loam soils, but can actually grow almost anywhere due to its relative drought resistant [Dickmann and Stuart, 1983:16]. Poplar trees offer distinct advantages for treatment of soils contaminated with organics. They are long-lived, fast growing, hardy, and tolerant of organics [Schnoor and others, 1995:4]. Poplars also are easily grown from cuttings planted deeply in the soil, with advantageous roots that will quickly

reach down to the water table, establishing a dense root mass for uptake of water [Dickmann, 1983:56-57; Schnoor and others, 1995:4].

Section	Species	Common Name
TURANGA	*Populus euphratica*	Euphrates poplar
LEUCOIDES	*Populus ciliata*	Himalayan poplar
	Populus heterophylla	Swamp cottonwood
	Populus lasiocarpa	
	Populus wilsonii	Wilson poplar
LEUCE		
Subsection ALBIDAE	*Populus alba*	White poplar
	Populus monticola	Mexican white poplar
Subsection TREPIDAE	*Populus adenopoda*	Chinese aspen
	Populus davidiana	Korean aspen
	Populus grandidentata	Bigtooth aspen
	Populus sieboldii	Japanese aspen
	Populus tremula	European aspen
	Populus tremuloides	Quaking aspen
TACAMAHACA	*Populus angustifolia*	Narow-leaved cottonwood
	Populus balsamifera	Balsam poplar
	Populus cathayana	
	Populus koreana	Korean poplar
	Populus laurifolia	Laurel poplar
	Populus maximowiczii	Japanese poplar
	Populus simonii	Simon poplar
	Populus suaveolens	
	Populus szechuanica	
	Populus trichocarpa	Black cottonwood
	Populus tristis	Himalayan balsam poplar
	Populus yunnanensis	
AIGEIROS	*Populus deltoides*	Eastern cottonwood
	Populus fremontii	Fremont cottonwood
	Populus nigra	Black poplar
ABASO	*Populus mexicana*	Mexican poplar

Source: Dickmann and Stuart, 1983:3

Table 2.5 Genus of *Populus deltoides*

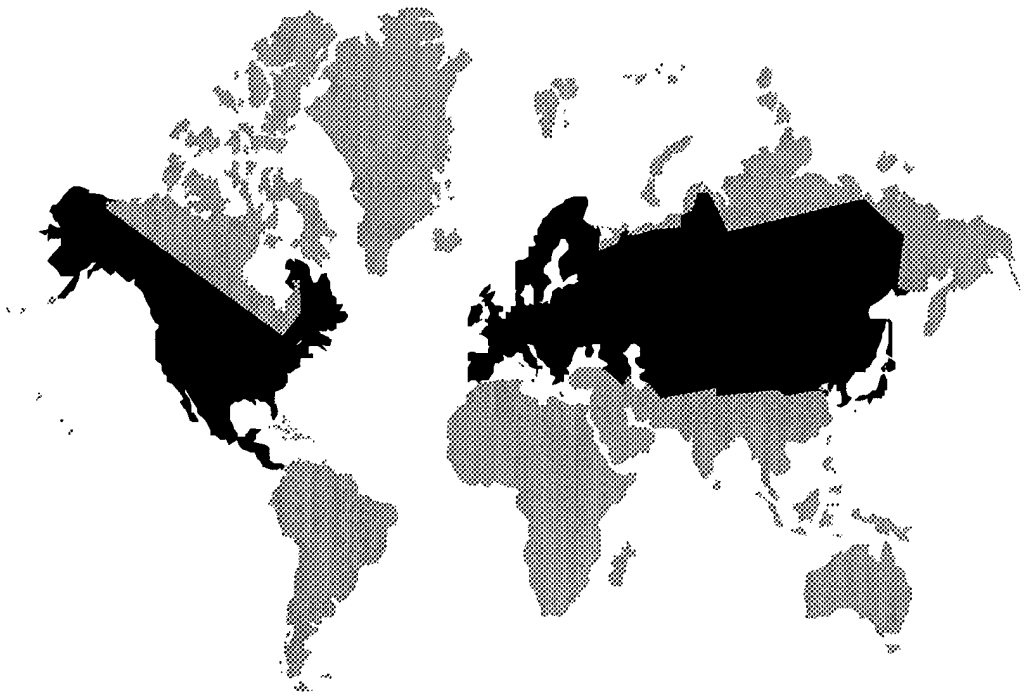

Figure 2.8 World Map of *Populus* Distribution

Rhizosphere Cometabolism of TCE

Degradability of TCE under aerobic and anaerobic conditions, until recently, was not well understood [Bouwer, 1981:596]. It is now known under anaerobic conditions that chloroethylenes are degraded through reductive dehalogenation [Anderson, 1994:18] to dichloroethylene (DCE) and vinyl chloride [Vogel and McCarty, 1985:1083] (Fig 2.10). Though anaerobic niches are not uncommon in aerobic soils [Hutchinson, 1979:1126], their significance is minimal around roots of phreatophytes due to their release of oxygen into the rhizosphere and soil. Under aerobic conditions, TCE is usually cometabolized or cooxidized via monooxygenase activity, which requires the presence of a cosubstrate [Mu, 1994:2661]; where cometabolism is defined as the process in

which microorganisms transform a substance, typically with no benefit to the microorganism itself, while growing on another substance [Anderson and others, 1993:2634]. Primary substrates include, ammonia [Arciero, 1989:641], isoprene [Ewers and others, 1990:412], methane [Fox and others, 1990:6419], propane [Wackett and others, 1989:2692], phenol, or toluene [Folsom and others, 1990:1279]. These substrates result in TCE cometabolically converting to TCE epoxide, which spontaneously breaks down into xenobiotics capable of mineralization by other microorganisms [Anderson, 1991:29] (Fig 2.11). TCE shows the best degradation by indigenous soil microorganisms when in the presence of toluene or phenol. This was confirmed in laboratory tests, verifying TCE would not degrade in the absence of toluene [Mu, 1994:2662]. The reason TCE is persistent in soil and groundwater is not only because it requires a substrate for cometabolism, but because the substrate itself is a competitive inhibitor to TCE [Ensley, 1991:296]. The cosubstrate must be present in the environment at high enough concentrations to induce the necessary oxygenase and regenerate reducing power into the cells lost during the oxidation of TCE. Otherwise, the microorganisms may be inactivated by the TCE or its metabolites, resulting in a new population of microorganisms necessary to continue the process. Conversely, the concentration of the cosubstrate must be low enough that it does not completely inhibit the oxidation of TCE through competition for the active site on the enzyme. This balance rarely exists in the natural environment, so TCE persists due to its resistance to microbial attack [Ensley,

1991:296; Wackett and others, 1989:2960]. Lab studies support this supposition, with no significant cometabolism of TCE found in the rhizosphere of *Populus* trees [Burken, 1997; Newman, 1997].

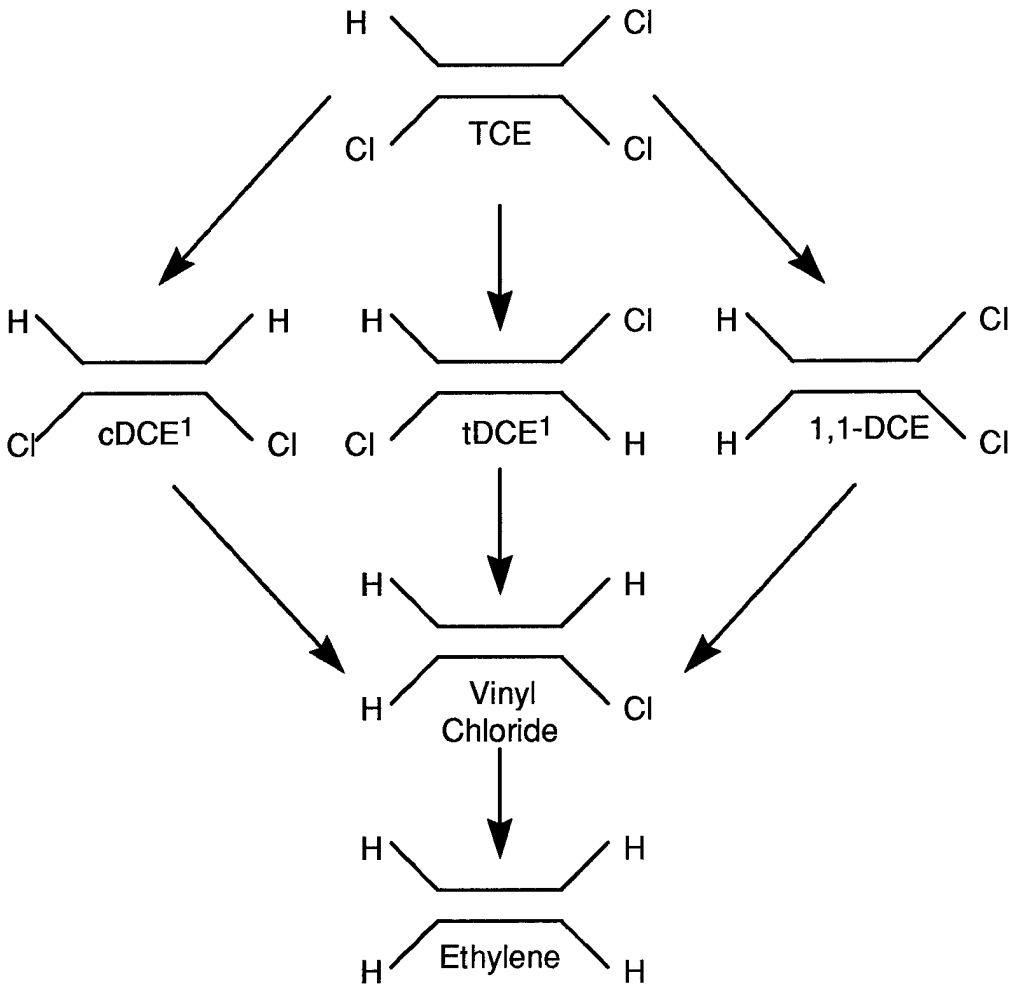

1 cDCE - cis-Dichloroethylene, trans-Dichloroethylene
Source: Vogel & McCarty, 1985:1083

Figure 2.9 Reductive Dechlorination Pathways of TCE Under Anaerobic Conditions

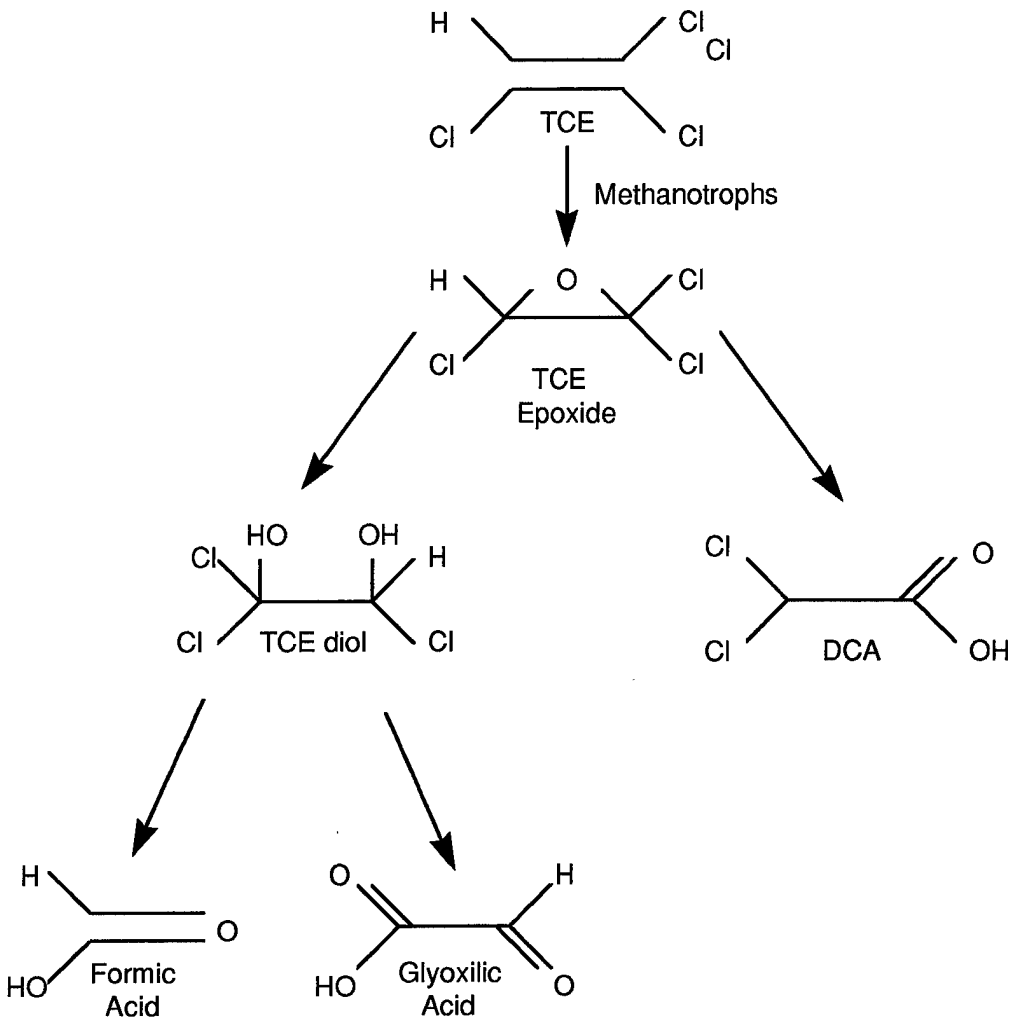

DCA - Dichloracetic Acid
Source: Anderson, 1991:24

Figure 2.10 Reductive Dechlorination Pathways of TCE Under Aerobic Conditions

Rhizosphere soils show a visible variation in cometabolic activity versus edaphosphere or nonrhizosphere soils, with TCE metabolizing much faster from rhizosphere soils in controlled experiments [Walton and others, 1990:1014]. Other experiments showed initial mineralization of TCE was 5-6.4% versus 1% in rhizosphere and edaphosphere soils, respectively, but over time the

edaphosphere soil mineralization caught up [Burken, November 1996:42]. TCE has also been found to degrade at extreme depths, up to 77' when present with a cometabolic substrate, in both saturated and unsaturated environments [Fuller, 1995:316-317].

In surface soils with plants and substrate, the metabolic rate or half-life for TCE is approximately 35 days at a soil TCE concentration of 1000 μg/L [Yagi, 1992:92]. Other studies show for TCE concentrations of 1 mg/L, .9 mg/L, and 1.1mg/L in the presence of an ammonia substrate in soil at 23 ^{o} C and a mixed microorganism culture, the half-life is 2 hours and at a higher concentration of 20 mg/L, the half-life drops to 10 days [Anderson, 1991:12-13]. Under similar conditions, but in the presence of glucose, and acetate, and a TCE concentration of 150mg/L, the half-life varies from 28 days to 58 days [Anderson, 1991:10]. In the presence of toluene, and a TCE concentration of 200 nM, the half-life is 4 days in ground water [Anderson, 1991:11].

Plant Metabolism of TCE

TCE transformation in eukaryotic systems has been investigated for several decades. The primary enzymes which oxidize TCE in mammals and yeasts is cytochrome P-450 [Nelson and others, 1993:29-30; Ensley, 1991:288]; reductive coupling by glutathione also reduces TCE [Hopkins, 1995:440]. These activities both produce mutagenic compounds in mammalian tissue [Henschler, 1990:526; Ensley, 1991:288]. Since both P-450 and glutathione are found in

plant tissue, it is plausible the same processes would take place or bear distinct similarities to the better understood mammalian metabolic pathways.

It is generally believed metabolism of xenobiotics proceeds in several phases: transformation of the contaminant, conjugation and compartmentalization, storage in storage sites, such as parenchyma cells, or metabolism or mineralization of the chemical to carbon dioxide and water [Sandermann, 1992:1; Schnoor and others, 1995:2]. Detoxification mechanisms may transform TCE to soluble conjugates, which are stored in the vacuole of cells or into insoluble conjugates, which are stored in the cell wall. Evidence of TCE plant metabolism and mineralization is supported by both experimental and theoretical considerations. Several investigations of TCE uptake by poplars have proven metabolism is predominant in the plants with a substantial portion binding irreversibly to plant tissue, specifically in the stem [Strand and others, 1995:605; Newman and others, 1997:1067; Gordon and others, 1997:7] (Table 2.2). It has also been established that plants can produce trichloroethanol, trichloroacetic acid, and dichloroacetic acid from TCE [U.S. DOE, 1994:15; Strand and others, 1995:605; Newman and others, 1997:1067; Gordon and others, 1997:7] (Figure 2.12). Recently, chloral hydrate was also found in poplar tissue [Gordon, 1997].

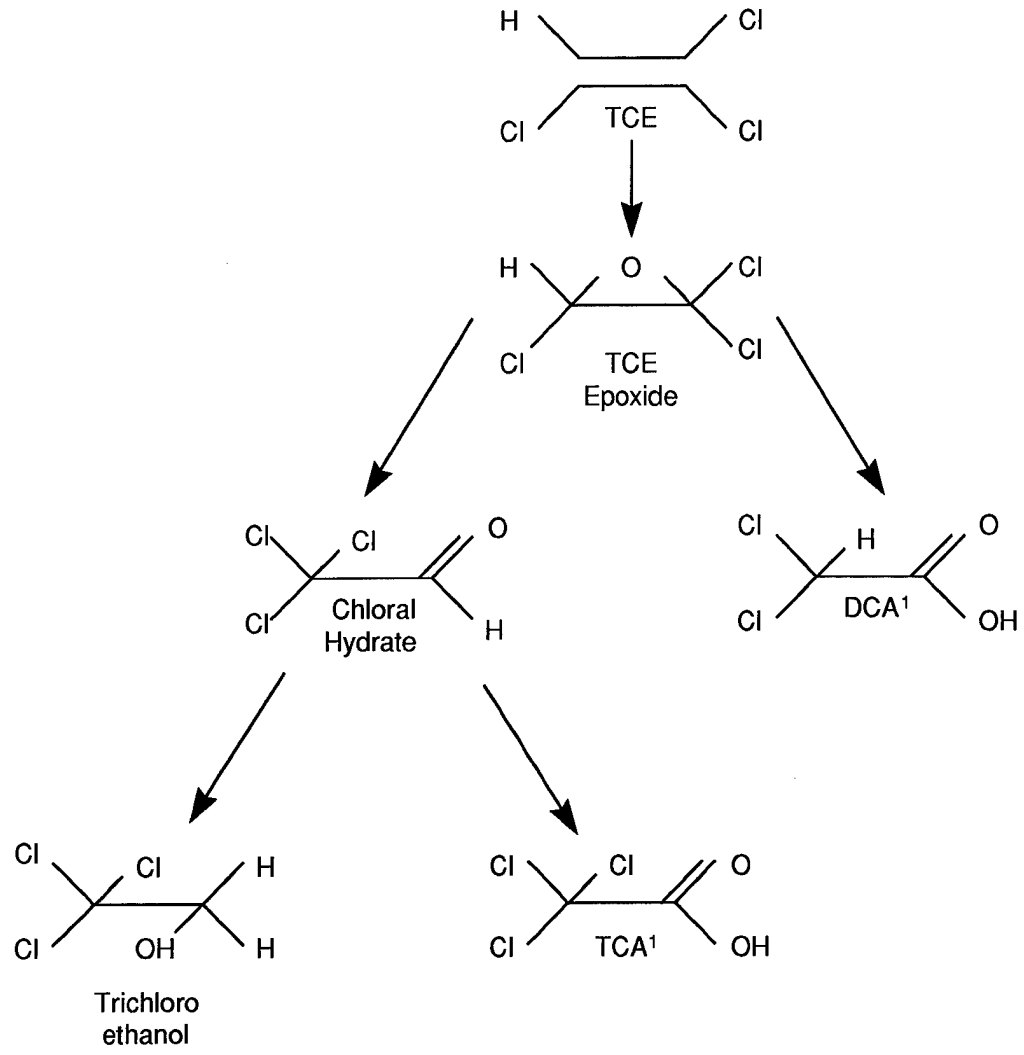

1 DCA - Dichloroacetic acid; TCA - Trichloroacetic acid
Source: Bruckner, 1989:31

Figure 2.11 Degradation Pathways of TCE in Plant Tissue

Growth of Poplars

As trees age they change physiologically and morphologically. Their photosynthetic rates decrease along with slower height and diameter rates of increase [Ryan and Yoder, 1997:241]. Since hydraulic resistance varies with path length and permeability of sapwood, as a tree grows the hydraulic

resistance increases, slowing the growth of the tree [Ryan and Yoder, 1997:238]. The forest industry has completed an incredible amount of research on stem growth and volume of production over time in softwoods. Most research has concentrated on poplar tree growth in the first few years [Sheikh, 1977:105; Sheikh, 1983: 220; Krinard, 1981:2; Stringer, 1987:74; Maisenhelder, 1970:300], but a number of researchers have completed studies over 10 to 30 years [Krinard, 1984,222; Krinard, December 1984:9; Krinard, 1985:3; Sharma, 1979:102]. These studies have analyzed varied growth with soil type, spacing, and geographic location. These studies showed poplars have rapid early diameter and height growth characteristics, with both peaking in the third or fourth year, regardless of tree spacing [Krinard, December 1984:9]. Growth in the first year varies from 1-4 m and from 10-20 years decreases to .8-2.0 m, with trees reaching a height in excess of 35 m. From these studies, various volume equations have been developed for stems, branches, bark, and leaves of poplars [Alan and Dawson, 1976:134; Alexander, 1976:407; Tingle and van Laar, 1977:14,19; Krinard, 1983:2; Krinard, 1988:1; Joshi and Pande, 1979:104; Tritton and Hornbeck, 1982:20]. These volume equations typically are based on diameter at base height (dbh) and height of the tree. The leaf volume equations are asymptotic, approaching a steady state with increasing age while the stem volume equations continually increase with age.

Much less research has been completed on root growth. It is known that high soil bulk densities severely impede root growth [Wild, 1988:133]. An

equation predicting the stump-taproot dry weight was found, relating volume to dbh. This equation increases continually with increasing age, but at a lower rate than the stem volume.

Studies of cottonwoods in clay and silty clay loam soils relating root volume to whole tree volume gave results ranging from 19-37.1%, for an average of 27.2% [Francis, 1985:3]. The higher value is typically seen in younger trees, and as the tree ages, the ratio decreases to the lower value. Ceuleman found *Populus deltoides* clone root to shoot (root to stem) ratios at .27 for the first year and .20 for the second year [1991:99]. Other authors state the root to shoot (root to stem) ratio varies from .34 to .42 [Heilman, 1994:1188]. By the sixth year in Populus deltoides, the root to shoot ratio is .25, approaching a constant ratio [Dickmann and Pregitzer, 1992:103].

Another area of debate is the mass of fine roots over time with respect to the whole phreatophytic root mass. Authors have found in studies of 2-year old *Populus deltoides* and *P. trichocarpa* that fine roots make up, on average, 6.8% of the root mass [Heilman, 1994:1188]. Most forest stands of mixed tree species report a value of 5%, regardless of age [Santantonio, 1989:57]. Other authors have found fine roots make up 40% of the total root in the second year [Friend and others, 1991:110] and 21-34% of the total root in 4-year old trees [Heilman 1994:1191]. Actual values of fine roots may be even higher, due to the difficulty in removing them from soil material.

Many experts also disagree on the growth characteristics of fine roots. Some authors state fine roots are primarily found in the top 1.5 feet of soil [Heilman, 1994:1191]. Researchers at Argon National Laboratory have found the same correlation, with fine roots decreasing in an inverse exponential rate with depth [Hinchman, 22 Aug 1997]. It should be pointed out though that in the first set of experiments the trees were surface irrigated near Seattle, Washington, an area of high annual rainfall. Dr. Gatliff, President of Applied Natural Sciences, stated in drier climates, the roots extend down into the capillary fringe with a mass of fine roots [24 Aug 1997]. Other authors substantiate a high amount of small roots and root hairs in proximity to the capillary fringe [Simon, 1996:11].

Populus roots are characterized by strongly developed horizontal roots, growing radially away from the taproot at depths of 5 to 20 cm below the soil surface, with vertical roots branching off of them, growing to a depth of 1 to 3 meters or more, depending on the phreatophyte in question [Dickmann and Stuart, 1983:98] (Fig 2.6). These roots grow in a linear relationship to height and can be found several tree lengths from the stem. The basal roots and tap roots continue to grow in diameter through secondary growth, increasing water transport capability [Zobel, 1991:65]. This type of development reduces the need for adventitious roots in most dicotyledonous species, yielding a mature root system which can be characterized as an expanded primary root system [Zobel, 1991:65]. In general, phreatophytes are also able to maintain their roots

in flooded anoxic conditions due to the vascular oxygen flow through the leaves, bark, and lenticels. There is some discussion though whether this is true in *Populus* trees. Some scientists feel there is no significant evidence of *Populus* extending its roots beyond the top of the capillary fringe [Licht, 1997]. Other scientists feel these trees will extend their roots into the capillary fringe and even 6-12" into the saturated zone [Ferro, 1997]. Greenhouse studies conclusively show Populus trees extend their fine roots into the saturated zone, but when exposed to TCE in the saturated zone, fine roots were nonexistent [Gordon, 1997].

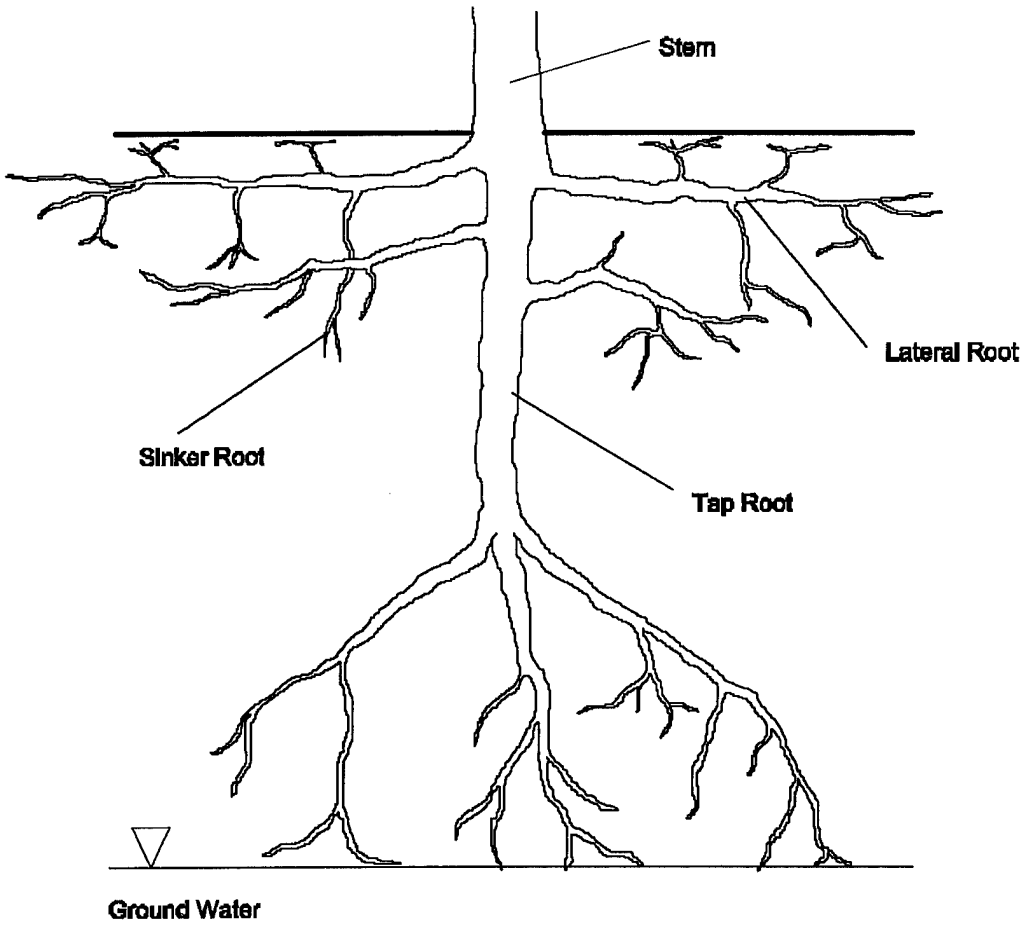

Adapted from Dickmann and Pregitzer, 1992:98

Figure 2.12 *Populus* Root Diagram

When initially planted as cuttings, which vary in length from 20 - 50 cm, approximately 15 - 40 cm is below ground [Dickman and Stuart, 1983:58]. One-year poplars have a reported root depth of 1.7 meters [Heilman, 1994:911]. Two-year poplars have a reported rooting depth of 3.35 to 4 meters [Tech Demo Plan, 1996:8-9; Simon, 1996:11]. Cottonwoods roots typically reach depths of 10 meters, when the ground water is at sufficient depth, and may even extend to 20 meters under optimal conditions [Gatliff, 14 Oct 1997].

Under favorable conditions, the life function of the root may continue through the winter. If the plant's roots are not exposed to freezing temperatures and drought in the winter season, then they will grow all year around [Simon, 1996:3].

Models

A review was accomplished of current models dealing with the movement of TCE in the soil column, rhizosphere interactions, TCE uptake, metabolism, translocation, and storage, tree growth, and TCE transpiration. The majority of models looked at the effects of TCE uptake; in all, eleven models looking at uptake were investigated. Most organic uptake models base their uptake on the transpiration stream concentration factor (TSCF), root concentration factor (RCF), and a stem concentration factor (SCF). These values were found by researchers studying the relationship between the K_{ow} and uptake of xenobiotics by barley plants [Briggs and others, 1982:495]. The TSCF is a ratio of the transpiration stream concentration of xenobiotic to the external soil concentration of xenobiotic. The RCF is the root concentration of xenobiotic to the external soil concentration of xenobiotic. The SCF is the stem concentration of xenobiotic to the external soil concentration of xenobiotic. All these relationships take on a linear form, so as the external soil concentration increases, the transpiration stream, root, and stem concentrations increase proportionally. In a natural system, xenobiotic plant contamination is a saturable

process that asymptotically approaches a saturation point. In the model developed by Briggs et. al., they assumed a constant external concentration, and once it goes to equilibrium, that it is independent of time and concentration. Other researchers found TSCF values on 27 compounds using 22 different species of plants [Polder, 1995:1618-1619]. In one test, 9 of 16 substances involved in the test deviated by more than a factor of five from Briggs' SCF values. Variability was also shown in the TSCF, with three values varying by more than five times those expected in Briggs' TSCF. Other tests suggested the equations do not work well for plants with woody roots; roots, like poplars, that have secondary growth [Briggs and others, 1982:501]. Numerous other models have used Briggs' equations, fitting Gaussian curves to data with a great deal of variability [Trapp and McFarlane, 1995:50]. These models show similar results to actual research experiments, but usually do not vary concentration and constrict their modeling time frame to 60-300 hours [Trapp and McFarlane, 1995:197; Trapp and others, 1994:415; Burken, 1996:960; Burken and Schnoor, 1997:1405]. Other models using the fugacity concept also have estimated the uptake of TCE over similar time frames [McFarlane and others, 1994:2263; Trapp and others, 1990:1248].

Another model investigated defines a plant as a set of compartments, separating the stem/branch sections and leaf clusters into their own respective compartments [Lindstrom, 1991:129]. This model is very complex, even for a very young plant with only a few branches and leaves, with 24 differential

equations and 24 unknowns. The final equation set takes on a matrix form, but the author does not present any results in the paper.

A model investigating the uptake, adsorption to root, and evapotranspiration of atrazine by plants was analyzed. This model also used the TSCF, but included a sink term to represent the contaminant lost from soil into the plant over time [Davis and others, 1993:68]. This model is extremely complicated, but still did not include biodegradation and assumed the root density was constant over the eight year time of study.

Volatilization of contaminants is another area of concern in the environment, so researchers have attempted to model this process. Two papers were analyzed which addressed the translocation to leaves and the diffusion process to the atmosphere [Trapp and Matthies, 1995:2333; Trapp and Matthies, 1997:71]. One used fugacity concepts and the other the TSCF to approximate flow to leaves through the xylem vascular system. Neither model allowed for variation in contaminant concentrations.

The rhizosphere is an extremely complicated system with much disagreement on how to exactly model its processes. Some models have only looked at the rhizoplane, discounting the rhizosphere under the assumption that microorganisms decrease rapidly within millimeters of the rhizoplane. Other modelers feel this planar relationship is not exact, so choose to include the entire rhizosphere. Another point of disagreement is on how to model microbial activity. Some models assume microbial activity is random, when instead it

tends to be clumped or discontinuous. Finally, most models to this date assume a constant microbial population [Curl and Truelove, 1986:246]., which in fact is not true, since the microorganisms primarily live off of rhizodeposition. As stated before, rhizodeposition consists of exudates, leakages, lysates, secretions, etc., which vary over a growing season since they are related to photosynthetic activity. One model investigated includes the rhizosphere and root growth as parameters [Newman, 1977:18]. They also consider two substrates for microorganisms, not only rhizodeposition but insoluble organic matter from the bulk soil. Michaelis-Menten kinetics estimates the transfer of substrate into microorganisms coupled with a doubling time of 3.5 hours for organisms. Assuming a rhizosphere of 1 mm in thickness, the author found the rhizoplane had extremely high counts of microorganisms, 1509 $\mu g/cm^3$, and at a distance of 1.8 mm, counts of microorganisms dropped to 2.2 $\mu g/cm^3$. This model did not include root hairs, due to the difficulty in modeling the rhizosphere around this complicated surface. It also did not include microbial migration, that substrate moves only by diffusion, that the substrate was the limiting factor for growth, and that rhizodeposition decreases as a plant ages. A comparison of actual data to model output showed the model slightly underestimated microorganism populations. Actual bacteria coverage is .3-9% and ectomycorrhizal coverage is .2-4% of root surface area, with similar colonization found in the tip, middle, and basal roots [Newman, 1977:43-44].

Another model, representing the growth of vesicular-arbuscular mycorrhizae (VAM), was investigated. This model used values of rate of infection by VAM, rate of increase in infection per unit length, the total length of root, the total length of infected root, and total infection units in the root [Walker and Smith, 1984:56]. The authors found VAM rate of infection greatest in new roots, which then dropped asymptotically to a lower value as main and lateral roots aged. In main roots, not only did the rate of infection decrease with age, but the rate of increase in infection per unit length dropped as well.

Several models also sought to replicate the movement of ground water and contaminants through the soil column [Tracy and others, 1989:608]. Two models looked at the saturated, capillary, and unsaturated zones [McCarthy and Johnson, 1993:1675; Narayanan, 1996:5]. These authors concluded that aqueous phase transport into the ground water was the primary transport pathway into the saturated zone and that vertical dispersion was related to molecular diffusion. At a groundwater velocity of .1 m/d a vertical dispersivity of .0005 m was calculated [McCarthy and Johnson, 1993:1678]. Both authors found TCE drops by nearly 3 orders of magnitude between the saturated and unsaturated zones in field studies. The majority of this decrease was in the upper portion of the capillary fringe. Narayanan quantified this further by showing TCE concentrations in the top vegetative layer is always less than 20% of TCE concentrations in the saturated zone. The authors then developed intricate three-dimensional equations, closely replicating their field studies.

The last model investigated is a whole tree model, called ECOPHYS, that models the growth of *Populus* during its first year [Host and others, 1990:1]. This model looks at processes of growth rather than relationships. A three-dimensional array simulates tree growth through leaf photosynthesis, leaf shading, leaf orientation, weather data, respiration, leaf, stem, and root dry weight, etc.. It also uses a saturable type equation for the carbon dioxide exchange rate. This model closely replicates growth of *Populus* at different locations throughout the country, within one standard deviation for two *Populus* clones, but has a drawback of only simulating juvenile tree development.

Site Conditions

The site conditions at Air Force Plant 4 near Fort Worth, TX, are highly conducive to phytoremediation. The climate is arid to humid with mild winters and hot, humid summers. The average annual precipitation is 31.5 inches, with the majority falling between April and October. The average annual temperature is 66 ^{o} F. July is the hottest month with an average monthly temperature of 86 ^{o} F, while January is the coldest month with an average monthly temperature of 45 ^{o} F. The average annual relative humidity is 63% and the average wind speed is 8 knots, primarily from the south.

The Terrace Alluvium Aquifer is the uppermost aquifer at the phytoremediation site at approximately 10-12 feet below grade. Recent excavation show this depth to vary from 2.5 to 3.3 meters in late summer,

[Hendrick, 1997:1]. The Terrace Alluvium Aquifer is approximately 3.5 feet thick, is an aerobic aquifer, and has hydraulic conductivities ranging from 10^{-6} to 10^{-1} centimeters per second [Tech Demo Plan, 1996:4-3]. Soils above the water table are composed of clayey sands/sandy clays that are underlain by clayey gravely sands [Tech Demo Plan, 1996:2-7]. The capillary fringe extends 18 inches to 36 inches above the saturated zone into this layer. Soil pH ranges from 7.6 to 8.7 in the phytoremediation area, which is in the optimal range for phytoremediation. Soil porosity ranges from 18.6-28.8% and organic content varies from 2-4.6%, with an average of 2.1% [MVTL, 1996; SAIC, 1996].

The concentrations of TCE at the phytoremediation site is approximately 230-970 ugm per liter and implementation of the phytoremediation process is not expected to interfere with the operations of Air Force Plant 4 or NAS Fort Worth [Tech Demo Plan, 1996:2-1 & 2-2].

Both whips and two year old trees were planted in the spring of 1996 at 8 feet spacing perpendicular to the plume flow (Fig 1.1) [Harvey, 1997]. Half of the trees planted were whips, the other, two year old trees. Each group, whips and trees, was planted in rectangular areas 250 feet by 50 feet. Growth of the whips in the first growing season was estimated as 6 to 12 feet and 8 to 10 feet each year thereafter. Total growth at year 10 is approximated at 50 feet and 7 inches diameter at breast height [Tech Demo Plan, 1996:8-6].

An existing mature cottonwood tree near the phytoremediation site shows the potential for phytoremediation. The uptake rate for this tree during the

summer months is between 300-350 gallons per day [Harvey, 1997:6]. The concentration of TCE under this mature cottonwood is about 80% less than concentrations anywhere else at the site [Lee, 1997:1].

III. Methodology

Overview

The modeling process itself proceeds through four stages; 1) conceptualization, 2) formulation, 3) testing, and 4) implementation [Randers, 1996:285]. It should be noted that this is an iterative process which requires modelers to return to earlier stages as they progress in their model construction. The following is a brief overview of each of these stages and what they entail.

In the first stage, conceptualization, the modeler becomes familiar with the topic and then defines the question to be addressed. Second, a reference mode which portrays the expected model behavior of key entities over a given time frame of interest is developed. Third, the system boundary and level of detail the structure will include is defined. Last, the modeler develops an influence diagram which represents significant cause and affect influences and entities in the system describing basic mechanisms.

After these steps, model formulation takes place. In this process, concepts are organized and the model structure is expanded to an acceptable level of detail while still closely replicating the reference mode. This level of detail is based on the amount of disaggregation the modeler needs to take to represent the system realistically, but still at a simplified level in comparison to the real world system This simplified representation captures the key influences

necessary for the particular system behavior being studied. Also, initial approximated parameters used in some entities are refined to better represent the dynamic system.

After the conceptualization and formulation stages, testing of the model takes place. This includes testing of the reference mode and assumptions. The reference mode is typically compared to the behavior of significant entities in the final model. If these two give similar results, it shows the model structure is replicating the initial perceived behavior. Also, assumptions on important variables, parameters, and relationships must be validated. If important variables are accurately included and parameters and relationships are of a reasonable nature, this further strengthens the reliability of the model structure. These values must be backed by other research, literature, expert opinion, or reasonable intuition to instill this confidence.

The last stage in the modeling process is implementation. This is where the model output is tested for realistic behavior in several validation scenarios as well as sensitivity to parameter minimum and maximum values. This is the stage where confidence is built into the usefulness of the model. Also, different scenarios are run against varying policies or characteristics of a location. Finally, insights gained through this process are translated and dispersed to the customer.

In this chapter I will cover the first three stages of the modeling process, conceptualization, formulation, and testing. I will also provide a discussion of

the implementation process in this chapter. In the following chapter I will produce results from the selected validation tests.

Conceptualization

Reference Mode. The reference mode is an initial estimation, through graphical or verbal representation, of the behavior of the system over a certain time frame of interest. This initial reference mode is then used to ascertain the reliability of the model output during each step in the iterative construction of the model; it is compared to the model output to ensure the model is behaving as expected. Since there was no historical data on TCE uptake over an extended time frame, a hypothesized reference mode was developed for this thesis. This reference mode was based on an initial understanding of the rhizosphere and phreatophytic tree and the expected uptake, translocation, storage, metabolism, and transpiration of TCE through this system. As the modeler's understanding of the system improved, the hypothesized reference mode went through iterative improvements. The hypothesized reference mode is shown in Figure 3.1.

Reference Mode

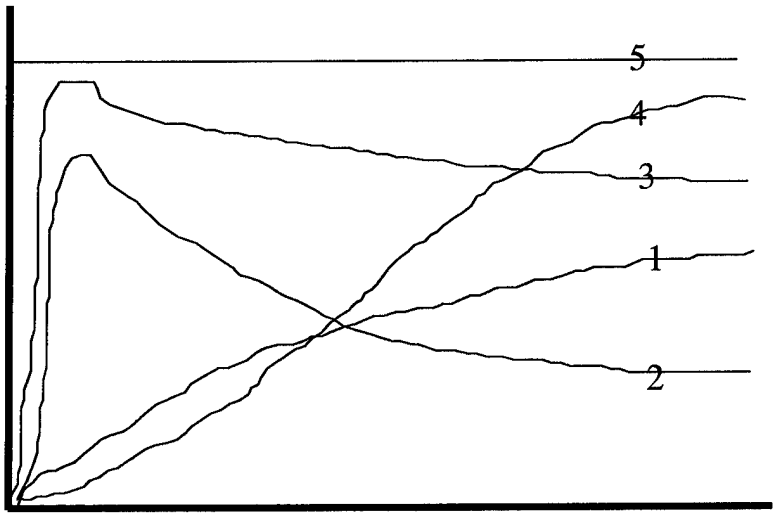

1 Leaf Conc 2 Stem Conc 3 Root Conc 4 Rhizo Conc 5 GW Conc

Figure 3.1 Hypothesized Reference Mode

The abscissa in Figure 3.1 is Time and the ordinate is Concentration for each compartment. The reference mode for this thesis does not show seasonal fluctuation, but instead was meant to represent the peak values seen each season. Also, the time frame for this reference mode was set at 50 years. This is the expected life span of a typical phreatophytic tree. Further explanation of the reference mode will occur under the Influence Diagram sub-heading.

Boundary. The boundary of this model was fairly straightforward in nature. To replicate the rhizosphere and phreatophytic tree and uptake and transpiration in these systems, the modeler sought to capture entities of primary importance in those two regions. This included various root, stem, and leaf compartments in the phreatophytic tree. The root was further separated into root hair zone and

secondary growth root compartments as well as portions of the root in the unsaturated zone and capillary fringe to give a better level of representation. The rhizosphere is a very complex system of interrelationships, but was given a simple level of detail to approximate the causal mechanisms in question.

Influence Diagram. The influence diagram ties in with the boundary analysis as a graphical tool to represent the entities and their interrelationships within the boundary of the system. Figure 3.2 is a high level representation of the influence diagram.

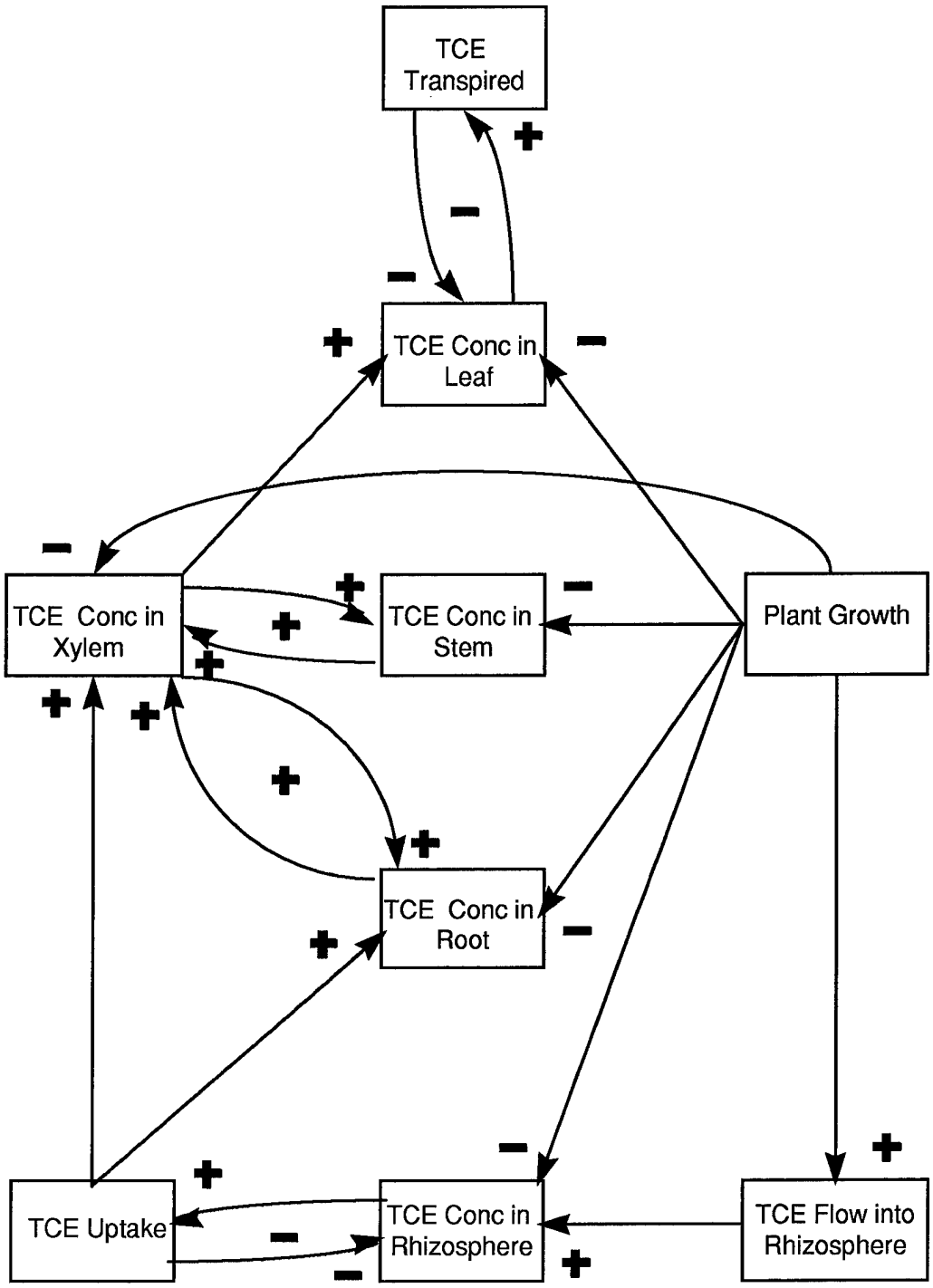

Figure 3.2 High Level Influence Diagram

This high level influence diagram does not capture all the entities and interrelationships of the final model, but gives the reader an overview of the model boundary and structure and its relation to the reference mode. The high level influence diagram shows the primary mechanisms for uptake and transpiration of TCE.

Influences from one entity to another are shown as arrows, with positive and negative influences depicted by plus and minus signs, respectively. For example, with an increase in Tree Growth the TCE Concentration in the Stem will decrease. This is a negative influence. Influences that form loops between entities also have a sign in their center which depicts the overall influence of the loop.

The following description ties the output from the reference mode (Figure 3.1) together with the interrelationships pictured in the high level influence diagram (Figure 3.2). The five lines portrayed in the reference mode are; 1) leaf, 2) stem, 3) root, 4) rhizosphere, and 5) ground water concentrations. Each respective line or compartment is discussed in order.

Initially in the leaf, the TCE mass will be lower than in the stem and root. This is because it is the final destination of the TCE xylem flow. The xylem first passes the root and stem apoplastic tissue, both of which remove contaminant from the xylem, causing the amount of TCE in the xylem to decrease as it passes up the phreatophytic tree. With increased TCE concentration in the xylem, the mass of TCE reaching the leaf compartment increases. The influence of TCE

Concentration in the Xylem is therefore a positive influence on the TCE Concentration in the Leaf. As TCE Concentration in the Leaf increases, TCE Transpiration will increase, resulting in a negative influence on the TCE in the leaf. TCE Transpiration will therefore balance the effects of TCE Concentration in the Xylem. The leaf volume increases over time, so Tree Growth will negatively influence TCE Concentration in the Leaf. With maturity, the volume of the leaf approaches an asymptotic or constant value. Taking these three factors into consideration, it is expected TCE Concentration in the Leaf will also approach a steady asymptotic value over time.

In the stem and root the majority of tissue is apoplast tissue; nonliving tissue which serves as structural support and as a storage media for the tree. As the amount of TCE in the xylem increases with uptake, the amount of TCE in these two compartments is expected to initially rise quickly as an equilibrium is reached and continue to rise over time as the amount of TCE in the xylem continually increases. This is the positive influence from the TCE Concentration in the Xylem to the TCE Concentration in the Stem and Root compartments. Also, as the TCE Concentrations in the Stem and Root increase, this will cause the TCE Concentration in the Xylem to increase. This is also a positive influence. Because of this reinforcing behavior, one would expect the stem and root concentrations to increase without bound. This does not occur due to the flow from the xylem, to the leaf, and ultimately TCE transpiration controlling the flow through the phreatophytic tree. This flow continually increases with growth,

forcing TCE through the plant over flow into the stem and root tissue. Therefore, the amount of TCE in the stem and root increases slowly over time.

Tree Growth is the sum of the leaf, stem, and root volumes which all increase over time. Therefore, Tree Growth has a negative influence on the TCE Concentration in the Stem and Root. The flow into the adjacent stem and root apoplastic tissue proceeds at a slower rate than the stem and root growth, so after reaching an initial equilibrium, the concentration in these two compartments is expected to decrease to a minimum value asymptotically with tree maturity.

Further discussion of the flow process into the stem and root compartments will be covered under the next section, Formulation.

The root also has a small proportion of storage tissue in the root hair zone or fine roots which comes into direct contact with the contaminant during TCE uptake. When contaminant is taken up by the fine roots it passes through the fine root tissue into the fine root xylem by mass flow. Because of this continual contact with the contaminant over time by the fine root tissue and also due to the secondary root's smaller cross-section with growth, the total root tissue TCE concentration does not decrease as fast as the stem apoplast tissue.

In the rhizosphere, the contaminant concentration is expected to initially increase rapidly, but approach an asymptotic value with tree maturity. As the TCE flow into the rhizosphere increases over time with tree growth, the amount of TCE inhibited from uptake by the tree will increase, based on the saturable

uptake process. Saturable uptake was used to represent the means of mass flow of contaminant into the plant and will be discussed in greater length later in this chapter. Due to the form of the saturable uptake equation, the amount of TCE inhibited from uptake will increase rapidly once the maximum uptake into the plant is reached. Therefore, as TCE Concentration in the Rhizosphere increases, TCE Uptake will increase, up to an asymptotic value, creating a positive influence from TCE Concentration in the Rhizosphere to TCE Uptake. In turn, a negative influence will develop from TCE Uptake to TCE Concentration in the Rhizosphere as TCE is removed from the rhizosphere. As the tree grows to maturity, TCE Flow into the Rhizosphere will increase, approaching an asymptotic value. This results in a positive influence on the TCE Concentration in the Rhizosphere. Also, as the tree grows to maturity, Tree Growth increases, approaching an asymptotic value. This increases the volume of the rhizosphere, which in turn decreases the TCE Concentration in the Rhizosphere. Taking all these influences into account, TCE Concentration in the Rhizosphere will increase rapidly in the first half of the phreatophytic tree life due to a small rhizosphere volume, a rapid flow increase into the rhizosphere, and the TCE Uptake rapidly reaching its maximum value. With tree maturity, TCE Concentration in the Rhizosphere will approach an asymptotic value as the TCE Flow into the Rhizosphere, Tree Growth, and TCE Uptake all approach asymptotic values.

For this model, it was assumed the ground water concentration of TCE would remain constant throughout the testing. TCE plumes typically bleed off of a concentrated dense nonaqueous phase liquid (DNAPL) source, providing a constant and persistent flow of TCE into adjacent ground water.

Formulation

Assumptions. The following are key assumptions used in the formulation of the model. These assumptions assisted in selection of the primary mechanisms of the model and to establish representation of the dynamic system.

- Soil and background atmosphere TCE concentrations remain constant throughout the modeling time frame
- TCE adsorption to soil particles in the rhizosphere is not considered
- Diffusion of TCE from the rhizosphere during seasonal uptake is considered minimal
- All TCE considered for uptake is in the aqueous form
- Phreatophytic tree roots extend to the ground water table
- TCE concentration in the capillary fringe is equivalent to the ground water concentration
- Initial plant compartments contain no TCE
- Each plant and rhizosphere compartment is a homogeneous unit with complete mixing

- Effects of metabolites are not considered in the phreatophytic tree or rhizosphere
- Phytotoxic affects of TCE on the plant are not considered
- Rhizosphere assumed continuous across all root surfaces
- Microbial populations and therefore cometabolism continuous across all root surfaces

Detailed Structure and Parameters. The ensuing discussion is devoted to the primary mechanisms used in the model. Explanations are given to support and defend the model structure and parameters. The complete model diagram and code are found in Appendix 1 and 2, respectively.

TCE Uptake. Plant uptake of solutes depends on plant, soil, and contaminant characteristics. Methods for predicting uptake should then account for these interactions. A great deal of research has been accomplished on plant uptake of solutes and is generally described through mathematical equations. When it comes to organic uptake, most researchers use the Transpiration Stream Concentration Factor (TSCF) as outlined in the literature review.

Authors state the movement of contaminants through the soil to the root occurs by diffusion and mass flow, with uptake depending on the concentration at the root surface [Barber and Claassen, 1975:358]. Since the mass flow into the plant root is inhibited by the casparian strip, a build up of contaminant around the root surface is expected.

In this model, the root uptake relation is described as a rate limiting or saturable process. That is, there is some theoretical maximum uptake the plant will approach as the contaminant concentration on the root surface continually increases. The saturable process is generally accepted for uptake of contaminants, but some researchers feel the uptake of TCE takes on a linear form, up to toxic levels. There is no conclusive evidence that the uptake of TCE takes on this linear form in plants, while saturable uptake of organic contaminants is found in numerous articles [Folsom, 1990:1280; Fox, 1990:6421; Nissen, 1991:488; Arciero, 1989:642].

The saturable uptake equation takes on the form:

$$\text{ContaminantUptake} = \frac{V_{max} \cdot C}{K_m + C} \qquad (1)$$

where V_{max} (mg TCE/kg plant-month) is the maximum uptake of contaminant by the tree over time, K_m (mg TCE/m3) is the concentration of TCE in the rhizosphere at which the contaminant uptake is half of V_{max}, and C (mg TCE/m3) is the concentration of TCE in the rhizosphere over time. This equation is then multiplied by the plant mass in kilograms to find the uptake mass of TCE over time. Figure 3.3 shows a typical saturable uptake curve with the values of V_{max} and K_m annotated on the graph.

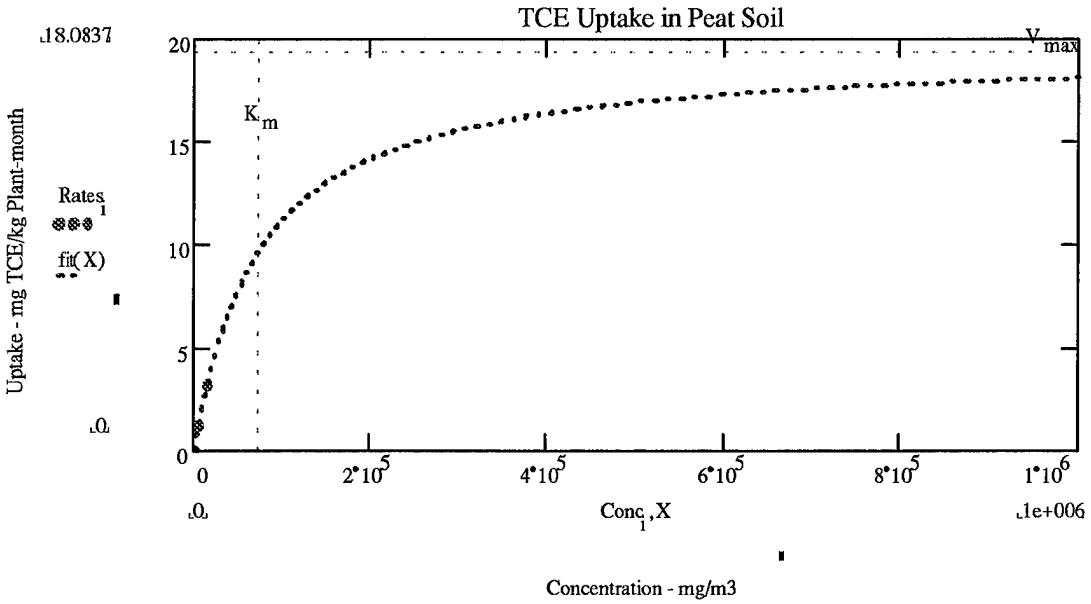

Figure 3.3 Typical Saturable Uptake Curve

To approximate the saturable equation, data was gathered from experimental research accomplished on phreatophytic whips grown in peat soil [Newman, 24 Jul 1997]. This information was used to identify data points on a graph whose abscissa is the rhizosphere TCE concentration and the ordinate is the contaminant uptake in units of mg TCE/(kg plant - month). Using a mathematical fitting program, an equation was developed to represent the graphical relation between TCE rhizosphere concentration and the subsequent TCE uptake into a phreatophytic tree (Figure 3.3). Detailed information on the formulation of the saturable curve can be found in Appendix 3.

Once the uptake curve was established, the weights of this uptake were identified between the secondary growth root and fine root. As covered in the Literature Review, researchers have found fine root ground water uptake varies from 2 to 70% of total uptake [Gatliff, 24 Aug 1997]. As an approximation, the

uptake weight by the fine root was assumed as 30% in the model. Breaking this down further, the secondary growth root and fine roots were differentiated between the unsaturated and capillary fringe soil horizons. The fine root ground water uptake of 30% was separated into 5% uptake in the unsaturated zone and the remainder in the capillary fringe. The secondary growth root ground water uptake of 70% was separated into 10% in the unsaturated zone and the remainder in the capillary fringe. This division of the weighting factors was based on discussions with experts in the field of root physiology and intuition of the uptake process. These weighted values also vary with the ratio of unsaturated soil depth to capillary fringe soil depth. The respective weighting factor is then multiplied by its rhizosphere compartment; 1) unsaturated fine root rhizosphere, 2) unsaturated secondary growth root rhizosphere, 3) capillary fringe fine root rhizosphere, and 4) capillary fringe secondary growth rhizosphere, to find the contaminant uptake in that portion of the phreatophytic tree.

Cometabolism. As covered in the literature review, the rhizosphere is the root soil interface where high numbers of microorganisms live in a symbiotic relationship with the phreatophytic tree. The root itself releases exudates, secretions, lysates through cell death, mucilage, and mucigel into the rhizosphere. Some of the exudates include phenolic substances which are proven primary substrates for microorganisms capable of releasing enzymes which degrade TCE. In the model, this cometabolic activity was represented by

a reaction rate equation [Masters, 1991:71] in the rhizosphere; the half-life was based on research in TCE contaminated soils with rice, lotus, and vegetable plants [Yagi, 1992:421]. The reaction rate equation takes on the form:

$$\text{Cometabolism} = \frac{\ln 2}{TCE_{\text{halflife}}} \cdot \text{TCEinRhizosphere} \qquad (2)$$

where the TCE half-life (months) or time for half the TCE in the rhizosphere to break down through cometabolism is approximated, through literature research, as 1.167 months and TCEinRhizosphere (mg TCE) is the mass of TCE in the rhizosphere. This gives an expression for the rate of TCE loss from the rhizosphere through cometabolism.

Rhizosphere. To approximate the rhizosphere and the various interactions taking place, a simplified approximation was required. The rhizosphere varies along a root surface due to the dynamic nature of its relationships. To approximate the rhizosphere volume, it was assumed the rhizosphere was continuous across all root surfaces. The surface area of the root was developed from the root volume graph, which was in turn based on the stem volume graph. Then using literature estimates of the rhizosphere thickness, 2 - 5mm, the rhizosphere volume was calculated with plant growth. Figure 3.4 depicts the volume of the secondary growth rhizosphere and fine root rhizosphere with tree growth. This output is at an average rhizosphere thickness of 3.5 mm. These curves were then copied into the model program to represent the rhizosphere volume over a 50 year time frame. Appendix 4 further outlines

the steps taken in establishing the secondary growth and fine root rhizosphere volumes.

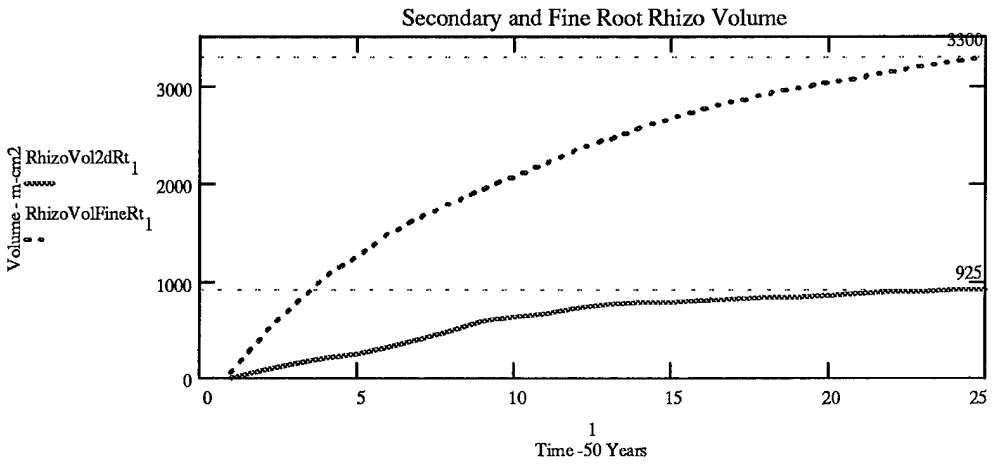

Figure 3.4 Rhizosphere Volume

The rhizosphere volumes asymptotically approach their maximum with tree growth. This behavior is due to the rapid increase in surface area of the root with growth. The value of 3300 m-cm^2 represents the secondary root rhizosphere volume at maturity and the value of 925 m-cm^2 represents the fine root rhizosphere volume at maturity. The fine root rhizosphere volume approaches a much higher volume due to the large surface area of the fine roots.

Vascular Flow. The xylem and phloem flow are based on literature which established both in relation to leaf area [McFarlane and other, 1981:93, Crank and others, 1981:32]. Since it is suggested the movement of contaminant through the plant is by mass flow [Bleckmann, 4 Sep 1997], the xylem flow drives the contaminant flow through the whole system, from the flow of TCE into the

rhizosphere to the flow into the leaves. The return vascular flow, or phloem flow, passes from the leaf to stem to root. The literature xylem flow rate is .019 mg/(m^3 leaf-month) and the phloem flow rate is .000162 mg/(m^3 leaf-month). A further description of these flow rates can be found in Appendix 5.

Plant Growth. Various literature was found which, through extensive experimental and statistical analysis, approximated phreatophytic tree growth using equations based on dbh and height [Ek and Dawson, 1978:134, Krinard, 1988:2 , Tritton and Hornbeck, 1982:20-21, Tingle and van Laar, 1977:14 , Francis, 1985:3]. Using this information, coupled with tree height and dbh data [Tingle and van Laar, 1977:21], curves were developed for phreatophytic tree growth over a 50 year time frame.

The leaf volume equation developed by Ek and Dawson is as follows:

$$\text{LeafVol} = \frac{.2243 \cdot \left(\frac{\text{dbh}}{2.54}\right)^{2.0892} \cdot (\text{H} \cdot 3.28083)^{-.17178}}{2.20462 \cdot 700 \cdot .05} \qquad (3)$$

where dbh (cm) is the diameter of the tree at breast height, H (m) is the height of the tree, 2.20462 (lb/kg) is a conversion factor, 700 (kg/m^3) is the leaf density, and 5% is the percent dry weight. These conversions are necessary since their original equation gives results in leaf dry weight (lbs). Figure 3.5 shows the output of this equation.

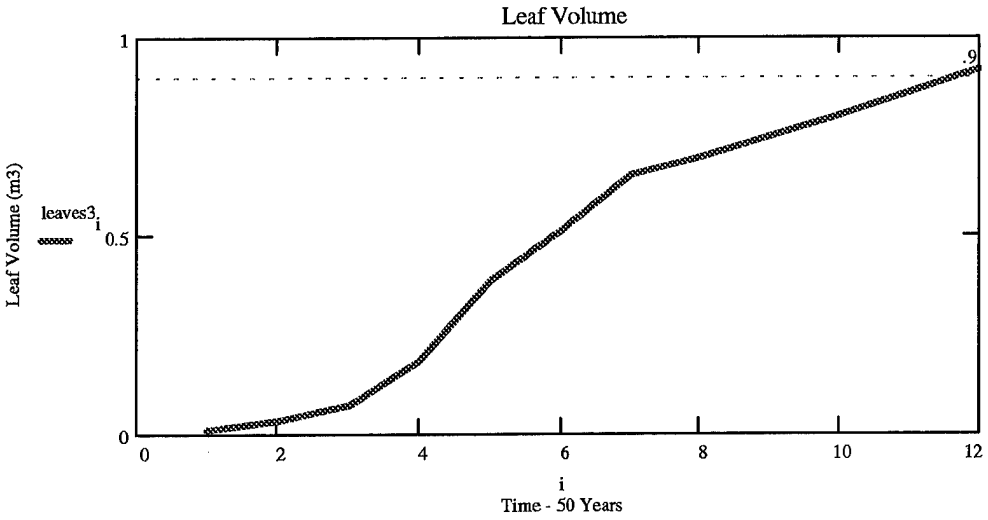

Figure 3.5 Leaf Volume

The leaf volume increases slowly at first, and once the tree is established, increases quickly. Upon reaching maturity, the leaf volume increase slows, ultimately it should approach a maximum volume at canopy closure.

The following three stem volume equations are from Tritton, Krinard, and Tingle, respectively:

$$StemVol1 = \frac{.1856 + .002074 \cdot \left(\frac{dbh}{2.54}\right)^2 \cdot H \cdot 3.28083}{35.147} \qquad (5)$$

$$StemVol2 = \frac{.00246 \cdot dbh^{1.84763} \cdot H^{1.7235}}{600} \qquad (6)$$

$$StemVol3 = \frac{.00231 \cdot \left(\frac{dbh}{2.54}\right)^{1.77593} \cdot (H \cdot 3.28083)^{1.11983}}{35.147} \qquad (7)$$

where dbh (cm) is the diameter at breast height, H (m) is the height of the tree, 35.147 (ft^3/m^3) is a conversion factor, and 600 (kg/m^3) is the stem density. Equations 5 and 7 give results in cubic feet, so the conversion factor from cubic feet to cubic meters is necessary. Equation 6 gives results in kilograms, so the result is divided by the stem density to convert the output to cubic meters. Figure 3.6 shows the results of all three of the stem volume equations.

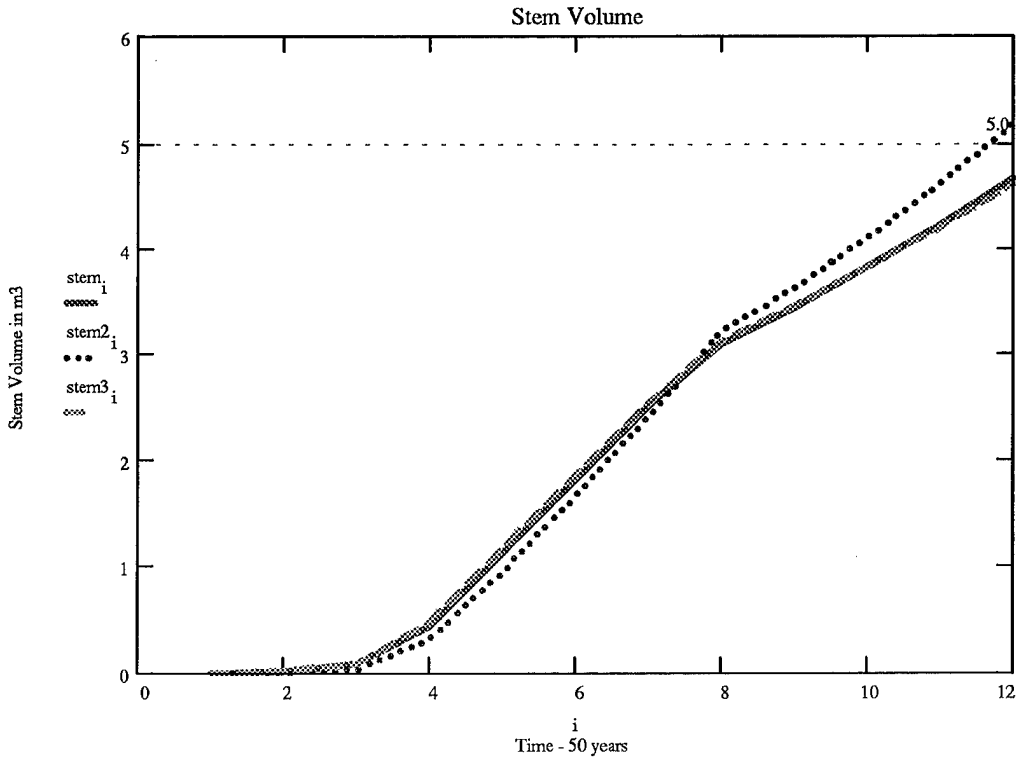

Figure 3.6 Stem Volume

Comparing Figure 3.6 to 3.5, the stem volume increases faster than the leaf volume, and continues to increase as the tree reaches maturity. This continual increase is due to the seasonal addition of growth rings about the stem and branch tissue.

The following root volume equation is from research by Francis:

$$\text{RootVol} = \frac{-17.386 + 1.328 \cdot \left(\frac{\text{dbh}}{2.54}\right)^{1.7}}{.125 \cdot 2.20462 \cdot (750 \cdot .93 + 1000 \cdot .07)} \qquad (8)$$

where dbh (cm) is diameter at breast height, 12.5% is the root dry weight, 2.20462 (lb/kg) is a conversion factor, 750 and 1000 are densities of the secondary and fine roots, and 93% and 7% are the approximate masses of secondary and fine roots. Equation 8 gives results in pounds dry weight, so the result is divided by the aforementioned conversion factors to transform the output to cubic meters.

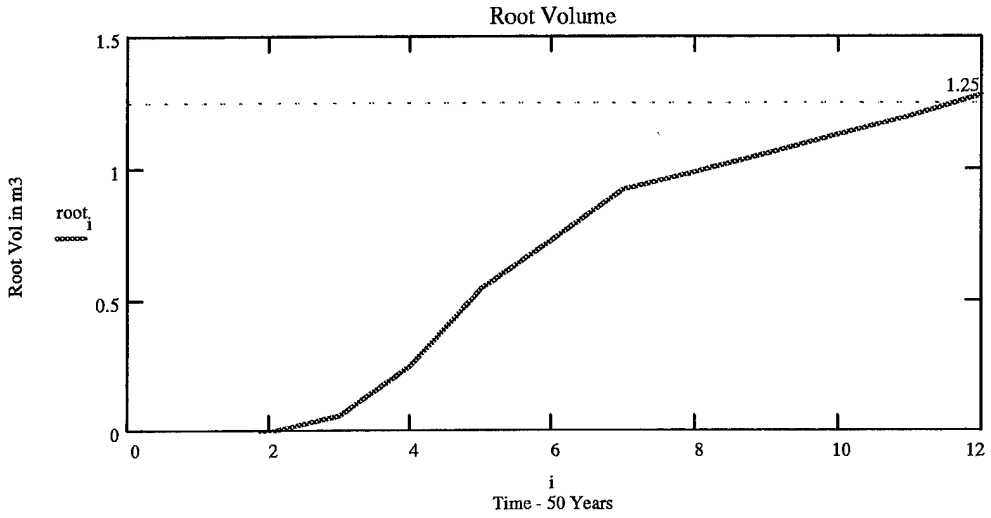

Figure 3.7 Root Volume

Comparing Figure 3.7 to Figures 3.6 and 3.5, the root volume increases faster than the leaf volume, but slower than the stem volume. With maturity, the root volume continues to increase, but not as fast as the stem volume, since secondary root growth proceeds at a slower rate than stem growth.

Appendix 6 further outlines the methodology used to approximate the leaf, stem, and root volumes.

The root, stem, and leaf volumes at maturity were calculated as 5, 1.25, and .9 cubic meter, respectively. The 5 cubic meter value closely corresponded to a mature stem volume given by Tingle and van Laar at a value of 4.75 m^3 for a tree 35 meters in height and 60 cm dbh [Tingle and van Laar, 1977:21]. Equations 4 through 8 were not developed for the complete life span of a tree; they do not represent the initial stage of growth or sapling stage accurately.

Because of this, they could not be directly used in the model. Instead, model graphs replicate their output over the known values and then volumes in the sapling stage were extrapolated. The extrapolation was based on stem sizes for whips and cuttings from which the root and leaf were then approximated. Since the stem equations from Tritton, Krinard, and Tingle all corresponded closely, there was a great deal of confidence in their output. Once the full stem curve was established in the model, the root volume was then checked against it.

Knowing roots make up approximately 40% of the root-stem mass in young trees and decreases to a constant value of approximately 25% by age six, an estimation was made of the root growth over time in relation to the stem volume. Given the mature stem volume is 5 cubic meters and the mature root volume is 1.25 cubic meters, the root to shoot ratio is then .25. This establishes the accuracy of the mature root volume. Also, to approximate the higher root to shoot ratio in the first 6 years, the root to stem ratio was started at .4 initially and stepped down to .25 by year six.

Since the vascular flow was in m3/(m2 leaf-month), the leaf area was required to estimate the flow. To find the leaf area the leaf volume was divided by an average leaf thickness to establish the surface area. According to Nobel, the typical leaf is 4 to 10 cells thick with a typical leaf cell 50 μm in thickness [1991:3,18]. Knowing tree leaves are on the thicker side, the leaf thickness was approximated as 10 cells or .05 cm thick. This gave a total leaf area at maturity of 1800 square meters, which closely corresponded to an expected area at

canopy closure of 2000 square meters [Harvey, 12 Jul 1997]. Figure 3.8 shows the leaf area with tree growth.

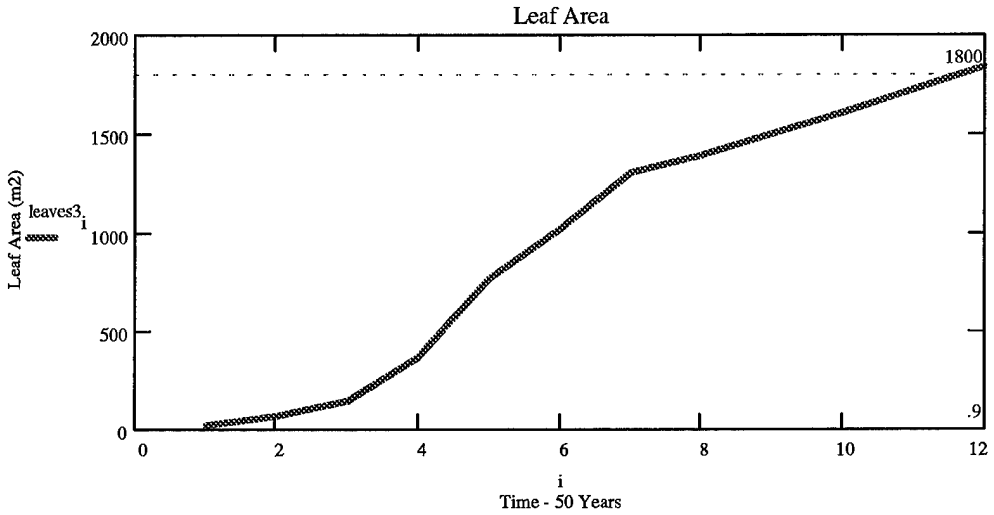

Figure 3.8 Leaf Area

Equation 4 was used to calculate the leaf area, with the addition of a value of .0005 meters in the denominator, which represented the thickness of a leaf. The same behavior was seen in this graph as in Figure 3.5.

Growth of the root network into the soil horizon proved a difficult undertaking. Estimates of fine root mass to total root volume vary from 5% to 40%. Actual values of fine roots may be even higher, due to the difficulty in removing them from soil material. As an estimate, it was assumed the fine roots made up 20% of the root mass and volume.

Many experts also disagree on the growth characteristics of fine roots. Some authors state fine roots are primarily found in the top 1.5 feet of soil while others state the roots extend down into the capillary fringe with a mass of fine

roots. The former research was in a humid environment with high rainfall, while the second statement was from a site with a moderate to dry climate. Since the model is for a moderate climate in Texas, it was assumed there would be a balance of fine roots found in both the capillary fringe and in the unsaturated zone.

The growth of the root through the soil horizons was also established. Known depths of roots at given tree ages were used to identify a curve of root depth with tree age.

The unsaturated soil, capillary fringe, and ground water depth are also input variables in the model. It is generally believed the roots extend to the ground water surface [Gatliff, 24 Aug 97, Hinchman, 22 Aug 97, Gordon, 17 Jun 97], so the model allows the roots to extend to this depth and no further. The ground water is assumed to remain at a constant level, so a yearly average is used. This provides the modeler the ability to vary each soil horizon parameter to a given site condition, soil type, and give a realistic representation of root growth in the soil horizon and subsequent uptake and transpiration.

Vascular Volume. To ensure the vascular flow and their concentrations were realistic, it was necessary to establish volumes for the vascular elements in the stem as well as in the different portions of the root. Using the known growth volumes of each compartment, the surface area of each was established, xylem and phloem thickness approximated, and then the vascular volume of the stem and root were found. The root compartment was then further broken down into

its four compartments to establish their individual vascular volumes. Figure 3.9 and 3.10 depict the curves developed from the analysis for the stem and total root vascular volume, respectively. Appendix 7 and 8 further outline the steps taken to approximate the stem and root vascular volumes.

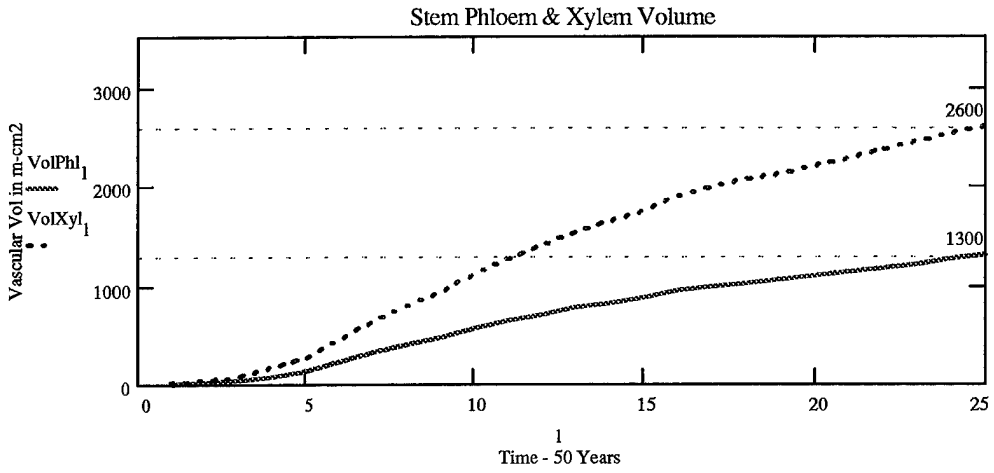

Figure 3.9 Stem Vascular Volume

The stem xylem volume at maturity was calculated as 2600 m-cm^2 and the stem phloem volume at maturity was calculated as 1300 m-cm^2. This curve produces similar behavior to the stem volume curve, but shows a more asymptotic behavior, due to the rapid increase in surface area over time. The total stem vascular volume was 7.8% of the total volume at maturity.

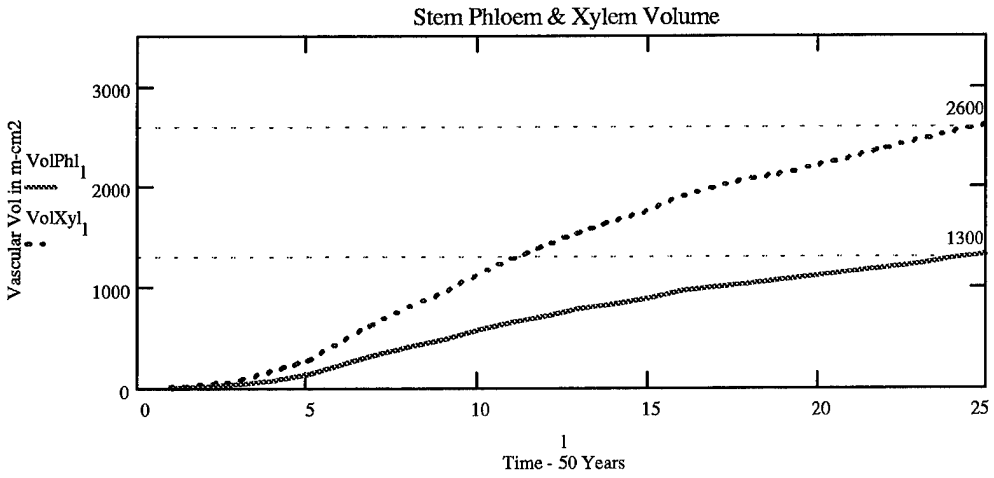

Figure 3.10 Root Vascular Volume

The root xylem volume at maturity was calculated as 1375 m-cm^2 and the stem phloem volume at maturity was calculated as 687.5 m-cm^2. Since there is more surface area in the root than the stem, the total vascular volume was expected to be higher in the root than in the stem. The total vascular volume makes up 16.5% of the root volume at maturity. The shape of the curve also changed, due to the effect of the rapid increase in the root surface area.

Flow/Gradient Equations. The flow of contaminants into the apoplast or nonliving stem and root tissue immediately adjacent to the xylem vascular members was represented by a flow equation, which in turn was based on a gradient equation and transfer rate coefficient. Once TCE flowed into these adjacent stem and root tissues, it was expected that diffusion would effectively distribute the TCE across all stem and root tissues. This was based on analysis of diffusion in an aqueous solution progressing faster than the incremental tree ring growth. Therefore, instead of a high concentration of TCE at the xylem

member and stem/root interface, a lower concentration of TCE at this interface was expected. Also, instead of a rapid decrease in TCE concentration as one progressed into the center of the tree, this decrease in concentration was much more gradual. Since the TCE gradient was low across the stem and root, it was assumed these compartments were homogeneously mixed, and therefore an average mass of TCE was assumed across the whole stem and root compartments. This resulted in an average concentration across these compartments. The variables in the following gradient equation took this assumption into account:

$$\text{Gradient} = \text{ConcY} \cdot K_{xy} - \text{ConcX} \qquad (9)$$

where ConcY (mg TCE/m^3) is the concentration in the xylem, K_{xy} is a dimensionless partition coefficient, and ConcY (mg TCE/m^3) is the average concentration in each tree compartment. The equation used to estimate the partition coefficient took on the form:

$$K_{xy} = \left(W_x + L_x \cdot K_{ow}^{\,b_x}\right) \cdot \frac{\rho_x}{\rho_y} \qquad (10)$$

where W_x is the water content in the x compartment, L_x is the lipid content in the x compartment, K_{ow} is the octanol-water coefficient of the contaminant, b_x is a coefficient for the x compartment, ρ_x is the density of the x compartment, and ρ_y is the density of the y compartment. These parameters were based on data from researchers [Dickmann, 8 Jul 1997; Gartner, 1995:126; Hendrick, 10 Jul 1997;

Nobel, 1991:423; Trapp, 1995:116-117]. Appendix 9 further outlines the equations used to establish the partition coefficients.

The gradient equation was then coupled with a transfer rate coefficient in the following equation:

$$Flow = \left(ConcY \cdot K_{xy} - ConcX\right) \cdot TransRateCoeff \qquad (11)$$

where K_{xy} is the result of equation 10, ConcY and ConcX (mg/m3) are the concentrations in the respective compartments of the plant from equation 9, and TransRateCoeff (m^3/month) is the transfer rate coefficient establishing the flow rate from one compartment to the other.

Transfer rate coefficients were estimated through intuition and a progressive understanding of the model structure and expected behavior.

Plant Metabolism. Phreatophytic trees actively metabolize TCE into its metabolites. Current research shows this metabolic rate is highest in the leaves, somewhat lower in the root, and very low in the stem [Newman, 23 Jul 1997]. According to other researchers, the half-life of TCE in the leaves of plants is approximately 2 days [Trapp, Stefan, from thesis by Capt Roy-Alan Augustin, 1994:43]. With this background knowledge, half-lives of TCE were established in individual compartments, and then using a reaction rate equation [Masters, 1991:71], the TCE metabolic rate for each compartment was established. The reaction rate equation takes on the form:

$$Metabolism = \frac{ln2}{TCE_{halflife}} \cdot TCEinPlant \qquad (12)$$

where the TCE half-life (months) or time for half the TCE in the plant compartment to break down through metabolism is approximated as 0.0667 months in the leaf, 1 month in the stem, and .5 months in the root. TCEinPlant (mg TCE) is the mass of TCE in the respective plant compartment. This gives an expression for the rate of TCE loss from the various plant compartments through metabolism.

Selection of Parameters. An integral part of formulation is refinement and selection of parameters for the model. Table 3.1 and 3.2 portray all the literature and soft parameters used in this model, their source, the value of each parameter, and if available, the minimum and maximum values found in literature or expected through intuition, research, and expert analysis.

LITERATURE PARAMETERS			
Variable	**Source**	**Value**	**Min/Max Value**
Rhizosphere TCE Half Life	Yagi, 1992	1.167 months	.33-1.93 months
Leaf Air Partition Coefficient	Burken, 1996	4.1	
TCE Air Concentration	ATSDR, 1989	.0205 ppb	.011-.03 ppb
Leaf Partition Coefficient	Trapp & McFarlane, 1995 - Appendix 9	0.549	
Xylem Flow Rate/Leaf Area	Crank, 1991	.019 m3/m2 leaf-month	.0065-.032 m3/m2 leaf-month
Phloem Flow Rate/Leaf Area	Crank, 1991	.000162 m3/m2 leaf-month	
Leaf Density	Nobel, 1991	700 kg/m3	
Stem Partition Coefficient	Trapp & McFarlane, 1995 - Appendix 9	0.43	
Secondary Growth Root to Fine Root Ratio	Hielmann, 1994; Friend, 1991	80%	60-95%
Secondary Growth Root Partition Coefficient	Trapp & McFarlane, 1995 - Appendix 9	0.68	
Fine Root Partition Coefficient	Trapp & McFarlane 1995 - Appendix 9	0.923	
Secondary Growth Root Flow Weight	Gatliff, 1997	70%	30-98%
Fine Root Flow Weight	Gatliff, 1997	30%	2-70%
Rhizosphere Thickness	Schmidt, 1991	.35 cm	.2-.5 cm
V_{max}	Newman, 1997 - Appendix 3	20 mg TCE/kg plant-month	
K_m	Newman, 1997 - Appendix 3	75,000 mg TCE/m3	
Capillary Fringe Soil Thickness @ AF Plant 4	Tech Demo Plan, 1996	0.605 cm	.45-.76 cm
TCE Concentration in GW @ AF Plant 4	Tech Demo Plan, 1996	605 ppb	240-970 ppb
Depth to GW @ AF Plant 4	Tech Demo Plan, 1996	3.3 m	3.05-3.65 m

Table 3.1 Literature Parameters

SOFT PARAMETERS			
Parameter	**Source**	**Value**	**Min/Max Value**
Leaf Vascular Ratio	Bleckmann, 1997	5%	
Leaf Air Transfer Rate Coefficient	[1]	1 m3/month	
Leaf TCE Half Life	Augustin, 1994; Newman, 1997	0.0667 month	
Stem Xylem Transfer Rate Coefficient	[1]	0.05 m3/month	
Phloem Xylem Transfer Rate Coefficient	Nobel, 1991	0.001 m3/month	
Stem Density	Hendrick, 1997; Dickmann, 1997	600 kg/m3	
Stem TCE Half Life	Newman, 1997	1 month	
Root TCE Half Life	Newman, 1997	.5 months	
Root Xylem Transfer Rate Coefficient	[1]	0.04 m3/month	
Fine Root Tissue Volume Coefficient	Bleckmann, 1997	30%	20-40%
Fine Root to Fine Root Xylem Ratio	Appendix 7	13.30%	6.67-20%
Secondary Growth Root Tissue Volume Coefficient	Bleckmann, 1997	30%	20-40%
Secondary Growth Root Density	Dickmann, 1997; Hendrick, 1997	750 kg/m3	
Fine Root Density	Source Unknown	1000 kg/m3	
Rhizosphere Flow Coefficient	[1]	.001 m3/month	

[1] Values developed through intuition and progressive development and analysis of model structure.

Table 3.2 Soft Parameters

An explanation of the testing and validation methods employed to verify these parameters follows. Actual output and discussion of the parameters can be found in Chapter IV, Results and Discussion.

Testing and Implementation

Under testing and implementation, the model is tested or compared to intuitive or experimental evidence to strengthen or refute the reliability of the model. It will include comparing the model structure to similar real world systems and model output to actual system behavior. Since absolute correctness of the model to reality is not feasible, various tests are run to validate the system dynamics model. An individual test does not prove or disprove the model, but instead builds confidence in it. Through a series of these validation tests, the confidence in the model's usefulness and soundness is established. After the model reaches this state of confidence, it is then disseminated to potential interested parties for application. In the following sections, the reference mode is compared to model output, a description is made of the parameters which require sensitivity testing, and a description of the validation tests themselves takes place.

Reference Mode Comparison. With the reference mode previously shown (Figure 3.1) and discussed, the final model output can now be compared against it as a reliability test. The reference mode comparison is shown in Figure 3.11.

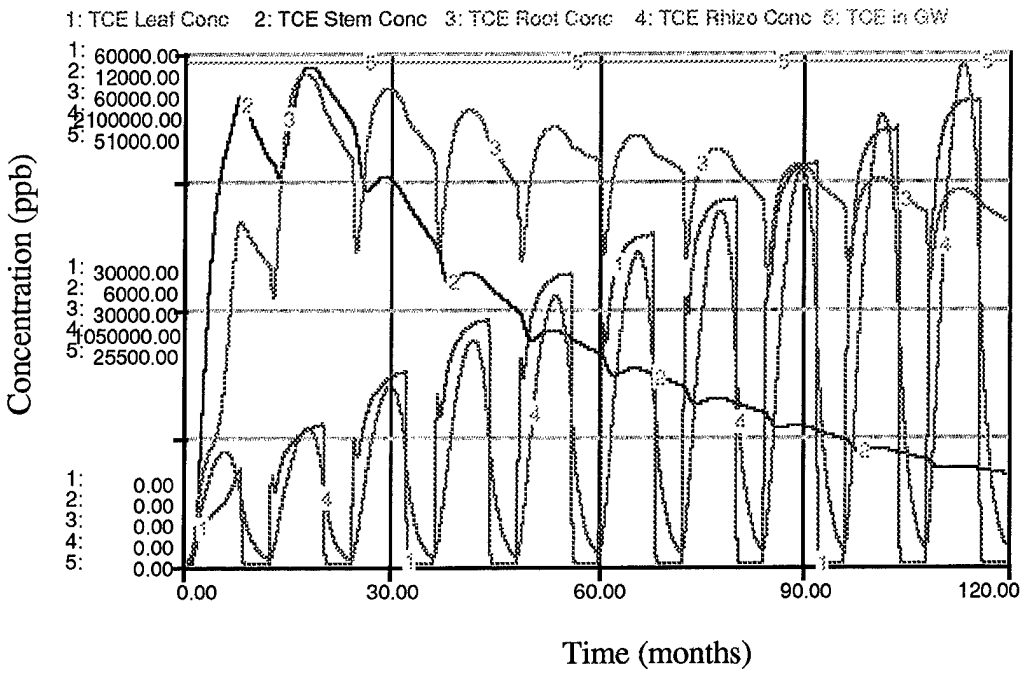

Figure 3.11 Reference Mode Comparison

The output of this graph closely corresponds to the reference mode. The abscissa of this graph is time in months, for a total of 120 months or 10 years. Because of this, only the first portion of the 50 year reference mode is compared to this output. The 10 year time frame was selected since the harvest time of a short rotation woody crop is typically seven years. The fluctuation of the output is due to the seasonal growth of the phreatophytic tree. The peaks signify the hottest part of the summer months when ground water and therefore, TCE uptake, are the greatest. The troughs in the rhizosphere represent the winter months, when the trees are dormant and TCE diffuses back into the ground water. Also, at the beginning of the dormant months, the TCE in the leaves disappear as the leaves senesce in the fall. Finally, the stem and root concentrations show a slight decrease in the spring when uptake is first initiated

and the TCE concentration is lower in the xylem than in the stem and root compartments. This causes a flow to take place out of the stem and root compartments into the xylem.

The ordinate shows concentrations in each compartment; 1) Leaf Concentration, 2) Stem Concentration, 3) Root Concentration, 4) Rhizosphere Concentration, and 5) Ground Water Concentration. All concentrations are in mg/m^3 or ppb. As expected, the leaf concentration is slowly reaching a steady asymptotic value. Both the stem and root concentrations show an initial increase and then decrease with time, with the stem decreasing more than the root due to its larger volume. The rhizosphere concentration is increasing almost at a linear rate, and with tree maturity, will eventually approach a maximum value. Finally, the ground water concentration is constant as a given parameter.

Parameters Requiring Testing and Sensitivity Analysis. All parameters in Tables 3.1 and 3.2 require analysis, since they influence either the uptake or transpiration of TCE from the system. Some parameters, such as leaf, stem, and root density; stem and root partition coefficients; and stem and root transfer rate coefficients, will be combined under sensitivity testing to simplify this testing and because they do not directly impact the uptake and transpiration of TCE in the phreatophytic tree. Sensitivity of parameters without known minimum and maximum values necessitate an approximation. For literature values lacking extremes in Table 3.1, 50% and 150% of the known value will give the approximate minimum and maximum values for analysis. For values in Table 3.2

lacking extreme values, approximated extremes will vary. For those soft parameters which are based on expert opinion, extremes will vary by a factor of five from the estimated average. This will more than cover plausible values for these parameters while still producing realistic output. For those soft parameters which are based on intuition, extremes will vary by a factor of 10 from the estimated average. The wider variation is due to the tentative value of these parameters. Also, five values will be selected in the sensitivity analysis on all parameters. This will give a good representation of the variation of output as one departs from an expected or average value.

Validation Tests. There are numerous validation tests, with at least 17 identified by Forrester and Senge [1980:209-227]. Though carrying out all these tests greatly validates a model, all are not always applicable to a given situation. Forrester and Senge identify a core of tests for system dynamics which were modified for application to this thesis model [1980:226-227]. Some additional tests were also added to further validate the model. The tests used to validate this model are as follows:

I. Tests of Model Structure
    a. Structural Verification
    b. Parameter Verification
    c. Extreme Conditions
    d. Boundary Adequacy
    e. Dimensional Consistency

II. Tests of Model Behavior

a. Behavior Reproduction

b. Behavior Anomaly

c. Behavior Sensitivity

d. Soft Parameter Sensitivity

e. Changed-Behavior Prediction

III. Other Validation Tests

a. Test of Site Parameters

b. Comparison to Real World Data

The following is a description of each of the 12 tests which will serve to validate this thesis model.

Tests of Model Structure.

Structure Verification. In this validation test, the structure of the model is compared to the real system. To gain confidence in the model using this test, the model structure must coincide with the structure of the real-world system. Verification may include review of the model by experts in the field in which the model pertains and through descriptions found in pertinent literature.

Parameter Verification. This entails verifying parameters against observations of real life or through experimentation and research of real life mechanisms. Parameter verification can take two forms, conceptual and numerical. In conceptual parameter verification, parameters are investigated to see if they actually exist and if they match elements of the real system. In

numerical parameter verification, assumed parameters are investigated to ensure they fall within a reasonable range of the real system.

Under conceptual parameter verification analysis of the parameters obtained through literature will take place and under numerical parameter verification analysis of soft parameters will take place.

Extreme Conditions. Extreme conditions in a model may reveal inconsistencies not realized through typical parameter inputs. By correcting these inconsistencies, an improved model in the normal operating region is realized. There are two reasons for development of these inconsistencies in a model. First, flaws in model structure may develop in extreme conditions which can pinpoint structural weakness. Second, extreme conditions force the system to operate outside existing but possible regions of behavior.

Not only were all the variables in Table 3.1 and 3.2 analyzed for this test, but other influences to the model as well. Extreme conditions of ground water concentration, ground water depth, unsaturated soil depth, time, V_{max}, and K_m were considered for this test. The first three variables were deemed essential for this test since soil horizons may vary a great deal between sites and even within a site. Therefore, these extremes require testing to ensure model output at any potential site.

The model currently is modeling uptake and transpiration over a 10 year time frame. There is a potential for longer studies, so the time of analysis will be increased to test its influence.

The values of V_{max} and K_m greatly influence the uptake and transpiration in a phreatophytic tree. Coupled with the fact that the V_{max} and K_m values were extrapolated from only three data points, their accuracy is not supported with a great deal of confidence. By testing their extremes, a better understanding of their influence on the system is anticipated.

Boundary Adequacy. This test looks at the level of aggregation of the model and whether it is appropriate and if all the associated model structure is included. If the necessary structure is represented, the model serves its purpose. This does not mean the model structure should necessarily represent the whole real-world system, but that it gives a representation of elements coincident with the model purpose.

Dimensional-Consistency. The dimensional-consistency test considers the reliability of model rate equations. If rate equations have a scaling factor or some factor with no real-life corresponding value, the model fails this test [Forrester and Senge, 1980:215].

Parmeters considered under this test will include those used in rate equations which affect the uptake and transpiration of TCE. This will include all transfer coefficients, partition rates, and ratios.

Tests of Model Behavior.

Behavior Anomaly. When the model produces unrealistic output, this is an indication of an anomaly in the model. Usually, these anomalies are found during model construction, but may develop during model validation.

Also, behavior anomaly testing builds confidence in soft parameters or assumed parameters. If unrealistic behavior is produced when the soft parameter is altered beyond its expected bounds, confidence is built in the accuracy of the assumed parameter bounds [Forrester and Senge, 1980:220].

This test was used frequently in the model construction phase. Anomalous behavior found included; fine root tissue concentrations due to the use of gradients over flows, the use of conductance equations over transpiration gradients, compartment flows not correctly related in parallel or in series, fine root and secondary growth root volumes not accurately related, and uptake into different root compartments not accurately established.

Working through the final model, several instances of anomalous behavior were discovered. There output will appear in the following results and discussion chapter. Since the anomalous behavior test also has the potential to increase confidence in soft parameters, Table 3.2 was analyzed for parameters which have potential for this test. The parameters were selected on the basis of greatest expected influence on uptake and transpiration in the model. They were also selected based on the degree of confidence in their values. Parameters selected include all transfer rates, the root hair volume coefficient, and the secondary growth tissue volume coefficient.

Behavior Sensitivity. Sensitivity tests are one of the more important tests run on a model. By running the model through maximum and minimum plausible extremes of a parameter, reliability of the model is improved.

This test also serves to indicate parameters to which the model is sensitive. If the real world system is sensitive and insensitive to the same parameters as the model, it builds confidence in the structure and behavior of the model. Also, if the model is sensitive to a parameter, future research has a focus for parameter and model improvement.

This test will cover all literature parameters in Table 3.1 except those covered under the extreme conditions test and the site parameter test. As stated before, some aggregation or combination of parameters which do not directly influence TCE uptake and transpiration will take place.

Soft Parameter Sensitivity. This test reveals the influence of soft or assumed parameters on the behavior of the model. If these uncertain parameters greatly influence the model output, the inherent risk of implementing this model at a potential site increases; cumulative TCE uptake and transpiration values may vary to such an extent that they may not give an accurate representation at a site.

This test will cover all literature parameters in Table 3.2. Some aggregation or combination of parameters which do not directly influence TCE uptake and transpiration will take place.

Changed-Behavior Prediction. If the model produces realistic output under different scenarios confidence is built in the model. There are two ways of accomplishing this test. First, by changing the scenario of the model and verifying the model behavior under these different scenarios. Second, by

comparing differing scenarios to real life output. If the model behavioral changes correspond to real life behavioral changes, confidence is built in the model representation. Since there is no variation in real life data, analysis under this test will consist of verifying the plausibility of model behavior under different scenarios. This test considers whether the model is able to generate more than one mode of behavior.

The model will portray different uptake and transpiration modes of behavior with changes in characteristics of the TCE concentration in ground water, unsaturated/capillary fringe soil horizon, and depth to ground water. All other parameters in the model increase or decrease the level of model output, but still give the same mode of behavior. The following is a description of the expected changed modes of behavior for the TCE concentration in ground water, unsaturated/capillary fringe soil horizon, and depth to ground water.

With the ground water TCE concentration set to zero, the TCE uptake by the tree will be nonexistent. Therefore, the only source of TCE will be from the TCE air background concentration. TCE transpiration from the phreatophytic leaves will then be reversed, as the tree takes up TCE from the air background concentration. At the other extreme, the ground water TCE concentration will be set to 100 ppm. In this scenario, the TCE uptake and transpiration by the phreatophytic tree will be dramatic. Figures 4.1 and 4.2 depict the two extremes of TCE ground water concentration.

When the unsaturated soil layer is not present, roots will immediately grow into the capillary fringe, where the TCE aqueous concentration is high. This will dramatically affect the uptake initially and over time. As the unsaturated soil layer increases, the roots will take longer to reach the capillary fringe, thus delaying the rapid TCE uptake. Also, a larger portion of the root will exist in the unsaturated soil as this layer increases in depth. Because the TCE aqueous concentration is lower in the unsaturated soil, TCE uptake will not reach as high a value over time with increased unsaturated soil depth. Figures 4.3 and 4.4 depict this change in behavior. Extremes of ground water depth are expected to give similar output, since all these parameters are interrelated.

Additional Validity Tests.

Test of Site Parameters. Soil and ground water conditions at Air Force Plant 4 show variability. This includes the depth to the ground water, the thickness of the capillary fringe, the thickness of the unsaturated zone, and TCE concentration in the ground water. This test will serve to establish the influence each of these parameters has on the uptake of TCE by a phreatophytic tree at Air Force Plant 4.

Comparison to Real World Data. This validation test will compare actual data from a research project against the model output. Washington State University recently completed greenhouse studies on *Populus* hybrids. This experiment was run over an eight month time frame on cuttings planted in 90 centimeters of soil and exposed to 50 ppm of TCE. By inputting

their parameters into the model and comparing them to the research results, the model output will give a good indication of the model's accuracy and reliability.

IV. Results and Discussion

In this chapter the results of the validation tests presented in Chapter III will be presented along with a discussion of these results.

Testing and Implementation

Validation Tests.

Tests of Model Structure.

Structure Verification. In this validation test, the structure of the model was compared to the real system. First this was accomplished by improving the modeler's knowledge of the system through literature review, pertinent classes, and discussion with experts on plant physiology, contaminant uptake, and other phreatophyte and rhizosphere processes. This was further augmented by analysis of the model by committee members during committee meetings and during individual discussions.

The stocks portrayed in the model, including; leaf, stem, root, and rhizosphere compartments, are all found in the real-world. This includes the separate root and rhizosphere compartments in the various soil horizons and the differentiation of the root into fine root and secondary root zones. Also, the representation of the vascular elements, their flow patterns, and the compartments to which they come into contact replicate an actual phreatophytic tree. Though some aggregation took place, the basic structure of the

rhizosphere and phreatophytic tree received a level of representation necessary to model uptake and transpiration of TCE over the time frame of a short rotation woody crop. Through additional validation tests and comparison to real world data, confidence in the reliability of the model structure was established.

Parameter Verification. Parameters outlined in Table 3.1 exist in the natural system or are part of mechanistically based equations which, through research and experimentation, were found to closely replicate real-world behavior. Also, all these parameters fall within the range of real-world parameters as reported in literature, and are typically taken as their average. All these values will be further analyzed under behavior sensitivity analysis.

Parameters outlined in Table 3.2 are soft parameters and exist in the real world system or represent actual influences of a real-world behavior. All soft parameters are supported by professional opinion or intuition, are based on literature variables and equations through research, or are established through intuition and progressive development and analysis of model structure. All these values will be further analyzed under soft parameter sensitivity analysis.

Extreme Conditions. Tests run under this section are extremes of TCE concentrations in ground water, ground water depth, unsaturated soil depth, time, V_{max}, and K_m. Unless otherwise noted, the ground water depth in all these scenarios is 3.3 meters and the capillary fringe is 0.605 meters. These are the average values at AF Plant 4. Figures 4.1 and 4.2 show extremes of TCE concentrations in ground water and their affect on uptake and transpiration.

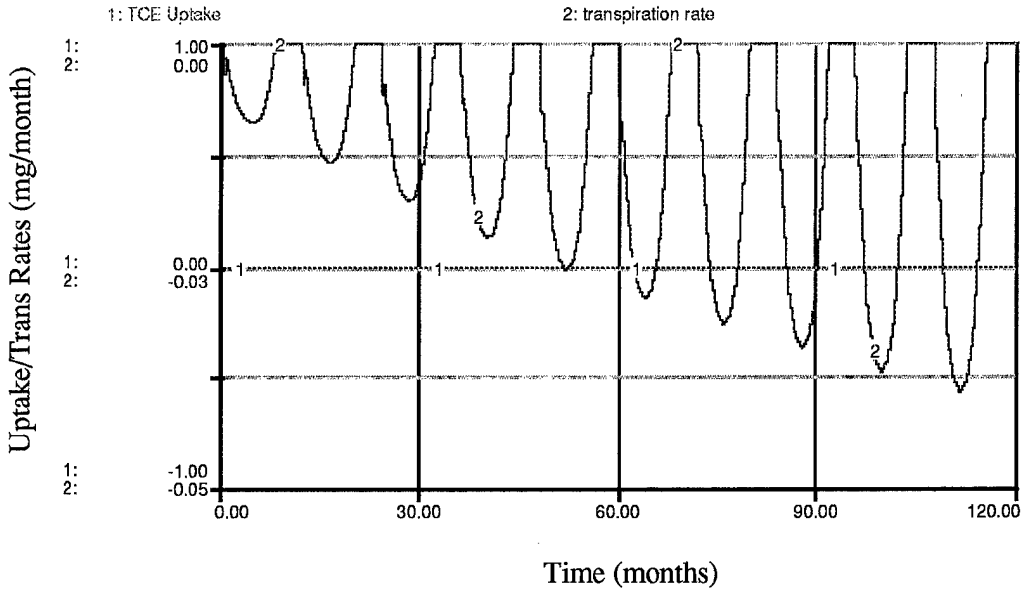

Figure 4.1 TCE Uptake and Transpiration at a TCE Ground Water Concentration of 0 ppm

In Figure 4.1, there is no TCE uptake since the ground water TCE concentration is zero. The tree is taking up TCE from the background air TCE concentration because the gradient is now reversed, so negative flow is expected. Also, because the TCE background air concentration is very small, the flow into the tree is minimal.

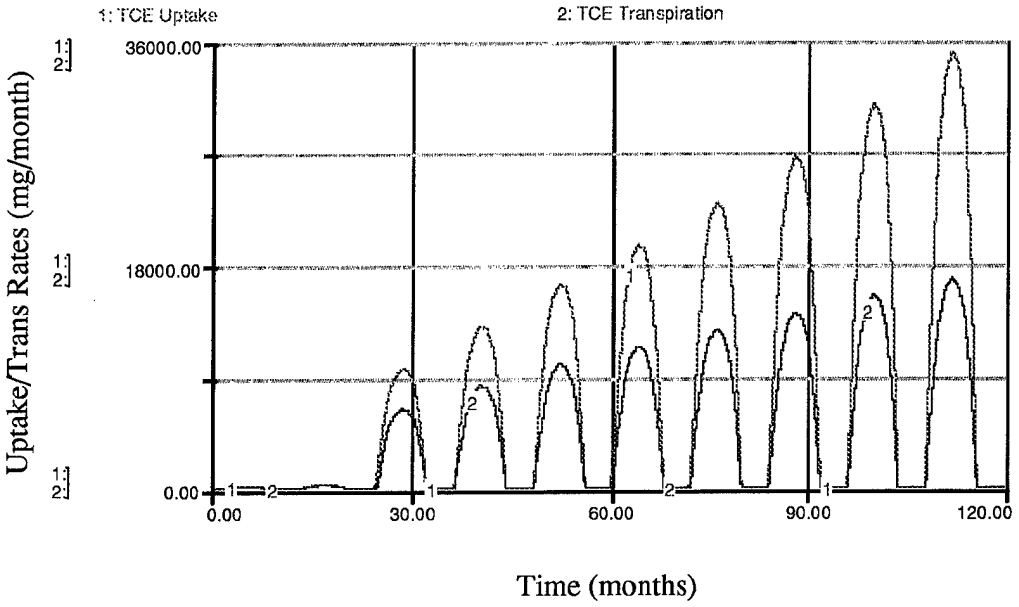

Figure 4.2 TCE Uptake and Transpiration at a TCE Ground Water Concentration of 100 ppm

In Figure 4.2, the ground water TCE concentration is 100 ppm, resulting in high TCE uptake and transpiration. TCE uptake is increasing at a gradual exponential rate while transpiration is increasing to an asymptotic value. The exponential uptake mode of behavior is due to several interactions. The flow of TCE into the rhizosphere is high, since the TCE ground water concentration is set at 100 ppm. This means the concentration of TCE in the rhizosphere is high, and therefore, the uptake is on the upper side of the saturable uptake curve; it is approaching a constant value (See Figure 3.3). The other variable which affects uptake is the tree mass, which in this case controls TCE uptake. The tree mass with growth follows a gradual exponential curve in the first half of its life and then approaches an asymptotic value with maturity. In this figure, the TCE uptake shows a gradual exponential increase due to the tree mass growth curve.

Transpiration increases each season as the TCE xylem flow into the leaf increases each season. It will eventually approach a maximum as the xylem flow into the leaf reaches a maximum with tree maturity. The step at the beginning of year three is due to the tree root reaching the higher TCE concentration in the capillary fringe and increasing TCE uptake into the tree.

The next two graphs represent extreme depths of unsaturated soil, from 0 meters in Figure 4.3 to 10 meters in Figure 4.4. This extreme test considers both the extremes of ground water depth as well as unsaturated soil depth.

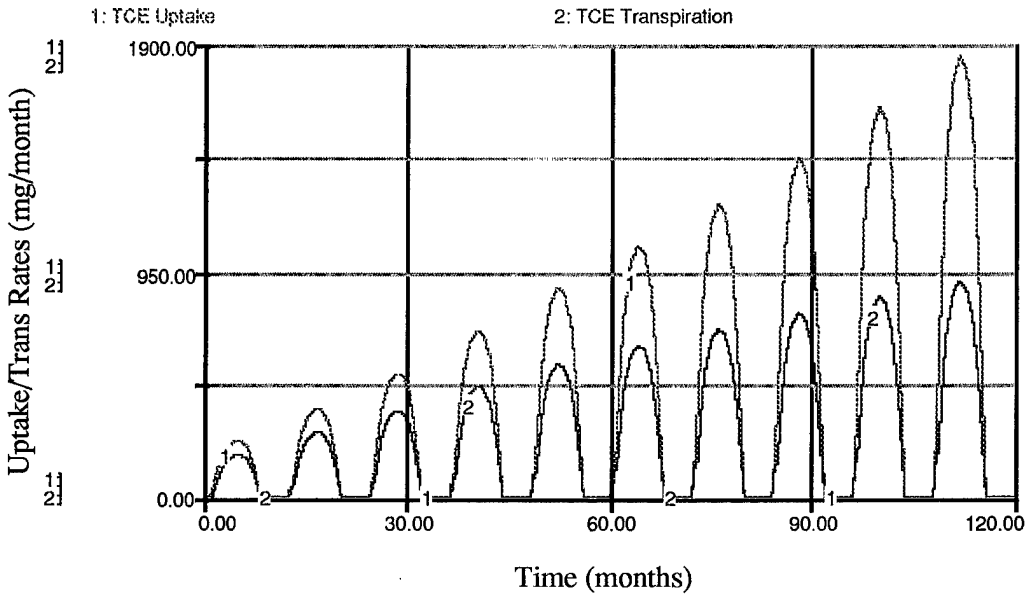

Figure 4.3 TCE Uptake and Transpiration at an Unsaturated Depth of 0 Meters

As seen in Figure 4.3, with the unsaturated depth set to zero and a ground water TCE concentration of 605 ppb, uptake is immediate and significant. This is because all of the roots' growth is in the capillary fringe, where the TCE concentration is typically 100 times higher than that of the

unsaturated zone. The model output is similar to the previous uptake in Figure 4.2. Transpiration also increases immediately and then follows the same behavior as outlined in Figure 4.2.

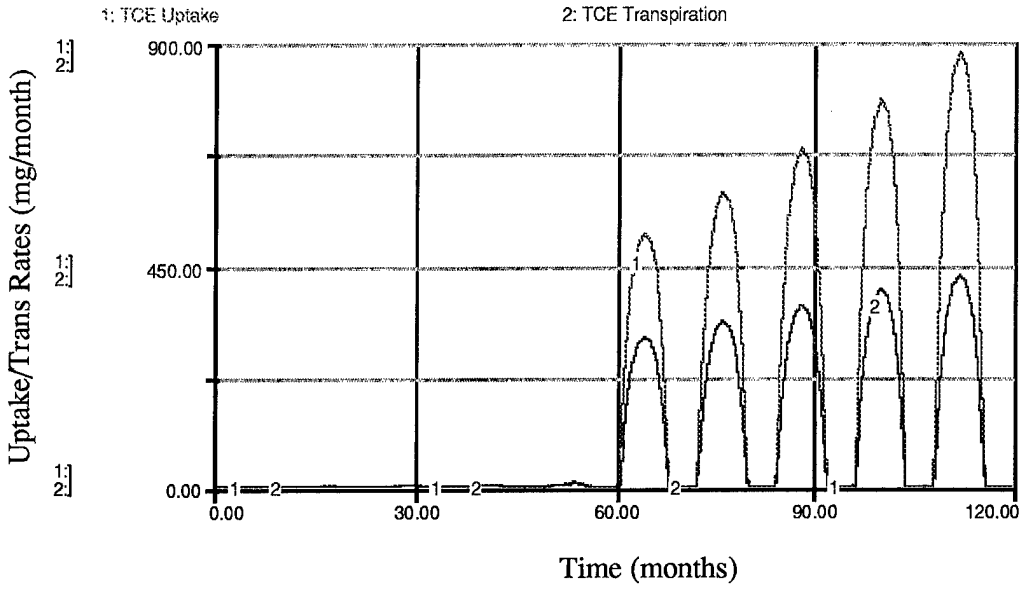

Figure 4.4 TCE Uptake and Transpiration at an Unsaturated Depth of 10 Meters

Figure 4.4, with the unsaturated depth set to 10 meters and a ground water TCE concentration of 605 ppb, shows little uptake or transpiration until year five. This is when the root finally extends to the capillary fringe and starts to take up larger quantities of contaminant. The output then takes on a form similar to prior runs at this concentration. Comparing Figures 4.3 to 4.4, the uptake and transpiration in the latter is approximately half of the former at year 10. The lower uptake and transpiration in Figure 4.4 is due to the increased amount of root in the unsaturated zone. With this increased root mass comes a higher uptake ratio from the unsaturated zone to the capillary fringe. Because

the unsaturated zone has up to 100 times less TCE in aqueous concentration, the total uptake and transpiration therefore decreases.

Figure 4.5 represents an extreme scenario of TCE uptake and transpiration over an extended time frame. The time frame of 216 months or 18 years was selected for this scenario since extended time periods exceeded computer memory capabilities.

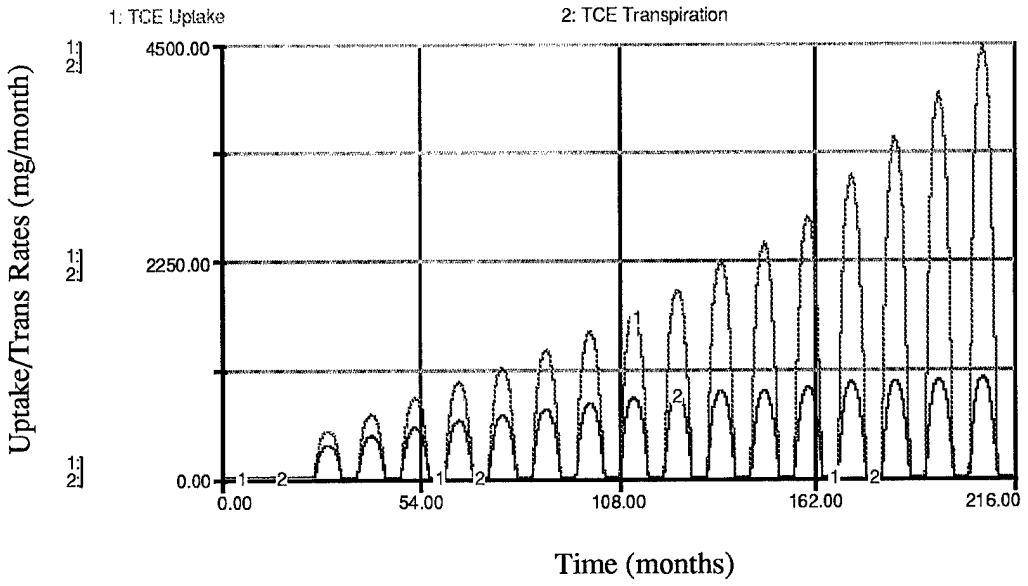

Figure 4.5 TCE Uptake and Transpiration Over 18 Years

At a time frame of 18 years the mode of behavior of uptake and transpiration is further represented; the exponential mode of behavior by uptake and asymptotic mode of behavior by transpiration are more apparent.

Figure 4.6 represents the extremes of uptake with changes in the value of the V_{max} parameter. Transpiration was not depicted in this scenario since the V_{max} parameter affects the uptake mechanism only and transpiration will mirror prior figures.

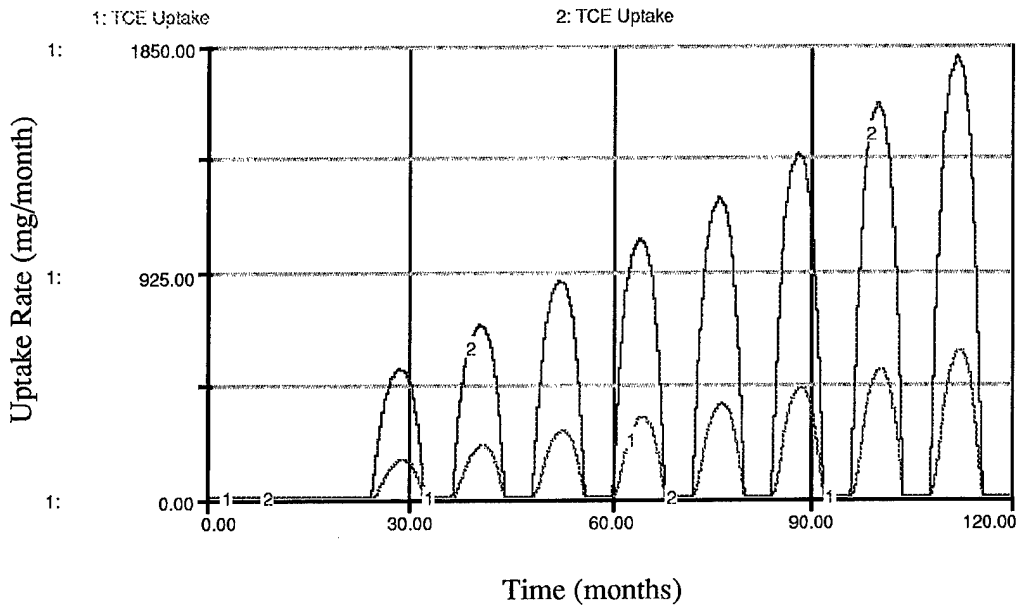

Figure 4.6 TCE Uptake with Extremes of V_{max}

Because the value for V_{max} was based on minimal research data which established only two points for extrapolating the saturable uptake curve, V_{max} was given large variation to test its effect on the model under extreme conditions. Plausible extreme values selected for this test were 1 and 200 mg TCE/(kg plant-month). These values were based on intuition and V_{max} values calculated by previous research in this field [Peake, 1996:87-90]. In Figure 4.6, values of V_{max} for each curve were as follows; 1) 1, 2) 200 mg TCE/(kg plant-month). With extremes in the value of V_{max}, the model showed the capability of producing plausible output outside an expected range for this parameter.

Figure 4.7 represents extreme changes in the uptake variable K_m and its effect on the uptake of TCE in the model tree.

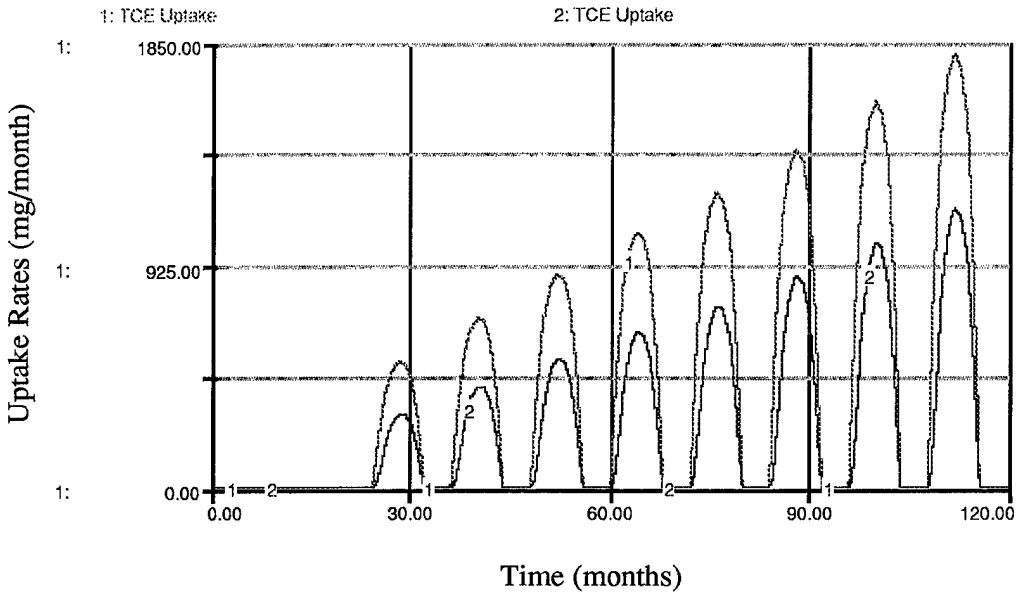

Figure 4.7 TCE Uptake with Extremes of K_m

Because the value for K_m was based on minimal research data which established only two points for extrapolating the saturable uptake curve, K_m was given large variation to test its effect on the model under extreme conditions. Plausible extreme values selected for this test were 7,500 and 750,000 mg TCE/m^3. These values were based on intuition and K_m values calculated by previous research in this field [Peake, 1996:87-90]. In Figure 4.7, extreme values of K_m were as follows; 1) 7,500, 2) 750,000 mg TCE/m^3. For the values portrayed in Figure 4.7, the model showed the capability of producing plausible output at extreme values of system conditions.

All tests of extremes produced reasonable behavior. No structural weaknesses were therefore realized and the model proved capable of operating outside existing but possible system conditions.

Boundary Adequacy. Since the purpose of this model was to estimate the uptake and transpiration of TCE over time, disaggregation of compartments influencing these factors was necessary. The phreatophytic tree received ample disaggregation to reach this purpose. Disaggregation of the rhizosphere was complete, accept in respect to the influence of cometabolism. Current scientific understanding and published articles on this topic are lacking so the desired level of disaggregation did not occur. Instead, a simplified reaction rate equation was used to represent rhizosphere cometabolism. This aggregation is a weakness in the model and has potential for future thesis research.

Dimensional-Consistency. Scaling factors used in this model include all coefficients, transfer rates, and ratios. As discussed in parameter verification, these values are part of equations or serve to disaggregate flows and volumes in the model into different compartments. All scaling factors represent corresponding real-life values or are part of equations which represent real-life processes. These values are based on literature parameters, professional intuition, research, or an understanding of the model structure and its progressive development. All scaling factors will receive further analysis under behavior sensitivity and soft parameter sensitivity.

Tests of Model Behavior.

Behavior Anomaly. Two instances of anomalous behavior were discovered in the final model. The first was an anomaly found in the amount of TCE in the leaf over time. Figure 4.8 shows this behavior.

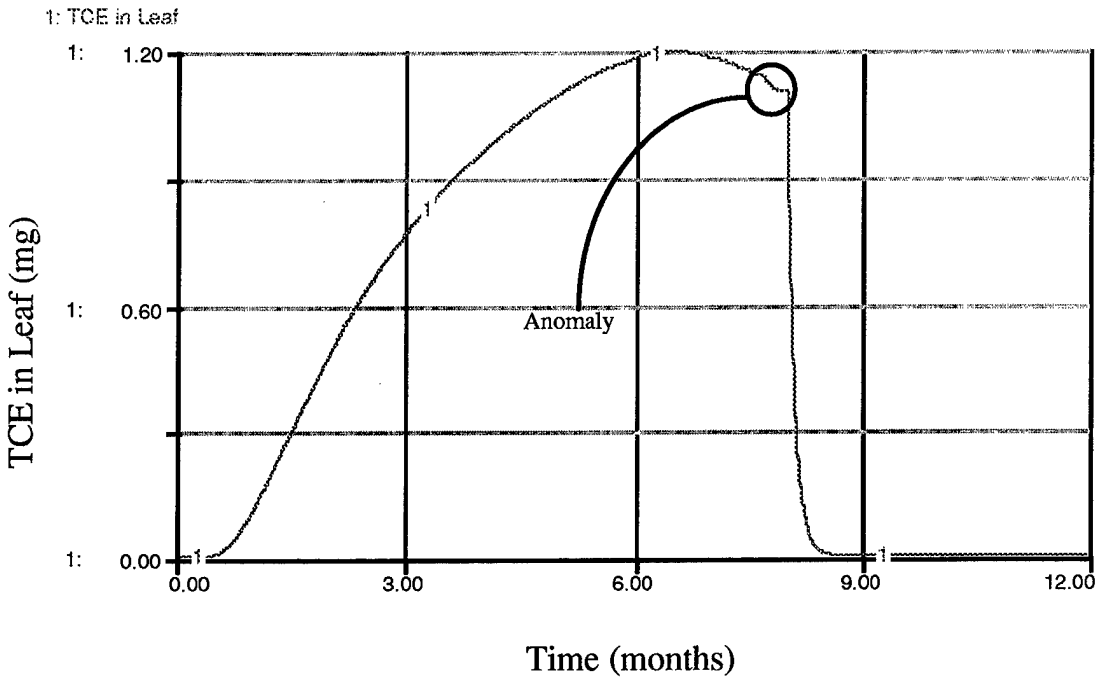

Figure 4.8 TCE Leaf Mass Anomaly

Line 1 in Figure 4.8 is TCE Mass in Leaf. As the TCE Mass in Leaf curve approaches month eight, there is a very slight abnormality or dip in the curve immediately before the end of the season. This abnormality is seen in all leaf mass curves over time. Initially it was thought the onset of leaf senescence triggered this abnormality, but leaf senescence does not begin until after month eight. Another parameter which was thought to possibly cause this behavior was the rhizosphere TCE loss rate. The loss or diffusion from the rhizosphere starts

in month seven and rapidly increases by month eight. When the flows in and out of the leaf were analyzed however, no reflection of this behavior was found. The flows in and out of the leaf compartment were then summed to find the cumulative flow. Figure 4.9 depicts this summed flow.

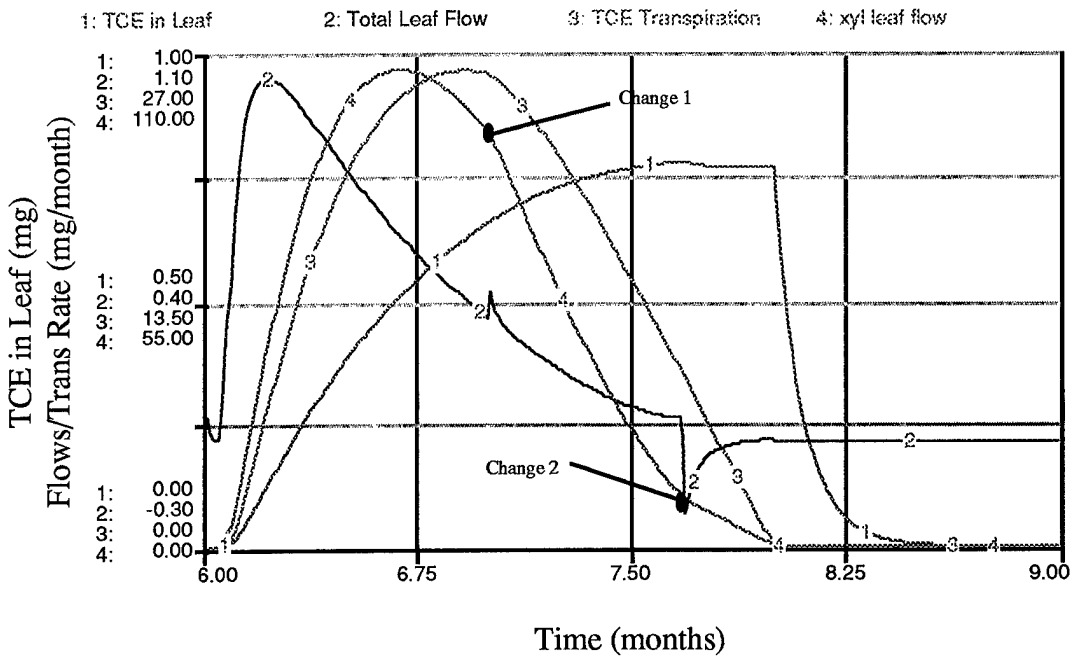

Figure 4.9 TCE Leaf Anomaly with Total Flows

Figure 4.9 was run from month six to month nine to better view the anomalous behavior at approximately month eight. Line 1 is the TCE Mass in Leaf, line 2 is the total flow of TCE in and out of the leaf, line 3 is TCE Transpiration, and line 4 is the TCE xylem to leaf flow. The cause of this anomaly is now apparent. At the end of the season, flows out of the leaf exceed flows into the leaf, causing TCE Mass in Leaf to drop suddenly to meet this demand. The reason for the change in total flow is as follows: the TCE xylem flow into the leaf is based on a seasonal fluctuation which does not follow a

smooth curve or cycle. This is because seasonal fluctuation was graphed by hand in Stella. The TCE xylem flow is influenced by the seasonal fluctuation, so shows similar behavior. Change 1 and 2 in the TCE Xylem Flow correspond to changes in the seasonal fluctuation. With these abrupt changes in slope of the Xylem Leaf Flow, the flows out of the leaf have a delay in their response due to an integration error in the program. This causes the anomalous spikes in Total Leaf Flow at Changes 1 and 2. The anomalous behavior at Change 2 is larger due to the lower flow rates in and out of the leaf coupled with the larger change in negative slope of the Total Leaf Flow. This anomaly in turn causes the slight anomaly in TCE Mass in Leaf.

This behavior is not expected in the real world and is due to the manual approximation of seasonal fluctuation in the model. Since TCE Transpiration is decreasing at a linear rate from month six to eight with no observable change, the anomalous behavior is not expected to have any significant effect on model uptake and transpiration output.

The second instance of anomalous behavior was also found in the leaf. Figure 4.10 represents the anomalous behavior.

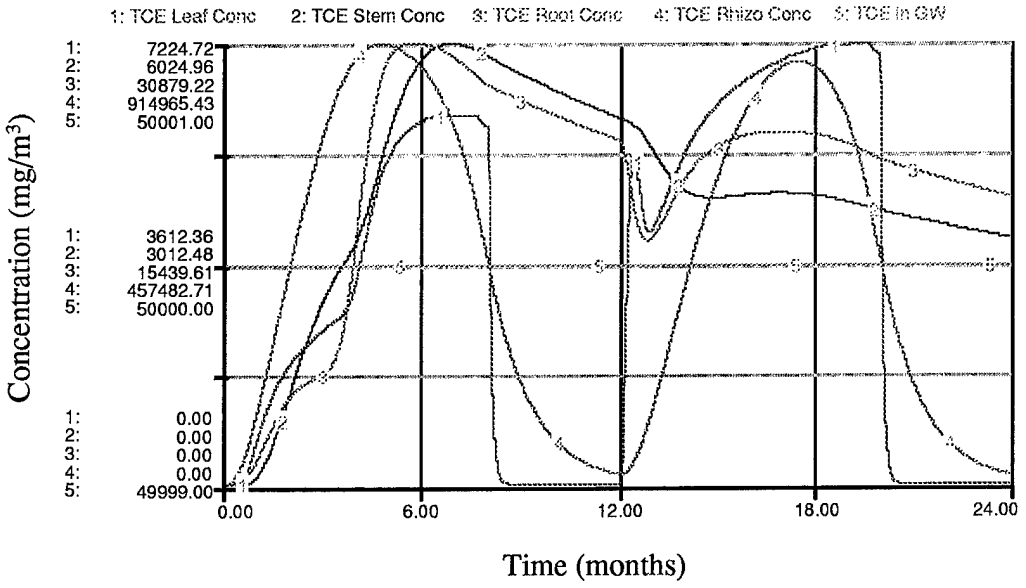

Figure 4.10 TCE Concentration in Leaf Anomaly

The output in Figure 4.10 are as follows; 1) TCE Leaf Concentration, 2) TCE Stem Concentration, 3) TCE Root Concentration, 4) TCE Rhizosphere Concentration, and 5) TCE Ground Water Concentration. In the beginning of the second year (month 12-13), the TCE Leaf Concentration curve makes a sharp drop. At first, this was thought to be anomalous behavior on the part of the model. Upon further analysis it was discovered all tree compartments, root, stem, and leaf, showed the same behavior. The description of this behavior is as follows: at the beginning of the season, due to the structure of the model the root and stem TCE concentrations are higher than the xylem TCE concentration, so flow takes place out of the root and stem into the xylem. This increases the xylem TCE concentration, which in turn rapidly increases the leaf TCE concentration. The rapid increase in the leaf TCE concentration continues until the xylem TCE concentration approaches the root and stem TCE concentrations.

As the xylem TCE concentration approaches the root and stem TCE concentration, the rapid increase decreases and the leaf TCE concentration subsequently drops. When the compartments are all at the same concentration, this influence ceases to affect the leaf concentration and it reaches a local minimum. Thereafter, the xylem TCE concentration exceeds the root and stem TCE concentrations and flow proceeds in the opposite direction. By running the model over a season, such as from month 12 to 24, the anomalous behavior was no longer present. This was due to all stocks having an initial value of 0 at time 12, so no initial flow out of the stem and root was seen. This scenario was compared to the initial time period of 0 to 24 months and it was found that the maximum rate of uptake and transpiration did not vary between the two scenarios. Therefore, this anomalous behavior was not deemed of significance to model output.

Another potential for behavior anomaly testing is its use in increasing confidence in soft variables. By running soft parameters outside their expected range, if anomalous behavior is seen, then this builds confidence in the selected value of the soft variable [Forrester and Senge, 1980:220]. Several soft parameters were selected for this analysis. The first was the leaf air transfer rate coefficient, which was solely based on intuition and was expected to influence the rate of transpiration.

TCE transpiration rates in greenhouse and field studies have been related to TCE uptake rates. There is a great deal of variability between these

studies, with ~ 70% and ~ 10% of the TCE taken up transpired in the respective studies. This information was used to approximate plausible extremes for this test. At a value of .05 m^3/month TCE transpiration was below the lower bound, approximately 5%, and at a value of 5 m^3/month the TCE transpiration was above the upper bound, approximately 75%. This test then brackets the leaf air transfer rate between these two extremes. Figure 4.11 depicts the behavior of the leaf transfer rate coefficient at extreme values of .05 and 5.

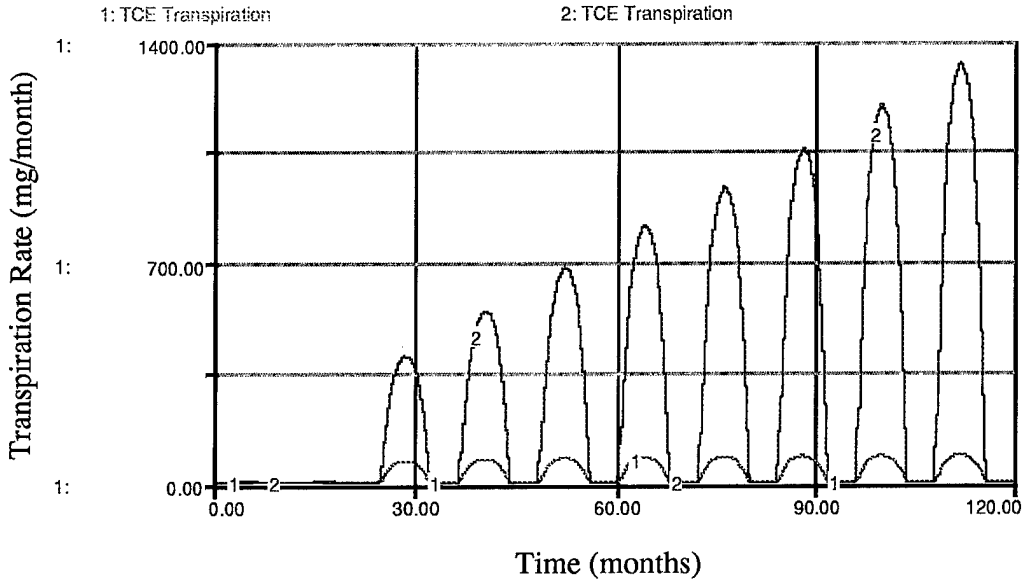

Figure 4.11 Leaf Air Transfer Rate Coefficient Behavior Anomaly Test

Line 1 in Figure 4.11 represents TCE transpiration with a leaf air transfer rate coefficient of .01 m^3/month and line 2 represents transpiration with a leaf air transfer rate coefficient of 5 m^3/month. This test shows the selected value for the leaf air transfer rate coefficient is realistic and builds confidence in its reliability.

Figure 4.12 and 4.13 test the fine root tissue volume coefficient and the secondary root tissue volume coefficient for anomalous behavior.

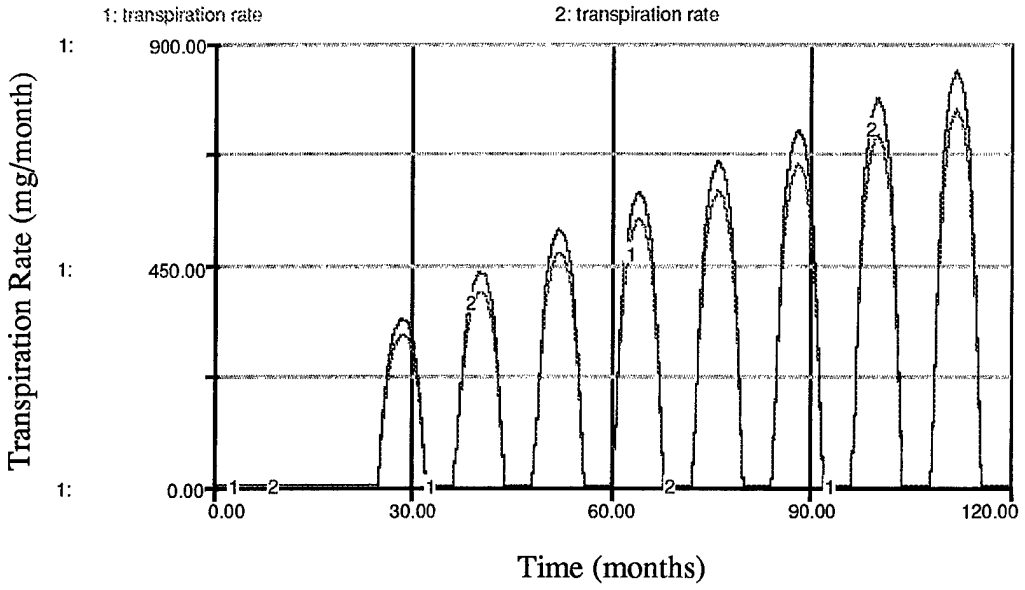

Figure 4.12 Fine Root Tissue Volume Coefficient Behavior Anomaly Test

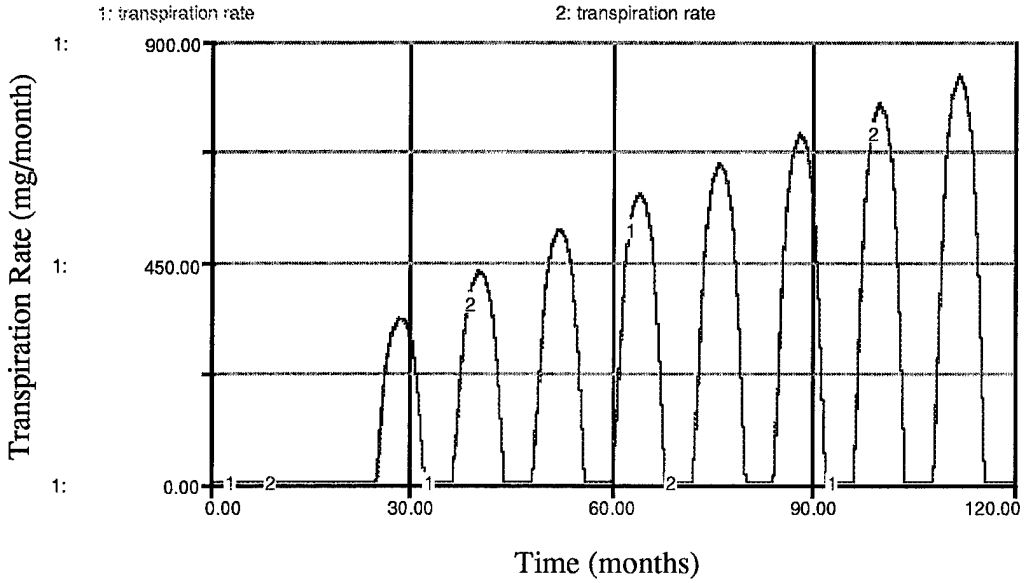

Figure 4.13 Secondary Growth Root Tissue Volume Coefficient Behavior Anomaly Test

The expected range for both the Fine Root and Secondary Growth Root Tissue Volume Coefficients was 20% to 40%. Extreme values of 5% and 70%

showed no anomalous behavior on TCE transpiration. Under the following section, soft parameter sensitivity, it was found these parameters did not affect TCE transpiration so further analysis in this section was not deemed necessary.

Other soft parameters, especially the stem and root transfer rate coefficients which were based on intuition, were not tested under this section, since they were also found to have no significant affect on TCE transpiration. Since these soft parameters do not affect TCE transpiration it was not felt that their approximated values required further analysis.

The behavior anomaly test helped provide extreme bounds for the Leaf Air Transfer Rate Coefficient, but was inconclusive in testing other soft variables at values beyond their expected ranges. TCE uptake and transpiration output on these latter soft parameters was still realistic and gave expected behavior.

Behavior Sensitivity. This test will cover all parameters in Table 3.1. Unless otherwise noted, the TCE ground water concentration was set at 605 ppb, the ground water depth was set at 3.3 meters, and the time frame of interest was set at 120 months or 10 years. The first two values correspond with average values found at Air Force Plant 4. Figure 4.12 represents the sensitivity of TCE uptake to cometabolism of TCE in the rhizosphere.

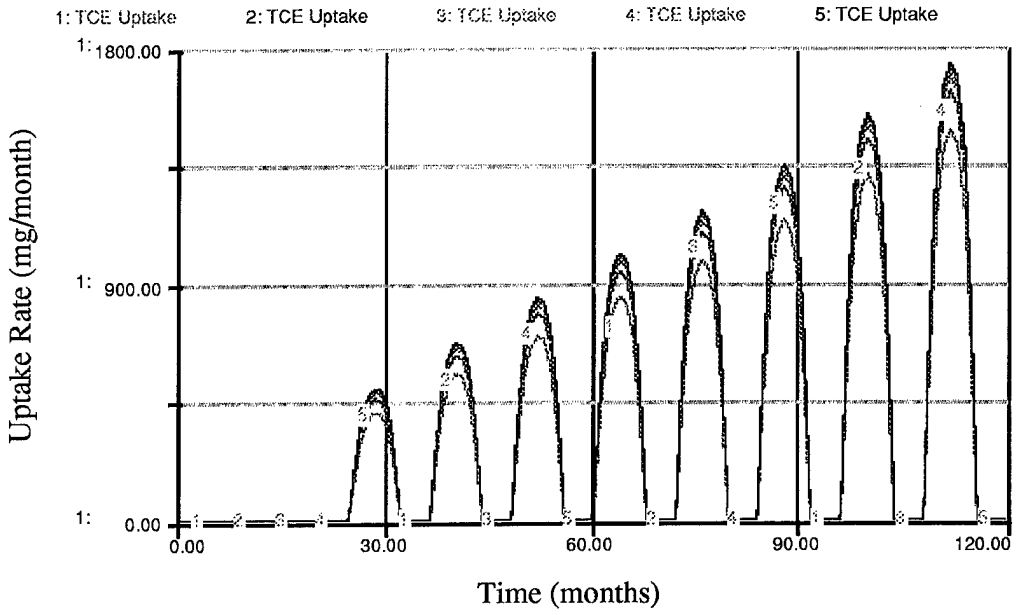

Figure 4.14 TCE Uptake Sensitivity to the Rhizosphere TCE Half Life

The Rhizosphere TCE Half Life represents the half life of TCE in the rhizosphere. It is an input parameter in equation 2. Literature values varied from .33 months to 1.93 months, so they bracketed the analysis. Values used in Figure 4.14 were as follows: 1) 0.33 months, 2) 0.73 months, 3) 1.13 months, 4) 1.53 months, and 5) 1.93 months. The model shows a slight sensitivity to changes in the TCE rhizosphere half life, especially at the lower value. At year 10 the difference between the highest and lowest parameters was approximately 13%. To further test this parameter, the sensitivity analysis was again carried out at a TCE ground water concentration of 50 ppm.

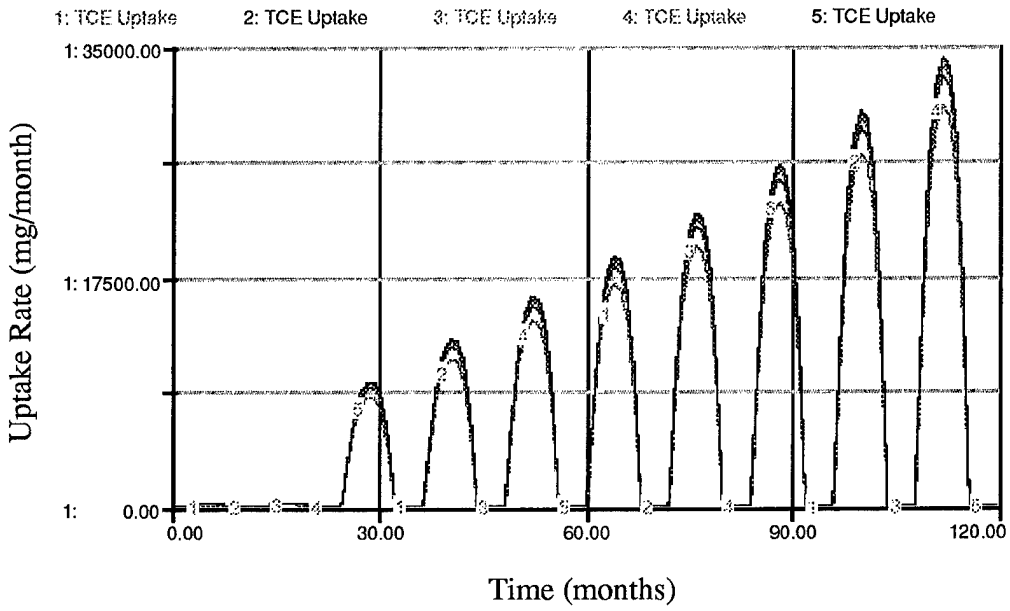

Figure 4.15 TCE Uptake Sensitivity to the Rhizosphere TCE Half Life at a TCE Ground Water Concentration of 50 ppm

Figure 4.15 gives the same output as Figure 4.14. At lower values of the rhizosphere TCE half life, cometabolism increases, thereby decreasing the amount of TCE available for uptake. As the rhizosphere TCE half life increases to the maximum value, cometabolism decreases, thereby increasing the amount of TCE available for uptake. This increased amount of TCE is not significant enough to greatly affect the uptake. This results in little change in uptake rates; at year 10 the difference between the highest and lowest parameters was approximately 13%. Overall, the model is slightly sensitive to the rhizosphere TCE half life parameter.

Figure 4.16 depicts the sensitivity of TCE transpiration to changes in the leaf air partition coefficient. TCE transpiration was selected as the output for this

scenario since this parameter is part of the TCE transpiration equation and does not affect TCE uptake.

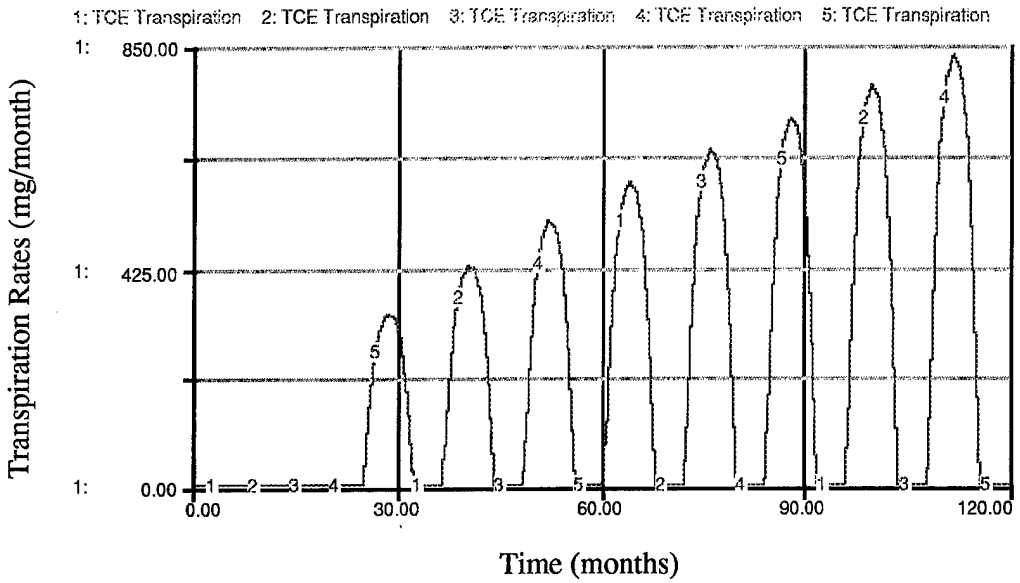

Figure 4.16 TCE Transpiration Sensitivity to the Leaf Air Partition Coefficient

The leaf air partition coefficient was used in equation 11 to establish the TCE flow between the phreatophytic tree leaves and the TCE air background concentration. Values used for the leaf air partition coefficient in Figure 4.16 were as follows: 1) 2.05, 2) 3.08, 3) 4.1, 4) 5.13, and 5) 6.15. The minimum and maximum were based on 50% and 150% of the literature value. The model proved insensitive to this parameter with no change in TCE transpiration with changes in the leaf air partition coefficient; at year 10 the difference between the highest and lowest parameters was 0%. This is because the phreatophytic tree leaf TCE concentration is much greater than the air background TCE

concentration, so controls this equation. The same behavior is expected in the real world system due to the higher phreatophytic tree TCE concentration.

Figure 4.17 represents the sensitivity of the model to the TCE air background concentration. TCE transpiration was selected as the output for this scenario since this parameter is part of the TCE transpiration equation and does not affect TCE uptake.

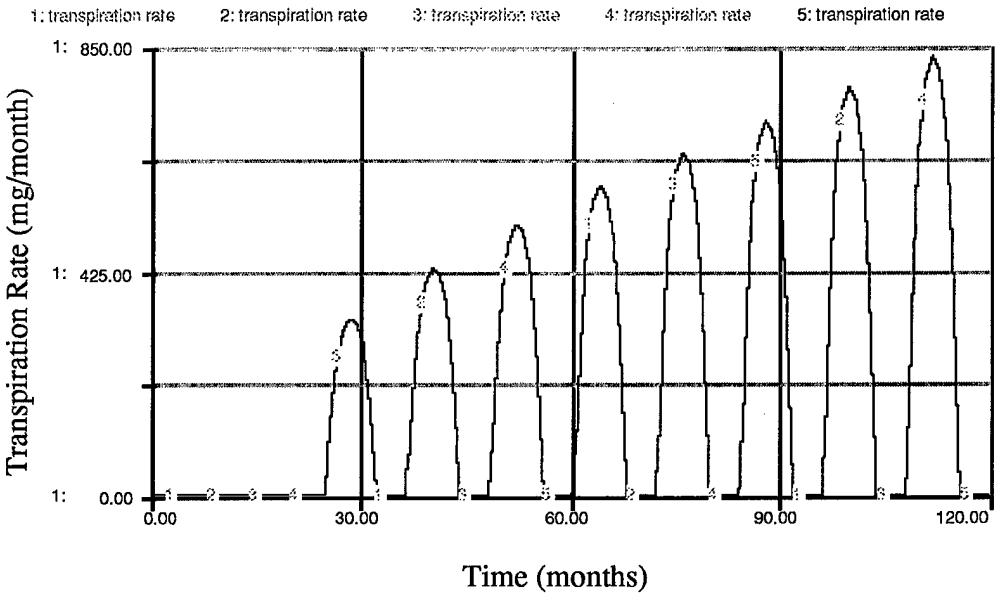

Figure 4.17 TCE Transpiration Sensitivity to the TCE Air Background Concentration

The TCE air background concentration was used in equation 11 to establish the TCE flow between the phreatophytic tree leaves and the TCE air background concentration. Values for the TCE air background concentration were varied from the known values of 0.011 ppb to 0.03 ppb. Values used in Figure 4.15 were as follows: 1) 0.011 ppf, 2) 0.0158 ppb, 3) 0.0205 ppb, 4) 0.0253 ppb, and 5) 0.03 ppb. The model proved insensitive to this parameter.

This was due to the high tree TCE concentration in comparison to the TCE air background concentration; the tree TCE concentration was at least 10 times that of the TCE air background concentration. This resulted in the parameter having no influence on the model; at year 10 the difference between the highest and lowest parameters was 0%.

Figure 4.18 depicts the sensitivity of the model to changes in the leaf partition coefficient. TCE transpiration was selected as the output for this scenario since this parameter is part of the TCE transpiration equation and does not affect TCE uptake.

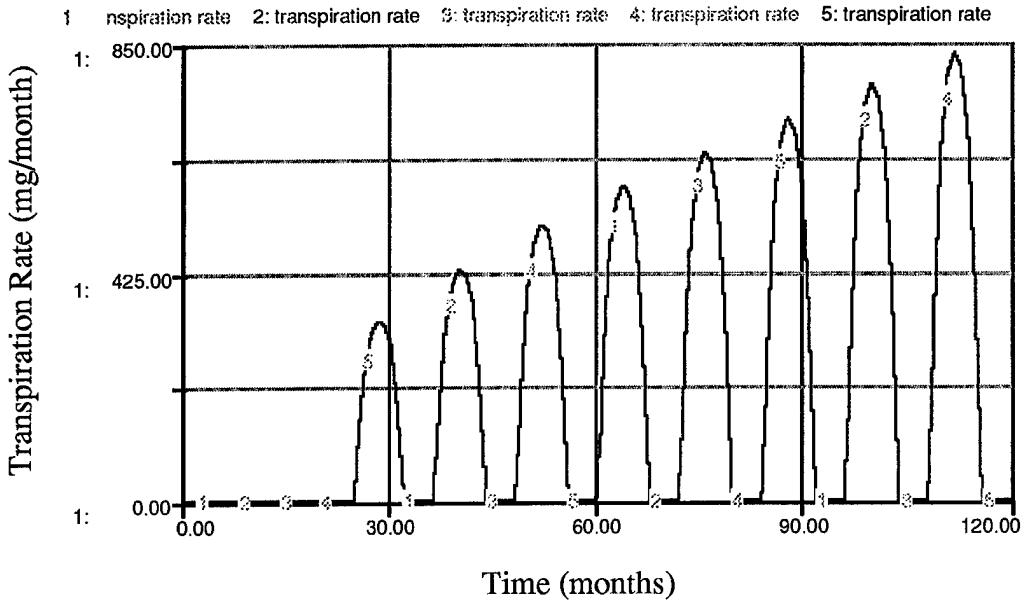

Figure 4.18 TCE Transpiration Sensitivity to the Leaf Partition Coefficient

The leaf partition coefficient was used in the flow equation between the xylem and phloem in the leaf. The leaf partition coefficient was varied from 50% to 150% of the calculated value of .549 m^3/month. Values used in Figure4.18

were as follows: 1) 0.275 m^3/month, 2) 0.412 m^3/month, 3) 0.549 m^3/month, 4) 0.688 m^3/month, and 5) 0.823 m^3/month. The model TCE transpiration proved insensitive to this variable; at year 10 the difference between the highest and lowest parameters was 0%. This was due to the insignificant diffusion flow from these two compartments in comparison to the TCE xylem flow. Real world systems are expected to show similar results.

Figure 4.19 and 4.20 represent the sensitivity of TCE uptake and transpiration to the xylem flow rate per leaf area.

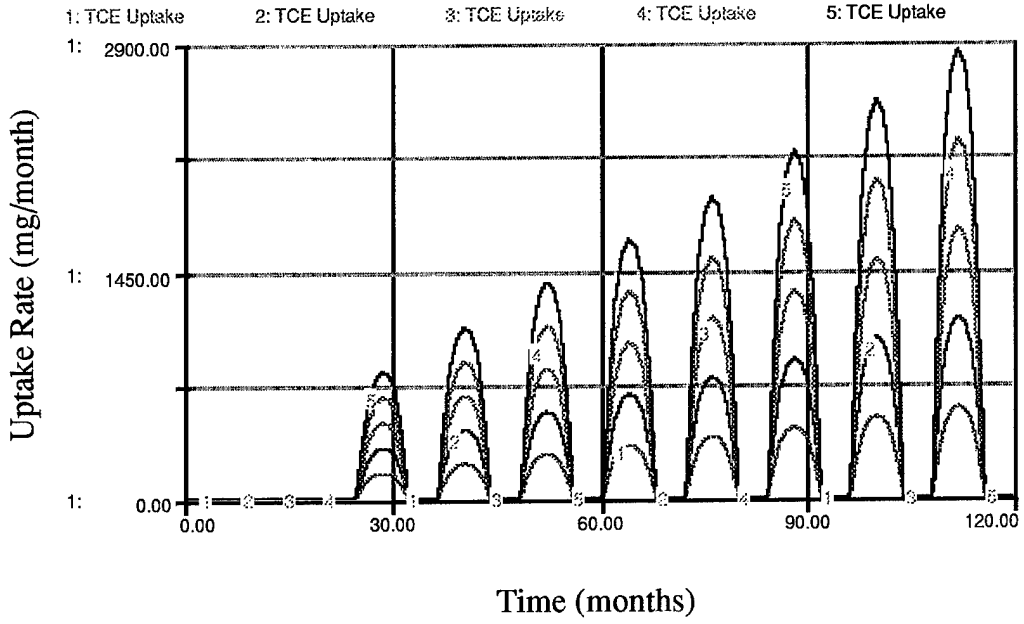

Figure 4.19 TCE Uptake Sensitivity to the Xylem Flow Rate per Leaf Area

The Xylem Flow Rate per Leaf Area drove the contaminant flow into the rhizosphere and through the phreatophytic tree xylem vascular system. Values of the Xylem Flow Rate per Leaf Area were varied from those found in literature. Values used in Figure 4.19 were as follows: 1) 0.0065 , 2) 0.0129, 3) 0.019, 4)

0.0256, and 5) 0.032 $m^3/(m^2$ leaf-month) TCE uptake into the model proved sensitive to the Xylem Flow Rate per Leaf area throughout all values; at year 10 the difference between the highest and lowest parameters was approximately 81%. This was due to TCE uptake being controlled by the saturable uptake equation, which, among other parameters, was based on the TCE concentration in the rhizosphere (See equation 1). As the flow of TCE increased into the rhizosphere, TCE rhizosphere concentration increased, and therefore uptake increased. As the tree reaches maturity the uptake is expected to reach a single maximum value, regardless of flow rates. With increased TCE uptake and transpiration in a real world system, TCE uptake is also expected to increase, approaching a maximum with tree maturity.

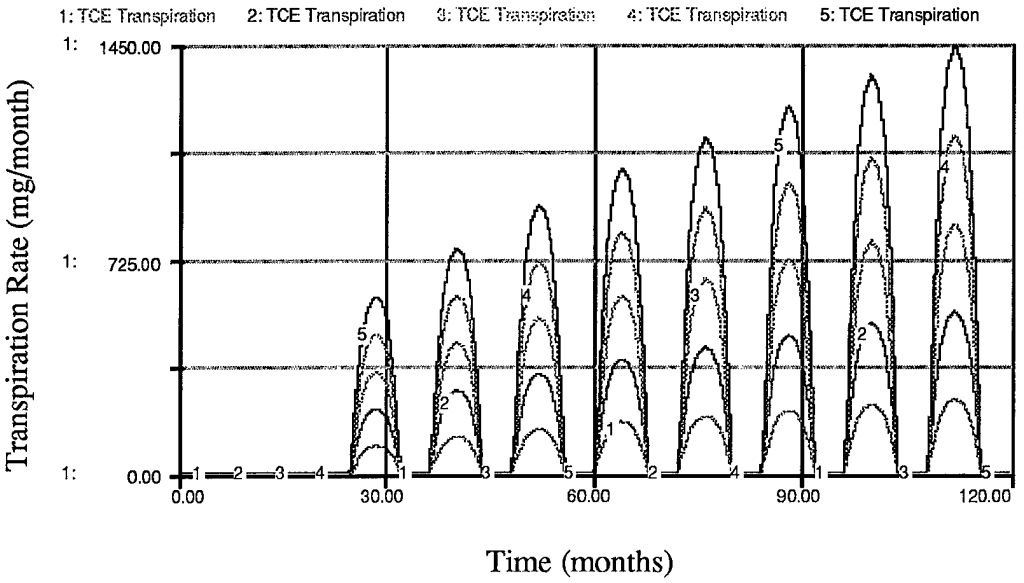

Figure 4.20 TCE Transpiration Sensitivity to the Xylem Flow Rate per Leaf Area

Figure 4.20 depicts the effect of changes in the xylem flow rate per leaf area on TCE transpiration. Values used in this figure were the same as in Figure 4.19. Once again, the model was sensitive to the xylem flow rate per leaf area throughout all values; at year 10 the difference between the highest and lowest parameters was approximately 81%.

Figure 4.21 depicts the sensitivity of TCE transpiration to the phloem flow rate per leaf area. TCE transpiration was selected as the output for this scenario since this parameter does not affect the flow of TCE into the phreatophyte, but serves as a return flow mechanism from the leaf to the root.

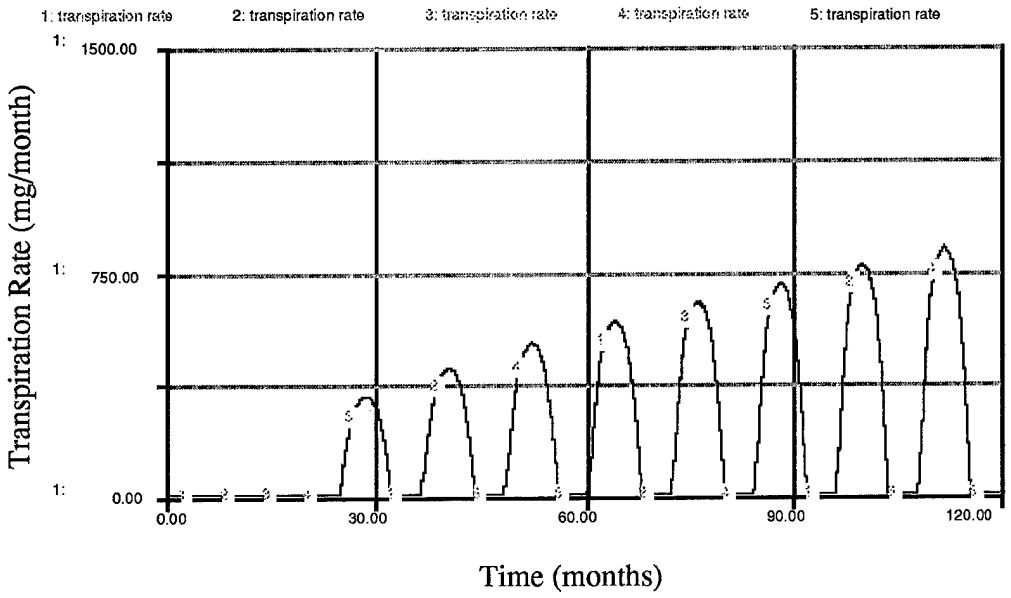

Figure 4.21 TCE Transpiration Sensitivity to the Phloem Flow Rate per Leaf Area

The Phloem Flow Rate per Leaf Area drove the contaminant from the leaf tissue down into the root. Values of the Phloem Flow Rate per Leaf Area were varied from 50% to 150% of the literature value of 0.000162 mg TCE/(kg plant-

month). Values used in Figure 4.19 were as follows: 1) 0.000081 , 2) 0.000012, 3) 0.000162, 4) 0.000208, and 5) 0.000243 mg TCE/(kg plant-month). TCE transpiration in the model proved insensitive to the Phloem Flow Rate per Leaf Area; at year 10 the difference between the highest and lowest parameters was 0%. This is because the phloem flow rate is insignificant in comparison to the xylem flow rate, which dominates the transport of contaminant. Phloem flow in the real world system is also insignificant in relation to the xylem flow, so will not affect TCE transpiration.

Figure 4.22 and 4.23 represents the sensitivity of the model to the leaf, stem, secondary root, and fine root densities.

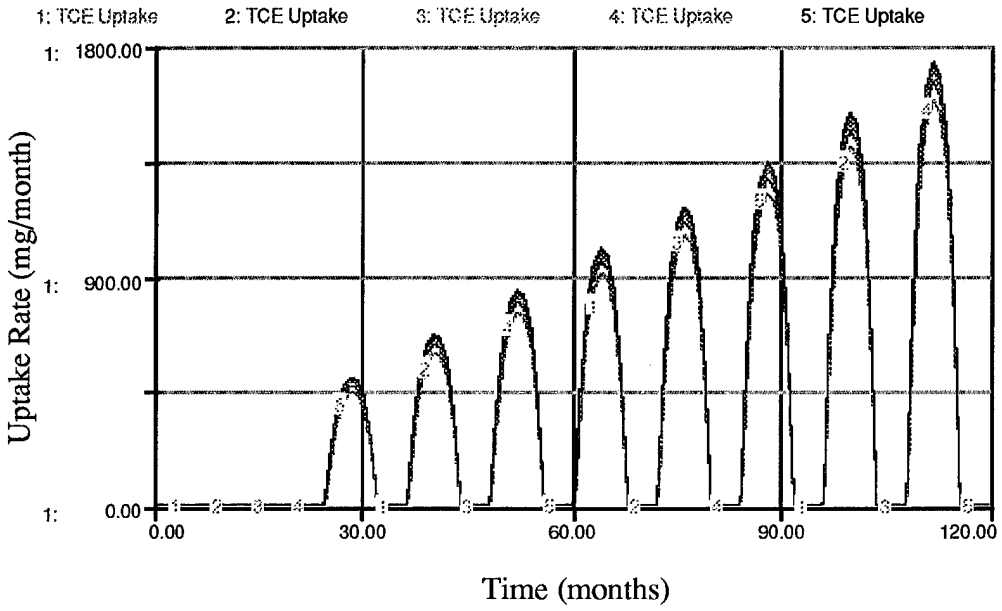

Figure 4.22 TCE Uptake Sensitivity to the Phreatophytic Tree Densities

It was felt the leaf, stem, and root densities would not significantly affect the model output, so were aggregated in one test. Each parameter was varied

50% to 150% of literature or approximated values. Values for each parameter used in Figure 4.22 were as follows: Leaf - 1) 350, 2) 525, 3) 700, 4) 875, and 5) 1050 kg/m^3; Stem - 1) 300, 2) 450, 3) 600, 4) 750, and 5) 900 kg/m^3; Secondary Root - 1) 325, 2) 563, 3) 750, 4) 938, and 5) 1125 kg/m^3; and Fine Root - 1) 500, 2) 750, 3) 1000, 4) 1250, and 5) 1500 kg/m^3. Densities were used to calculate tree mass which in turn was used in the calculation of TCE uptake. Because of this, the densities showed a slight influence on TCE uptake. Therefore, the model proved slightly sensitive to the density parameters; at year 10 the difference between the highest and lowest parameters was approximately 9%. In a natural system, it is expected that increased densities would also slightly change the uptake of TCE. Higher plant density equates to a higher amount of water weight in tree cells, which in turn would increase the amount of TCE to saturate the uptake into the plant.

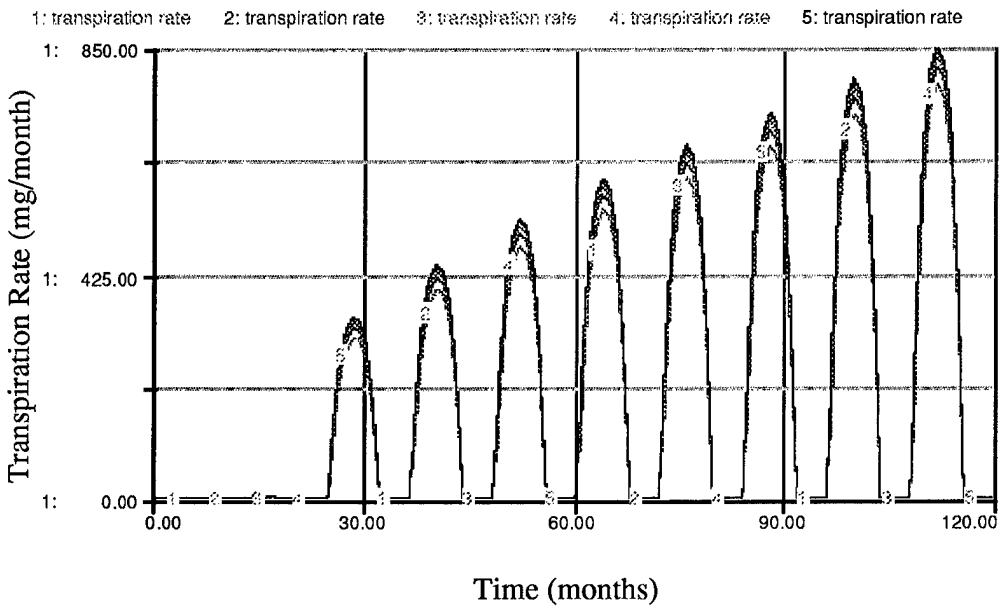

Figure 4.23 TCE Transpiration Sensitivity to the Phreatophytic Tree Densities

The same parameters in Figure 4.22 were used for the output in Figure 4.23. The effects of changing the leaf, stem, and root densities on the transpiration rate proved themselves minimal. Overall, the model proved itself slightly sensitive to changes in the various tree densities; at year 10 the difference between the highest and lowest parameters was approximately 7%.

Figure 4.24 represents the sensitivity of the model to changes in partition coefficients. TCE transpiration was selected as the output for this scenario since these parameters affect how the TCE flow is distributed once it is in the phreatophyte.

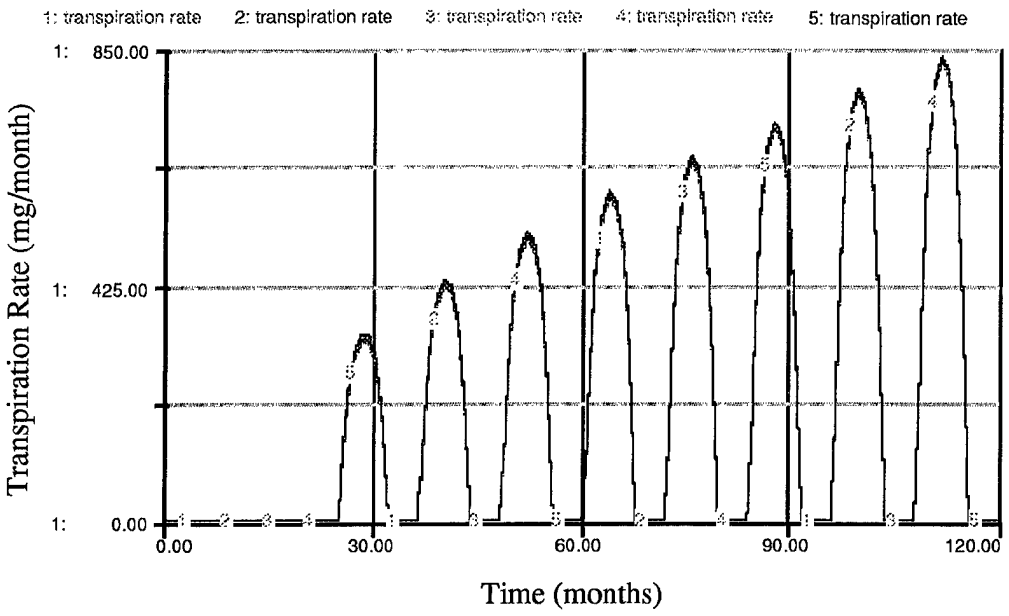

Figure 4.24 TCE Transpiration Sensitivity to the Stem and Root Partition Coefficients

The stem, secondary root, and fine root partition coefficients were used in equation 11 to represent flow between respective tree compartments. These parameters were aggregated for this sensitivity test since they did not directly influence TCE transpiration from the tree. Minimum and maximum values of 50% and 150% of the calculated values were used as bounds in this analysis. The parameters used in Figure 4.24 were as follows: Stem Partition Coefficient - 1) 0.215, 2) 0.323, 3) 0.43, 4) 0.538, and 5) 0.645 m^3/month; Secondary Root Partition Coefficient - 1) 0.34 2) 0.51, 3) 0.68, 4) 0.85, and 5) 1.02 m^3/month; Fine Root Partition Coefficient - 1) 0.462, 2) 0.692, 3) 0.963, 4) 1.15, and 5) 1.385 m^3/month. Model TCE transpiration proved slightly sensitive to changes in these parameters; at year 10 the difference between the highest and lowest parameters was approximately 3%. This is due to the small amount of TCE flow

into the tree tissue in relation to the total flowing through the xylem and subsequently being transpired.

Figure 4.25 and 4.26 represent the sensitivity of the model to the variations in the ratio of secondary and fine roots.

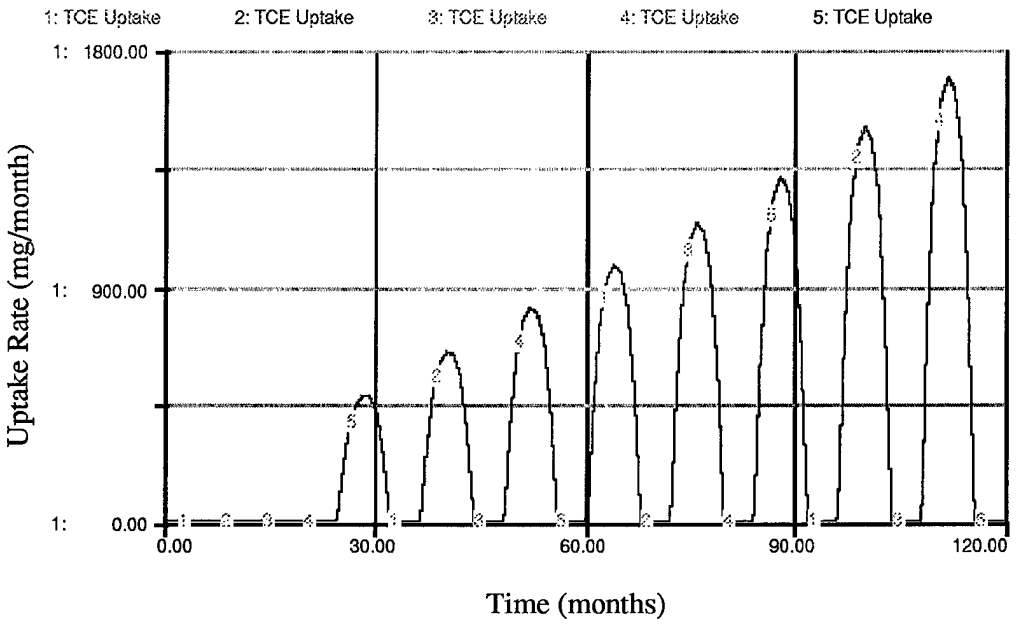

Figure 4.25 TCE Uptake Sensitivity to the Secondary Growth Root to Fine Root Ratio

The Secondary Growth to Fine Root Ratio represents the amount of the total root which is secondary growth root versus fine root. Maximum and minimum literature values range from 60% to 95% of the total root as secondary root. The values used Figure 4.25 were as follows: 1) 0.6, 2) 0.688, 3) 0.78, 4) 0. 862, and 5) 0.95. The model uptake showed no sensitivity to this variable; at year 10 the difference between the highest and lowest parameters was 0%.

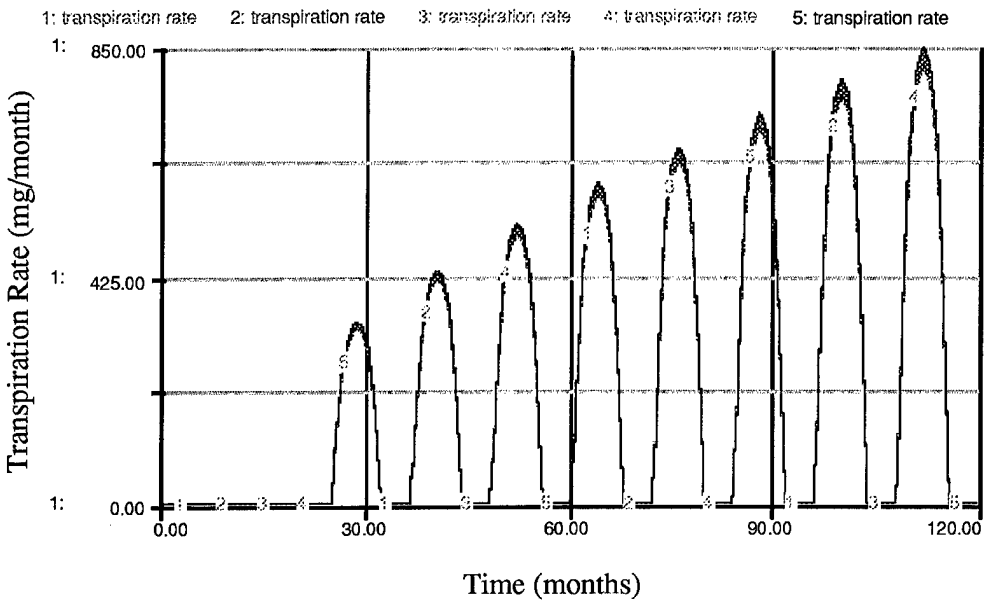

Figure 4.26 TCE Transpiration Sensitivity to the Secondary Growth to Fine Root Ratio

TCE transpiration was then tested against changes in the Secondary Growth to Fine Root Ratio. Values used in Figure 4.26 were the same as those in Figure 4.25. TCE transpiration proved slightly sensitive to the Secondary Growth to Fine Root Ratio; at year 10 the difference between the highest and lowest parameters was approximately 6%. The fine root tissue stores more TCE than the secondary root tissue on a volumetric basis. This is because the fine root tissue is saturated in contaminant due to mass flow through it while the secondary root tissue takes up contaminant through indirect flow. Therefore, as the fine root decreases, the amount of TCE passing into the xylem increases and subsequently increases TCE transpiration. In a real world system this behavior is expected for the same reasons. Overall, model TCE uptake is insensitive and

model TCE transpiration is slightly sensitive to the Secondary Growth to Fine Root Ratio.

Figures 4.27 and 4.28 represent the sensitivity of the model to variation in the flow of contaminant into root compartments.

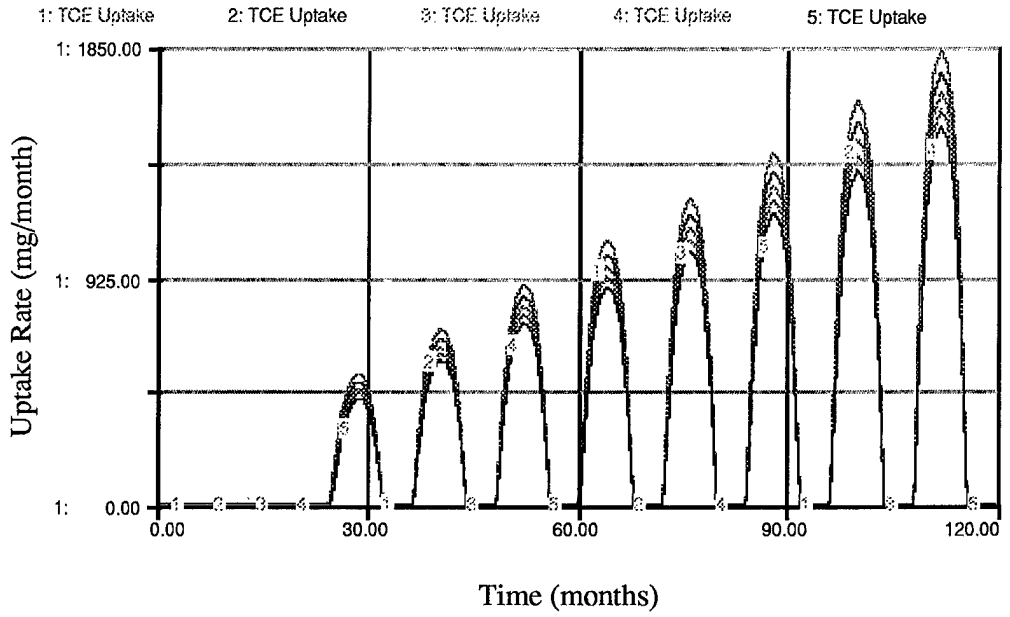

Figure 4.27 TCE Uptake Sensitivity to the Fine Root Flow Weight

The Fine Root Flow Weight represents the percentage of water uptake by fine roots. Literature values for fine root uptake ranged from 2% to 70% of the total uptake. Values used in Figure 4.27 were as follows: 1) 0.02, 2) 0.19, 3) 0.36, 4) 0.53, and 5) 0.70. TCE uptake by the model proved sensitive to changes in the fine root flow weight; at year 10 the difference between the highest and lowest parameters was approximately 18%. Fine Root Flow Weight only influences Fine Root Uptake Coefficient. The Fine Root Uptake Coefficient separates the flow into the respective rhizosphere compartments. It does not

affect the Fine Root Volume Coefficient, which separates the rhizosphere volume between root compartments. Because of this, the Fine Root Volume Coefficient can be assumed as constant in this sensitivity test while the Fine Root Volume Coefficient varies with the Fine Root Flow Weight. Because of this, as the Fine Root Flow Weight increases into the fine roots, the uptake will decrease, since the fine root zone has a much larger volume than the secondary growth root. The larger fine root volume slows the increase of the TCE concentration in the fine root rhizosphere, and therefore decreases TCE uptake.

In a real world system, with increased flow into the same volume of fine roots, the same behavior is expected. The larger surface are of fine roots would result in a slower build up of the TCE concentration in its rhizosphere, decreasing TCE uptake as the flow into the fine root rhizosphere increases.

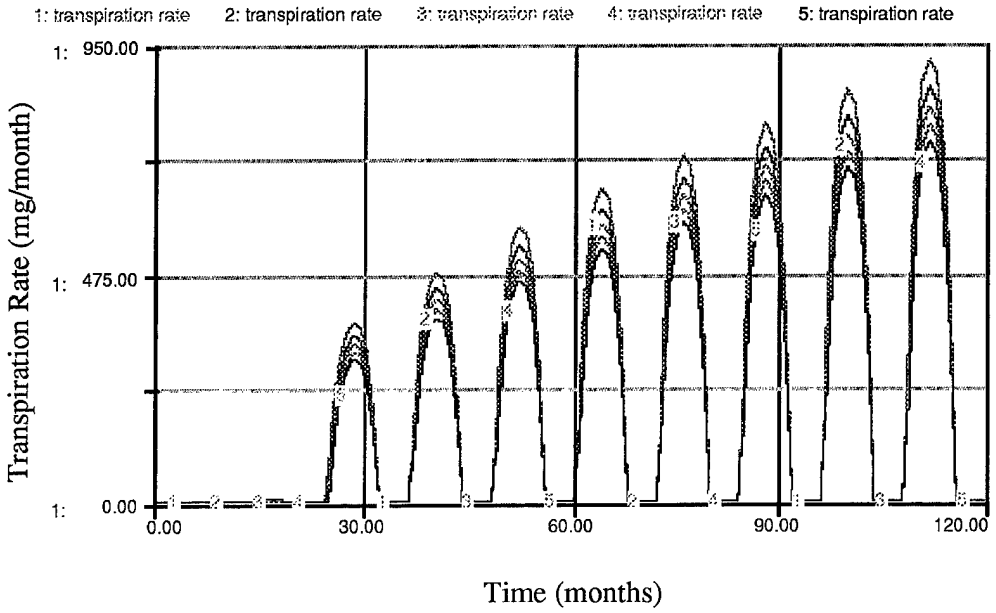

Figure 4.28 TCE Transpiration Sensitivity to the Fine Root Flow Weight

TCE transpiration was then tested with variation in the Fine Root Flow Weight. Values used were the same as in Figure 4.27. TCE transpiration was somewhat more sensitive to the Fine Root Flow Weight than TCE uptake; at year 10 the difference between the highest and lowest parameters was approximately 20%. As the uptake into the fine roots decreases, the ratio of TCE stored in fine root tissue versus what passes through increases. This results in the slight divergence of the output in Figure 4.28. Since the same process would take place in a real world system, the same results are expected. Overall, TCE uptake and transpiration proved sensitive to the Fine Root Flow Weight.

Figure 4.29 represents the sensitivity of the model to the thickness of the rhizosphere.

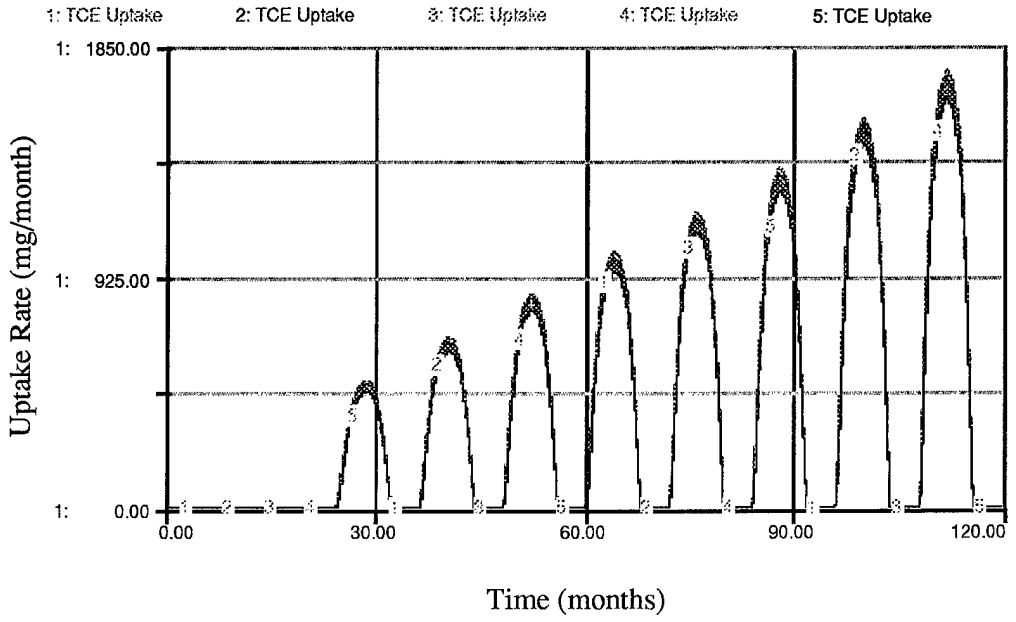

Figure 4.29 TCE Uptake Sensitivity to Rhizosphere Thickness

The thickness of the rhizosphere was varied from literature values of 2 mm to 5 mm. Values used in Figure 4.29 were as follows: 1) 0.2 cm, 2) 0.2625 cm, 3) 0.35 cm, 4) 0.4375 cm, and 5) 0.5 cm. TCE uptake proved slightly sensitive to variation in the rhizosphere thickness; at year 10 the difference between the highest and lowest parameters was less than 1%. This slight sensitivity was expected, since the surface area of the roots or rhizoplane is very large in respect to the rhizosphere thickness. This means the rhizoplane will dominate the calculated volume. Over time the effect of the variation in the rhizosphere thickness will become more pronounced. This is due to the flow into the rhizosphere escalating faster than root growth. This in turn causes the TCE rhizosphere concentration to increase, which increases saturable uptake (See equation 1). Overall, the model was slightly sensitive to changes in rhizosphere thickness.

Figure 4.30 represents the sensitivity of the model to V_{max}, a parameter used in the saturable uptake equation.

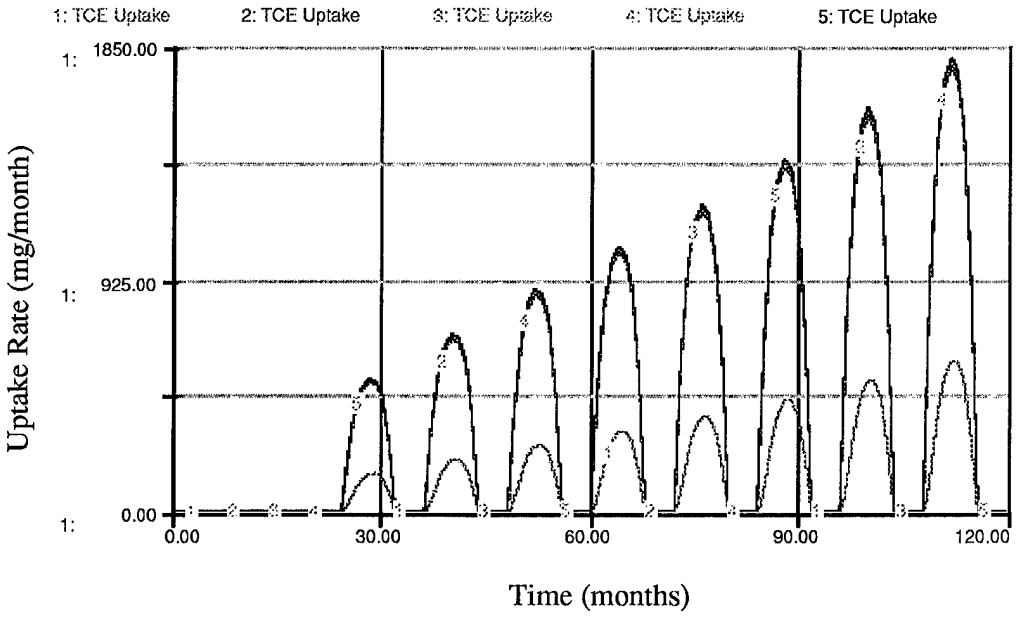

Figure 4.30 TCE Uptake Sensitivity to V_{max} at a Ground Water TCE Concentration of 605 ppb

Values used in Figure 4.30 were as follows: 1) 1, 2) 50, 3) 100, 4) 150, and 5) 200 mg TCE/(kg plant-month). Only at the lowest value of V_{max} was there a noticeable difference in the uptake of TCE. Since the ground water concentration in this scenario was set at 605 ppb, the rhizosphere concentration does not increase enough for the uptake per mass of plant to reach the V_{max} value (See Figure 3.3). In fact, the rhizosphere concentration does not reach the K_m value of 75,000 mg TCE/m^3. This means the uptake values are very low in comparison to V_{max}, and at this low concentration, curves with V_{max} values varying from 50 to 200 mg TCE/(kg plant-month) follow a similar path. At higher ground water concentrations, it is expected the variation between the uptake

rates with changing V_{max} values will become more marked. Figure 4.31 tests this theory.

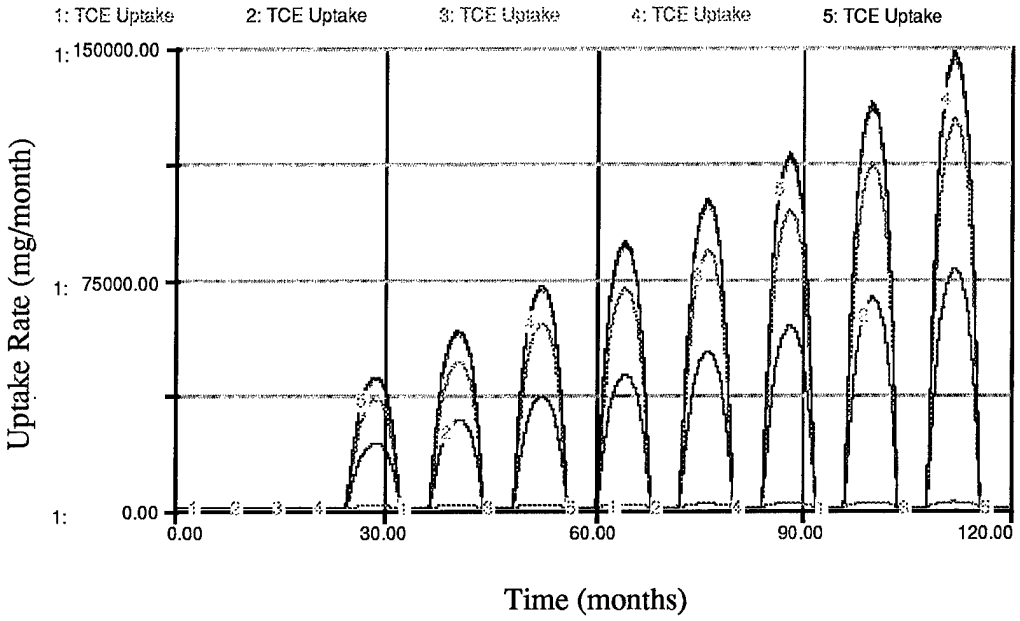

Figure 4.31 TCE Uptake Sensitivity to V_{max} at a Ground Water TCE Concentration of 50 ppm

As expected, Figure 4.31 shows with an increased ground water concentration of 50 ppm, the variation in uptake is marked, except for at the highest V_{max} values of 150 and 200 mg TCE/(kg plant-month). As the ground water TCE concentration is increased further, the rhizosphere concentration will also increase, causing even the highest values of V_{max} to diverge. By varying the V_{max} value, as well as the ground water concentrations, the model was shown to be sensitive to this parameter; at year 10 the difference between the highest and lowest parameters was approximately 69% at a ground water

concentration of 605 ppb and approximately 99% at a ground water concentration of 50 ppm.

Figure 4.32 represents the sensitivity of the model to K_m, a parameter used in the saturable uptake equation.

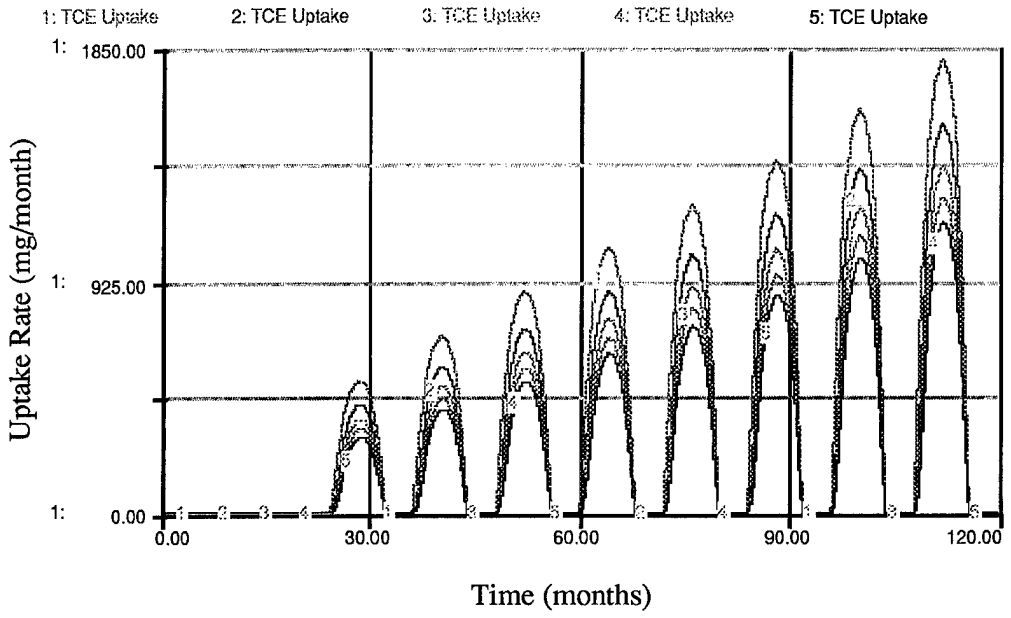

Figure 4.32 TCE Uptake Sensitivity to K_m

Values used in Figure 4.32 were as follows: 1) 7,500, 2) 193,125, 3) 378,750, 4) 564375, and 5) 750,000 mg TCE/m^3. The model proved itself sensitive to this parameter; at year 10 the difference between the highest and lowest parameters was approximately 38%.

Figure 4.33 represents the sensitivity of the model to changes in the TCE ground water concentration.

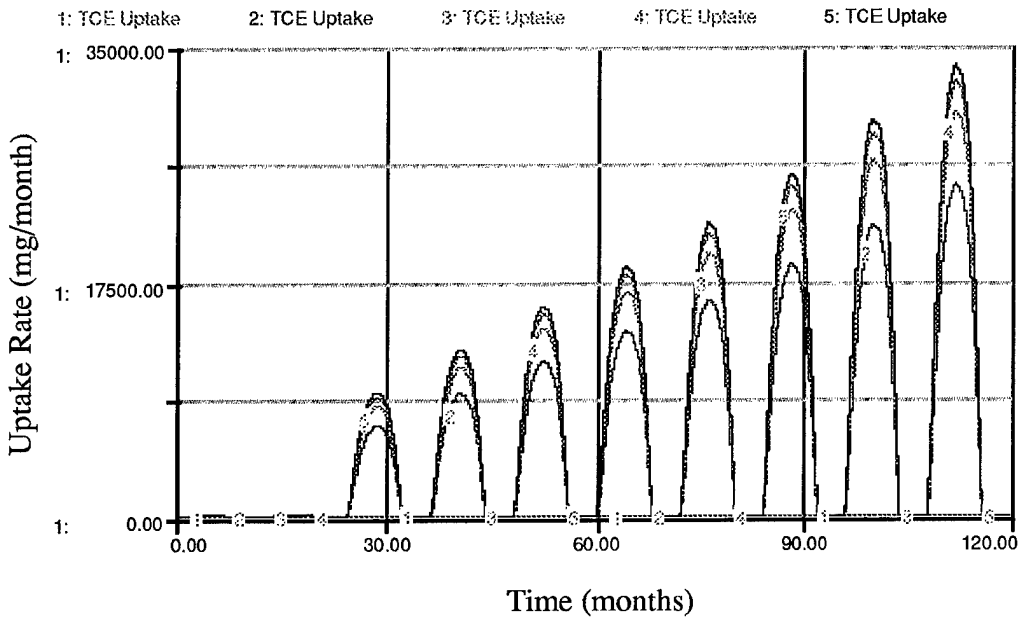

Figure 4.33 TCE Uptake Sensitivity to TCE Ground Water Concentration

The TCE ground water concentration was varied from known values found in the field and used in research studies. Values used in Figure 4.33 were as follows: 1) 0 ppm, 2) 12,500 ppm, 3) 37,500 ppm, 4) 50,000 ppm, and 5) 50,000 ppm. TCE uptake proved sensitive to variation in the TCE ground water concentration; at year 10 the difference between the highest and lowest parameters was 100%. With increasing TCE ground water concentration, uptake increases, approaching a maximum value. This was due to contaminant saturating uptake.

Figure 4.34 represents the sensitivity of the model to changes in the ground water depth.

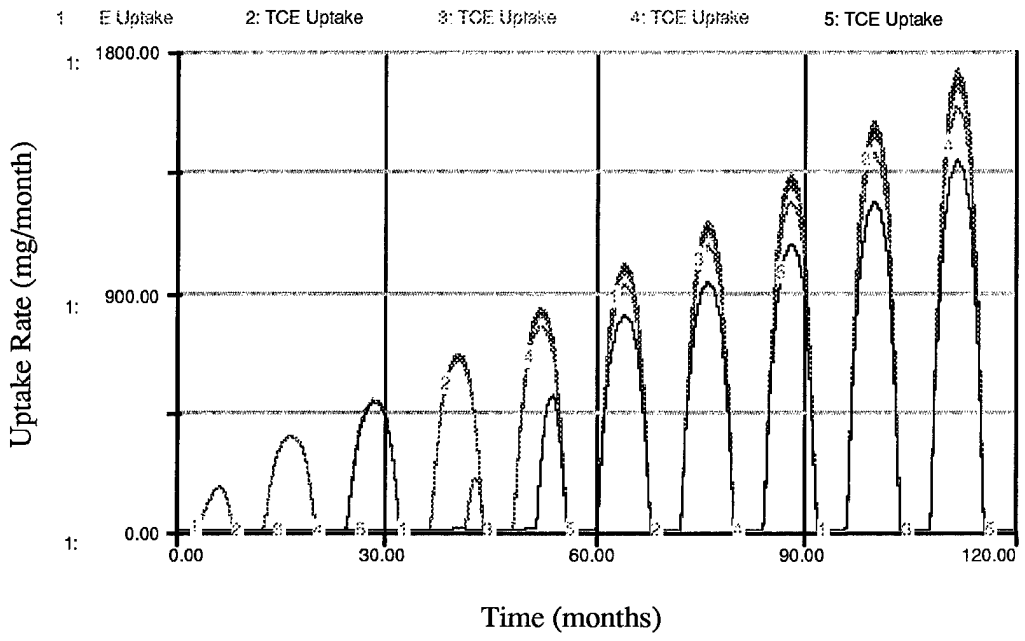

Figure 4.34 TCE Uptake Sensitivity to Ground Water Depth

The ground water depth was varied from known values capable of sustaining phreatophytic growth. Values used in Figure 4.34 were as follows: 1) 1 m, 2) 3.25 m, 3) 5.5 m, 4) 7.75 m, and 5) 10 m. TCE uptake proved sensitive to variation in the ground water depth; at year 10 the difference between the highest and lowest parameters was approximately 25%. In the first five years there was a great deal of variability in the output. This was due to the changing ground water depth. The capillary fringe was held constant at a value of 1 meter, so with increasing ground water depth, the root took longer to reach the higher TCE concentration in the capillary fringe. Also, with increasing ground water depth, more root volume occupied the unsaturated zone, so total TCE uptake decreased.

Figure 4.35 represents the sensitivity of the model to changes in the unsaturated/capillary fringe soil thickness.

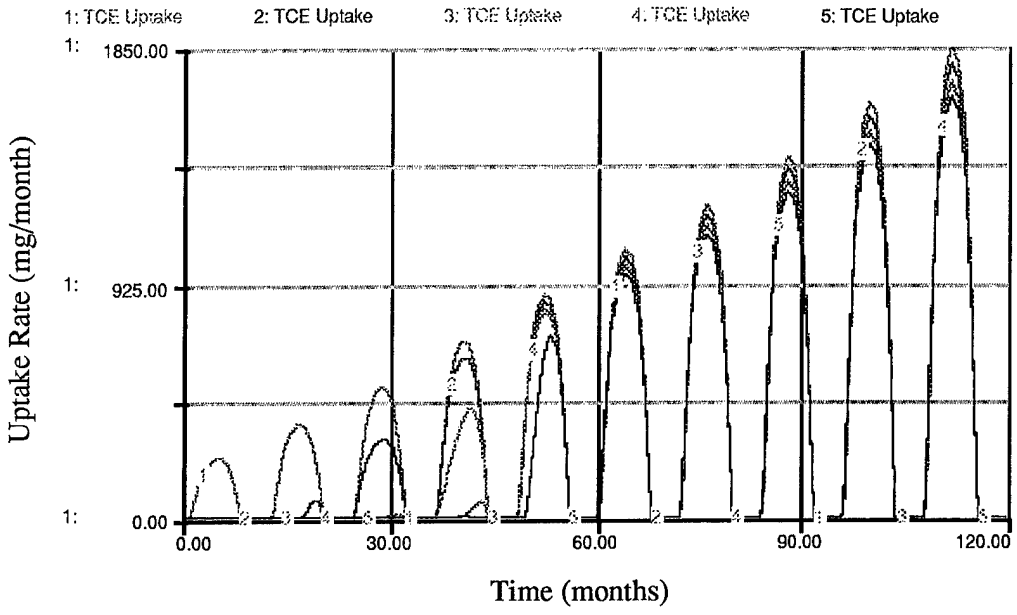

Figure 4.35 TCE Uptake Sensitivity to Unsaturated/Capillary Fringe Soil Thickness

The unsaturated zone and capillary fringe soil thickness were varied from known values capable of sustaining phreatophytic growth. Values used in Figure 4.35 were as follows: Unsaturated Zone Thickness - 1) 0.5 m, 2) 2.75 m, 3) 5.0 m, 4) 7.25 m, and 5) 9.5 m; Capillary Fringe Thickness - 1) 10 m, 2) 7.75 m, 3) 5.5 m, 4) 3.25 m, and 5) 1 m. TCE uptake proved slightly sensitive to variation in the ground water depth; at year 10 the difference between the highest and lowest parameters was approximately 13%. In the first five years there was a great deal of variability in the output. This was due to the changing depth of the capillary fringe. As the capillary fringe decreased, the root took longer to reach the higher TCE concentration in this soil horizon. Also, with

decreasing capillary fringe thickness, more root volume occupied the unsaturated zone, so total TCE uptake decreased.

Soft Parameter Sensitivity. This test will cover all parameters in Table 3.2. Unless otherwise noted, the TCE ground water concentration was set at 605 ppb, the ground water depth was set at 3.3 meters, and the time frame of interest was set at 120 months or 10 years. The first two values correspond with average values found at Air Force Plant 4.

Figure 4.36 represents the sensitivity of the model to the xylem and phloem volume in the leaf. TCE transpiration was selected as the output for this scenario since this parameter is part of the TCE transpiration equation and does not effect TCE uptake.

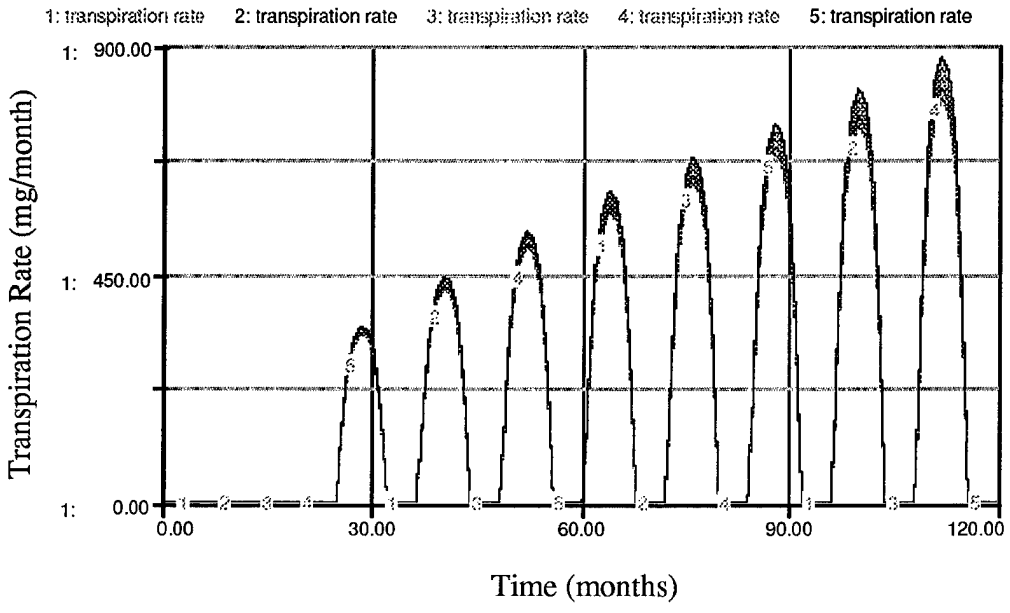

Figure 4.36 TCE Transpiration Sensitivity to the Leaf Vascular Ratio

The Leaf Vascular Ratio represents the amount of xylem and phloem vascular elements in the leaf. Since this was an approximated value, the expected value of the Leaf Vascular Ratio was varied by a factor of 5. Values used in Figure 4.36 were as follows: 1) 0.01, 2) 0.0325, 3) 0.05, 4) 0.0775, and 5) 0.1. With an increase in the vascular volume the flow of TCE into the leaf increased, and therefore, increased the amount and concentration of TCE in the leaf tissue. This in turn increased the TCE transpiration rate. TCE transpiration by the model proved slightly sensitive to changes in the Leaf Vascular Ratio; at year 10 the difference between the highest and lowest parameters was approximately 11%.

Figure 4.37 represents the sensitivity of the model to variation in the flow rate coefficient. TCE transpiration was selected as the output for this scenario since this parameter is part of the TCE transpiration equation and does not affect TCE uptake.

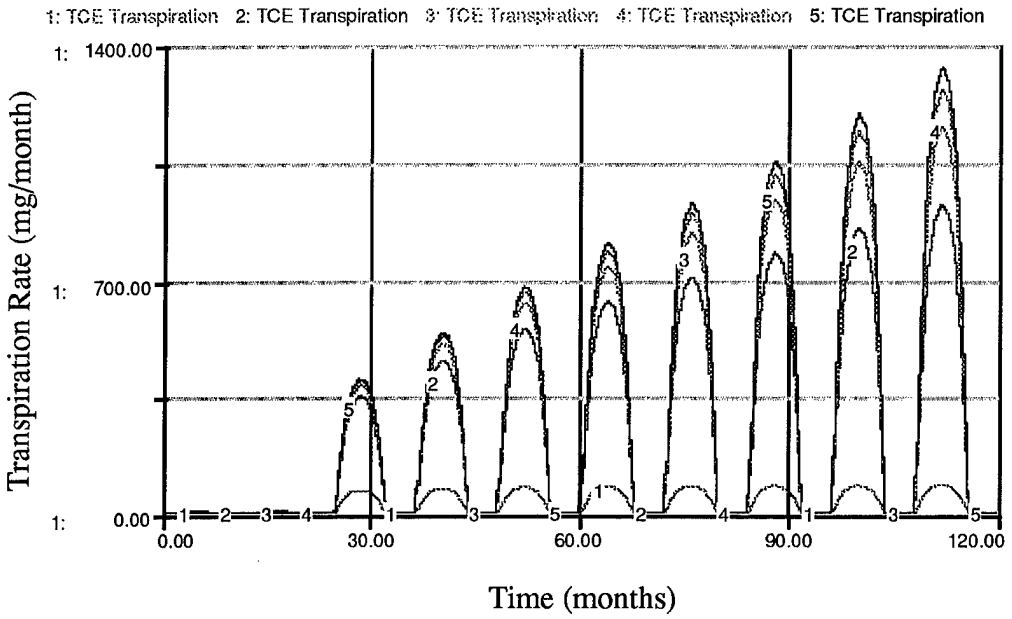

Figure 4.37 TCE Transpiration Sensitivity to the Leaf Air Transfer Rate Coefficient

The Leaf Air Transfer Rate Coefficient was used in the flow equation between the leaf and air (See equation 11). In the Behavior Anomaly Test, the upper and lower bounds for this parameter were identified as 5 and .05, so these were the values used in this sensitivity analysis. Values used in Figure 4.37 were as follows: 1) 0.05 m^3/month, 2) 1.29 m^3/month, 3) 2.53 m^3/month, 4) 3.76 m^3/month, and 5) 5 m^3/month. This variable strongly influenced the flow equation. TCE transpiration by the model proved sensitive to changes in the Leaf Air Transfer Rate Coefficient; at year 10 the difference between the highest and lowest parameters was approximately 90%.

Figure 4.38 represents the sensitivity of the model to metabolism of TCE in the leaf tissue. TCE transpiration was selected as the output for this scenario since the parameter does not affect the uptake of TCE.

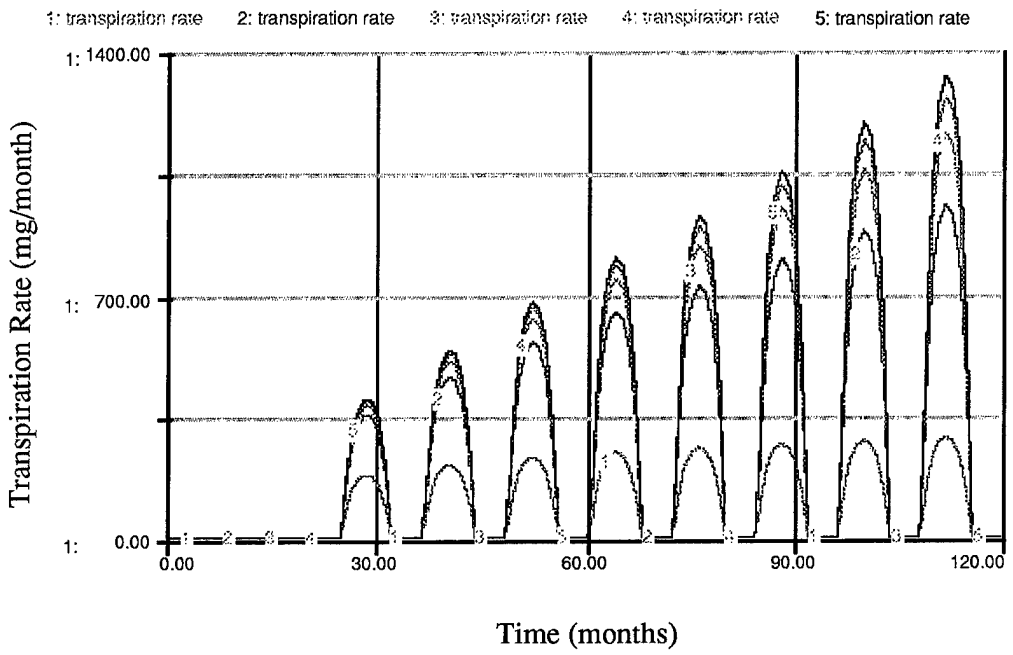

Figure 4.38 TCE Transpiration Sensitivity to the Leaf TCE Half Life

The Leaf TCE Half Life represents the half life of TCE in the leaf of the phreatophytic tree. This variable is used in equation 12 to represent the metabolism of TCE in the leaf tissue. The expected value for the Leaf TCE Half Life was varied by a factor of 5. Values used in Figure 4.38 were as follows: 1) 0.0133 months, 2) 0.0934 months, 3) 0.0667 months, 4) 0.253 months, and 5) 0.334 months. As the half life increases, less TCE is metabolized in the leaf, therefore, more TCE is available for transpiration. The transpiration rate approaches a maximum with an increase in Leaf TCE Half Life. TCE transpiration by the model proved sensitive to changes in the Leaf TCE Half Life; at year 10 the difference between the highest and lowest parameters was approximately 25%.

Figure 4.39 represents the sensitivity of the model to variation in metabolism in the stem and root. TCE transpiration was selected as the output for this scenario since these parameters are not coupled with TCE uptake.

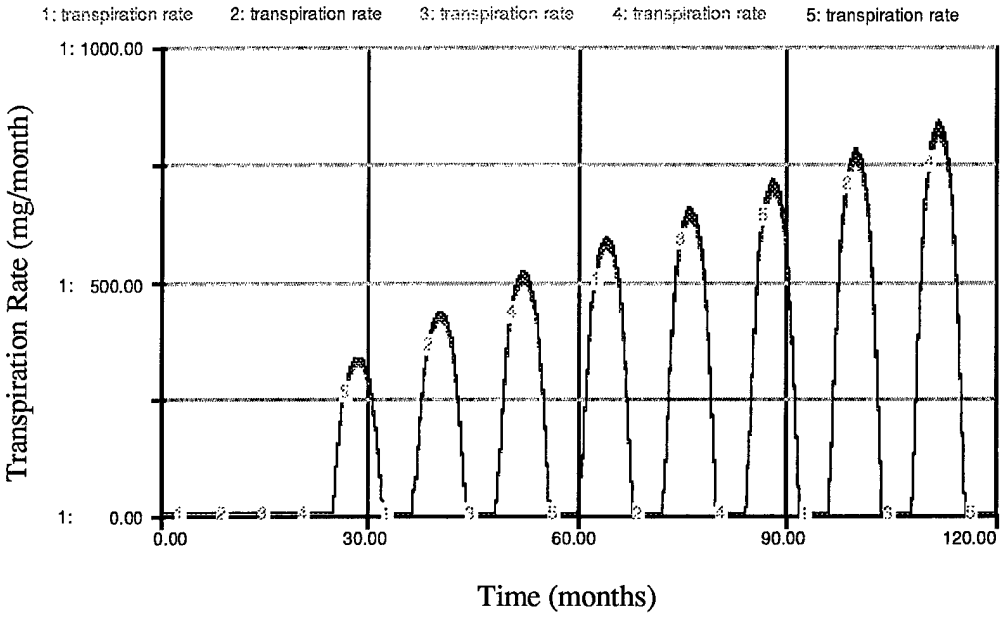

Figure 4.39 TCE Transpiration Sensitivity to the Stem and Root TCE Half Lives

The Stem TCE Half Life and Root TCE Half Life represent the half lives of TCE in the stem and root of the phreatophytic tree, respectively. These parameters were used in equation 12 to represent the metabolism of TCE in the stem and root tissue. Their analysis was aggregated because they do not directly influence the transpiration of TCE from the phreatophytic tree. Expected values for the Stem and Root TCE Half Lives were varied by a factor of 5. Values used in Figure 4.39 were as follows: Stem TCE Half Life - 1) 0.2 month, 2) 0.6 month, 3) 1.0 month, 4) 3 months, and 5) 5 months; Root TCE Half Life - 1) 0.1 month, 2) 0. 3 month, 3) 0.5 month, 4) 0.75 month, and 5) 1.0 month.

With an increase in the Stem and Root TCE Half Lives, the xylem flow TCE concentration increases slightly, increasing the rate of transpiration of TCE. TCE transpiration by the model proved insensitive to changes in the Stem and Root TCE Half Lives; at year 10 the difference between the highest and lowest parameters was approximately 5%.

Figure 4.40 represents the sensitivity of the model to variation in the various transfer rate coefficients in the stem and root of the phreatophytic tree. TCE transpiration was selected as the output for this scenario since these parameters do not affect TCE uptake.

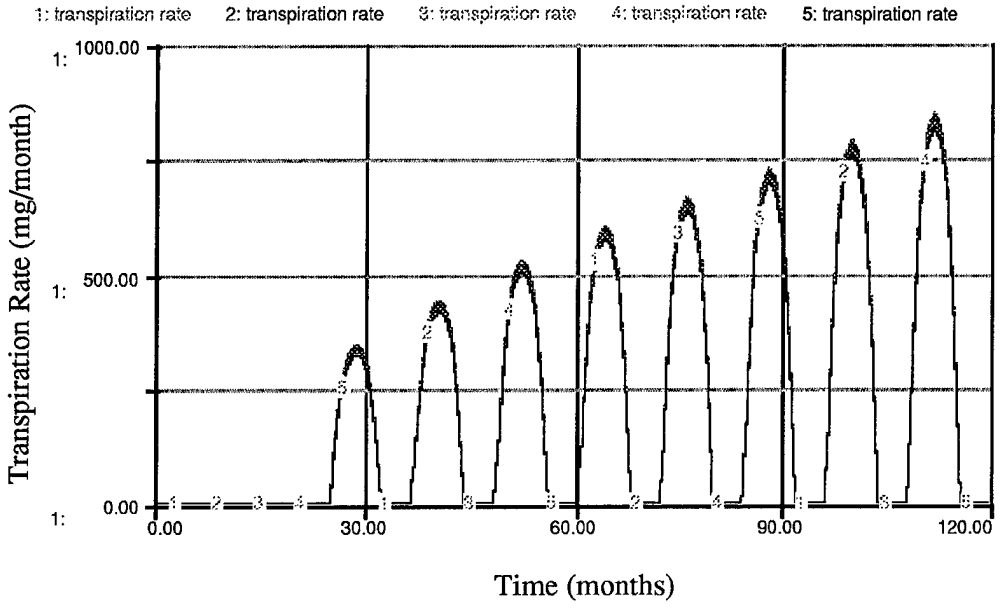

Figure 4.40 TCE Transpiration Sensitivity to the Stem, Phloem, and Root Transfer Rate Coefficients

The Stem, Phloem, and Root Transfer Rate Coefficients were used in equation 10 to represent the flow of TCE between various compartments in the plant. Their analysis was aggregated because they do not directly influence the

transpiration of TCE from the phreatophytic tree. Due to the approximate nature of these variables, expected values for the Stem, Phloem, and Root Transfer Rate Coefficients were varied by a factor of 10. Values used in Figure 4.40 were as follows: Stem Flow Rate Coefficient - 1) 0.006 m^3/month, 2) 0.033 m^3/month, 3) 0.06 m^3/month, 4) 0.33 m^3/month, and 5) 0.6 m^3/month; Root Flow Rate Coefficient - 1) 0.006 m^3/month, 2) 0.033 m^3/month, 3) 0.06 m^3/month, 4) 0.033 m^3/month, and 5) 0.6 m^3/month; Phloem Flow Rate Coefficient - 1) 0.0005 m^3/month, 2) 0.00075 m^3/month, 3) 0.001 m^3/month, 4) 0.00055m^3/month, and 5) 0.01 m^3/month. With an increase in these transfer rate coefficients, the xylem flow TCE concentration decreased slightly. This decrease resulted in the amount of TCE transpired to decrease slightly. TCE transpiration by the model proved insensitive to these variables, even when aggregated and varied to extremes. At year 10 the difference between the highest and lowest parameters was approximately 5%

Figure 4.41 represents the sensitivity of the model to variation in the tissue volume coefficient in the root. TCE transpiration was selected as the output for this scenario since these parameters do not affect TCE uptake.

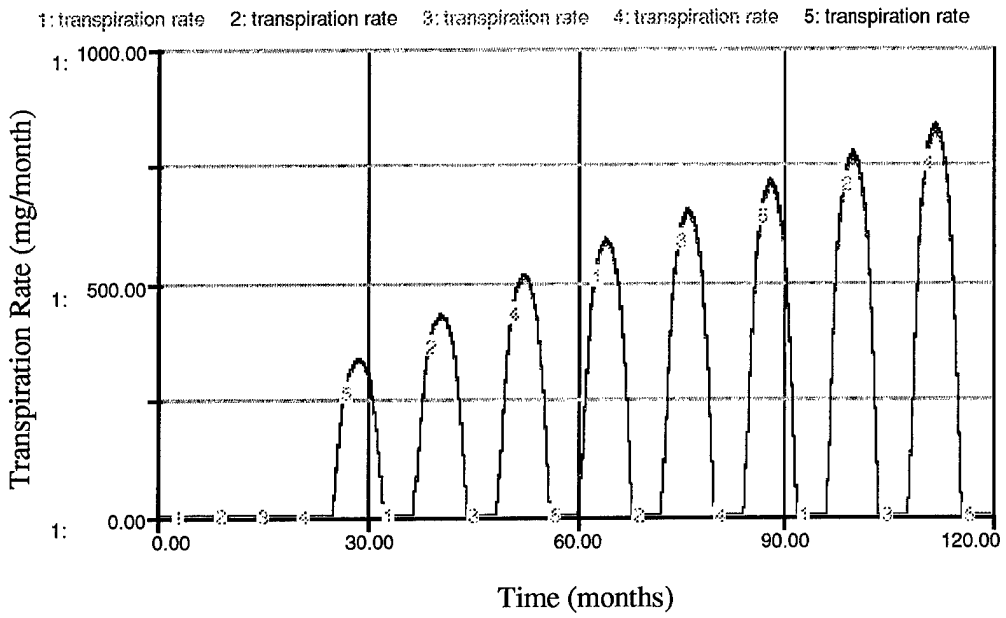

Figure 4.41 TCE Transpiration Sensitivity to the Fine Root and Secondary Root Tissue Volume Coefficients

The Fine Root and Secondary Root Tissue Volume Coefficients were used in several root flow equations to represent the limited flow through living or symplast root tissue and their apoplast or cell wall tissue. Since flow is limited through the cell vacuole, these coefficients represent the volume of symplast and apoplast tissue available for flow. The analysis of these variables was aggregated because they do not directly influence the transpiration of TCE from the phreatophytic tree. Expected values for the Fine Root and Secondary Root Tissue Volume Coefficients were varied from 50% to 150%. Values used in Figure 4.41 were as follows: Fine Root Tissue Volume Coefficient - 1) 0.2, 2) 0.25, 3) 0.3, 4) 0.35, and 5) 0.4; Secondary Root Tissue Volume Coefficient - 1) 0.2, 2) 0.25, 3) 0.3, 4) 0.35, and 5) 0.4. As expected, TCE transpiration by the model proved insensitive to changes in the Fine Root and Secondary Root

Tissue Volume Coefficients; at year 10 the difference between the highest and lowest parameters was approximately 3%.

Figure 4.42 represents the sensitivity of the model to the ratio of fine root tissue to fine root xylem. TCE transpiration was selected as the output for this scenario since this parameter does not affect TCE uptake.

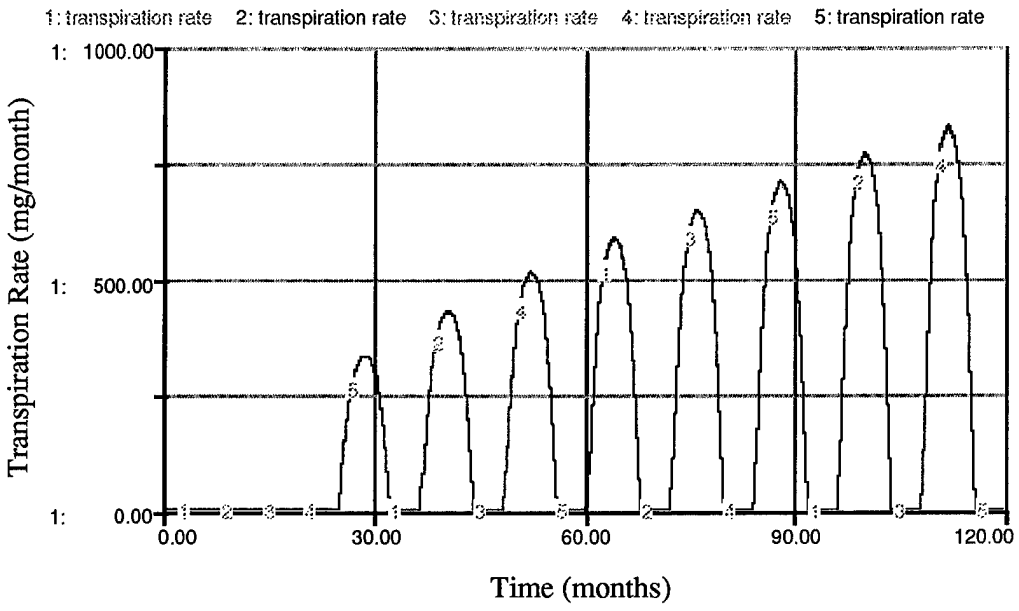

Figure 4.42 TCE Transpiration Sensitivity to the Fine Root to Fine Root Xylem Ratio

The Fine Root to Fine Root Xylem Ratio was used in the fine root flow equation to represent the amount of fine root xylem in the fine roots. Expected values for the Fine Root to Fine Root Xylem Ratio were varied from 50% to 150%. Values used in Figure 4.42 were as follows: 1) 0.0667, 2) 0.1, 3) 0.133, 4) 0.167, and 5) 0.2. As expected, TCE transpiration by the model proved

insensitive to changes in the Fine Root to Fine Root Xylem Ratio; at year 10 the difference between the highest and lowest parameters was 0%.

Figure 4.43 represents the sensitivity of the model to diffusion of TCE from the rhizosphere.

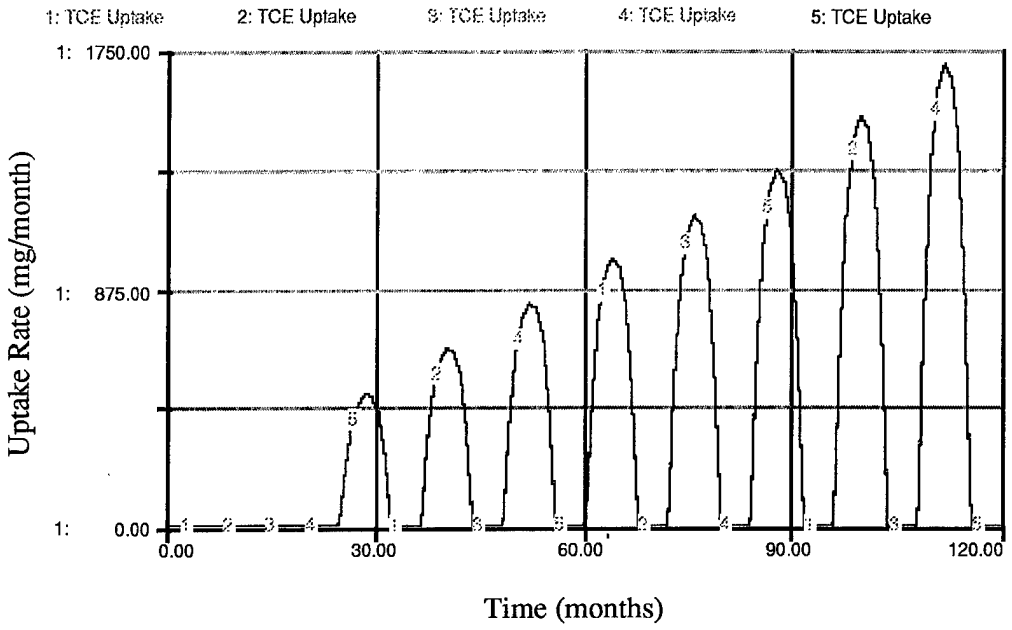

Figure 4.43 TCE Uptake Sensitivity to the Rhizosphere Diffusion Coefficient

The Rhizosphere Diffusion Coefficient was used to represent the diffusion of TCE from the rhizosphere at the end of the growing season, during the dormant months, and at the beginning of the growing season. Due to the uncertainty of this variable, the expected values for the Rhizosphere Diffusion Rate was varied by a factor of 10. Values used in Figure 4.43 were as follows: 1) 0.0001 m^3/month, 2) 0.00055 m^3/month, 3) 0.001 m^3/month, 4) 0.0055 m^3/month, and 5) 0.01 m^3/month. As expected, TCE uptake by the model

proved insensitive to changes in the Rhizosphere Diffusion Rate; at year 10 the difference between the highest and lowest parameters was 0%.

Table 4.1 and 4.2 show the results of the sensitivity tests on the parameters used in the model. Table 4.1 covers the sensitivity of the model to literature parameters and Table 4.2 covers the sensitivity of the model to soft parameters. The second column, Level of Parameter Precision, gives a weight of the precision with which the parameter was established. Parameters established from literature with little error in their bounds were weighted as high, parameters from literature with a great deal of variance and soft parameters based on expert opinion with a small variance were weighted as moderate, and soft parameters based on intuition were weighted as low. The third column, Model Process Assessed, refers to the mechanism assessed in the sensitivity test, either TCE uptake or transpiration. The last column, Percent Difference Between Highest to Lowest Parameter, shows the results of the sensitivity analysis. The value shows the percent difference in uptake or transpiration output between the highest to lowest parameter run in the test at the tenth season. By looking at these percentages, an idea of the most influential parameters on the model is possible. Also, the parameters level of precision can also be established. Parameters can then be ranked from those most sensitive and with the least amount of precision to those least sensitive with the greatest precision. An idea of the parameters needing further analysis will then be known.

LITERATURE PARAMETERS			
Parameter	**Level of Parameter Precision**	**Model Process Assessed**	**% Difference High to Low Parameter**
Rhizosphere TCE Half Life	moderate	uptake	13%
Leaf Air Partition Coefficient	moderate	transpiration	0%
TCE Air Background Concentration	high	transpiration	0%
Leaf Partition Coefficient	moderate	transpiration	0%
Xylem Flow Rate/Leaf Area	moderate	uptake/transpiration	81%/81%
Phloem Flow Rate/Leaf Area	moderate	transpiration	0%
Leaf Density	high	uptake/transpiration	9%/7%
Stem Partition Coefficient	moderate	transpiration	3%
Secondary Growth Root to Fine Root Ratio	high	uptake/transpiration	0%/6%
Secondary Growth Root Partition Coefficient	moderate	transpiration	3%
Fine Root Partition Coefficient	moderate	transpiration	3%
Secondary Growth Root Flow Weight	moderate	uptake/transpiration	18%/20%
Fine Root Flow Weight	moderate	uptake/transpiration	18%/20%
Rhizosphere Thickness	moderate	uptake	<1%
V_{max}	moderate	uptake	69-99%
K_m	moderate	uptake	38%
Capillary Fringe Soil Thickness	high	uptake	13%
TCE Concentration in GW	high	uptake	100%
Depth to GW	high	uptake	25%

Table 4.1 Sensitivity of Literature Parameters

SOFT PARAMETERS			
Parameter	**Level of Parameter Precision**	**Model Process Assessed**	**% Difference High to Low Parameter**
Leaf Vascular Ratio	moderate	transpiration	11%
Leaf Air Transfer Rate Coefficient	low	transpiration	90%
Leaf TCE Half Life	moderate	transpiration	25%
Stem Xylem Transfer Rate Coefficient	low	transpiration	5%
Phloem Xylem Transfer Rate Coefficient	low	transpiration	5%
Stem Density	moderate	uptake/transpiration	9%/7%
Stem TCE Half Life	moderate	transpiration	5%
Root TCE Half Life	moderate	transpiration	5%
Root Xylem Transfer Rate Coefficient	low	transpiration	5%
Fine Root Tissue Volume Coefficient	moderate	transpiration	3%
Fine Root to Fine Root Xylem Ratio	low	transpiration	0%
Secondary Growth Tissue Volume Coefficient	moderate	transpiration	3%
Secondary Growth Root Density	moderate	uptake/transpiration	9%/7%
Root Hair Density	moderate	uptake/transpiration	9%/7%
Rhizosphere Diffusion Coefficient	low	uptake	0%

Table 4.2 Sensitivity of Soft Parameters

Changed-Behavior Prediction. Parameters tested under Changed-Behavior Prediction were already tested under the Extreme Conditions Test. Figures 4.1 and 4.2 represent the changed behavior of TCE uptake and transpiration with extremes of the TCE ground water concentration. At a TCE ground water concentration of 0 ppm (Figure 4.1), there is no TCE uptake and

TCE transpiration is reversed, due to the air background TCE concentration flowing into the tree. At a TCE ground water concentration of 100 ppm (Figure 4.2), TCE uptake and transpiration is significant. The output between these two figures changes drastically, showing the ability of the model to produce changed behavior under differing contaminant ground water concentrations.

Figures 4.3 and 4.4 represent the changed behavior of TCE uptake and transpiration with extremes of the unsaturated soil, capillary fringe, and ground water depth. At an unsaturated soil depth of 0 meters and the capillary fringe and ground water depth set to 1 meter (Figure 4.3), the tree root immediately contacts the capillary fringe. Due to the higher TCE concentration in the capillary fringe, TCE uptake and transpiration are significant. At an unsaturated soil depth of 10 meters, a capillary fringe depth of .5 meters, and the ground water depth set to 10.5 meters (Figure 4.4), the tree root must grow through a great deal of unsaturated soil to reach the capillary fringe. This results in a delay of several years before the TCE jumps due contact with the capillary fringe. Also, since a larger portion of the root is in the unsaturated soil TCE uptake does not increase to the same level as in the prior figure. Once again, the model showed its ability to portray different TCE uptake and transpiration output with changes in hydrogeological characteristics.

Additional Validity Tests.

Test of Site Parameters. By testing site parameters, an idea of the sensitivity of the model to these parameters was established. Unless

otherwise noted, the capillary fringe thickness was set at 0.605 meters; the TCE ground water concentration was set at 605 ppb; and the depth to ground water was set at 3.3 meters. Parameters analyzed in this test were the capillary fringe thickness, TCE ground water concentration, and depth to ground water.

Figure 4.44 represents the sensitivity of the model to variation in the capillary fringe thickness at Air Force Plant 4.

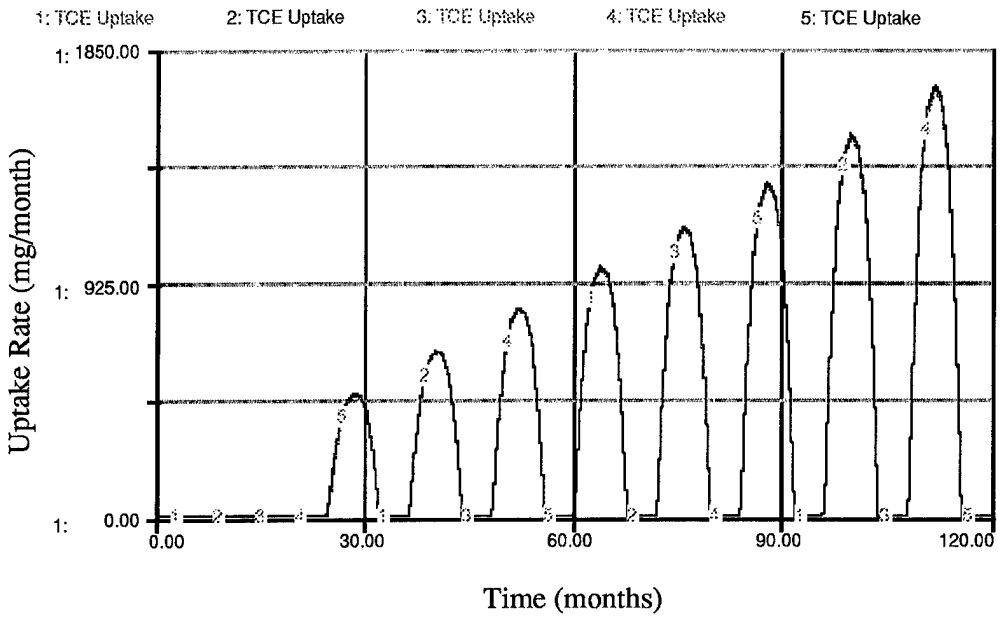

Figure 4.44 TCE Uptake Sensitivity to the Capillary Fringe Thickness at AF Plant 4

The capillary fringe at Air Force Plant 4 was estimated, through expert opinion, to vary from 0.45 to 0.76 meters. Values used in Figure 4.44 were as follows: 1) 0.45 meters, 2) 0.528 meters, 3) 0.605 meters. 4) 0.683 meters, and 5) 0.76 meters. As the Capillary Fringe Thickness at AF Plant 4 increased in thickness, the TCE uptake showed an almost negligible increase. This was due to a larger portion of the root existing in the capillary fringe and therefore

increasing TCE uptake. Also, the root reached the capillary fringe slightly sooner in year three as the capillary fringe thickness increased. Overall, TCE uptake by the model proved insensitive to changes in the Capillary Fringe Thickness at AF Plant 4; at year 10 the difference between the highest and lowest parameters was 0%.

Figure 4.45 represents the sensitivity of the model to variation in TCE ground water concentration at Air Force Plant 4.

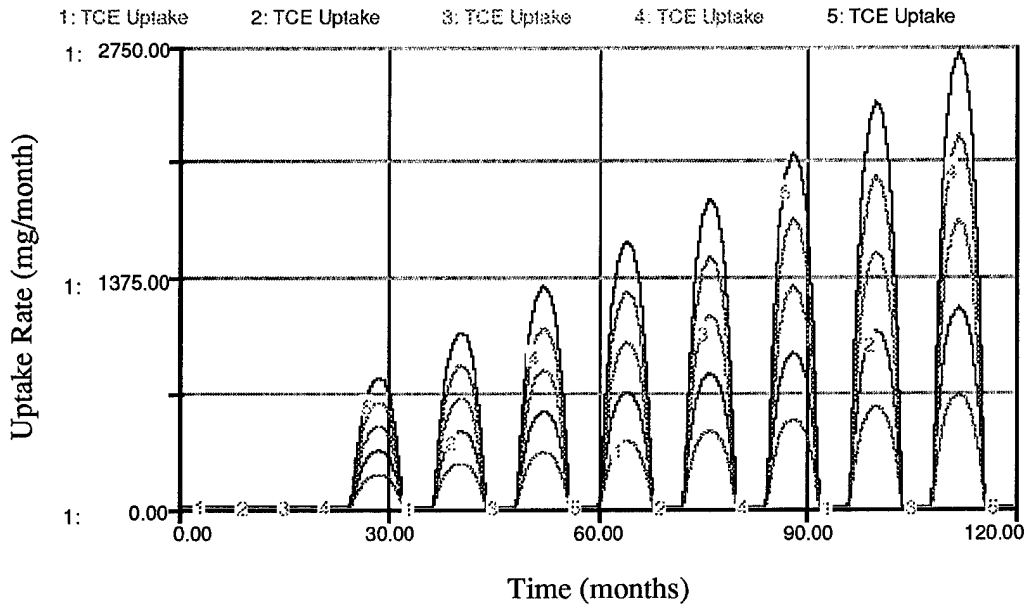

Figure 4.45 TCE Uptake Sensitivity to the TCE Ground Water Concentration at AF Plant 4

The TCE ground water concentration at Air Force Plant 4 was found, through field analysis, to vary from 240 ppb to 970 ppb. Values used in Figure 4.45 were as follows: 1) 240 ppb, 2) 423 ppb, 3) 605 ppb. 4) 788 ppb, and 5) 970 ppb. As the TCE Ground Water Concentration at AF Plant 4 increases, the flow into the rhizosphere increases. This in turn increases the TCE rhizosphere

concentration which in turn increases TCE uptake. Because of this, the incremental behavior in output is expected. As the uptake is saturated and the tree reaches maturity, it is anticipated the values will all approach the same maximum value. TCE uptake by the model proved sensitive to changes in the TCE Ground Water Concentration at AF Plant 4; at year 10 the difference between the highest and lowest parameters was approximately 25%.

Figure 4.46 represents the sensitivity of the model to variation in depth to ground water at Air Force Plant 4.

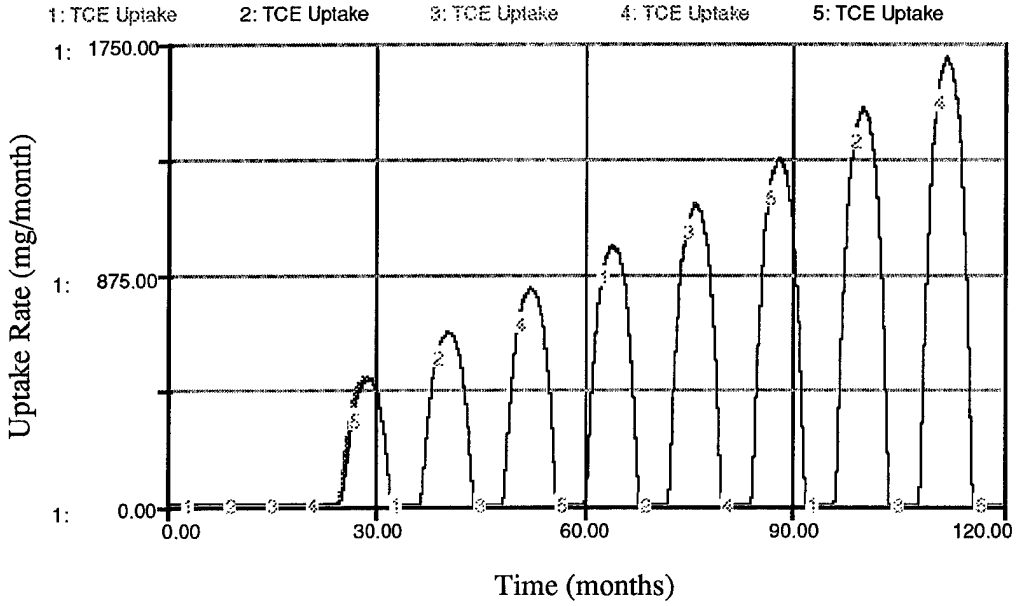

Figure 4.46 TCE Uptake Sensitivity to the Depth to Ground Water at AF Plant 4

The Depth to Ground Water at Air Force Plant 4 was found, through field analysis, to vary from 3.05 meters to 3.65 meters. Values used in Figure 4.46 were as follows: 1) 3.05 meters, 2) 3.20 meters, 3) 3.3 meters. 4) 3.50 meters, and 5) 3.65 meters. With increasing depth to ground water, the root takes

slightly longer to reach the capillary fringe, which is held at a constant value. This causes the slight change in TCE uptake at the beginning of year 3. The slightly larger amount of unsaturated soil versus capillary fringe soil is not of enough significance to alter the uptake of TCE over time. TCE uptake by the model proved insensitive to changes in the Depth to Ground Water at AF Plant 4; at year 10 the difference between the highest and lowest parameters was 0%.

Table 4.3 shows the results of the sensitivity tests on the site parameters used in the model. This table follows the same guidelines as tables 4.1 and 4.2.

SITE PARAMETERS			
Parameters	**Level of Parameter Precision**	**Model Process Assessed**	**% Difference High to Low Parameter**
Capillary Fringe Soil Thickness @ AF Plant 4	moderate	uptake	0%
TCE Concentration in GW @ AF Plant 4	high	uptake	25%
Depth to GW @ AF Plant 4	high	uptake	0%

Table 4.3 Sensitivity of Air Force Plant 4 Parameters

Comparison to Real World Data. The final validation test will compare actual data from a research project against model output. Washington State University recently completed greenhouse studies on *Populus* hybrids. This experiment was run over an eight month time frame on cuttings planted in 0.9 meters of soil and exposed to 50 ppm of TCE. By inputting these parameters into the model, the results should give a good indication of its accuracy and

reliability. Figure 4.47 shows the model output with a discussion following on the experimentally derived values.

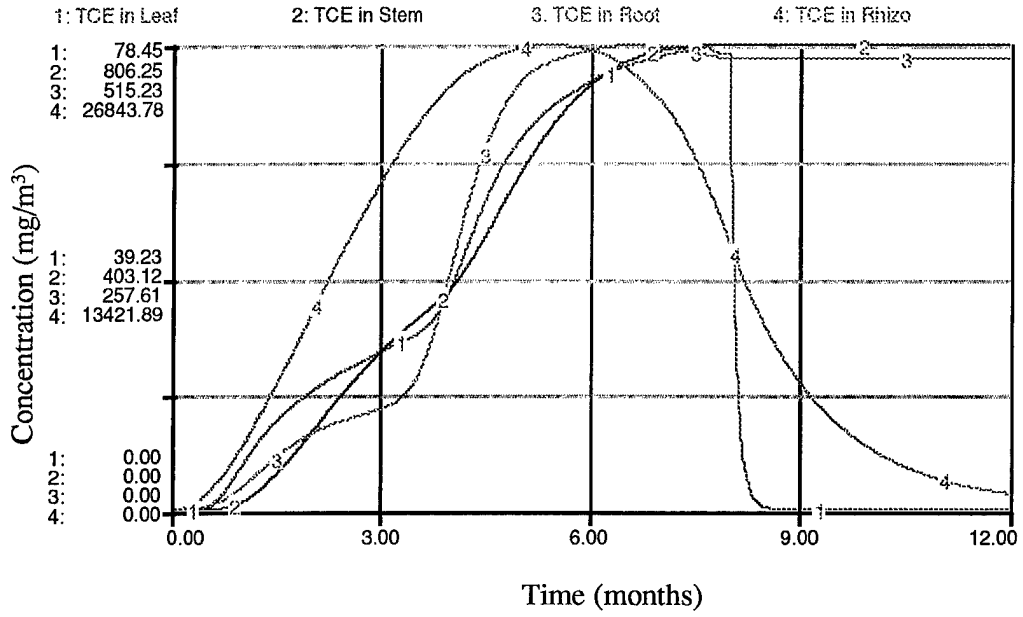

Figure 4.47 Comparison to Real World Data

Table 4.47 depicts amounts of TCE in the leaf, stem, root, and rhizosphere over a time frame of a year. At eight months, the values are maximum, and this is where the comparison of data takes place. In the model, the amounts of TCE in the leaf, stem, and root are 78.45, 806.25, and 515.23 ppb, respectively. The researchers analyzed three trees for their leaf and stem TCE amounts and one tree for its root TCE amount. Their results showed negligible amounts in the leaf, approximately 806 ppb in the stem, and approximately 602 ppb in the root. The root value in the model is within 15% of

the expected value and the stem value is within 1% of the expected value. This gives high reliability of the model to simulate real world behavior.

Summary

All parameters in the model were analyzed in this chapter. The parameters tested improved the confidence in the model structure as well as the model behavior. The parameters presented offer a better understanding of the complex interactions of the rhizosphere and phreatophytic tree in the uptake and transpiration of TCE.

The validation tests proved the model's ability to produce varying output through numerous tests. The model showed an ability to handle extreme conditions as well as producing different output or modes of behavior in different scenarios.

Conclusions can also be drawn from the numerous sensitivity tests accomplished. Some parameters were identified as having very little effect on the model output while others significantly altered the model output.

Through the validation process, the model output produced expected behavior through its verified structure. Each validation test and model run increased the confidence in the structure and resulting behavior. The real world system supports the model output and, through modeling, future uptake and transpiration can now be reliably projected.

V. Conclusions and Recommendations

The purpose of this thesis was to develop quantitative concepts to understand the dynamics of TCE uptake, cometabolism, translocation, storage, metabolism, and transpiration in the rhizosphere and phreatophytic tree. Through all stages of this research project, additional attributes and influences were discovered which added new insights and facets to the work. This chapter is devoted to summarizing conclusions and making recommendations on the direction of future research projects.

Conclusions

Using a system dynamics model, different scenarios using phreatophytic trees to remove TCE from contaminated soils were tested. This included varying the soil and ground water contaminant levels, varying the depth to ground water and of the capillary fringe and unsaturated soil thickness, the phytoremediation time frame, and characteristics of the phreatophytic tree and its rhizosphere.

It was found that higher TCE ground water levels initially showed a higher percentage of uptake. As the phreatophytic tree grew however, the xylem flow rate increased, resulting in greater flows into the rhizosphere. At a point, the tree uptake became saturated, resulting in a constant uptake and a greater build-up of TCE in the rhizosphere which also reached a maximum with tree maturity.

As the ground water depth increased the level of TCE uptake decreased. This is expected, since with increasing depth, more of the root occupies the unsaturated zone which has aqueous TCE levels approximately 100 time lower than the capillary fringe soil. Also, as the ratio of unsaturated soil to capillary fringe soil decreases, more TCE is removed by the phreatophytic tree, once again due to the difference in TCE aqueous concentrations between the unsaturated and capillary fringe soils. Therefore, at sites with ground water at extreme depths the removal of TCE will take years longer to reach the same level of required remediation.

With increasing time, the phreatophytic tree showed increased uptake of TCE in all scenarios. This is expected, because with growth, the phreatophytic tree continually increases its uptake of water and therefore contaminants from the ground water. The model was run out for 10 years since typical short rotation woody crops are harvested at 7 to 8 years. The model proved a useful tool to remediation managers in establishing the approximate TCE removal amounts over the crops life span.

By varying the phreatophytic tree characteristics, an idea of the rate and degree of removal of TCE from the ground water were established. Also, the levels of storage, metabolism, and transpiration within the phreatophytic tree itself were demonstrated. This information may prove useful in identifying the amount of TCE released into the atmosphere during potential remediation projects at highly contaminated sites as well as the amount released seasonally

over the projects expected life span. It will also assist in estimating the removal rates over time and the expected remediation time frame.

Characteristics of the rhizosphere showed varying levels of influence in the phytoremediation process. With increasing rhizosphere thickness the uptake of TCE decreased dramatically. This was due to the model representation of the uptake process which may not accurately portray natural uptake. In a real world system, saturable uptake is based on the concentration of the aqueous phase contaminant on the rhizoplane. In the model, a rhizosphere with a thickness from 2 to 5 mm was assumed. The rhizosphere was also assumed as continuous across all root surfaces. As the rhizosphere thickness increased in the model the rhizosphere concentration decreased, decreasing contaminant uptake, therefore, TCE uptake was underestimated by the model. Conversely, adsorption of TCE to soil particles and diffusion during a majority of the growing season were not accounted for in the model. Both these influences would decrease TCE uptake. Cometabolism was assumed as continuous across all surfaces, even though real world microorganisms exist in colonies. This resulted in an averaging of cometabolism in comparison to the variability seen in the real world system. The assumptions in the rhizosphere were necessary to aggregate the intricate influences while still giving an adequate approximation of the expected behavior.

Recommendations

There are several recommendations for further research in the area of this thesis. All recommendations pertain to parameter and processes estimated in the model. This model proved itself extremely complex, so not all factors reached a desired level of disaggregation.

The most important factor in this model, the uptake process, requires further research. There is some debate whether the uptake of TCE by plants is a saturable process or a linear uptake process up to toxic levels. At higher concentrations, these two schools of thought show a major divergence in TCE removal by the phreatophytic tree. Further experimental research using various types of plants at extreme TCE aqueous concentrations will greatly enhance this debate.

The rhizosphere is a dynamic system which constantly changes throughout a growing season as well as the life of the plant. Because of this, the rhizosphere representation was extremely simplified. One example is the concentration of TCE for uptake by the phreatophytic tree. The model representation of the rhizosphere does not take TCE absorption to soil particles into account. Also, the uptake concentration may be underrepresented due to an averaging across the rhizosphere, especially at higher concentrations.

Another simplification in the rhizosphere was the cometabolic relationship. Through the photosynthetic process, substances are released into the rhizosphere which various microorganisms then subsist on in a symbiotic

relationship with the plant. Some of these substances are proven substrates for the cometabolism of TCE by microorganisms. This relationship is dependent on the levels of substrate and TCE in the rhizosphere as well as the amount of microorganisms themselves. Further research and analysis is necessary to develop a better understanding and less aggregated representation of this process.

The growth of tree roots and degree of ground water uptake by the root hairs versus the secondary root are hotly debated topics in literature today. New research by plant physiologists, agronomists, and biologists in the near future will hopefully shed light on the exact ratios of plant root masses and their respective functions in uptake.

The conclusions and recommendations made on this research are instrumental in expanding the knowledge and understanding of the phytoremediation process, especially in the area of uptake of TCE by phreatophytic trees. Increased public awareness of environmental issues and the continual push for natural and less intrusive remediation processes further strengthens the potential of phytoremediation. Effectively remediating some of the numerous contaminated ground water systems through phytoremediation is currently being investigated in several field studies, with positive initial results. Through a better understanding of the phytoremediation process, the use of phreatophytes to remediate ground water contaminants will continue to grow.

Appendix 1

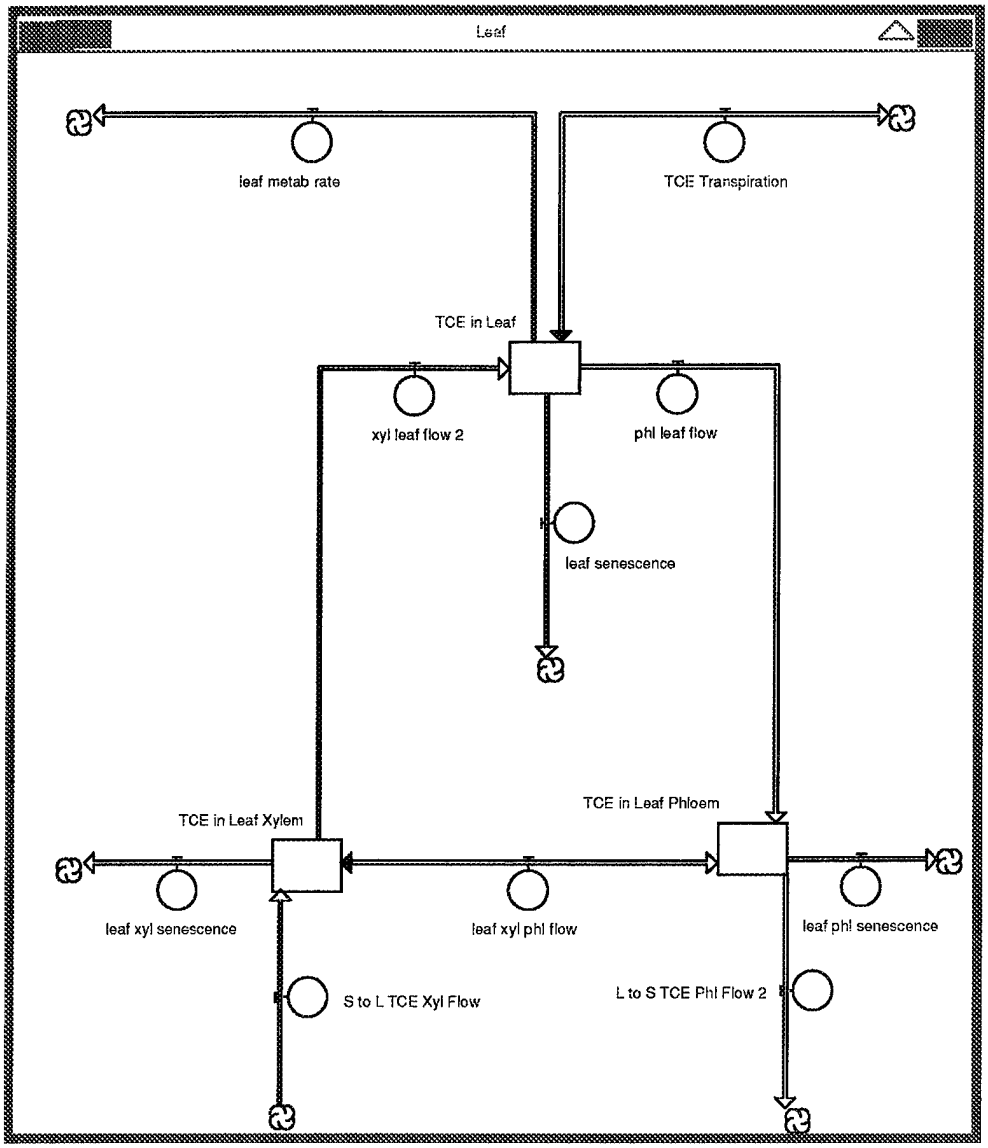
Leaf
leaf metab rate
TCE Transpiration
TCE in Leaf
xyl leaf flow 2
phl leaf flow
leaf senescence
TCE in Leaf Xylem
TCE in Leaf Phloem
leaf xyl senescence
leaf xyl phl flow
leaf phl senescence
S to L TCE Xyl Flow
L to S TCE Phl Flow 2

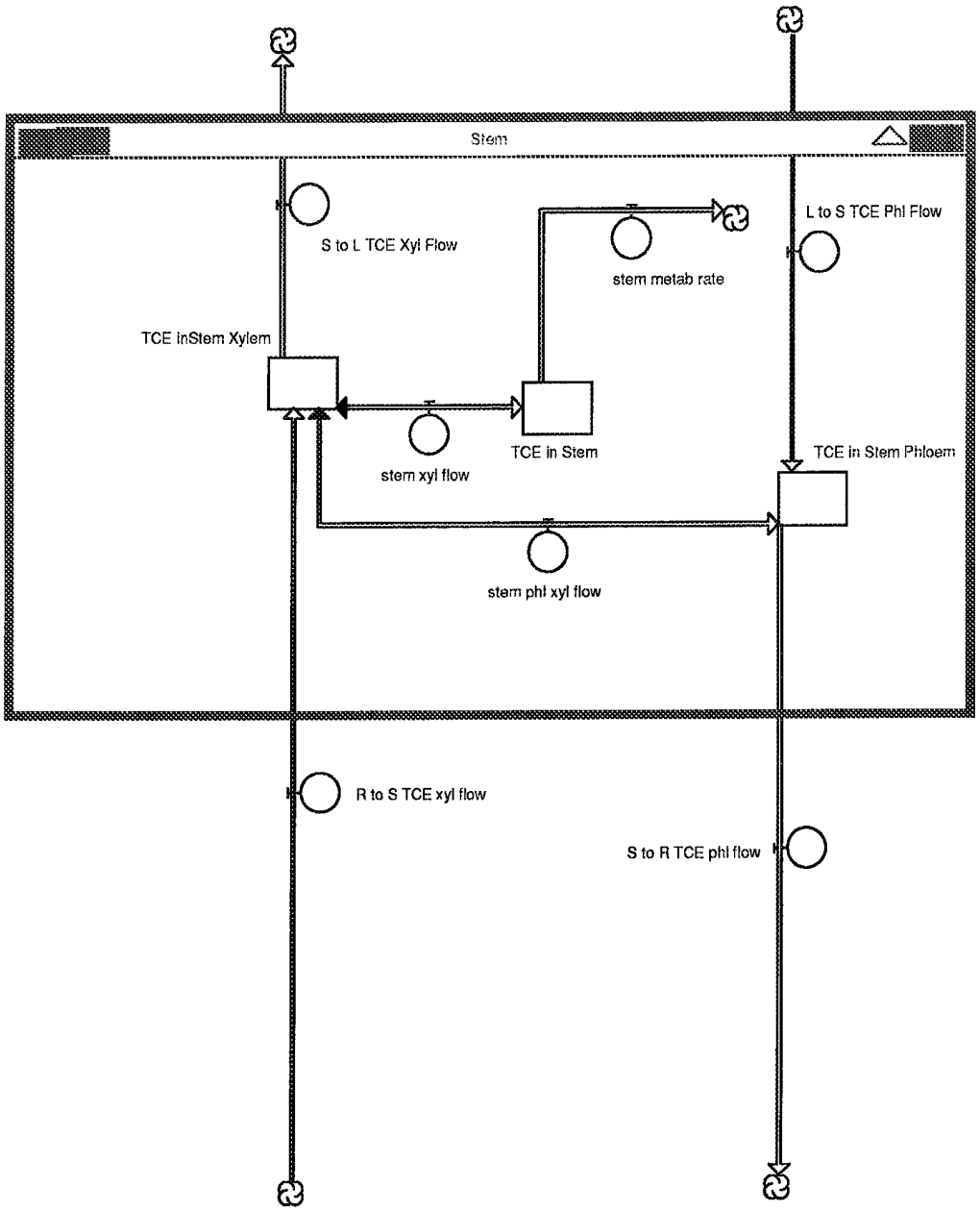
Stem
S to L TCE Xyl Flow
stem metab rate
L to S TCE Phl Flow
TCE inStem Xylem
TCE in Stem
TCE in Stem Phloem
stem xyl flow
stem phl xyl flow
R to S TCE xyl flow
S to R TCE phl flow

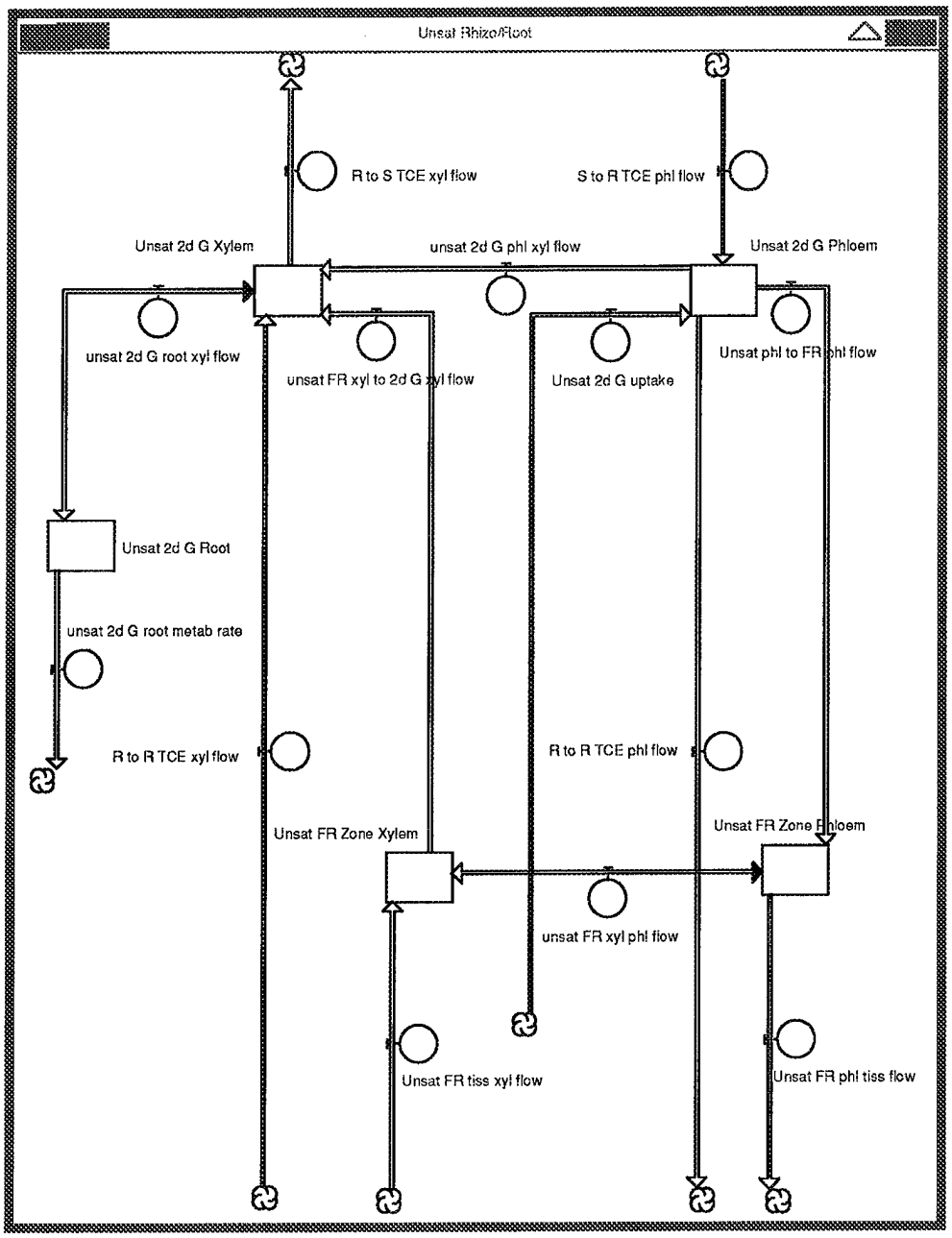
Unsat Rhizo/Root
R to S TCE xyl flow
S to R TCE phl flow
Unsat 2d G Xylem
unsat 2d G phl xyl flow
Unsat 2d G Phloem
unsat 2d G root xyl flow
unsat FR xyl to 2d G xyl flow
Unsat 2d G uptake
Unsat phl to FR phl flow
Unsat 2d G Root
unsat 2d G root metab rate
R to R TCE xyl flow
R to R TCE phl flow
Unsat FR Zone Xylem
Unsat FR Zone Phloem
unsat FR xyl phl flow
Unsat FR tiss xyl flow
Unsat FR phl tiss flow

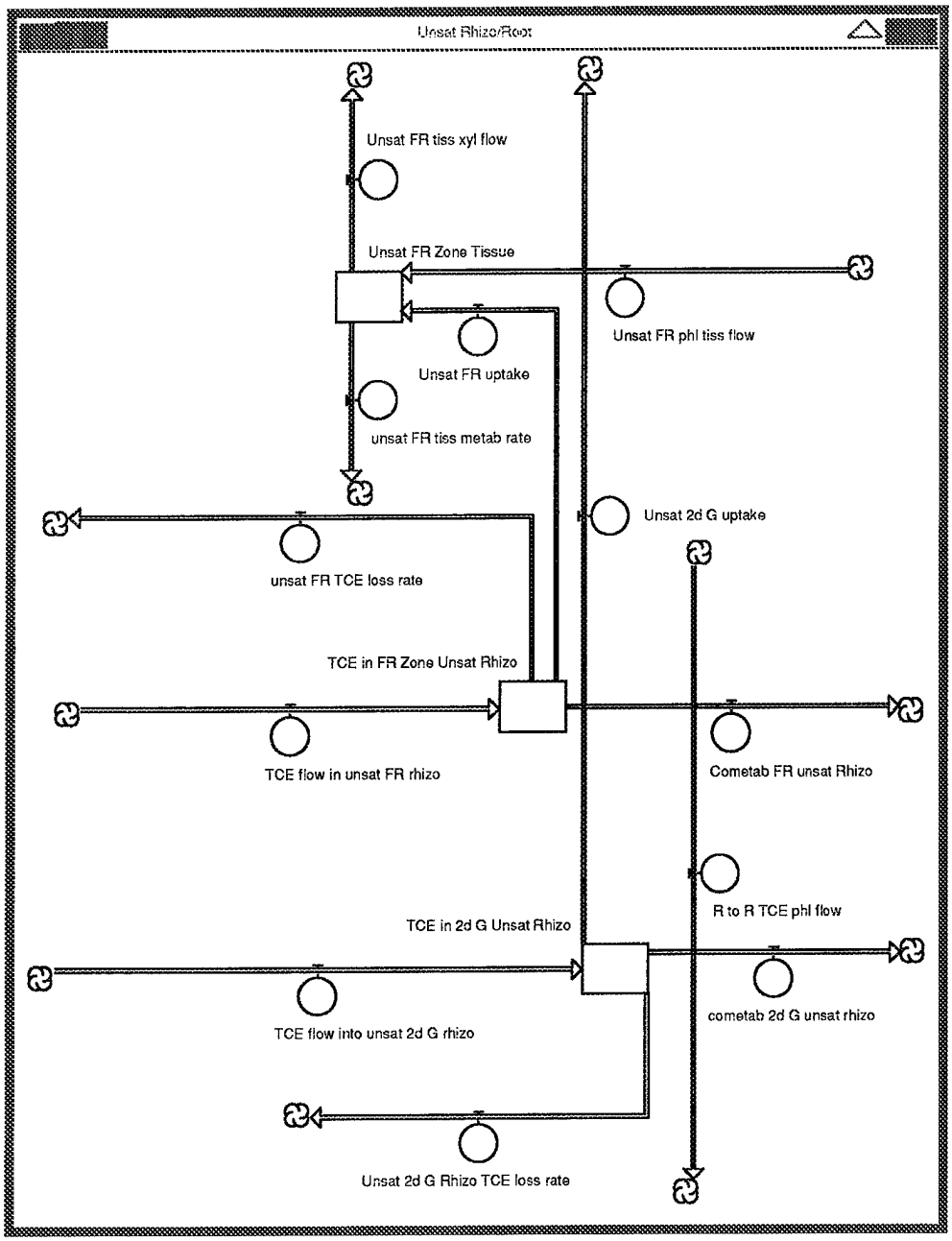
Unsat Rhizo/Root
Unsat FR tiss xyl flow
Unsat FR Zone Tissue
Unsat FR phl tiss flow
Unsat FR uptake
unsat FR tiss metab rate
Unsat 2d G uptake
unsat FR TCE loss rate
TCE in FR Zone Unsat Rhizo
TCE flow in unsat FR rhizo
Cometab FR unsat Rhizo
R to R TCE phl flow
TCE in 2d G Unsat Rhizo
TCE flow into unsat 2d G rhizo
cometab 2d G unsat rhizo
Unsat 2d G Rhizo TCE loss rate

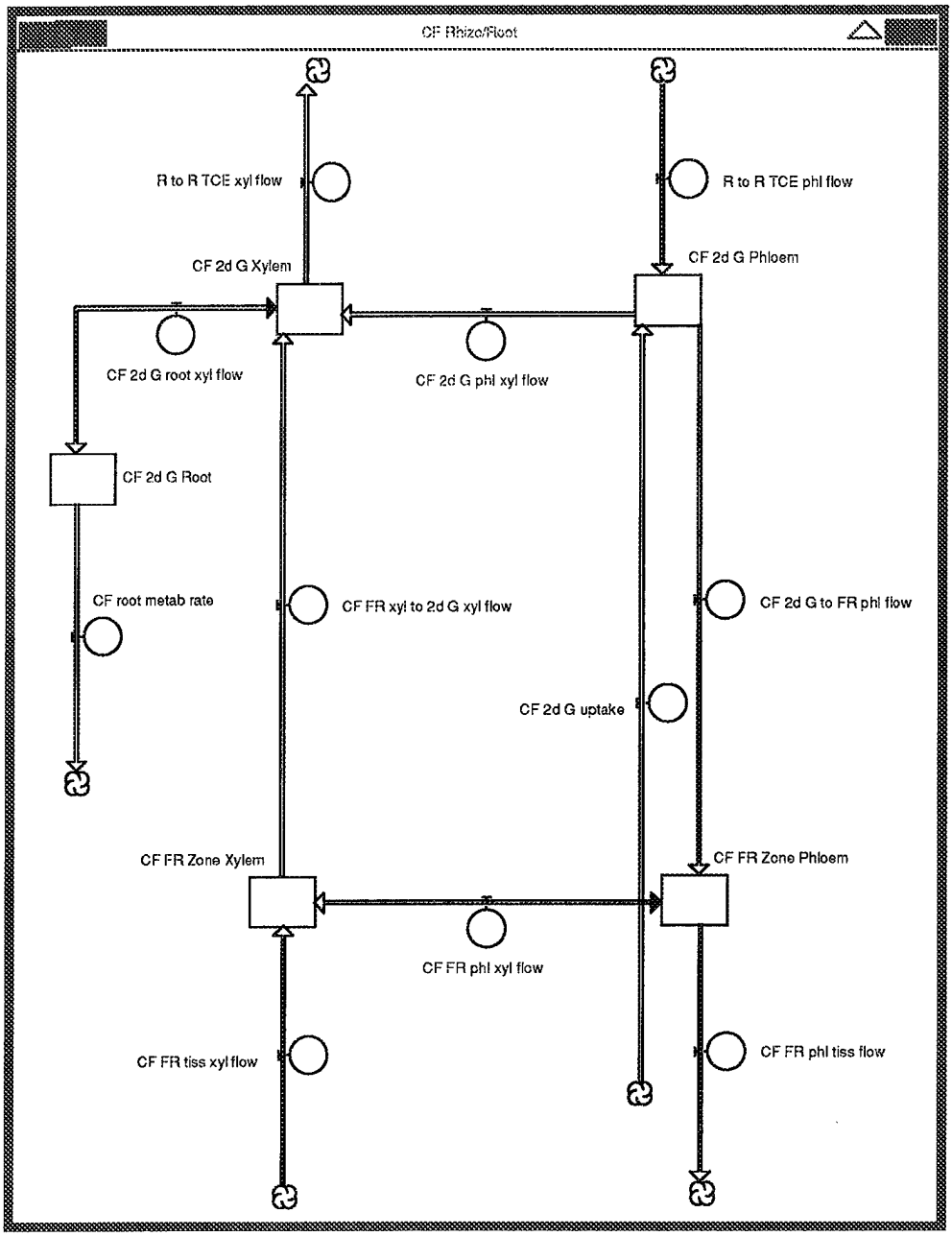
CF Rhize/Root
R to R TCE xyl flow
R to R TCE phl flow
CF 2d G Xylem
CF 2d G Phloem
CF 2d G root xyl flow
CF 2d G phl xyl flow
CF 2d G Root
CF root metab rate
CF FR xyl to 2d G xyl flow
CF 2d G to FR phl flow
CF 2d G uptake
CF FR Zone Xylem
CF FR Zone Phloem
CF FR phl xyl flow
CF FR tiss xyl flow
CF FR phl tiss flow

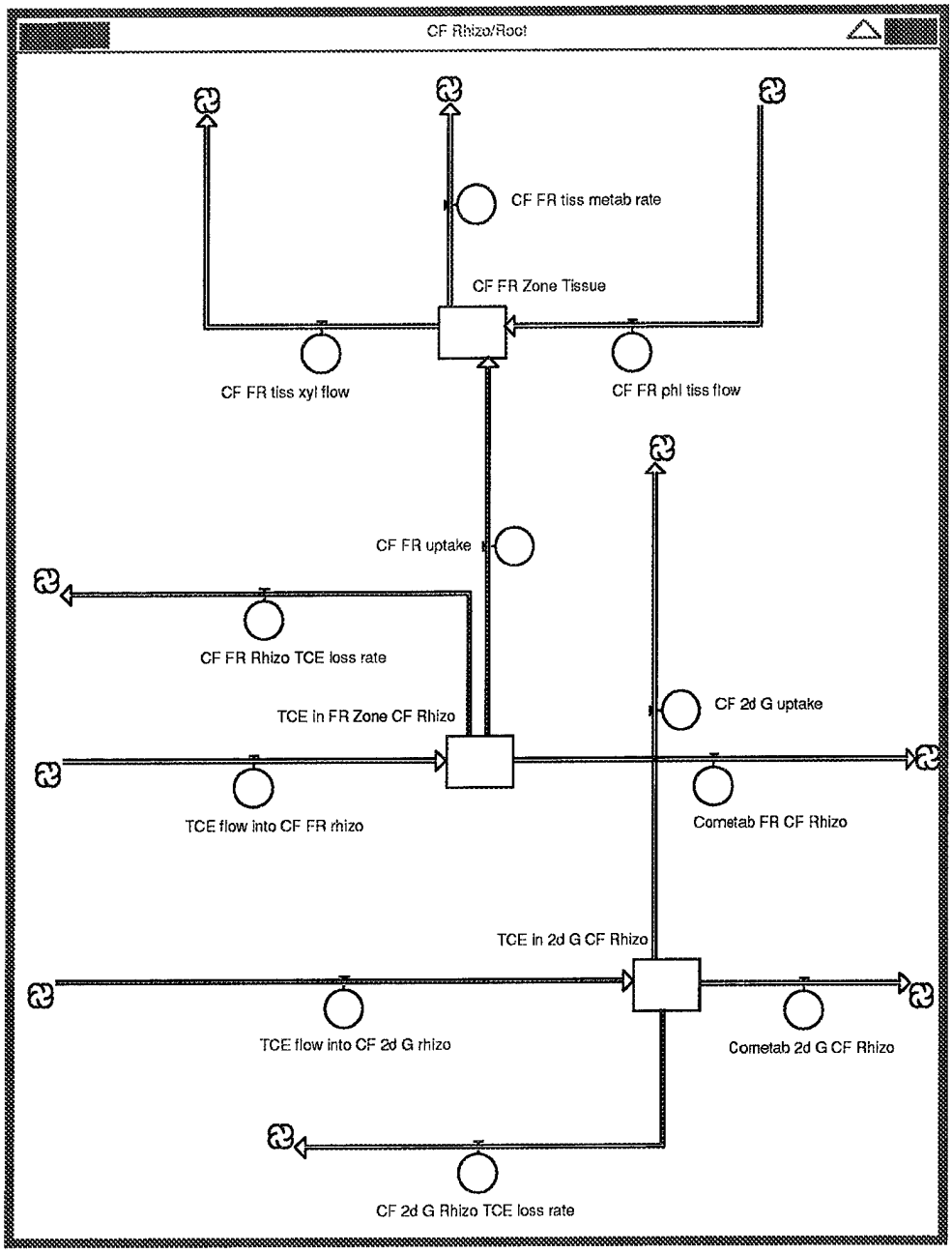
CF Rhizo/Root
CF FR tiss metab rate
CF FR Zone Tissue
CF FR tiss xyl flow
CF FR phl tiss flow
CF FR uptake
CF FR Rhizo TCE loss rate
TCE in FR Zone CF Rhizo
CF 2d G uptake
TCE flow into CF FR rhizo
Cometab FR CF Rhizo
TCE in 2d G CF Rhizo
TCE flow into CF 2d G rhizo
Cometab 2d G CF Rhizo
CF 2d G Rhizo TCE loss rate

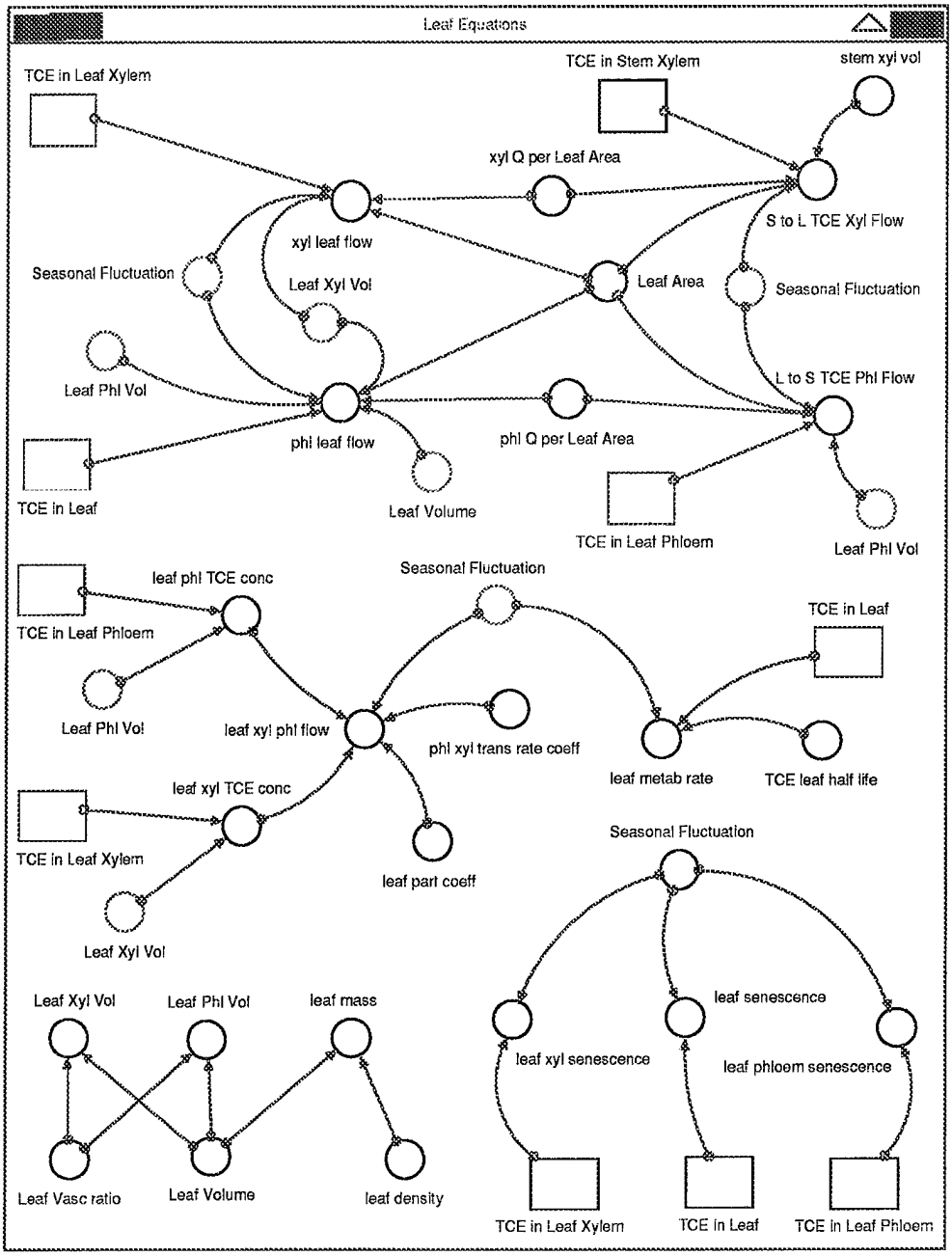
Leaf Equations
TCE in Leaf Xylem
TCE in Stem Xylem
stem xyl vol
xyl Q per Leaf Area
S to L TCE Xyl Flow
xyl leaf flow
Seasonal Fluctuation
Leaf Xyl Vol
Leaf Area
Seasonal Fluctuation
Leaf Phl Vol
L to S TCE Phl Flow
phl leaf flow
phl Q per Leaf Area
TCE in Leaf
Leaf Volume
TCE in Leaf Phloem
Leaf Phl Vol
leaf phl TCE conc
Seasonal Fluctuation
TCE in Leaf
TCE in Leaf Phloem
Leaf Phl Vol
leaf xyl phl flow
phl xyl trans rate coeff
leaf metab rate
TCE leaf half life
leaf xyl TCE conc
TCE in Leaf Xylem
leaf part coeff
Seasonal Fluctuation
Leaf Xyl Vol
Leaf Xyl Vol
Leaf Phl Vol
leaf mass
leaf senescence
leaf xyl senescence
leaf phloem senescence
Leaf Vasc ratio
Leaf Volume
leaf density
TCE in Leaf Xylem
TCE in Leaf
TCE in Leaf Phloem

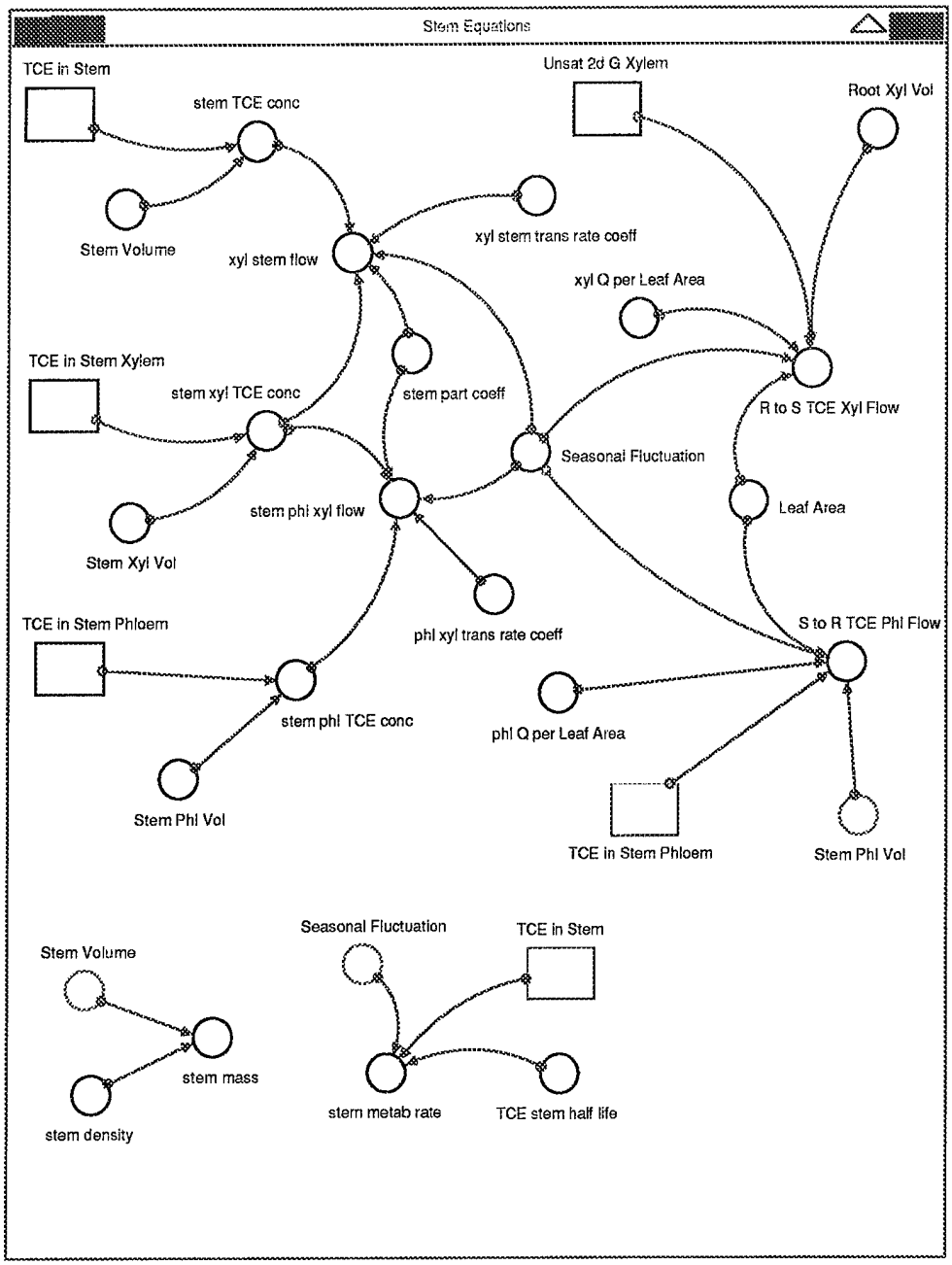
Stem Equations
TCE in Stem
stem TCE conc
Stem Volume
xyl stem flow
xyl stem trans rate coeff
Unsat 2d G Xylem
Root Xyl Vol
xyl Q per Leaf Area
TCE in Stem Xylem
stem xyl TCE conc
stem part coeff
R to S TCE Xyl Flow
Seasonal Fluctuation
stem phi xyl flow
Leaf Area
Stem Xyl Vol
TCE in Stem Phloem
phl xyl trans rate coeff
S to R TCE Phl Flow
stem phl TCE conc
phl Q per Leaf Area
Stem Phl Vol
TCE in Stem Phloem
Stem Phl Vol
Stem Volume
stem mass
stem density
Seasonal Fluctuation
TCE in Stem
stem metab rate
TCE stem half life

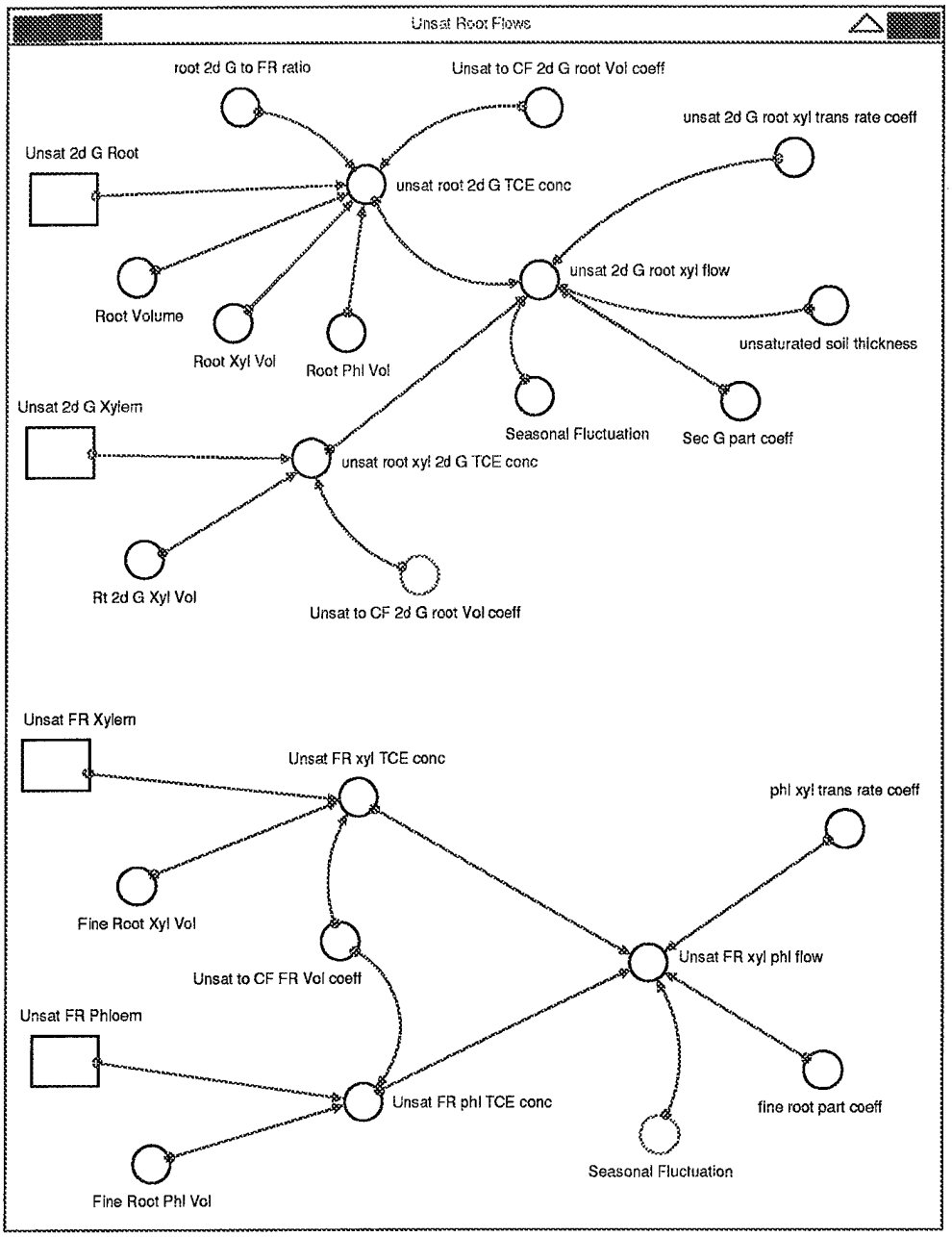
Unsat Root Flows
root 2d G to FR ratio
Unsat to CF 2d G root Vol coeff
unsat 2d G root xyl trans rate coeff
Unsat 2d G Root
unsat root 2d G TCE conc
unsat 2d G root xyl flow
Root Volume
Root Xyl Vol
Root Phl Vol
unsaturated soil thickness
Seasonal Fluctuation
Sec G part coeff
Unsat 2d G Xylem
unsat root xyl 2d G TCE conc
Rt 2d G Xyl Vol
Unsat to CF 2d G root Vol coeff
Unsat FR Xylem
Unsat FR xyl TCE conc
phl xyl trans rate coeff
Fine Root Xyl Vol
Unsat to CF FR Vol coeff
Unsat FR xyl phl flow
Unsat FR Phloem
Unsat FR phl TCE conc
fine root part coeff
Seasonal Fluctuation
Fine Root Phl Vol

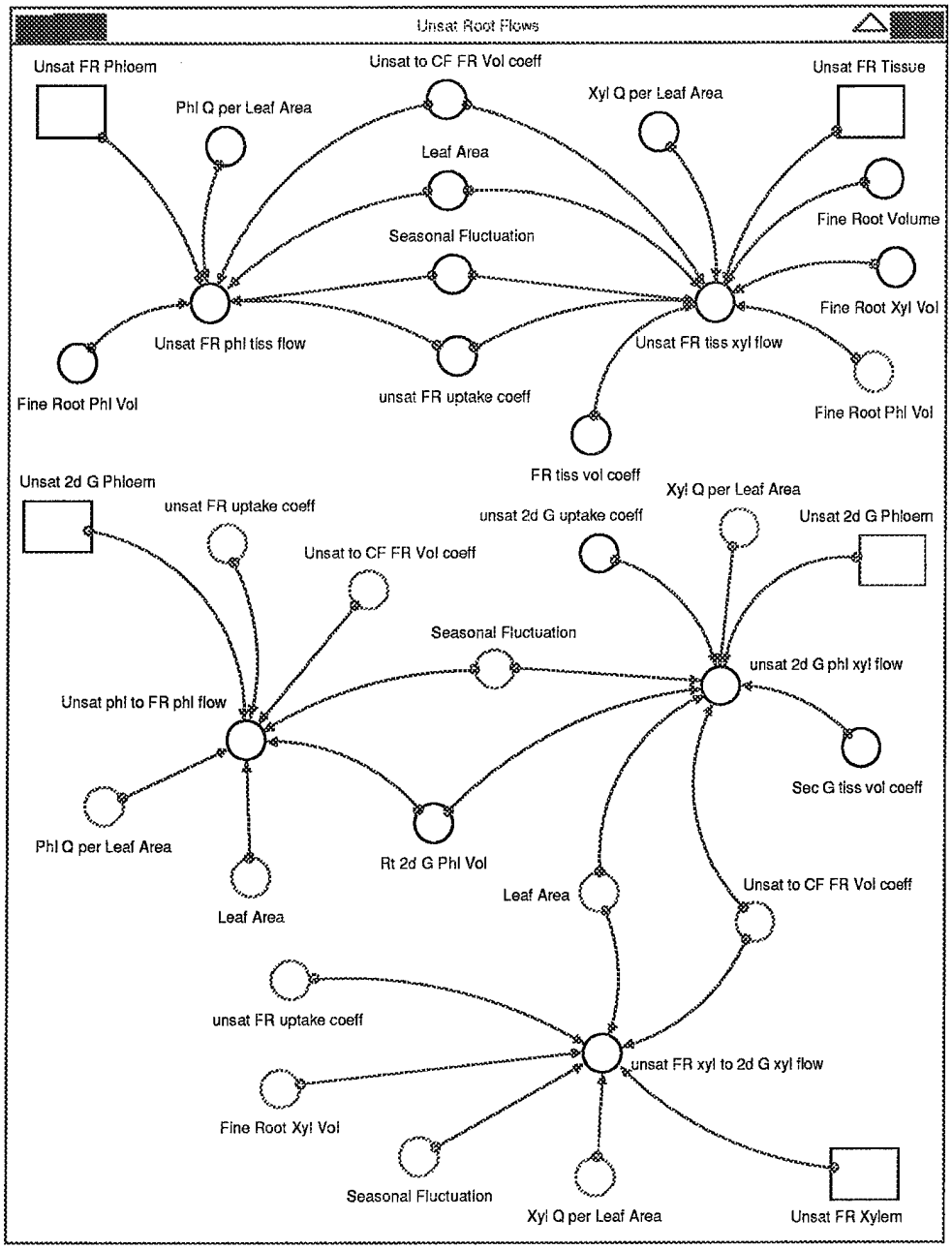
Unsat Root Flows
Unsat FR Phloem
Phl Q per Leaf Area
Unsat to CF FR Vol coeff
Leaf Area
Seasonal Fluctuation
Xyl Q per Leaf Area
Unsat FR Tissue
Fine Root Volume
Fine Root Xyl Vol
Unsat FR phl tiss flow
Unsat FR tiss xyl flow
Fine Root Phl Vol
unsat FR uptake coeff
FR tiss vol coeff
Fine Root Phl Vol
Unsat 2d G Phloem
unsat FR uptake coeff
Unsat to CF FR Vol coeff
unsat 2d G uptake coeff
Xyl Q per Leaf Area
Unsat 2d G Phloem
Seasonal Fluctuation
unsat 2d G phl xyl flow
Unsat phl to FR phl flow
Sec G tiss vol coeff
Phl Q per Leaf Area
Rt 2d G Phl Vol
Leaf Area
Leaf Area
Unsat to CF FR Vol coeff
unsat FR uptake coeff
unsat FR xyl to 2d G xyl flow
Fine Root Xyl Vol
Seasonal Fluctuation
Xyl Q per Leaf Area
Unsat FR Xylem

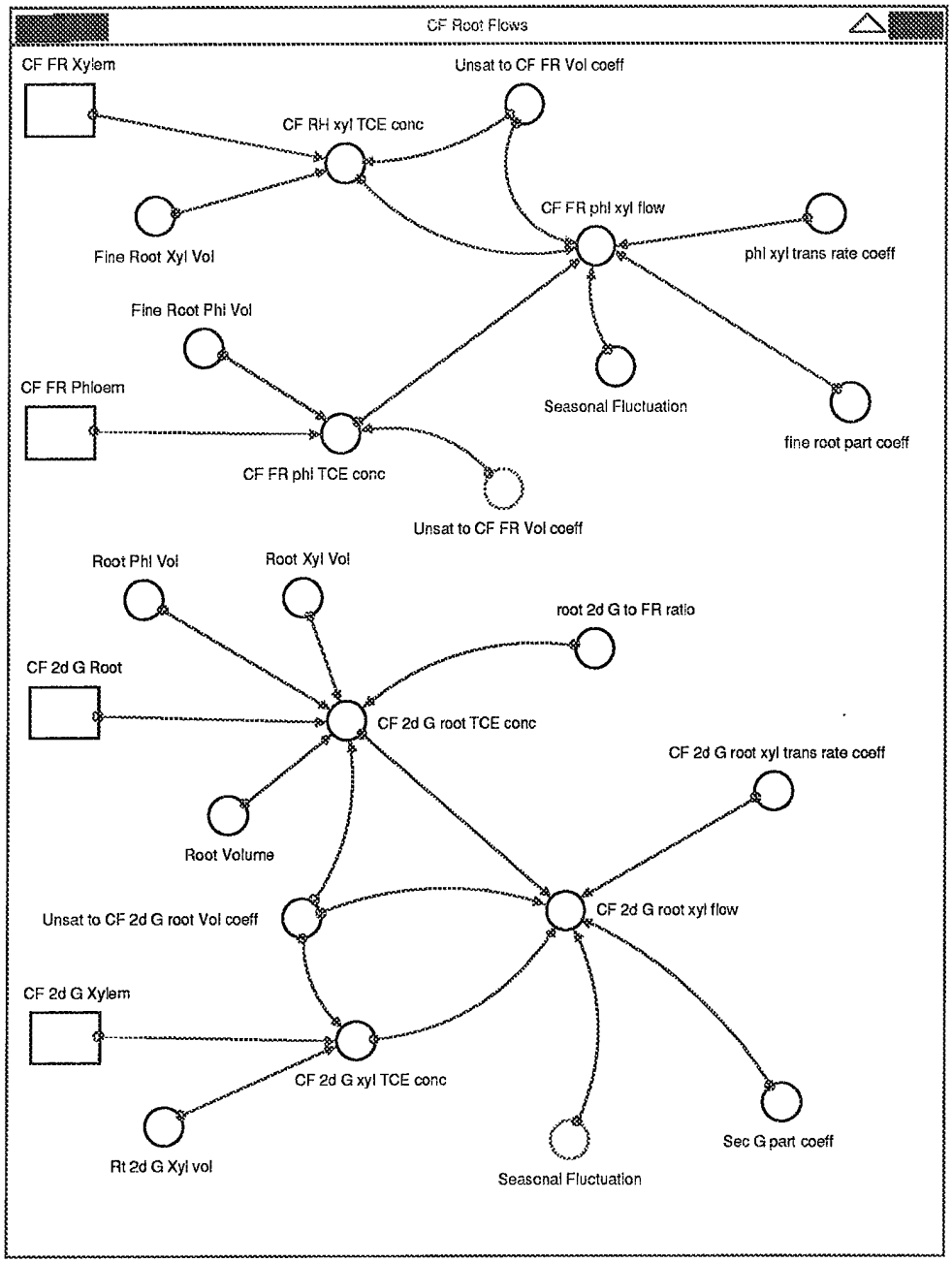
CF Root Flows
CF FR Xylem
Unsat to CF FR Vol coeff
CF RH xyl TCE conc
CF FR phl xyl flow
Fine Root Xyl Vol
phl xyl trans rate coeff
Fine Root Phi Vol
Seasonal Fluctuation
CF FR Phloem
fine root part coeff
CF FR phl TCE conc
Unsat to CF FR Vol coeff
Root Phl Vol
Root Xyl Vol
root 2d G to FR ratio
CF 2d G Root
CF 2d G root TCE conc
CF 2d G root xyl trans rate coeff
Root Volume
Unsat to CF 2d G root Vol coeff
CF 2d G root xyl flow
CF 2d G Xylem
CF 2d G xyl TCE conc
Sec G part coeff
Rt 2d G Xyl vol
Seasonal Fluctuation

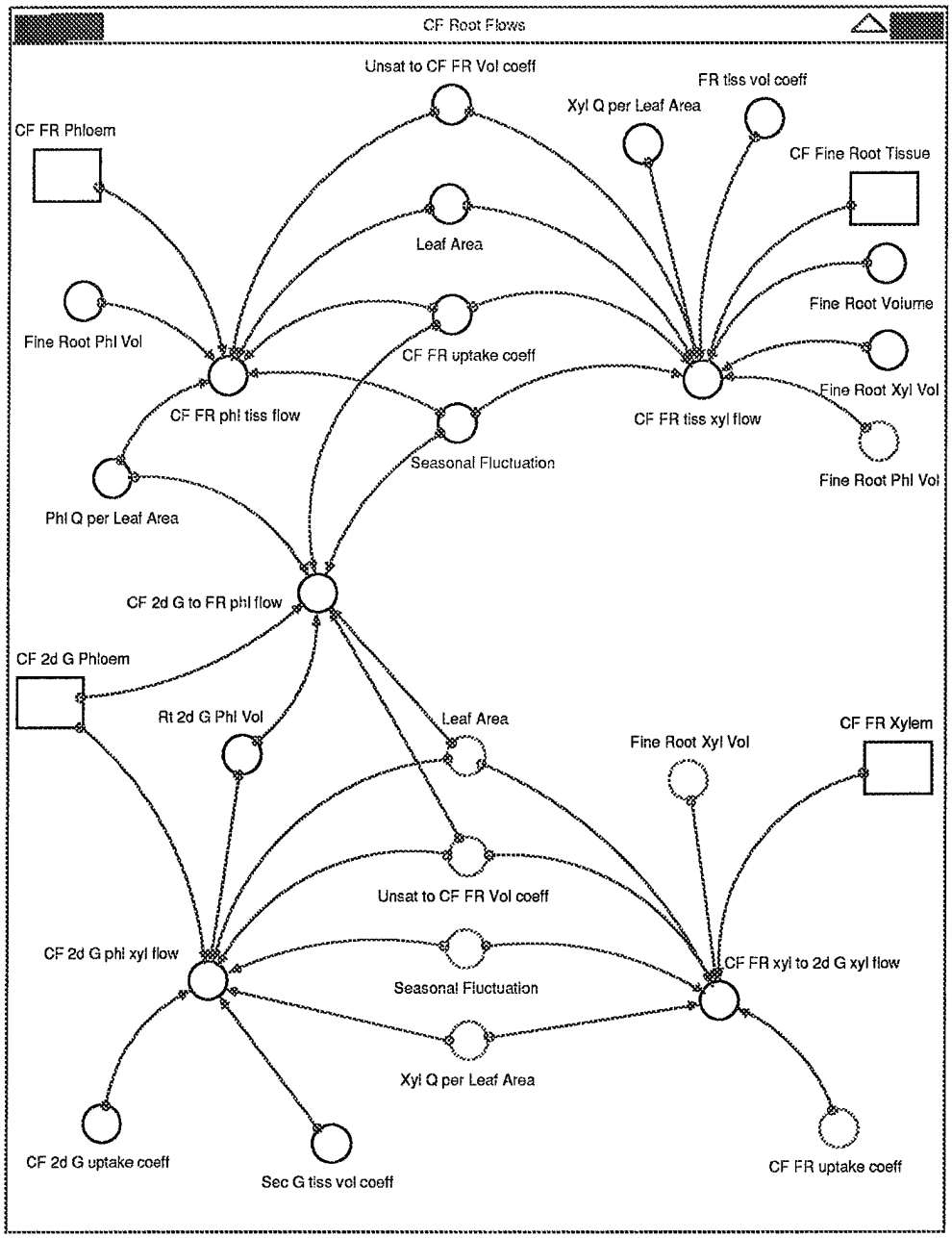
CF Root Flows
Unsat to CF FR Vol coeff
FR tiss vol coeff
Xyl Q per Leaf Area
CF FR Phloem
CF Fine Root Tissue
Leaf Area
Fine Root Volume
Fine Root Phl Vol
CF FR uptake coeff
Fine Root Xyl Vol
CF FR phl tiss flow
CF FR tiss xyl flow
Seasonal Fluctuation
Fine Root Phl Vol
Phl Q per Leaf Area
CF 2d G to FR phl flow
CF 2d G Phloem
Rt 2d G Phl Vol
Leaf Area
Fine Root Xyl Vol
CF FR Xylem
Unsat to CF FR Vol coeff
CF 2d G phl xyl flow
CF FR xyl to 2d G xyl flow
Seasonal Fluctuation
Xyl Q per Leaf Area
CF 2d G uptake coeff
Sec G tiss vol coeff
CF FR uptake coeff

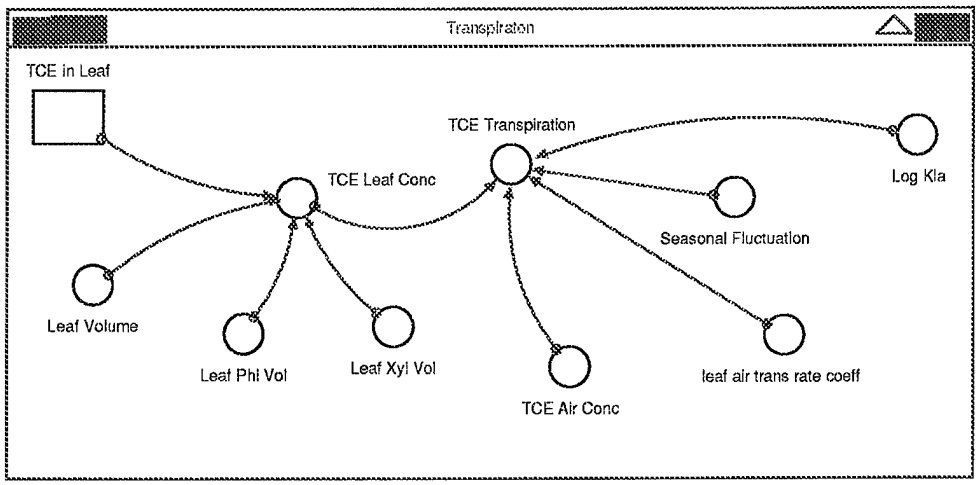
Transpiration
TCE in Leaf
TCE Transpiration
Log Kla
TCE Leaf Conc
Seasonal Fluctuation
Leaf Volume
Leaf Phi Vol
Leaf Xyl Vol
TCE Air Conc
leaf air trans rate coeff

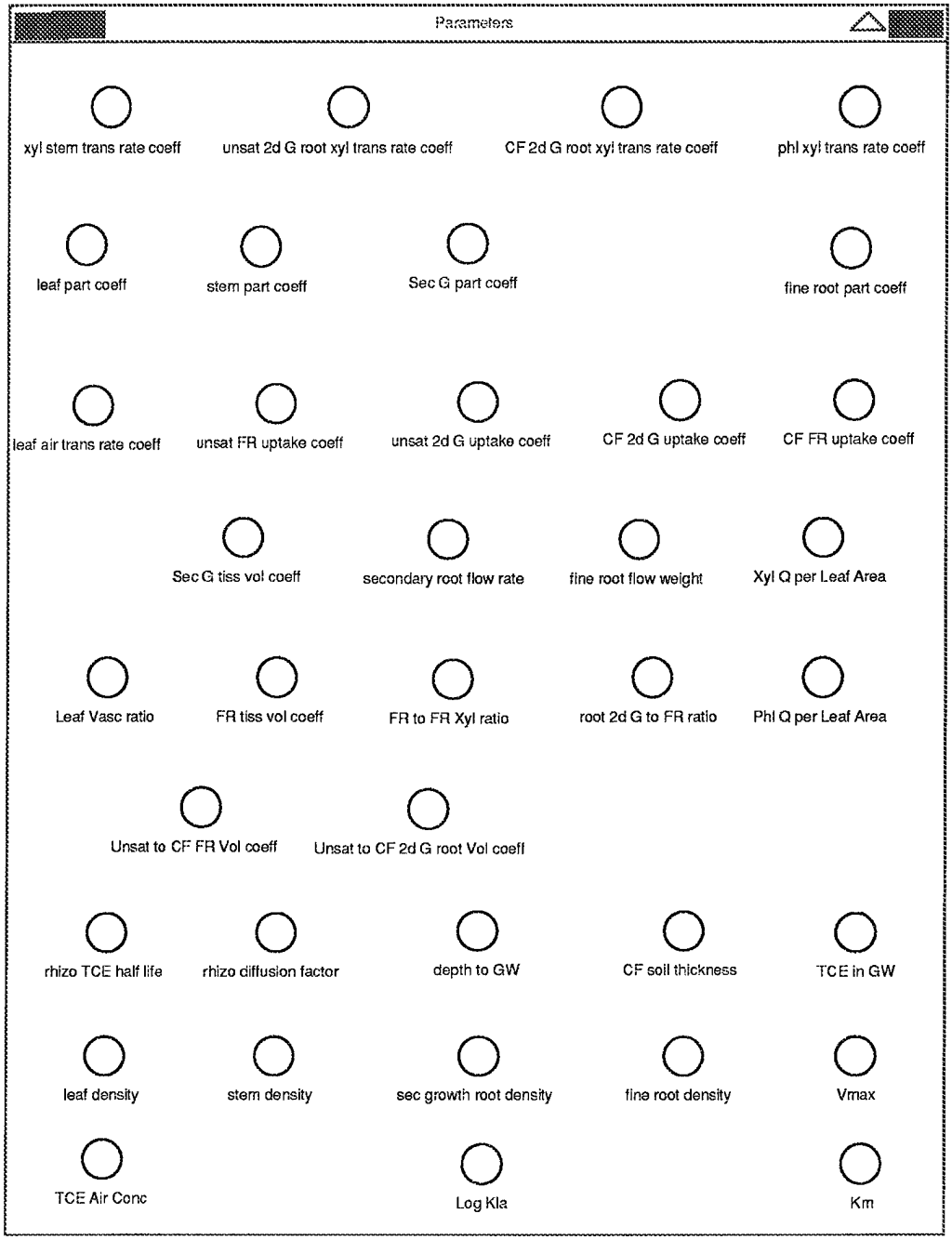
Parameters
xyl stem trans rate coeff
unsat 2d G root xyl trans rate coeff
CF 2d G root xyl trans rate coeff
phl xyl trans rate coeff
leaf part coeff
stem part coeff
Sec G part coeff
fine root part coeff
leaf air trans rate coeff
unsat FR uptake coeff
unsat 2d G uptake coeff
CF 2d G uptake coeff
CF FR uptake coeff
Sec G tiss vol coeff
secondary root flow rate
fine root flow weight
Xyl Q per Leaf Area
Leaf Vasc ratio
FR tiss vol coeff
FR to FR Xyl ratio
root 2d G to FR ratio
Phl Q per Leaf Area
Unsat to CF FR Vol coeff
Unsat to CF 2d G root Vol coeff
rhizo TCE half life
rhizo diffusion factor
depth to GW
CF soil thickness
TCE in GW
leaf density
stem density
sec growth root density
fine root density
Vmax
TCE Air Conc
Log Kla
Km

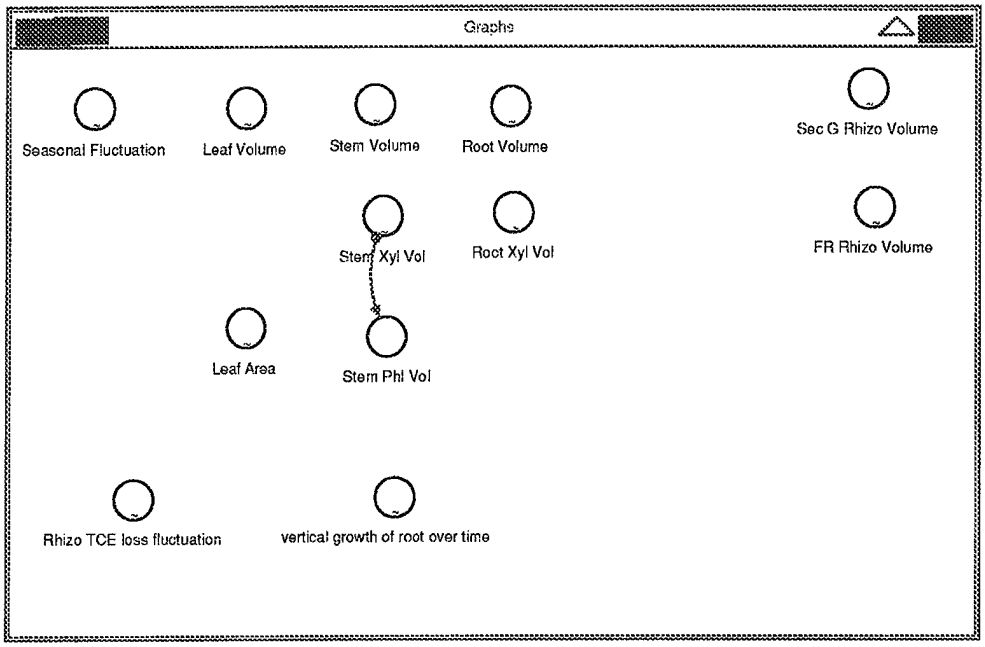
Graphs
Seasonal Fluctuation
Leaf Volume
Stem Volume
Root Volume
Sec G Rhizo Volume
Stem Xyl Vol
Root Xyl Vol
FR Rhizo Volume
Leaf Area
Stem Phl Vol
Rhizo TCE loss fluctuation
vertical growth of root over time

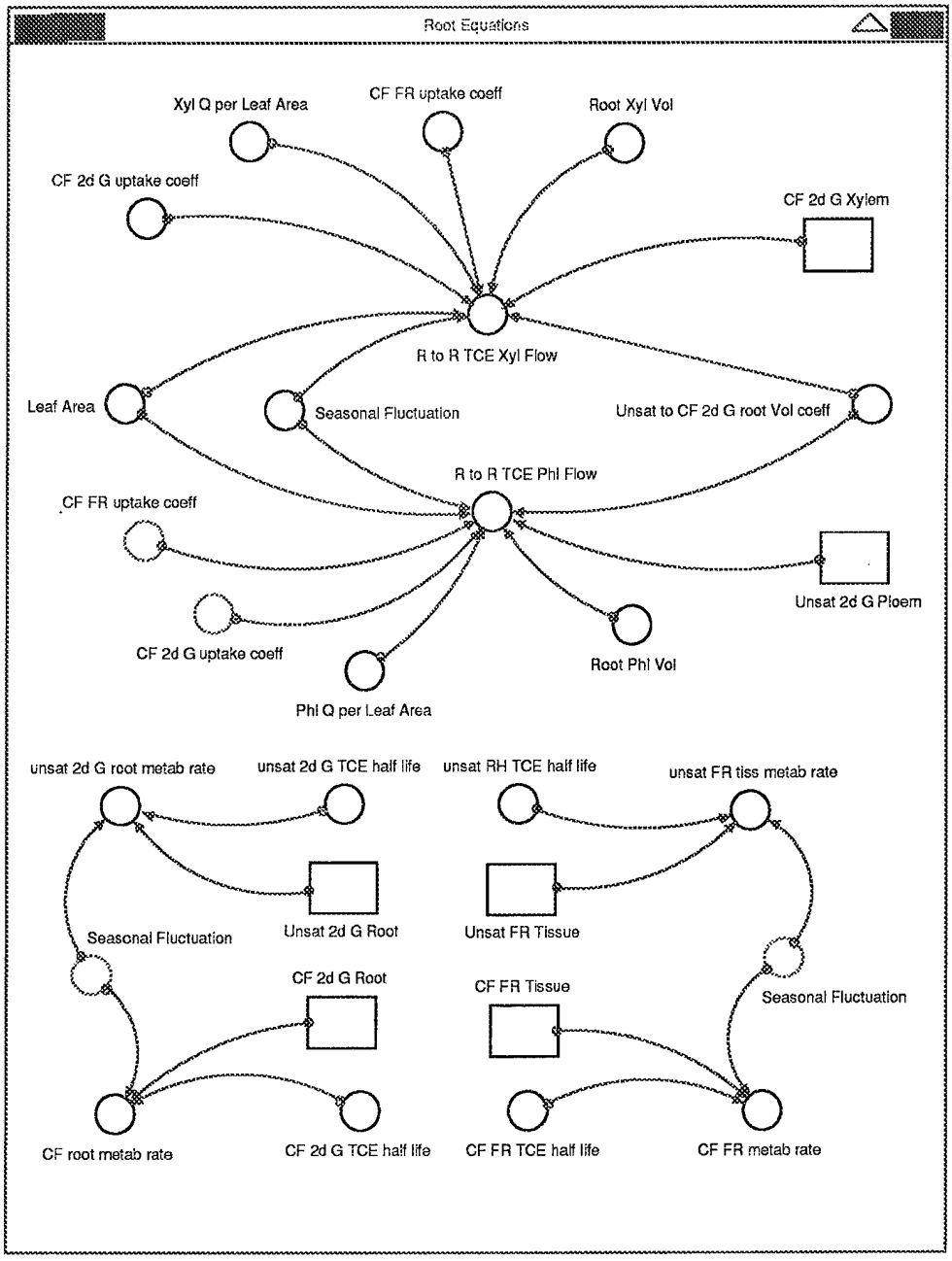
Root Equations
Xyl Q per Leaf Area
CF FR uptake coeff
Root Xyl Vol
CF 2d G uptake coeff
CF 2d G Xylem
R to R TCE Xyl Flow
Leaf Area
Seasonal Fluctuation
Unsat to CF 2d G root Vol coeff
R to R TCE Phl Flow
CF FR uptake coeff
Unsat 2d G Ploem
CF 2d G uptake coeff
Root Phl Vol
Phl Q per Leaf Area
unsat 2d G root metab rate
unsat 2d G TCE half life
unsat RH TCE half life
unsat FR tiss metab rate
Unsat 2d G Root
Unsat FR Tissue
Seasonal Fluctuation
CF 2d G Root
CF FR Tissue
Seasonal Fluctuation
CF root metab rate
CF 2d G TCE half life
CF FR TCE half life
CF FR metab rate

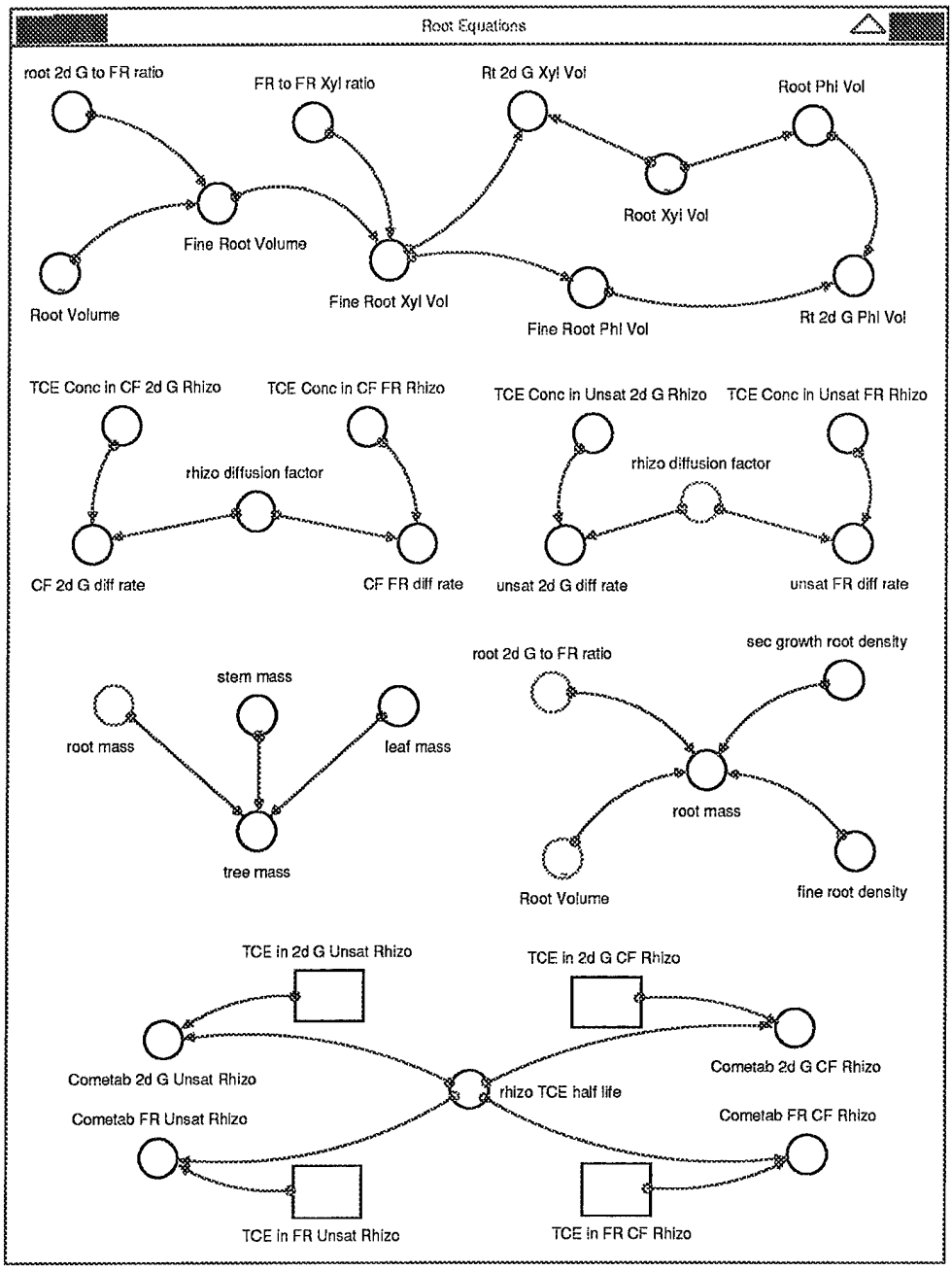
Root Equations
root 2d G to FR ratio
FR to FR Xyl ratio
Rt 2d G Xyl Vol
Root Phl Vol
Root Xyl Vol
Fine Root Volume
Root Volume
Fine Root Xyl Vol
Fine Root Phl Vol
Rt 2d G Phl Vol
TCE Conc in CF 2d G Rhizo
TCE Conc in CF FR Rhizo
rhizo diffusion factor
CF 2d G diff rate
CF FR diff rate
TCE Conc in Unsat 2d G Rhizo
TCE Conc in Unsat FR Rhizo
rhizo diffusion factor
unsat 2d G diff rate
unsat FR diff rate
stem mass
root mass
leaf mass
tree mass
root 2d G to FR ratio
sec growth root density
root mass
Root Volume
fine root density
TCE in 2d G Unsat Rhizo
TCE in 2d G CF Rhizo
Cometab 2d G Unsat Rhizo
Cometab 2d G CF Rhizo
rhizo TCE half life
Cometab FR Unsat Rhizo
Cometab FR CF Rhizo
TCE in FR Unsat Rhizo
TCE in FR CF Rhizo

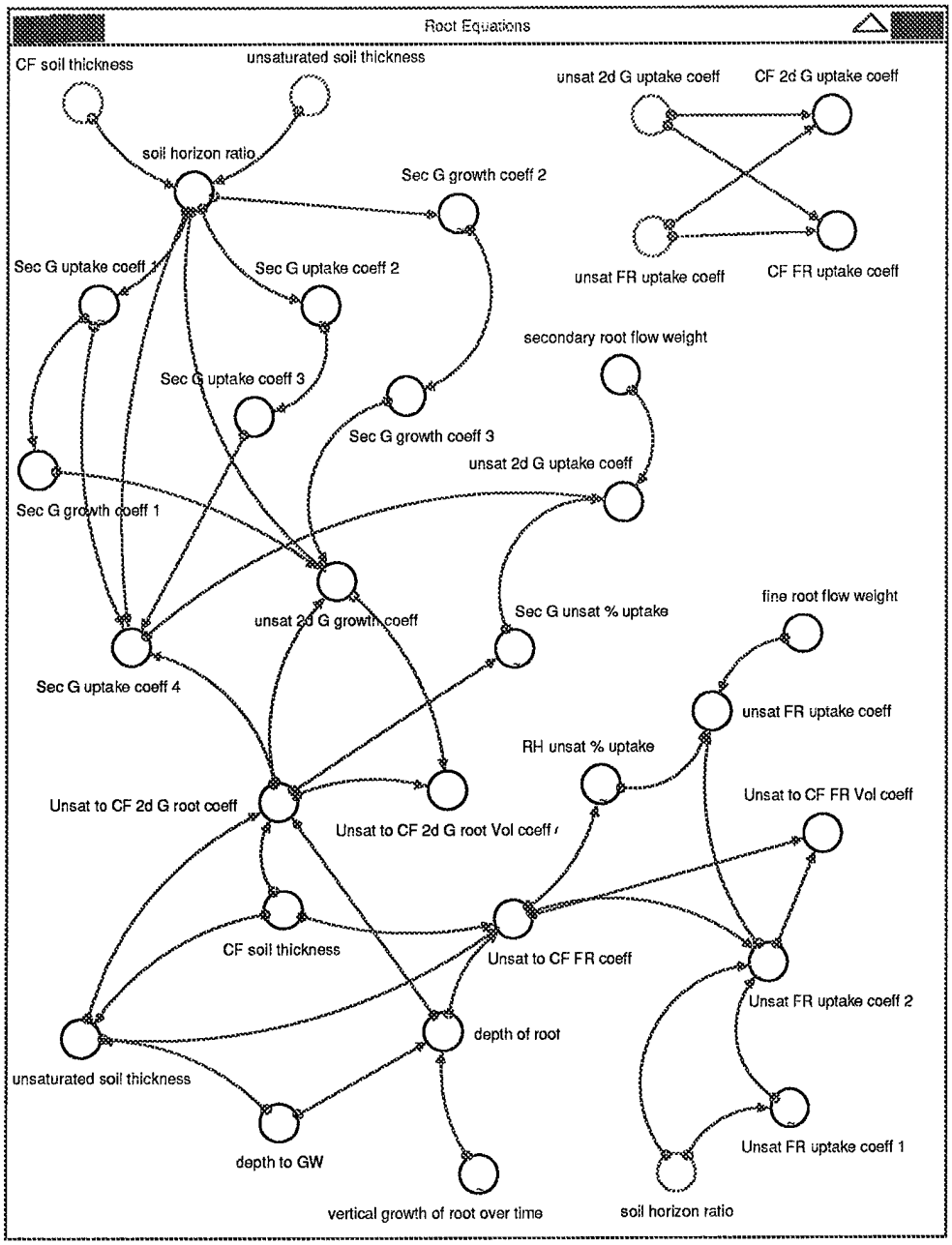
Root Equations
CF soil thickness
unsaturated soil thickness
soil horizon ratio
Sec G growth coeff 2
Sec G uptake coeff 1
Sec G uptake coeff 2
Sec G uptake coeff 3
Sec G growth coeff 3
Sec G growth coeff 1
unsat 2d G uptake coeff
unsat 2d G growth coeff
Sec G unsat % uptake
Sec G uptake coeff 4
Unsat to CF 2d G root coeff
Unsat to CF 2d G root Vol coeff
CF soil thickness
Unsat to CF FR coeff
depth of root
unsaturated soil thickness
depth to GW
vertical growth of root over time
unsat 2d G uptake coeff
CF 2d G uptake coeff
unsat FR uptake coeff
CF FR uptake coeff
secondary root flow weight
fine root flow weight
unsat FR uptake coeff
RH unsat % uptake
Unsat to CF FR Vol coeff
Unsat FR uptake coeff 2
Unsat FR uptake coeff 1
soil horizon ratio

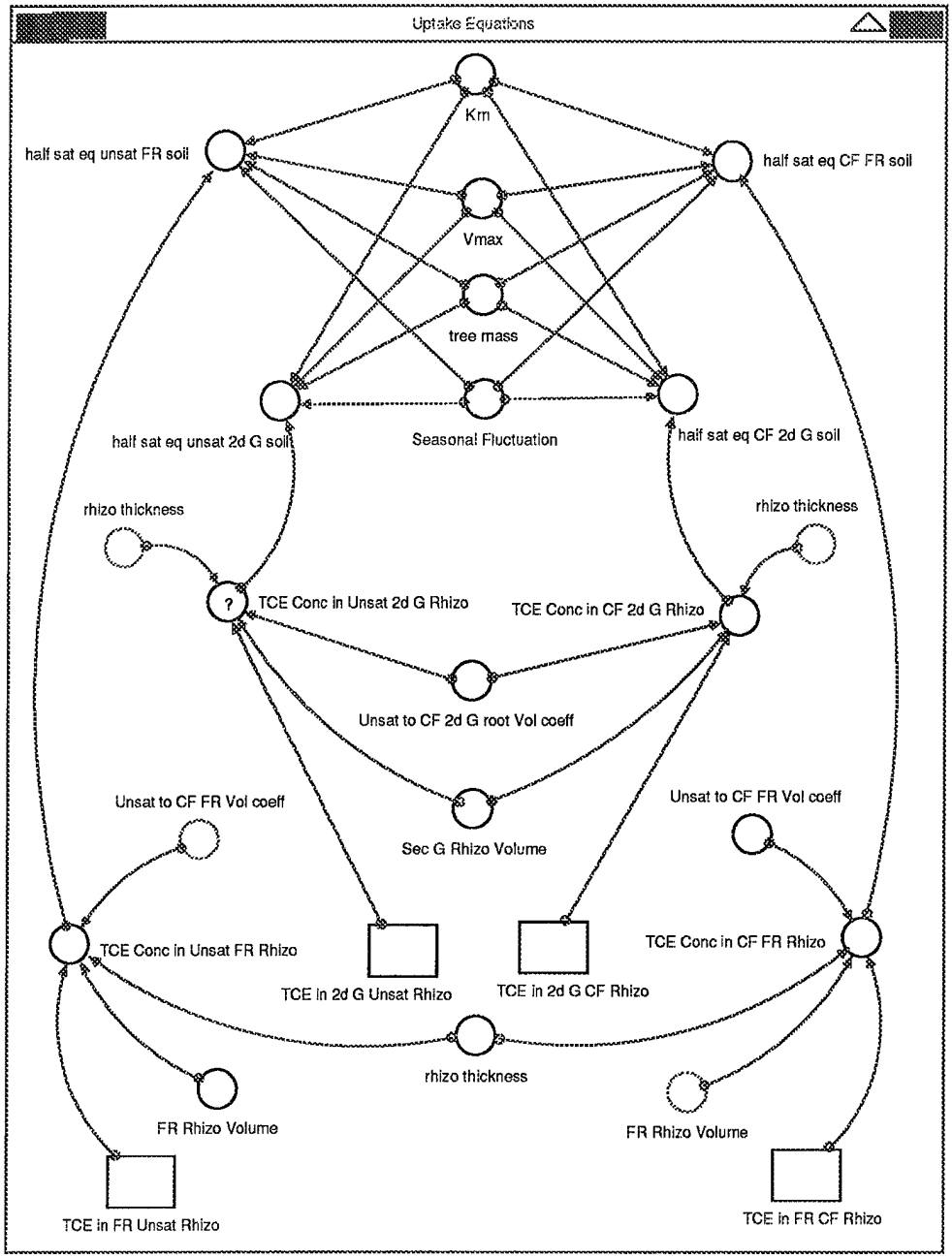
Uptake Equations
Km
half sat eq unsat FR soil
half sat eq CF FR soil
Vmax
tree mass
half sat eq unsat 2d G soil
Seasonal Fluctuation
half sat eq CF 2d G soil
rhizo thickness
rhizo thickness
?
TCE Conc in Unsat 2d G Rhizo
TCE Conc in CF 2d G Rhizo
Unsat to CF 2d G root Vol coeff
Unsat to CF FR Vol coeff
Unsat to CF FR Vol coeff
Sec G Rhizo Volume
TCE Conc in Unsat FR Rhizo
TCE Conc in CF FR Rhizo
TCE in 2d G Unsat Rhizo
TCE in 2d G CF Rhizo
rhizo thickness
FR Rhizo Volume
FR Rhizo Volume
TCE in FR Unsat Rhizo
TCE in FR CF Rhizo

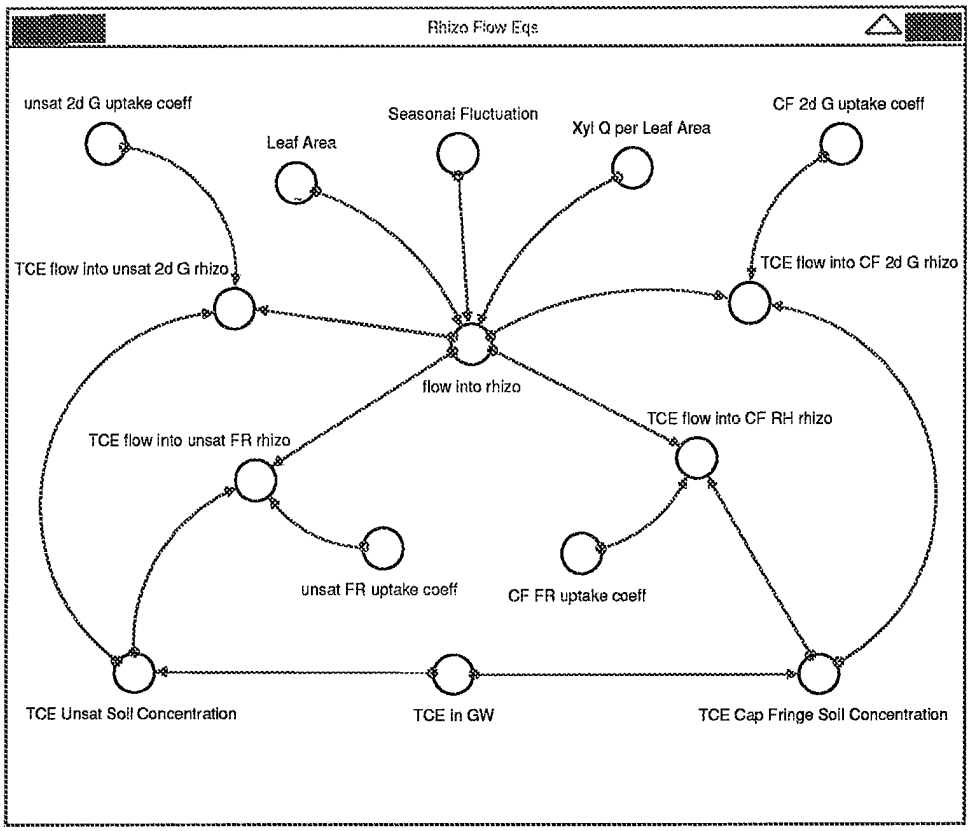
Rhizo Flow Eqs
unsat 2d G uptake coeff
Leaf Area
Seasonal Fluctuation
Xyl Q per Leaf Area
CF 2d G uptake coeff
TCE flow into unsat 2d G rhizo
TCE flow into CF 2d G rhizo
flow into rhizo
TCE flow into unsat FR rhizo
TCE flow into CF RH rhizo
unsat FR uptake coeff
CF FR uptake coeff
TCE Unsat Soil Concentration
TCE in GW
TCE Cap Fringe Soil Concentration

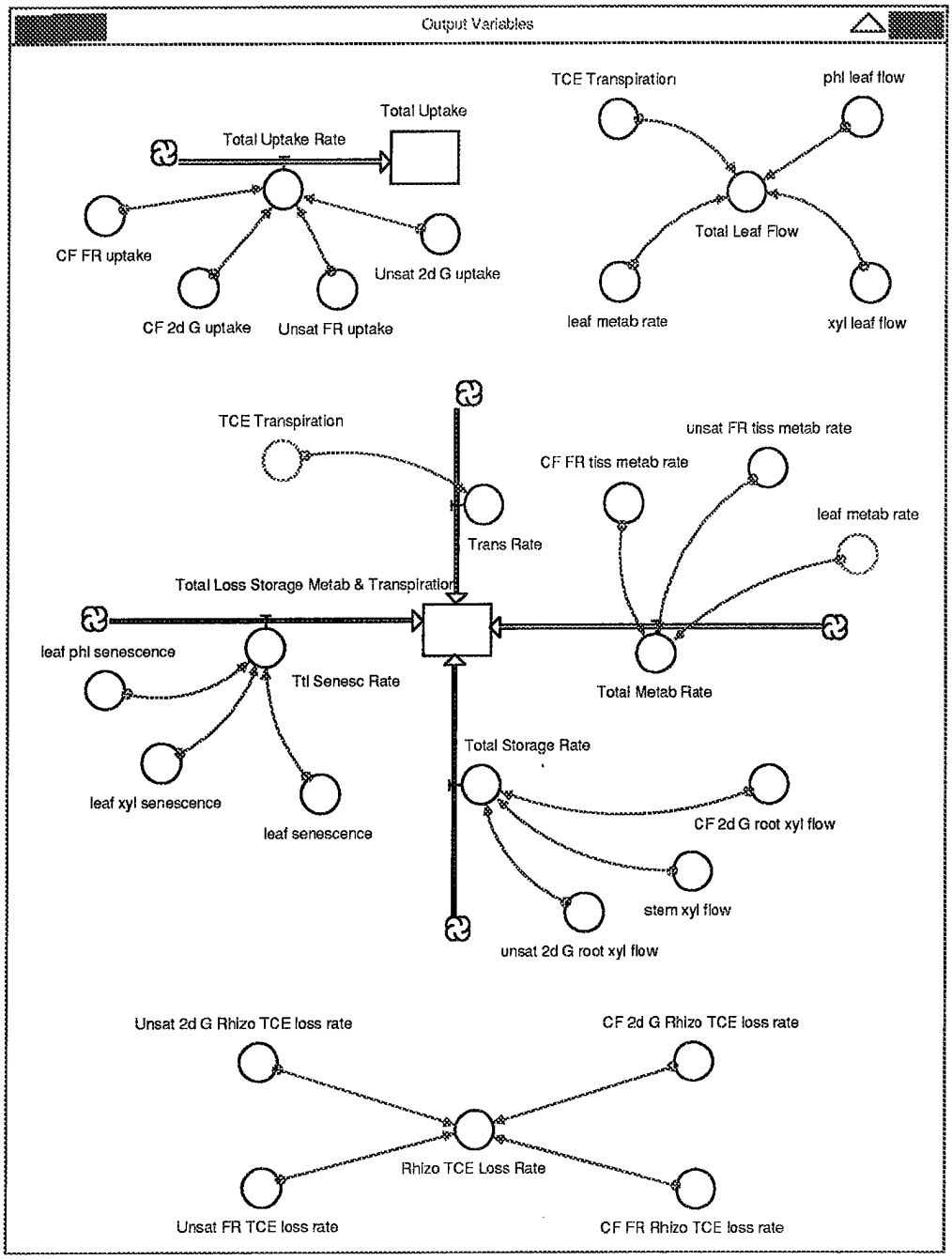
Output Variables
TCE Transpiration
phl leaf flow
Total Uptake
Total Uptake Rate
Total Leaf Flow
CF FR uptake
Unsat 2d G uptake
leaf metab rate
xyl leaf flow
CF 2d G uptake
Unsat FR uptake
TCE Transpiration
unsat FR tiss metab rate
CF FR tiss metab rate
leaf metab rate
Trans Rate
Total Loss Storage Metab & Transpiration
leaf phl senescence
Ttl Senesc Rate
Total Metab Rate
Total Storage Rate
leaf xyl senescence
leaf senescence
CF 2d G root xyl flow
stem xyl flow
unsat 2d G root xyl flow
Unsat 2d G Rhizo TCE loss rate
CF 2d G Rhizo TCE loss rate
Rhizo TCE Loss Rate
Unsat FR TCE loss rate
CF FR Rhizo TCE loss rate

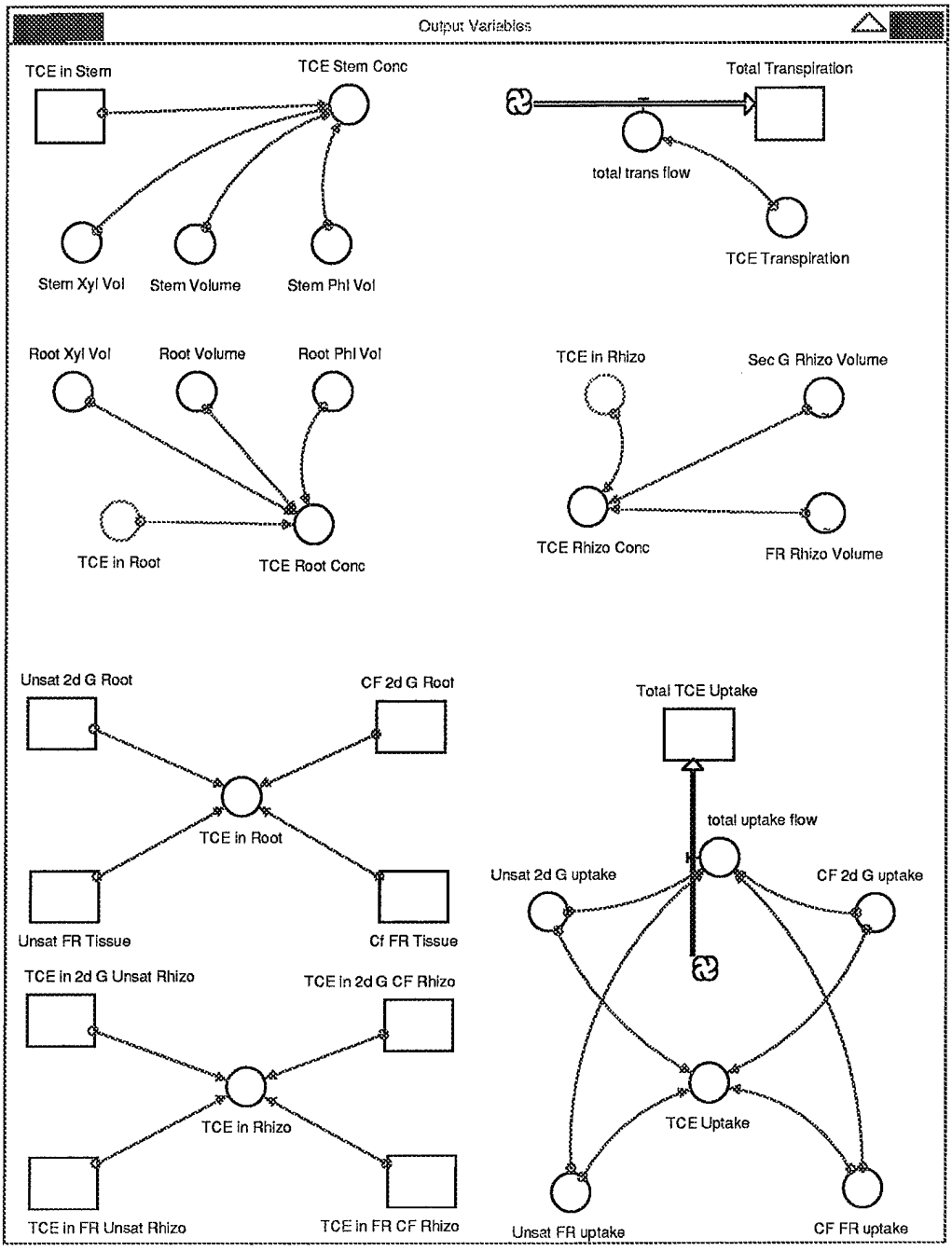
Output Variables
TCE in Stem
TCE Stem Conc
Stem Xyl Vol
Stem Volume
Stem Phl Vol
Total Transpiration
total trans flow
TCE Transpiration
Root Xyl Vol
Root Volume
Root Phl Vol
TCE in Root
TCE Root Conc
TCE in Rhizo
Sec G Rhizo Volume
TCE Rhizo Conc
FR Rhizo Volume
Unsat 2d G Root
CF 2d G Root
TCE in Root
Unsat FR Tissue
Cf FR Tissue
Total TCE Uptake
total uptake flow
Unsat 2d G uptake
CF 2d G uptake
TCE Uptake
Unsat FR uptake
CF FR uptake
TCE in 2d G Unsat Rhizo
TCE in 2d G CF Rhizo
TCE in Rhizo
TCE in FR Unsat Rhizo
TCE in FR CF Rhizo

Appendix 2

Equations from Stella II diagram.

Capillary Fringe Rhizosphere and Root

CF_2d_G_Phloem(t) = CF_2d_G_Phloem(t - dt) + (R_to_R_TCE_phl_flow_2 + CF_2d_G_uptake - CF_2d_G_to_FR_phl_flow_2 - CF_2d_G_phl_xyl_flow_2) * dt
INIT CF_2d_G_Phloem = 0

DOCUMENT: This is the amount of TCE in the phloem of the capillary fringe root.

Units: mg TCE

INFLOWS:

R_to_R_TCE_phl_flow_2 (IN SECTOR: Unsat Rhizo/Root)

CF_2d_G_uptake = half_sat_eq_CF_2d_G_soil

DOCUMENT: This is the uptake by the root in the capillary fringe secondary growth portion of the soil.

Units: mg TCE/month

OUTFLOWS:

CF_2d_G_to_FR_phl_flow_2 = CF_2d_G_to_FR_phl_flow

DOCUMENT: This is the flow rate of the TCE in the phloem transpiration stream, from the secondary growth root in the capillary fringe to the fine roots in the capillary fringe .

Units: mg TCE/month

CF_2d_G_phl_xyl_flow_2 = CF_2d_G_phl_xyl_flow

DOCUMENT: This is an approximation of the flow of TCE from the root phloem apoplast and symplast to the root xylem in the secondary growth root in the capillary fringe.

Units: mg TCE/month

CF_2d_G_Root(t) = CF_2d_G_Root(t - dt) + (CF_2d_G_root_xyl_grad_2 - CF_root_metab_rate_2) * dt
INIT CF_2d_G_Root = 0

DOCUMENT: This is the amount of TCE in the root in the capillary fringe of the soil.

Units: mg TCE

INFLOWS:

CF_2d_G_root_xyl_grad_2 = CF_2d_G_root_xyl_flow

DOCUMENT: This is an equilibrium flow equation, balancing the concentration of TCE between the root xylem to the root in the capillary fringe with a transfer rate coefficient between the two.

Units: mg TCE/month

OUTFLOWS:

CF_root_metab_rate_2 = CF_root_metab_rate

DOCUMENT: This is the metabolic rate of TCE IN the CF root of a tree.

Units: mg TCE/month

CF_2d_G_Xylem(t) = CF_2d_G_Xylem(t - dt) + (CF_FR_xyl_to_2d_G_xyl_flow_3 + CF_2d_G_phl_xyl_flow_2 - R_to_R_TCE_xyl_flow_2 - CF_2d_G_root_xyl_grad_2) * dt
INIT CF_2d_G_Xylem = 0

DOCUMENT: This is the amount of TCE in the xylem of the root in the capillary fringe of the soil.

Units: mg TCE

INFLOWS:

CF_FR_xyl_to_2d_G_xyl_flow_3 = CF_FR_xyl_to_2d_G_xyl_flow_2

DOCUMENT: This is the flow rate of the TCE in the xylem transpiration stream, from the root hair zone in the capillary fringe to the secondary growth root in the capillary fringe.

Units: mg TCE/month

CF_2d_G_phl_xyl_flow_2 = CF_2d_G_phl_xyl_flow

DOCUMENT: This is an approximation of the flow of TCE from the root phloem apoplast and symplast to the root xylem in the secondary growth root in the capillary fringe.

Units: mg TCE/month

OUTFLOWS:

R_to_R_TCE_xyl_flow_2 (IN SECTOR: Unsat Rhizo/Root)

CF_2d_G_root_xyl_flow_2 = CF_2d_G_root_xyl_flow

DOCUMENT: This is an equilibrium flow equation, balancing the concentration of TCE between the root xylem to the root in the capillary fringe using a transfer rate coefficient between the two.

Units: mg TCE/month

CF_FR_Zone_Phloem(t) = CF_FR_Zone_Phloem(t - dt) +
(CF_2d_G_to_FR_phl_flow_2 - CF_FR_phl_xyl_flow_2 - CF_FR_phl_tiss_flow_2) *
dt
INIT CF_FR_Zone_Phloem = 0

DOCUMENT: This stock represents the amount of TCE in the capillary fringe root hair zone phloem.

Units: mg TCE

INFLOWS:

CF_2d_G_to_FR_phl_flow_2 = CF_2d_G_to_FR_phl_flow

DOCUMENT: This is the flow rate of the TCE in the phloem transpiration stream, from the secondary growth root in the capillary fringe to the fine roots in the capillary fringe .

Units: mg TCE/month

OUTFLOWS:

CF_FR_phl_xyl_flow_2 = CF_FR_phl_xyl_flow

DOCUMENT: This is an equilibrium flow equation, balancing the concentration of TCE between the capillary fringe fine root phloem to the capillary fringe fine root xylem and the rate of transfer of contaminant between the two.

Units: mg TCE/month

CF_FR_phl_tiss_flow_2 = CF_FR_phl_tiss_flow

DOCUMENT: This is the flow rate from the capillary fringe fine root phloem to the capillary fringe fine root tissue.

Units: mg TCE/month

CF_FR_Zone_Tissue(t) = CF_FR_Zone_Tissue(t - dt) + (CF_FR_uptake + CF_FR_phl_tiss_flow_2 - CF_FR_tiss_xyl_flow_2 - CF_FR_tiss_metab_rate) * dt
INIT CF_FR_Zone_Tissue = 0

DOCUMENT: This stock represents the amount of TCE in the capillary fringe root hair zone tissue.

Units: mg TCE

INFLOWS:

CF_FR_uptake = half_sat_eq_CF_FR_soil

DOCUMENT: This is the TCE uptake by the root hair zone in the capillary fringe.

Units: mg TCE/month

CF_FR_phl_tiss_flow_2 = CF_FR_phl_tiss_flow

DOCUMENT: This is the flow rate from the capillary fringe fine root phloem to the capillary fringe fine root tissue.

Units: mg TCE/month

OUTFLOWS:

CF_FR_tiss_xyl_flow_2 = CF_FR_tiss_xyl_flow

DOCUMENT: This is the flow rate of the TCE in the xylem transpiration stream, from the fine root tissue in the capillary fringe to the fine root xylem in the capillary fringe.

Units: mg TCE/month

CF_FR_tiss_metab_rate = CF_FR_metab_rate

DOCUMENT: This is the metabolic rate of TCE from the CF fine roots of a tree.

Units: mg TCE/month

CF_FR_Zone_Xylem(t) = CF_FR_Zone_Xylem(t - dt) + (CF_FR_tiss_xyl_flow_2 + CF_FR_phl_xyl_flow_2 - CF_FR_xyl_to_2d_G_xyl_flow_3) * dt
INIT CF_FR_Zone_Xylem = 0

DOCUMENT: This stock represents the amount of TCE in the capillary fringe root hair zone xylem.

Units: mg TCE

INFLOWS:

CF_FR_tiss_xyl_flow_2 = CF_FR_tiss_xyl_flow

DOCUMENT: This is the flow rate of the TCE in the xylem transpiration stream, from the fine root tissue in the capillary fringe to the fine root xylem in the capillary fringe.

Units: mg TCE/month

CF_FR_phl_xyl_flow_2 = CF_FR_phl_xyl_flow

DOCUMENT: This is an equilibrium flow equation, balancing the concentration of TCE between the capillary fringe fine root phloem to the capillary fringe fine root xylem using a rate of transfer coefficient between the two.

Units: mg TCE/month

OUTFLOWS:

CF_FR_xyl_to_2d_G_xyl_flow_3 = CF_FR_xyl_to_2d_G_xyl_flow_2

DOCUMENT: This is the flow rate of the TCE in the xylem transpiration stream, from the root hair zone in the capillary fringe to the secondary growth root in the capillary fringe.

Units: mg TCE/month

TCE_in_2d_G_CF_Rhizo(t) = TCE_in_2d_G_CF_Rhizo(t - dt) +
(TCE_flow_into_CF_2d_G_rhizo_2 - Cometab_2d_G_CF_Rhizo_2 -
CF_2d_G_Rhizo_TCE_loss_rate - CF_2d_G_uptake) * dt
INIT TCE_in_2d_G_CF_Rhizo = 0

DOCUMENT: This is the approximation for the amount of TCE in the capillary fringe of the rhizosphere surrounding the secondary growth root.

Units: mg TCE

INFLOWS:

TCE_flow_into_CF_2d_G_rhizo_2 = TCE_flow_into_CF_2d_G_rhizo

DOCUMENT: This is the TCE flow into the 2d growth capillary fringe of the rhizosphere.

Units: mg TCE/month

OUTFLOWS:

Cometab_2d_G_CF_Rhizo_2 = Cometab_2d_G_CF_Rhizo

DOCUMENT: This is the metabolism of TCE in the capillary fringe of the rhizosphere.

Units: mg TCE/month

CF_2d_G_Rhizo_TCE_loss_rate =
Rhizo_TCE_loss_fluctuation*CF_2d_G_diff_rate

DOCUMENT: This gives a representation of the loss of TCE from the rhizosphere during the tree's dormant months when active uptake is not taking place.

Units: mg TCE/month

CF_2d_G_uptake = half_sat_eq_CF_2d_G_soil

DOCUMENT: This is the uptake by the root in the capillary fringe secondary growth portion of the soil.

Units: mg TCE/month

TCE_in_FR_Zone_CF_Rhizo(t) = TCE_in_FR_Zone_CF_Rhizo(t - dt) + (TCE_flow_into_CF_FR_rhizo_2 - Cometab_FR_CF_Rhizo_2 - CF_FR_uptake - CF_FR_Rhizo_TCE_loss_rate) * dt
INIT TCE_in_FR_Zone_CF_Rhizo = 0

DOCUMENT: This is the approximation for the amount of TCE in the capillary fringe of the rhizosphere surrounding the root hair zone.

Units: mg TCE

INFLOWS:

TCE_flow_into_CF_FR_rhizo_2 = TCE_flow_into_CF_RH_rhizo

DOCUMENT: This is the TCE flow into the fine root capillary fringe of the rhizosphere.

Units: mg TCE/month

OUTFLOWS:

Cometab_FR_CF_Rhizo_2 = Cometab_FR_CF_Rhizo

DOCUMENT: This is the metabolism of TCE in the fine root capillary fringe of the rhizosphere.

Units: mg TCE/month

CF_FR_uptake = half_sat_eq_CF_FR_soil

DOCUMENT: This is the TCE uptake by the root hair zone in the capillary fringe.

Units: mg TCE/month

CF_FR_Rhizo_TCE_loss_rate =
Rhizo_TCE_loss_fluctuation*CF_FR_diff_rate

DOCUMENT: This gives a representation of the diffusion of TCE from the capillary fringe fine root rhizosphere during the tree's dormant months when active uptake is not taking place.

Units: mg TCE/month

Capillary Fringe Root Flows

CF_2d_G_phl_xyl_flow =
IF(Unsat_to_CF_FR_Vol_coeff=1)THEN(0)ELSE((CF_2d_G_Phloem/((Rt_2d_G_Phl
_Vol)*(1-
Unsat_to_CF_FR_Vol_coeff))*Sec_G_tiss_vol_coeff)*(Xyl_Q_per_Leaf_Area*CF_2d
_G_uptake_coeff)*Leaf_Area*Seasonal_Fluctuation)

DOCUMENT: This is an approximation of the flow of TCE from the root phloem apoplast and symplast to the root xylem in the secondary growth root in the capillary fringe.

Units: mg TCE/month

CF_2d_G_root_TCE_conc = CF_2d_G_Root/((Root_Volume-
(Root_Phl_Vol+Root_Xyl_Vol))*(root_2d_G_to_FR_ratio)*(1-
Unsat_to_CF_2d_G_root_Vol_coeff))

DOCUMENT: This is the concentration of TCE in the secondary growth root in the capillary fringe of the soil.

Units: mg TCE/m3

CF_2d_G_root_xyl_flow =
IF(Unsat_to_CF_2d_G_root_Vol_coeff=1)THEN(0)ELSE((CF_2d_G_xyl_TCE_conc-
(CF_2d_G_root_TCE_conc*Sec_G_part_coeff))*CF_2d_G_root_xyl_trans_rate_coeff
*Seasonal_Fluctuation)

DOCUMENT: This is an equilibrium flow equation, balancing the concentration of TCE between the root xylem to the root in the secondary growth root in the capillary fringe using a transfer rate coefficient between the two.

Units: mg TCE/month

CF_2d_G_to_FR_phl_flow =
IF(Unsat_to_CF_FR_Vol_coeff=1)THEN(0)ELSE((CF_2d_G_Phloem/(Rt_2d_G_Phl
_Vol*(1-
Unsat_to_CF_FR_Vol_coeff)))*(Phl_Q_per_Leaf_Area)*CF_FR_uptake_coeff*Leaf_
Area*Seasonal_Fluctuation)

DOCUMENT: This is the flow rate of the TCE in the phloem transpiration stream, from the secondary growth root in the capillary fringe to the fine roots in the capillary fringe .

Units: mg TCE/month

CF_2d_G_xyl_TCE_conc = CF_2d_G_Xylem/(Rt_2d_G_Xyl_Vol*(1-
Unsat_to_CF_2d_G_root_Vol_coeff))
DOCUMENT: This is the concentration of TCE in the secondary growth root xylem in the capillary fringe of the soil.

Units: mg TCE/m3

CF_FR_phl_TCE_conc = CF_FR_Zone_Phloem/(Fine_Root_Phl_Vol*(1-
Unsat_to_CF_FR_Vol_coeff))

DOCUMENT: This is the concentration of TCE in the phloem root hair zone in the capillary fringe of the soil.

Units: mg TCE/m3

CF_FR_phl_tiss_flow =
IF(Unsat_to_CF_FR_Vol_coeff=1)THEN(0)ELSE((CF_FR_Zone_Phloem/(Fine_Root
_Phl_Vol*(1-
Unsat_to_CF_FR_Vol_coeff)))*(Phl_Q_per_Leaf_Area)*CF_FR_uptake_coeff*Leaf_
Area*Seasonal_Fluctuation)

DOCUMENT: This is the flow rate from the capillary fringe fine root phloem to the capillary fringe root hair tissue.

Units: mg TCE/month

CF_FR_phl_xyl_flow =
IF(Unsat_to_CF_FR_Vol_coeff=1)THEN(0)ELSE(CF_FR_phl_TCE_conc-
(CF_RH_xyl_TCE_conc*fine_root_part_coeff))*phl_xyl_trans_rate_coeff*Seasonal_F
luctuation

DOCUMENT: This is an equilibrium flow equation, balancing the concentration of TCE between the capillary fringe fine root phloem to the capillary fringe fine root xylem using a rate of transfer coefficient between the two.

Units: mg TCE/month

CF_FR_tiss_xyl_flow =
IF(Unsat_to_CF_FR_Vol_coeff=1)THEN(0)ELSE(((CF_FR_Zone_Tissue/(((Fine_Roo
t_Volume-(Fine_Root_Phl_Vol+Fine_Root_Xyl_Vol))*(1-
Unsat_to_CF_FR_Vol_coeff)))*FR_tiss_vol_coeff))*(Xyl_Q_per_Leaf_Area)*CF_FR
_uptake_coeff*Seasonal_Fluctuation*Leaf_Area)

DOCUMENT: This is the flow rate of the TCE in the xylem transpiration stream, from the fine root tissue in the capillary fringe to the fine root xylem in the capillary fringe.

Units: mg TCE/month

CF_FR_xyl_to_2d_G_xyl_flow =
IF(Unsat_to_CF_FR_Vol_coeff=1)THEN(0)ELSE(((CF_FR_Zone_Xylem/Fine_Root_
Xyl_Vol)*(1-
Unsat_to_CF_FR_Vol_coeff))*(Xyl_Q_per_Leaf_Area)*(CF_FR_uptake_coeff)*Leaf
_Area*Seasonal_Fluctuation)

DOCUMENT: This is the flow rate of the TCE in the xylem transpiration stream, from the root hair zone in the capillary fringe to the secondary growth root in the capillary fringe.

Units: mg TCE/month

CF_RH_xyl_TCE_conc = CF_FR_Zone_Xylem/(Fine_Root_Xyl_Vol*(1-
Unsat_to_CF_FR_Vol_coeff))

DOCUMENT: This is the concentration of TCE in the xylem root hair zone in the capillary fringe of the soil.

Units: mg TCE/m3

Graphs

Stem_Phl_Vol = Stem_Xyl_Vol/2

DOCUMENT: The total stem phloem volume comes out at approximately 1300 cm square by meter in height or .13 cubic meters. My graph approaches this max value.

Units: m3

FR_Rhizo_Volume = GRAPH(TIME)
(0.00, 165), (50.0, 792), (100, 1337), (150, 1815), (200, 2178), (250, 2459), (300, 2714), (350, 2904), (400, 3020), (450, 3119), (500, 3201), (550, 3267), (600, 3300)

DOCUMENT: This is the approximate volume of the rhizosphere. Authors estimate the rhizosphere thickness from 2 to 5 millimeters. These values give me a total rhizosphere volume of 2500 to 6000 cm2-m, with an average of around 4250. I am approximating that 3300 cm2-m of this average will be found in the fine root portion of the root. The values in this graph need to be divided by 10,000 to get it into cubic meters.

Units: m-cm2/10000

Leaf_Area = GRAPH(TIME)
(0.00, 20.0), (12.0, 35.0), (24.0, 49.0), (36.0, 67.4), (48.0, 86.4), (60.0, 105), (72.0, 122), (84.0, 140), (96.0, 161), (108, 182), (120, 202), (132, 240), (144, 260), (156, 280), (168, 330), (180, 370), (192, 420), (204, 470), (216, 530), (228, 600), (240, 660), (252, 720), (264, 780), (276, 840), (288, 900), (300, 950), (312, 1000), (324, 1060), (336, 1120), (348, 1170), (360, 1240), (372, 1290), (384, 1350), (396, 1390), (408, 1450), (420, 1490), (432, 1520), (444, 1550), (456, 1580), (468, 1610), (480, 1640), (492, 1650), (504, 1670), (516, 1690), (528, 1700), (540, 1720), (552, 1740), (564, 1750), (576, 1770), (588, 1790), (600, 1800)

DOCUMENT: Leaf area max is 1800 square meters. I came up with this figure by assuming the average leaf is .05 cm thick and knowing my max leaf volume is approximately .9 m3 at canopy closure. The leaf growth rapidly approaches this value until the canopy is closed.

Units: m2 leaf

Leaf_Volume = GRAPH(TIME)
(0.00, 0.01), (12.0, 0.017), (24.0, 0.025), (36.0, 0.034), (48.0, 0.043), (60.0, 0.052), (72.0, 0.061), (84.0, 0.07), (96.0, 0.081), (108, 0.091), (120, 0.101), (132, 0.135), (144, 0.155), (156, 0.175), (168, 0.195), (180, 0.235), (192, 0.275), (204, 0.315), (216, 0.365), (228, 0.41), (240, 0.455), (252, 0.48), (264, 0.51), (276, 0.54), (288, 0.555), (300, 0.585), (312, 0.6), (324, 0.625), (336, 0.645), (348, 0.66), (360, 0.68), (372, 0.7), (384, 0.72), (396, 0.745), (408, 0.77), (420, 0.78), (432, 0.8), (444, 0.81), (456, 0.825), (468, 0.835), (480, 0.84), (492, 0.85), (504, 0.855), (516, 0.865), (528, 0.875), (540, 0.88), (552, 0.885), (564, 0.892), (576, 0.896), (588, 0.898), (600, 0.9)

DOCUMENT: This graph is from my mathcad template. The max leaf volume approaches 1.0 cubic meter.

Units: m3 leaf

Rhizo_TCE_loss_fluctuation = GRAPH(TIME)
(0.00, 0.667), (1.00, 0.00), (2.00, 0.00), (3.00, 0.00), (4.00, 0.00), (5.00, 0.00), (6.00, 0.00), (7.00, 0.00), (8.00, 0.667), (9.00, 0.95), (10.0, 1.00), (11.0, 0.95), (12.0, 0.667), (13.0, 0.00), (14.0, 0.00), (15.0, 0.00), (16.0, 0.00), (17.0, 0.00), (18.0, 0.00), (19.0, 0.00), (20.0, 0.667), (21.0, 0.95), (22.0, 1.00), (23.0, 0.95), (24.0, 0.667), (25.0, 0.00), (26.0, 0.00), (27.0, 0.00), (28.0, 0.00), (29.0, 0.00), (30.0, 0.00), (31.0, 0.00), (32.0, 0.667), (33.0, 0.95), (34.0, 1.00), (35.0, 0.95), (36.0, 0.667), (37.0, 0.00), (38.0, 0.00), (39.0, 0.00), (40.0, 0.00), (41.0, 0.00), (42.0, 0.00), (43.0, 0.00), (44.0, 0.667), (45.0, 0.95), (46.0, 1.00), (47.0, 0.95), (48.0, 0.667), (49.0, 0.00), (50.0, 0.00), (51.0, 0.00), (52.0, 0.00), (53.0, 0.00), (54.0, 0.00), (55.0, 0.00), (56.0, 0.667), (57.0, 0.95), (58.0, 1.00), (59.0, 0.95), (60.0, 0.667), (61.0, 0.00), (62.0, 0.00), (63.0, 0.00), (64.0, 0.00), (65.0, 0.00), (66.0, 0.00), (67.0, 0.00), (68.0, 0.667), (69.0, 0.95), (70.0, 1.00), (71.0, 0.95), (72.0, 0.667), (73.0, 0.00), (74.0, 0.00), (75.0, 0.00), (76.0, 0.00), (77.0, 0.00), (78.0, 0.00), (79.0, 0.00), (80.0, 0.667), (81.0, 0.95), (82.0, 1.00), (83.0, 0.95), (84.0, 0.667), (85.0, 0.00), (86.0, 0.00), (87.0, 0.00), (88.0, 0.00), (89.0, 0.00), (90.0, 0.00), (91.0, 0.00), (92.0, 0.667), (93.0, 0.95), (94.0, 1.00), (95.0, 0.95), (96.0, 0.667), (97.0, 0.00), (98.0, 0.00), (99.0, 0.00), (100, 0.00), (101, 0.00), (102, 0.00), (103, 0.00), (104, 0.667), (105, 0.95), (106, 1.00), (107, 0.95), (108, 0.667), (109, 0.00), (110, 0.00), (111, 0.00), (112, 0.00), (113, 0.00), (114, 0.00), (115, 0.00), (116, 0.667), (117, 0.95), (118, 1.00), (119, 0.95), (120, 0.667), (121, 0.00), (122, 0.00), (123, 0.00), (124, 0.00), (125, 0.00), (126, 0.00), (127, 0.00), (128, 0.667), (129, 0.95), (130, 1.00), (131, 0.95), (132, 0.667), (133, 0.00), (134, 0.00), (135, 0.00), (136, 0.00), (137, 0.00), (138, 0.00), (139, 0.00), (140, 0.667), (141, 0.95), (142, 1.00), (143, 0.95), (144, 0.667), (145, 0.00), (146, 0.00), (147, 0.00), (148, 0.00), (149, 0.00), (150, 0.00), (151, 0.00), (152, 0.667), (153, 0.95), (154, 1.00), (155, 0.95), (156, 0.667), (157, 0.00), (158, 0.00), (159, 0.00), (160, 0.00), (161, 0.00), (162, 0.00), (163, 0.00), (164, 0.667), (165, 0.95),

(166, 1.00), (167, 0.95), (168, 0.667), (169, 0.00), (170, 0.00), (171, 0.00), (172, 0.00), (173, 0.00), (174, 0.00), (175, 0.00), (176, 0.667), (177, 0.95), (178, 1.00), (179, 0.95), (180, 0.667), (181, 0.00), (182, 0.00), (183, 0.00), (184, 0.00), (185, 0.00), (186, 0.00), (187, 0.00), (188, 0.667), (189, 0.95), (190, 1.00), (191, 0.95), (192, 0.667), (193, 0.00), (194, 0.00), (195, 0.00), (196, 0.00), (197, 0.00), (198, 0.00), (199, 0.00), (200, 0.667), (201, 0.95), (202, 1.00), (203, 0.95), (204, 0.667), (205, 0.00), (206, 0.00), (207, 0.00), (208, 0.00), (209, 0.00), (210, 0.00), (211, 0.00), (212, 0.667), (213, 0.95), (214, 1.00), (215, 0.95), (216, 0.667), (217, 0.00), (218, 0.00), (219, 0.00), (220, 0.00), (221, 0.00), (222, 0.00), (223, 0.00), (224, 0.667), (225, 0.95), (226, 1.00), (227, 0.95), (228, 0.667), (229, 0.00), (230, 0.00), (231, 0.00), (232, 0.00), (233, 0.00), (234, 0.00), (235, 0.00), (236, 0.667), (237, 0.95), (238, 1.00), (239, 0.95), (240, 0.667), (241, 0.00), (242, 0.00), (243, 0.00), (244, 0.00), (245, 0.00), (246, 0.00), (247, 0.00), (248, 0.667), (249, 0.95), (250, 1.00), (251, 0.95), (252, 0.667), (253, 0.00), (254, 0.00), (255, 0.00), (256, 0.00), (257, 0.00), (258, 0.00), (259, 0.00), (260, 0.667), (261, 0.95), (262, 1.00), (263, 0.95), (264, 0.667), (265, 0.00), (266, 0.00), (267, 0.00), (268, 0.00), (269, 0.00), (270, 0.00), (271, 0.00), (272, 0.667), (273, 0.95), (274, 1.00), (275, 0.95), (276, 0.667), (277, 0.00), (278, 0.00), (279, 0.00), (280, 0.00), (281, 0.00), (282, 0.00), (283, 0.00), (284, 0.667), (285, 0.95), (286, 1.00), (287, 0.95), (288, 0.667), (289, 0.00), (290, 0.00), (291, 0.00), (292, 0.00), (293, 0.00), (294, 0.00), (295, 0.00), (296, 0.667), (297, 0.95), (298, 1.00), (299, 0.95), (300, 0.667), (301, 0.00), (302, 0.00), (303, 0.00), (304, 0.00), (305, 0.00), (306, 0.00), (307, 0.00), (308, 0.667), (309, 0.95), (310, 1.00), (311, 0.95), (312, 0.667), (313, 0.00), (314, 0.00), (315, 0.00), (316, 0.00), (317, 0.00), (318, 0.00), (319, 0.00), (320, 0.667), (321, 0.95), (322, 1.00), (323, 0.95), (324, 0.667), (325, 0.00), (326, 0.00), (327, 0.00), (328, 0.00), (329, 0.00), (330, 0.00), (331, 0.00), (332, 0.667), (333, 0.95), (334, 1.00), (335, 0.95), (336, 0.667), (337, 0.00), (338, 0.00), (339, 0.00), (340, 0.00), (341, 0.00), (342, 0.00), (343, 0.00), (344, 0.667), (345, 0.95), (346, 1.00), (347, 0.95), (348, 0.667), (349, 0.00), (350, 0.00), (351, 0.00), (352, 0.00), (353, 0.00), (354, 0.00), (355, 0.00), (356, 0.667), (357, 0.95), (358, 1.00), (359, 0.95), (360, 0.667), (361, 0.00), (362, 0.00), (363, 0.00), (364, 0.00), (365, 0.00), (366, 0.00), (367, 0.00), (368, 0.667), (369, 0.95), (370, 1.00), (371, 0.95), (372, 0.667), (373, 0.00), (374, 0.00), (375, 0.00), (376, 0.00), (377, 0.00), (378, 0.00), (379, 0.00), (380, 0.667), (381, 0.95), (382, 1.00), (383, 0.95), (384, 0.667), (385, 0.00), (386, 0.00), (387, 0.00), (388, 0.00), (389, 0.00), (390, 0.00), (391, 0.00), (392, 0.667), (393, 0.95), (394, 1.00), (395, 0.95), (396, 0.667), (397, 0.00), (398, 0.00), (399, 0.00), (400, 0.00), (401, 0.00), (402, 0.00), (403, 0.00), (404, 0.667), (405, 0.95), (406, 1.00), (407, 0.95), (408, 0.667), (409, 0.00), (410, 0.00), (411, 0.00), (412, 0.00), (413, 0.00), (414, 0.00), (415, 0.00), (416, 0.667), (417, 0.95), (418, 1.00), (419, 0.95), (420, 0.667), (421, 0.00), (422, 0.00), (423, 0.00), (424, 0.00), (425, 0.00), (426, 0.00), (427, 0.00), (428, 0.667), (429, 0.95), (430, 1.00), (431, 0.95), (432, 0.667), (433, 0.00), (434, 0.00), (435, 0.00), (436, 0.00), (437, 0.00), (438, 0.00), (439, 0.00), (440, 0.667), (441, 0.95), (442, 1.00), (443, 0.95), (444, 0.667), (445, 0.00), (446, 0.00), (447, 0.00), (448, 0.00), (449, 0.00), (450, 0.00), (451, 0.00), (452, 0.667), (453, 0.95), (454, 1.00), (455, 0.95), (456, 0.667), (457, 0.00), (458, 0.00), (459, 0.00), (460, 0.00), (461, 0.00), (462, 0.00), (463, 0.00), (464, 0.667), (465, 0.95), (466, 1.00), (467, 0.95),

(468, 0.667), (469, 0.00), (470, 0.00), (471, 0.00), (472, 0.00), (473, 0.00), (474, 0.00), (475, 0.00), (476, 0.667), (477, 0.95), (478, 1.00), (479, 0.95), (480, 0.667), (481, 0.00), (482, 0.00), (483, 0.00), (484, 0.00), (485, 0.00), (486, 0.00), (487, 0.00), (488, 0.667), (489, 0.95), (490, 1.00), (491, 0.95), (492, 0.667), (493, 0.00), (494, 0.00), (495, 0.00), (496, 0.00), (497, 0.00), (498, 0.00), (499, 0.00), (500, 0.667), (501, 0.95), (502, 1.00), (503, 0.95), (504, 0.667), (505, 0.00), (506, 0.00), (507, 0.00), (508, 0.00), (509, 0.00), (510, 0.00), (511, 0.00), (512, 0.667), (513, 0.95), (514, 1.00), (515, 0.95), (516, 0.667), (517, 0.00), (518, 0.00), (519, 0.00), (520, 0.00), (521, 0.00), (522, 0.00), (523, 0.00), (524, 0.667), (525, 0.95), (526, 1.00), (527, 0.95), (528, 0.667), (529, 0.00), (530, 0.00), (531, 0.00), (532, 0.00), (533, 0.00), (534, 0.00), (535, 0.00), (536, 0.667), (537, 0.95), (538, 1.00), (539, 0.95), (540, 0.667), (541, 0.00), (542, 0.00), (543, 0.00), (544, 0.00), (545, 0.00), (546, 0.00), (547, 0.00), (548, 0.667), (549, 0.95), (550, 1.00), (551, 0.95), (552, 0.667), (553, 0.00), (554, 0.00), (555, 0.00), (556, 0.00), (557, 0.00), (558, 0.00), (559, 0.00), (560, 0.667), (561, 0.95), (562, 1.00), (563, 0.95), (564, 0.667), (565, 0.05), (566, 0.00), (567, 0.00), (568, 0.00), (569, 0.00), (570, 0.00), (571, 0.00), (572, 0.667), (573, 0.95), (574, 1.00), (575, 0.95), (576, 0.667), (577, 0.00), (578, 0.00), (579, 0.00), (580, 0.00), (581, 0.00), (582, 0.00), (583, 0.00), (584, 0.667), (585, 0.95), (586, 1.00), (587, 0.95), (588, 0.667), (589, 0.00), (590, 0.00), (591, 0.00), (592, 0.00), (593, 0.00), (594, 0.00), (595, 0.00), (596, 0.667), (597, 0.95), (598, 1.00), (599, 0.95), (600, 0.667)

DOCUMENT: To represent the loss of TCE from the rhizosphere during the tree's dormant months, I developed this graph over time which fluctuates from 0 to 1. This fluctuation occurs from November to March.

Units: NA

Root_Volume = GRAPH(TIME)
(0.00, 0.032), (12.0, 0.05), (24.0, 0.07), (36.0, 0.09), (48.0, 0.12), (60.0, 0.137), (72.0, 0.156), (84.0, 0.188), (96.0, 0.219), (108, 0.25), (120, 0.281), (132, 0.313), (144, 0.344), (156, 0.375), (168, 0.406), (180, 0.438), (192, 0.469), (204, 0.5), (216, 0.538), (228, 0.563), (240, 0.594), (252, 0.625), (264, 0.656), (276, 0.688), (288, 0.719), (300, 0.75), (312, 0.781), (324, 0.813), (336, 0.844), (348, 0.875), (360, 0.906), (372, 0.938), (384, 0.969), (396, 1.00), (408, 1.02), (420, 1.03), (432, 1.05), (444, 1.06), (456, 1.07), (468, 1.09), (480, 1.10), (492, 1.12), (504, 1.13), (516, 1.15), (528, 1.17), (540, 1.18), (552, 1.19), (564, 1.21), (576, 1.22), (588, 1.24), (600, 1.25)

DOCUMENT: This graph is from my mathcad template. The max root volume approaches 1.25 cubic meter. This rate of approach is between the leaf and stem volume rates of approach, with leaf volume approaching .9 cubic m and stem volume approaching 5 cubic m.

Units: m3 root

Root_Xyl_Vol = GRAPH(TIME)
(0.00, 0.0131), (50.0, 0.0393), (100, 0.0587), (150, 0.0752), (200, 0.0897), (250, 0.102), (300, 0.111), (350, 0.119), (400, 0.125), (450, 0.13), (500, 0.133), (550, 0.136), (600, 0.138)

DOCUMENT: From my Mathcad template I found the total root xylem volume comes out as 11% of the total root volume at maturity. This gives me a total root xylem volume of approximately 1375 cm square by meter in length or .1375 cubic meters.

Units: m3 root xylem

Seasonal_Fluctuation = GRAPH(TIME)
(0.00, 0.00), (1.00, 0.5), (2.00, 0.825), (3.00, 0.96), (4.00, 1.00), (5.00, 0.96), (6.00, 0.825), (7.00, 0.5), (8.00, 0.00), (9.00, 0.00), (10.0, 0.00), (11.0, 0.00), (12.0, 0.00), (13.0, 0.5), (14.0, 0.825), (15.0, 0.96), (16.0, 1.00), (17.0, 0.96), (18.0, 0.825), (19.0, 0.5), (20.0, 0.00), (21.0, 0.00), (22.0, 0.00), (23.0, 0.00), (24.0, 0.00), (25.0, 0.5), (26.0, 0.825), (27.0, 0.96), (28.0, 1.00), (29.0, 0.96), (30.0, 0.825), (31.0, 0.5), (32.0, 0.00), (33.0, 0.00), (34.0, 0.00), (35.0, 0.00), (36.0, 0.00), (37.0, 0.5), (38.0, 0.825), (39.0, 0.96), (40.0, 1.00), (41.0, 0.96), (42.0, 0.825), (43.0, 0.5), (44.0, 0.00), (45.0, 0.00), (46.0, 0.00), (47.0, 0.00), (48.0, 0.00), (49.0, 0.5), (50.0, 0.825), (51.0, 0.96), (52.0, 1.00), (53.0, 0.96), (54.0, 0.825), (55.0, 0.5), (56.0, 0.00), (57.0, 0.00), (58.0, 0.00), (59.0, 0.00), (60.0, 0.00), (61.0, 0.5), (62.0, 0.825), (63.0, 0.96), (64.0, 1.00), (65.0, 0.96), (66.0, 0.825), (67.0, 0.5), (68.0, 0.00), (69.0, 0.00), (70.0, 0.00), (71.0, 0.00), (72.0, 0.00), (73.0, 0.5), (74.0, 0.825), (75.0, 0.96), (76.0, 1.00), (77.0, 0.96), (78.0, 0.825), (79.0, 0.5), (80.0, 0.00), (81.0, 0.00), (82.0, 0.00), (83.0, 0.00), (84.0, 0.00), (85.0, 0.5), (86.0, 0.825), (87.0, 0.96), (88.0, 1.00), (89.0, 0.96), (90.0, 0.825), (91.0, 0.5), (92.0, 0.00), (93.0, 0.00), (94.0, 0.00), (95.0, 0.00), (96.0, 0.00), (97.0, 0.5), (98.0, 0.825), (99.0, 0.96), (100, 1.00), (101, 0.96), (102, 0.825), (103, 0.5), (104, 0.00), (105, 0.00), (106, 0.00), (107, 0.00), (108, 0.00), (109, 0.5), (110, 0.825), (111, 0.96), (112, 1.00), (113, 0.96), (114, 0.825), (115, 0.5), (116, 0.00), (117, 0.00), (118, 0.00), (119, 0.00), (120, 0.00), (121, 0.5), (122, 0.825), (123, 0.96), (124, 1.00), (125, 0.96), (126, 0.825), (127, 0.5), (128, 0.00), (129, 0.00), (130, 0.00), (131, 0.00), (132, 0.00), (133, 0.5), (134, 0.825), (135, 0.96), (136, 1.00), (137, 0.96), (138, 0.825), (139, 0.5), (140, 0.00), (141, 0.00), (142, 0.00), (143, 0.00), (144, 0.00), (145, 0.5), (146, 0.825), (147, 0.96), (148, 1.00), (149, 0.96), (150, 0.825), (151, 0.5), (152, 0.00), (153, 0.00), (154, 0.00), (155, 0.00), (156, 0.00), (157, 0.5), (158, 0.825), (159, 0.96), (160, 1.00), (161, 0.96), (162, 0.825), (163, 0.5), (164, 0.00), (165, 0.00), (166, 0.00), (167, 0.00), (168, 0.00), (169, 0.5), (170, 0.825), (171, 0.96), (172, 1.00), (173, 0.96), (174, 0.825), (175, 0.5), (176, 0.00), (177, 0.00), (178, 0.00), (179, 0.00), (180, 0.00), (181, 0.5), (182, 0.825), (183, 0.96), (184, 1.00), (185, 0.96), (186, 0.825), (187, 0.5), (188, 0.00), (189, 0.00), (190, 0.00), (191, 0.00), (192, 0.00), (193, 0.5), (194, 0.825), (195,

0.96), (196, 1.00), (197, 0.96), (198, 0.825), (199, 0.5), (200, 0.00), (201, 0.00), (202, 0.00), (203, 0.00), (204, 0.00), (205, 0.5), (206, 0.825), (207, 0.96), (208, 1.00), (209, 0.96), (210, 0.825), (211, 0.5), (212, 0.00), (213, 0.00), (214, 0.00), (215, 0.00), (216, 0.00), (217, 0.5), (218, 0.825), (219, 0.96), (220, 1.00), (221, 0.96), (222, 0.825), (223, 0.5), (224, 0.00), (225, 0.00), (226, 0.00), (227, 0.00), (228, 0.00), (229, 0.5), (230, 0.825), (231, 0.96), (232, 1.00), (233, 0.96), (234, 0.825), (235, 0.5), (236, 0.00), (237, 0.00), (238, 0.00), (239, 0.00), (240, 0.00), (241, 0.5), (242, 0.825), (243, 0.96), (244, 1.00), (245, 0.96), (246, 0.825), (247, 0.5), (248, 0.00), (249, 0.00), (250, 0.00), (251, 0.00), (252, 0.00), (253, 0.5), (254, 0.825), (255, 0.96), (256, 1.00), (257, 0.96), (258, 0.825), (259, 0.5), (260, 0.00), (261, 0.00), (262, 0.00), (263, 0.00), (264, 0.00), (265, 0.5), (266, 0.825), (267, 0.96), (268, 1.00), (269, 0.96), (270, 0.825), (271, 0.5), (272, 0.00), (273, 0.00), (274, 0.00), (275, 0.00), (276, 0.00), (277, 0.5), (278, 0.825), (279, 0.96), (280, 1.00), (281, 0.96), (282, 0.825), (283, 0.5), (284, 0.00), (285, 0.00), (286, 0.00), (287, 0.00), (288, 0.00), (289, 0.5), (290, 0.825), (291, 0.96), (292, 1.00), (293, 0.96), (294, 0.825), (295, 0.5), (296, 0.00), (297, 0.00), (298, 0.00), (299, 0.00), (300, 0.00), (301, 0.5), (302, 0.825), (303, 0.96), (304, 1.00), (305, 0.96), (306, 0.825), (307, 0.5), (308, 0.00), (309, 0.00), (310, 0.00), (311, 0.00), (312, 0.00), (313, 0.5), (314, 0.825), (315, 0.96), (316, 1.00), (317, 0.96), (318, 0.825), (319, 0.5), (320, 0.00), (321, 0.00), (322, 0.00), (323, 0.00), (324, 0.00), (325, 0.5), (326, 0.825), (327, 0.96), (328, 1.00), (329, 0.96), (330, 0.825), (331, 0.5), (332, 0.00), (333, 0.00), (334, 0.00), (335, 0.00), (336, 0.00), (337, 0.5), (338, 0.825), (339, 0.96), (340, 1.00), (341, 0.96), (342, 0.825), (343, 0.5), (344, 0.00), (345, 0.00), (346, 0.00), (347, 0.00), (348, 0.00), (349, 0.5), (350, 0.825), (351, 0.96), (352, 1.00), (353, 0.96), (354, 0.825), (355, 0.5), (356, 0.00), (357, 0.00), (358, 0.00), (359, 0.00), (360, 0.00), (361, 0.5), (362, 0.825), (363, 0.96), (364, 1.00), (365, 0.96), (366, 0.825), (367, 0.5), (368, 0.00), (369, 0.00), (370, 0.00), (371, 0.00), (372, 0.00), (373, 0.5), (374, 0.825), (375, 0.96), (376, 1.00), (377, 0.96), (378, 0.825), (379, 0.5), (380, 0.00), (381, 0.00), (382, 0.00), (383, 0.00), (384, 0.00), (385, 0.5), (386, 0.825), (387, 0.96), (388, 1.00), (389, 0.96), (390, 0.825), (391, 0.5), (392, 0.00), (393, 0.00), (394, 0.00), (395, 0.00), (396, 0.00), (397, 0.5), (398, 0.825), (399, 0.96), (400, 1.00), (401, 0.96), (402, 0.825), (403, 0.5), (404, 0.00), (405, 0.00), (406, 0.00), (407, 0.00), (408, 0.00), (409, 0.5), (410, 0.825), (411, 0.96), (412, 1.00), (413, 0.96), (414, 0.825), (415, 0.5), (416, 0.00), (417, 0.00), (418, 0.00), (419, 0.00), (420, 0.00), (421, 0.5), (422, 0.825), (423, 0.96), (424, 1.00), (425, 0.96), (426, 0.825), (427, 0.5), (428, 0.00), (429, 0.00), (430, 0.00), (431, 0.00), (432, 0.00), (433, 0.5), (434, 0.825), (435, 0.96), (436, 1.00), (437, 0.96), (438, 0.825), (439, 0.5), (440, 0.00), (441, 0.00), (442, 0.00), (443, 0.00), (444, 0.00), (445, 0.5), (446, 0.825), (447, 0.96), (448, 1.00), (449, 0.96), (450, 0.825), (451, 0.5), (452, 0.00), (453, 0.00), (454, 0.00), (455, 0.00), (456, 0.00), (457, 0.5), (458, 0.825), (459, 0.96), (460, 1.00), (461, 0.96), (462, 0.825), (463, 0.5), (464, 0.00), (465, 0.00), (466, 0.00), (467, 0.00), (468, 0.00), (469, 0.5), (470, 0.825), (471, 0.96), (472, 1.00), (473, 0.96), (474, 0.825), (475, 0.5), (476, 0.00), (477, 0.00), (478, 0.00), (479, 0.00), (480, 0.00), (481, 0.5), (482, 0.825), (483, 0.96), (484, 1.00), (485, 0.96), (486, 0.825), (487, 0.5), (488, 0.00), (489, 0.00), (490, 0.00), (491, 0.00), (492, 0.00), (493, 0.5), (494, 0.825), (495, 0.96), (496, 1.00), (497, 0.96), (498, 0.825), (499, 0.5), (500, 0.00), (501, 0.00), (502, 0.00), (503,

0.00), (504, 0.00), (505, 0.5), (506, 0.825), (507, 0.96), (508, 1.00), (509, 0.96), (510, 0.825), (511, 0.5), (512, 0.00), (513, 0.00), (514, 0.00), (515, 0.00), (516, 0.00), (517, 0.5), (518, 0.825), (519, 0.96), (520, 1.00), (521, 0.96), (522, 0.825), (523, 0.5), (524, 0.00), (525, 0.00), (526, 0.00), (527, 0.00), (528, 0.00), (529, 0.5), (530, 0.825), (531, 0.96), (532, 1.00), (533, 0.96), (534, 0.825), (535, 0.5), (536, 0.00), (537, 0.00), (538, 0.00), (539, 0.00), (540, 0.00), (541, 0.5), (542, 0.825), (543, 0.96), (544, 1.00), (545, 0.96), (546, 0.825), (547, 0.5), (548, 0.00), (549, 0.00), (550, 0.00), (551, 0.00), (552, 0.00), (553, 0.5), (554, 0.825), (555, 0.96), (556, 1.00), (557, 0.96), (558, 0.825), (559, 0.5), (560, 0.00), (561, 0.00), (562, 0.00), (563, 0.00), (564, 0.00), (565, 0.5), (566, 0.825), (567, 0.96), (568, 1.00), (569, 0.96), (570, 0.825), (571, 0.5), (572, 0.00), (573, 0.00), (574, 0.00), (575, 0.00), (576, 0.00), (577, 0.5), (578, 0.825), (579, 0.96), (580, 1.00), (581, 0.96), (582, 0.825), (583, 0.5), (584, 0.00), (585, 0.00), (586, 0.00), (587, 0.00), (588, 0.00), (589, 0.5), (590, 0.825), (591, 0.96), (592, 1.00), (593, 0.96), (594, 0.825), (595, 0.5), (596, 0.00), (597, 0.00), (598, 0.00), (599, 0.00), (600, 0.00)

DOCUMENT: I made a seasonal fluctuation graph to multiply each of my flow rates by to give them a seasonal shift. It is in months, and goes out 600 months, or 50 years.

Units: NA

Sec_G_Rhizo_Volume = GRAPH(TIME)
(0.00, 50.0), (50.0, 190), (100, 328), (150, 449), (200, 541), (250, 624), (300, 698), (350, 754), (400, 805), (450, 851), (500, 888), (550, 911), (600, 925)
DOCUMENT: This is the approximate volume of the rhizosphere. Authors estimate the rhizosphere thickness from 2 to 5 millimeters. These values give me a total rhizosphere volume of 2500 to 6000 m-cm2 , with an average of around 4250. I am approximating that 925 m-square centimeters of this average will be found in the secondary growth portion of the root. The values in this graph need to be divided by 10,000 to get it into cubic meters.

Units: m-cm2/10000

Stem_Volume = GRAPH(TIME)
(0.00, 0.1), (12.0, 0.175), (24.0, 0.25), (36.0, 0.35), (48.0, 0.45), (60.0, 0.55), (72.0, 0.65), (84.0, 0.75), (96.0, 0.875), (108, 1.00), (120, 1.13), (132, 1.25), (144, 1.38), (156, 1.50), (168, 1.63), (180, 1.75), (192, 1.88), (204, 2.00), (216, 2.13), (228, 2.25), (240, 2.38), (252, 2.50), (264, 2.63), (276, 2.75), (288, 2.88), (300, 3.00), (312, 3.13), (324, 3.25), (336, 3.38), (348, 3.50), (360, 3.63), (372, 3.75), (384, 3.88), (396, 4.00), (408, 4.06), (420, 4.12), (432, 4.18), (444, 4.24), (456, 4.29), (468, 4.35), (480, 4.41), (492, 4.47), (504, 4.53), (516, 4.59), (528, 4.65), (540, 4.71), (552, 4.76), (564, 4.82), (576, 4.88), (588, 4.94), (600, 5.00)

DOCUMENT: This graph is from my mathcad template. The max stem volume linearly approaches 5 cubic meters.

Units: m3 stem

Stem_Xyl_Vol = GRAPH(TIME)
(0.00, 50.0), (50.0, 208), (100, 377), (150, 637), (200, 936), (250, 1261), (300, 1560), (350, 1885), (400, 2197), (450, 2327), (500, 2431), (550, 2522), (600, 2600)

DOCUMENT: The total stem xylem volume comes out at approximately 2600 cm square by meter in height or .26 cubic meters. My graph approaches this max value.

Units: m3

Leaf

TCE_in_Leaf(t) = TCE_in_Leaf(t - dt) + (xyl_leaf_flow_2 - phl_leaf_flow_2 - transpiration_flow_rate_2 - leaf_metab_rate_2 - leaf_senescence_2) * dt
INIT TCE_in_Leaf = 0

DOCUMENT: This is the amount of TCE in the leaf.

Units: mg TCE

INFLOWS:

xyl_leaf_flow_2 = xyl_leaf_flow

DOCUMENT: This rate is based on the xylem to leaf flow, including a seasonal fluctuation.

Units: mg TCE/month

OUTFLOWS:

phl_leaf_flow_2 = phl_leaf_flow

DOCUMENT: This rate is based on the phloem to leaf gradient, including a seasonal fluctuation.

Units: mg TCE/month

transpiration_flow_rate_2 = transpiration_flow_rate

DOCUMENT: The transpiration flow rate tracks the outflow of TCE into/out of the leaf out of/into the atmosphere.

Units: mg TCE/month

leaf_metab_rate_2 = leaf_metab_rate

DOCUMENT: This equation takes the form of the half-life equation - ln2/T half life * mass TCE in leaf.

Units: mg TCE/month

leaf_senescence_2 = leaf_senescence

DOCUMENT: To model the leaf senescence in the fall, I am using a step function relating the seasonal fluctuation to the TCE in the leaf compartments, driving the mass of TCE to 0 as leaves fall.

Units: mg TCE/month

TCE_in_Leaf_Phloem(t) = TCE_in_Leaf_Phloem(t - dt) + (phl_leaf_flow_2 + leaf_xyl_phl_flow_2 - L_to_S_TCE_Phl_Flow_2 - leaf_phl_senescence_2) * dt
INIT TCE_in_Leaf_Phloem = 0

DOCUMENT: This is the amount of TCE in the phloem of the leaf.

Units: mg TCE

INFLOWS:

phl_leaf_flow_2 = phl_leaf_flow

DOCUMENT: This rate is based on the phloem to leaf flow, including a seasonal fluctuation.

Units: mg TCE/month

leaf_xyl_phl_flow_2 = leaf_xyl_phl_flow

DOCUMENT: This is an equilibrium flow equation, balancing the concentration of TCE between the leaf xylem and the leaf phloem and the rate of transfer between the two.

Units: mg TCE/month

OUTFLOWS:

L_to_S_TCE_Phl_Flow_2 (Not in a sector)

leaf_phl_senescence_2 = leaf_phloem_senescence

DOCUMENT: To model the leaf senescence in the fall, I am using a step function relating the seasonal fluctuation to the TCE in the leaf compartments, driving the mass of TCE to 0 as leaves fall.

Units: mg TCE/month

TCE_in_Leaf_Xylem(t) = TCE_in_Leaf_Xylem(t - dt) + (S_to_L_TCE_Xyl_Flow_2 - xyl_leaf_flow_2 - leaf_xyl_senescence_2 - leaf_xyl_phl_flow_2) * dt
INIT TCE_in_Leaf_Xylem = 0

DOCUMENT: This is the amount of TCE in the xylem of the leaf.

Units: mg TCE

INFLOWS:

S_to_L_TCE_Xyl_Flow_2 (Not in a sector)

OUTFLOWS:

xyl_leaf_flow_2 = xyl_leaf_flow

DOCUMENT: This rate is based on the xylem to leaf flow, including a seasonal fluctuation.

Units: mg TCE/month

leaf_xyl_senescence_2 = leaf_xyl_senescence

DOCUMENT: To model the leaf senescence in the fall, I am using a step function relating the seasonal fluctuation to the TCE in the leaf compartments, driving the mass of TCE to 0 as leaves fall.

Units: mg TCE/month

leaf_xyl_phl_flow_2 = leaf_xyl_phl_flow

DOCUMENT: This is an equilibrium flow equation, balancing the concentration of TCE between the leaf xylem and the leaf phloem using a rate of transfer coefficient between the two.

Units: mg TCE/month

Leaf Equations

leaf_mass = leaf_density*Leaf_Volume

DOCUMENT: Leaf mass is computed by multiplying the leaf density (kg/cubic meter) by the leaf volume (cubic meter), giving leaf mass.

Units: kg leaf

leaf_metab_rate = (.693/TCE_leaf_half_life)*TCE_in_Leaf*Seasonal_Fluctuation

DOCUMENT: This equation takes the form of the half-life equation - ln2/TCE half life * mass TCE in leaf.

Units: mg TCE/month

leaf_phloem_senescence = IF(Seasonal_Fluctuation=0)THEN(STEP(TCE_in_Leaf_Phloem*10,Seasonal_Fluctuation=0))ELSE(0)

DOCUMENT: To model the leaf senescence in the fall, I am using a step function relating the seasonal fluctuation to the TCE in the leaf compartments, driving the mass of TCE to 0 as leaves fall.

Units: mg TCE/month

leaf_phl_TCE_conc = TCE_in_Leaf_Phloem/Leaf_Phl_Vol

DOCUMENT: This is the concentration of TCE in the phloem of the leaf.

Units: mg TCE/m3

Leaf_Phl_Vol = Leaf_Vasc_ratio*Leaf_Volume

DOCUMENT: Since leaf structure does not change for a plant with age, that is, the cross-section shows the same physiology over time, I am assuming the leaf phloem volume will remain constant over the life of the tree. After talking to Dr. Bleckmann, I am assuming the leaf is made up of 5% phloem tissue [Bleckmann, 1997].

Units: m3

leaf_senescence =
IF(Seasonal_Fluctuation=0)THEN(STEP(TCE_in_Leaf*10,Seasonal_Fluctuation=0))ELSE(0)

DOCUMENT: To model the leaf senescence in the fall, I am using a step function relating the seasonal fluctuation to the TCE in the leaf compartments, driving the mass of TCE to 0 as leaves fall.

Units: mg TCE/month

leaf_xyl_phl_flow = (leaf_xyl_TCE_conc-
(leaf_phl_TCE_conc*leaf_part_coeff))*phl_xyl_trans_rate_coeff*Seasonal_Fluctuation

DOCUMENT: This is an equilibrium flow equation, balancing the concentration of TCE between the leaf xylem and the leaf phloem using a rate of transfer coefficient between the two.

Units: mg TCE/month

leaf_xyl_senescence =
IF(Seasonal_Fluctuation=0)THEN(STEP(TCE_in_Leaf_Xylem*10,Seasonal_Fluctuation=0))ELSE(0)

DOCUMENT: To model the leaf senescence in the fall, I am using a step function relating the seasonal fluctuation to the TCE in the leaf compartments, driving the mass of TCE to 0 as leaves fall.

Units: mg TCE/month

leaf_xyl_TCE_conc = TCE_in_Leaf_Xylem/Leaf_Xyl_Vol

DOCUMENT: This is the concentration of TCE in the xylem of the leaf.

Units: mg TCE/m3

Leaf_Xyl_Vol = Leaf_Vasc_ratio*Leaf_Volume

DOCUMENT: Since leaf structure does not change for a plant with age, that is, the cross-section shows the same physiology over time, I am assuming the leaf xylem volume will remain constant over the life of the tree. After talking to Dr. Bleckmann, I am assuming the leaf is made up of 5% xylem tissue [Bleckmann, 1997].

Units: m3

L_to_S_TCE_Phl_Flow =
(TCE_in_Leaf_Phloem/Leaf_Phl_Vol)*(Phl_Q_per_Leaf_Area)*Seasonal_Fluctuation
*Leaf_Area

DOCUMENT: This is the flow rate of the TCE in the phloem transpiration stream, from the leaf to the stem.

Units: mg TCE/month

phl_leaf_flow = (TCE_in_Leaf/(Leaf_Volume-
(Leaf_Phl_Vol+Leaf_Xyl_Vol)))*(Phl_Q_per_Leaf_Area)*Seasonal_Fluctuation*Leaf
_Area

DOCUMENT: This is an equilibrium flow equation, balancing the concentration of TCE between the leaf phloem to the leaf itself.

Units: mg TCE/month

S_to_L_TCE_Xyl_Flow =
TCE_inStem_Xylem*(Xyl_Q_per_Leaf_Area)*Seasonal_Fluctuation*Leaf_Area/(Ste
m_Xyl_Vol/10000)

DOCUMENT: This is the flow rate of the TCE in the xylem transpiration stream, from the stem to the leaf.

Units: mg TCE/month

TCE_leaf_half_life = 2/30

DOCUMENT: According to Dr. Newman, 23 Jul 97, in a telephone conversation, metabolism in poplars is highest in the leaves, somewhat lower in the root, and very low in the stem. According to lit from Dr. Trapp, the half life of TCE in plants is approximately 2 days. I am using this value of 2 days in the leaf.

Units: month

xyl_leaf_flow =
TCE_in_Leaf_Xylem*(Xyl_Q_per_Leaf_Area)*Seasonal_Fluctuation*Leaf_Area/(Lea f_Xyl_Vol)

DOCUMENT: This is an equilibrium equation, balancing the concentration of TCE between the leaf xylem to the leaf itself.

Units: mg TCE/month

Output Parameters

Total_Loss_Storage_Metab_&_Transpiration(t) =
Total_Loss_Storage_Metab_&_Transpiration(t - dt) + (Ttl_Senesc_Rate + Total_Storage_Rate + Total_Metab_Rate + Trans_Rate) * dt
INIT Total_Loss_Storage_Metab_&_Transpiration = 0

DOCUMENT: This is the total amount of TCE lost from the tree through senescence, metabolism, storage, and transpiration.

Units: mg TCE

INFLOWS:

Ttl_Senesc_Rate =
leaf_phl_senescence_2+leaf_senescence_2+leaf_xyl_senescence_2

DOCUMENT: This is the total rate of TCE lost from the tree due to leaf senescence over time.

Units: mg TCE/month

Total_Storage_Rate =
CF_2d_G_root_xyl_grad_2+stem_xyl_flow_2+unsat_2d_G_root_xyl_flow_2

DOCUMENT: This is the total rate of TCE stored in tree tissue over time.

Units: mg TCE/month

Total_Metab_Rate =
CF_FR_tiss_metab_rate+leaf_metab_rate_2+unsat_FR_tiss_metab_rate_2

DOCUMENT: This is the total rate of TCE metabolized in the tree over time.

Units: mg TCE/month

Trans_Rate = transpiration_flow_rate_2

DOCUMENT: This is the rate of transpiration of TCE over time.

Units: mg TCE/month

Total_TCE_Uptake(t) = Total_TCE_Uptake(t - dt) + (total_uptake_flow) * dt
INIT Total_TCE_Uptake = 0

DOCUMENT: This is the total TCE taken up by the plant over time.

Units: mg TCE

INFLOWS:
total_uptake_flow =
CF_2d_G_uptake+CF_FR_uptake+unsat_2d_G_uptake+Unsat_FR_uptake

DOCUMENT: This is the total uptake rate in all portions of the root.

Units: mg TCE/month

Total_Transpiration(t) = Total_Transpiration(t - dt) + (total_trans_flow) * dt

INIT Total_Transpiration = 0

DOCUMENT: This is the total TCE uptake rate over time.

Units: mg TCE/month

INFLOWS:

total_trans_flow = transpiration_flow_rate_2

DOCUMENT: This is the total transpiration rate over time.

Units: mg TCE/month

Total_Uptake(t) = Total_Uptake(t - dt) + (Total_Uptake_Rate) * dt
INIT Total_Uptake = 0

DOCUMENT: This is the total amount of TCE transpired by the phreatophytic tree over time.

Units: mg TCE

INFLOWS:

Total_Uptake_Rate = CF_2d_G_uptake+CF_FR_uptake+Unsat_2d_G_uptake+Unsat_FR_uptake

DOCUMENT: This is the total rate of uptake of TCE into the phreatophytic tree over time.

Units: mg TCE/month

Rhizo_TCE_Loss_Rate = CF_2d_G_Rhizo_TCE_loss_rate+CF_FR_Rhizo_TCE_loss_rate+Unsat_2d_G_Rhizo_TCE_loss_rate+unsat_FR_TCE_loss_rate

DOCUMENT: This is the total rate of TCE loss from all the rhizosphere compartments.

Units: mg TCE/month

TCE_in_Rhizo = TCE_in_2d_G_CF_Rhizo+TCE_in_2d_G_Unsat_Rhizo+TCE_in_FR_Zone_CF_Rhizo+TCE_in_FR_Zone_Unsat_Rhizo

DOCUMENT: This is the total amount of TCE in the whole tree rhizosphere.

Units: mg TCE

TCE_in_Root =
CF_2d_G_Root+CF_FR_Zone_Tissue+Unsat_2d_G_Root+Unsat_FR_Zone_Tissue

TCE_Rhizo_Conc =
TCE_in_Rhizo/((FR_Rhizo_Volume+Sec_G_Rhizo_Volume)/10000)

TCE_Root_Conc = TCE_in_Root/(Root_Volume-(Root_Xyl_Vol+Root_Phl_Vol))

TCE_Stem_Conc = TCE_in_Stem/(Stem_Volume-
((Stem_Phl_Vol+Stem_Xyl_Vol)/10000))

TCE_Uptake =
CF_2d_G_uptake+CF_FR_uptake+unsat_2d_G_uptake+Unsat_FR_uptake

Rhizosphere Flow Equations

flow_into_rhizo = Leaf_Area*Seasonal_Fluctuation*(Xyl_Q_per_Leaf_Area)

DOCUMENT: This is the total water flow rate into the rhizosphere.

Units: m3 TCE/month

TCE_Cap_Fringe_Soil_Concentration = TCE_in_GW

DOCUMENT: This is the approximation for the concentration of TCE in the capillary fringe of the bulk soil. I am assuming this value remains constant at an approximate value which is the same as in the saturated soil.

Units: mgTCE/m3

TCE_flow_into_CF_2d_G_rhizo =
TCE_Cap_Fringe_Soil_Concentration*flow_into_rhizo*(CF_2d_G_uptake_coeff)

DOCUMENT: This is the TCE flow into the secondary growth capillary fringe of the rhizosphere. It is found by multiplying the CF TCE concentration by the water flow into the rhizosphere.

Units: mg TCE/month

TCE_flow_into_CF_RH_rhizo =
TCE_Cap_Fringe_Soil_Concentration*flow_into_rhizo*(CF_FR_uptake_coeff)

DOCUMENT: This is the TCE flow into the fine root capillary fringe of the rhizosphere. It is found by multiplying the CF TCE concentration by the water flow into the rhizosphere.

Units: mg TCE/month

TCE_flow_into_unsat_2d_G_rhizo =
TCE_Unsat_Soil_Concentration*flow_into_rhizo*(unsat_2d_G_uptake_coeff)

DOCUMENT: This is the TCE flow into the secondary growth unsaturated rhizosphere. It is found by multiplying the unsat soil TCE concentration by the water flow into the rhizosphere.

Units: mg TCE/month

TCE_flow_into_unsat_FR_rhizo =
TCE_Unsat_Soil_Concentration*flow_into_rhizo*(unsat_FR_uptake_coeff)

DOCUMENT: This is the TCE flow into the fine root unsaturated rhizosphere. It is found by multiplying the unsat soil TCE concentration by the water flow into the rhizosphere.

Units: mg TCE/month

TCE_Unsat_Soil_Concentration = TCE_in_GW/100

DOCUMENT: This is the approximation for the concentration of TCE in the unsaturated portion of the bulk soil. I am assuming this value remains constant at an approximate value of .01 of the value in the saturated soil.

Units: mg TCE/m3

Root Equations

CF_2d_G_diff_rate = TCE_Conc_in_CF_2d_G_Rhizo*rhizo_diffusion_factor

DOCUMENT: This equation represents the rate of diffusion of TCE from the capillary fringe secondary growth portion of the rhizosphere.

Units: mg TCE/month

CF_2d_G_TCE_half_life = 15/30

DOCUMENT: According to Dr. Newman, 23 Jul 97, in a telephone conversation, metabolism in poplars is highest in the leaves, somewhat lower in the root, and very low in the stem. According to lit from Dr. Trapp, the half life of TCE in plants is approximately 2 days. I am using value of 15 days in the secondary growth portion of the root.

Units: month

CF_2d_G_uptake_coeff =
IF(unsat_2d_G_uptake_coeff=0)THEN(.7)ELSE((unsat_2d_G_uptake_coeff/(unsat_2d_G_uptake_coeff+unsat_FR_uptake_coeff))*(1-(unsat_2d_G_uptake_coeff+unsat_FR_uptake_coeff)))

DOCUMENT: This coefficient approximates the weighted flow in the capillary fringe root xylem.

Units: % flow rate

CF_FR_diff_rate = TCE_Conc_in_CF_FR_Rhizo*rhizo_diffusion_factor

DOCUMENT: This equation represents the rate of diffusion of TCE from the capillary fringe fine root portion of the rhizosphere.

Units: mg TCE/month

CF_FR_metab_rate =
(.693/CF_FR_TCE_half_life)*CF_FR_Zone_Tissue*Seasonal_Fluctuation

DOCUMENT: This equation takes the form of the half-life equation - ln2/T half life * mass TCE in capillary fringe fine roots.

Units: mg TCE/month

CF_FR_TCE_half_life = 15/30

DOCUMENT: According to Dr. Newman, 23 Jul 97, in a telephone conversation, metabolism in poplars is highest in the leaves, somewhat lower in the root, and very low in the stem. According to lit from Dr. Trapp, the half life of TCE in plants is approximately 2 days. I am using value of 15 days in the root hair zone.

Units: month

CF_FR_uptake_coeff =
IF(unsat_FR_uptake_coeff=0)THEN(.3)ELSE((unsat_FR_uptake_coeff/(unsat_FR_uptake_coeff+unsat_2d_G_uptake_coeff))*(1-(unsat_FR_uptake_coeff+unsat_2d_G_uptake_coeff)))

DOCUMENT: This coefficient approximates the weighted flow in the root hair zone vascular tissue.

Units: % flow rate

CF_root_metab_rate =
(.693/CF_2d_G_TCE_half_life)*CF_2d_G_Root*Seasonal_Fluctuation

DOCUMENT: This equation takes the form of the half-life equation - ln2/T half life * mass TCE in stem.

Units: mg TCE/month

CF_soil_thickness = .605

DOCUMENT: This is the thickness of the capillary fringe. At AF Plant 4 the capillary fringe is approximated as 18-30 inches or .45 to .76 meters, with an average of .605. The tests at WSU used a container 90 cm tall with a sand/water layer 30 cm deep.

Units: meters

Cometab_2d_G_CF_Rhizo = (.693/rhizo_TCE_half_life)*TCE_in_2d_G_CF_Rhizo

DOCUMENT: This converter represents the cometabolic rate in the secondary growth capillary fringe rhizosphere.

Units: mg TCE/month

Cometab_2d_G_Unsat_Rhizo =
(.693/rhizo_TCE_half_life)*TCE_in_2d_G_Unsat_Rhizo

DOCUMENT: This converter represents the cometabolic rate in the secondary growth unsaturated rhizosphere.

Units: mg TCE/month

Cometab_FR_CF_Rhizo = (.693/rhizo_TCE_half_life)*TCE_in_FR_Zone_CF_Rhizo

DOCUMENT: This converter represents the cometabolic rate in the fine root capillary fringe rhizosphere.

Units: mg TCE/month

Cometab_FR_Unsat_Rhizo =
(.693/rhizo_TCE_half_life)*TCE_in_FR_Zone_Unsat_Rhizo

DOCUMENT: This converter represents the cometabolic rate in the fine root unsaturated rhizosphere.

Units: mg TCE/month

depth_of_root =
IF(vertical_growth_of_root_over_time<depth_to_GW)THEN(vertical_growth_of_root_over_time)ELSE(depth_to_GW)

DOCUMENT: This is a If Then statement, which limits the vertical growth of the root to the ground water depth.

Units: NA

depth_to_GW = 3.3

DOCUMENT: This is the average depth to ground water at a given site. At AF Plant 4 the depth to ground water varies from 10 to 12 feet or 3.05 to 3.65 m and is approximated as 3.3 meters. For the tests at WSU the containers were 90 cm.

Units: meters

fine_root_flow_weight = .30

DOCUMENT: According to Dickmann and Stewart, Hofer, and Curl - the fine root or root hair zone is the zone of major water uptake. In a perennial plant, the root hair zone makes up only 1% of the root, the rest being suberized root [Kolek, 1992:183; Curl, 1986:47]. Some authors have found substantial uptake rates in the suberized portion of the root [Kolek, 1992:183]. Other authors have found uptake rates at different locations of the root change with rate of uptake; at low uptake rates the apical root is the major zone of uptake, while at high rates of uptake the basal root is the major zone of uptake [Brouwer, 1953:134; 1954:78]. Researchers have found root hair zone uptake varies from 2 to 70% of total uptake, which varies with water availability (the more water readily available the less root hairs necessary for uptake) [Gatliff, 1997]. Still other authors state root hairs perform no uptake function, basing this on the fact that the conductance of the root hairs is much lower than that of soil, making root hairs an unlikely media for water uptake [Weatherly, 1982:105]. I am assuming the uptake by the fine root is somewhere between the literature values, so I will assume a value of 30%.

Units: %

Fine_Root_Phl_Vol = Fine_Root_Xyl_Vol/2

DOCUMENT: In my Mathcad template I assumed the phloem was half the thickness of the xylem volume, so by dividing the xylem by 2, the fine root phloem volume is calculated.

Units: m3 root hair phloem

Fine_Root_Volume = Root_Volume*(1-root_2d_G_to_FR_ratio)

DOCUMENT: This is the volume of the fine roots in the phreatophyte tree root.

Units: m3 root hair

Fine_Root_Xyl_Vol = Fine_Root_Volume*FR_to_FR_Xyl_ratio

DOCUMENT: This is the volume of xylem in the fine root or root hair zone.

Units: m3 fine root xylem

FR_to_FR_Xyl_ratio = .133

DOCUMENT: From my Mathcad template, I found the fine root xylem volume makes up approximately 13.3% of the fine root volume. This converter represents this value.

Unit: % root hair volume

root_mass =
(sec_growth_root_density*Root_Volume*root_2d_G_to_FR_ratio)+(Root_Volume*fine_root_density*(1-root_2d_G_to_FR_ratio))

DOCUMENT: Root mass is computed by multiplying the root density (kg/cubic meter) by the root volume (cubic meter), giving root mass.

Units: kg root

Root_Phl_Vol = Root_Xyl_Vol/2

DOCUMENT: In my Mathcad template I assumed the phloem was half the thickness of the xylem volume, so by dividing the xylem by 2, the root phloem volume is calculated.

Units: m3 root phloem

Rt_2d_G_Phl_Vol = Root_Phl_Vol-Fine_Root_Phl_Vol

DOCUMENT: By subtracting the root hair phloem volume from the total root phloem volume, the amount of secondary growth phloem is found.

Units: m3 secondary growth root phloem

Rt_2d_G_Xyl_Vol = Root_Xyl_Vol-Fine_Root_Xyl_Vol

DOCUMENT: By subtracting the root hair xylem volume from the total root xylem volume, the amount of secondary growth xylem is found.

Units: m3 secondary growth root xylem

R_to_R_TCE_Phl_Flow =
(Unsat_2d_G_Phloem/(Root_Phl_Vol*Unsat_to_CF_2d_G_root_Vol_coeff))*(Phl_Q_per_Leaf_Area)*(CF_2d_G_uptake_coeff+CF_FR_uptake_coeff)*Leaf_Area*Seasonal_Fluctuation

DOCUMENT: This is the flow rate of the TCE in the phloem transpiration stream, from the root in the unsaturated zone to the root in the capillary fringe.

Units: mg TCE/month

R_to_R_TCE_Xyl_Flow =
IF(Unsat_to_CF_2d_G_root_Vol_coeff=1)THEN(0)ELSE((CF_2d_G_Xylem/(Root_Xyl_Vol*(1-
Unsat_to_CF_2d_G_root_Vol_coeff)))*(Xyl_Q_per_Leaf_Area)*(CF_2d_G_uptake_coeff+CF_FR_uptake_coeff)*Seasonal_Fluctuation*Leaf_Area)

DOCUMENT: This is the flow rate of the TCE in the xylem transpiration stream, from the root in the capillary fringe to the root in the unsaturated zone.

Units: mg TCE/month

secondary_root_flow_weight = .70

DOCUMENT: I am assuming 30% of the ground water uptake is through the root hair zone. Therefore, 70% is through the secondary root.

Units: % uptake

Sec_G_growth_coeff_1 = Sec_G_uptake_coeff_1

DOCUMENT: This graph represents the represents the change in root growth with variation in the ratio of unsaturated soil depth to capillary fringe depth from 0 to 1. As the ratio increases from 0 to 1, the output goes from 0 to 1.

Units: % growth in unsat secondary growth

Sec_G_growth_coeff_3 = SMTH3(Sec_G_growth_coeff_2,1)

DOCUMENT: This converter smoothes the % growth in the secondary growth root.

Units: NA

Sec_G_uptake_coeff_3 = SMTH3(Sec_G_uptake_coeff_2,1)

DOCUMENT: This converter smoothes the % uptake in the secondary growth root.

Units: NA

Sec_G_uptake_coeff_4 =
IF(Unsat_to_CF_2d_G_root_coeff=1)THEN(1)ELSE(IF(soil_horizon_ratio<1)THEN(
Sec_G_uptake_coeff_1)ELSE(Sec_G_uptake_coeff_3))

DOCUMENT: This converter ensures the root uptake ratio only is in place after the root has reached the capillary fringe and the correct root uptake ratio is represented.

Units: NA

soil_horizon_ratio = unsaturated_soil_thickness/CF_soil_thickness

DOCUMENT: This converter gives the ratio of unsaturated soil depth to capillary fringe soil depth.

Units: NA

tree_mass = leaf_mass+root_mass+stem_mass

DOCUMENT: This gives the total mass of the tree.

Units: kg tree

unsaturated_soil_thickness = depth_to_GW-CF_soil_thickness

DOCUMENT: This is the depth of the usaturated soil.

Units: meters

unsat_2d_G_diff_rate = TCE_Conc_in_Unsat_2d_G_Rhizo*rhizo_diffusion_factor

DOCUMENT: This equation represents the rate of diffusion of TCE from the unsaturated secondary growth portion of the rhizosphere.

Units: mg TCE/month

unsat_2d_G_growth_coeff =
IF(Unsat_to_CF_2d_G_root_coeff=1)THEN(1)ELSE(IF(soil_horizon_ratio<1)THEN(
Sec_G_growth_coeff_1)ELSE(Sec_G_growth_coeff_3))

DOCUMENT: This converter ensures the root growth ratio only is in place after the root has reached the capillary fringe and the correct root growth ratio is represented.

Units: NA

unsat_2d_G_root_metab_rate =
(.693/unsat_2d_G_TCE_half_life)*Unsat_2d_G_Root*Seasonal_Fluctuation

DOCUMENT: This equation takes the form of the half-life equation - ln2/T half life * mass TCE in stem.

Units: mg TCE/month

unsat_2d_G_TCE_half_life = 15/30

DOCUMENT: According to Dr. Newman, 23 Jul 97, in a telephone conversation, metabolism in poplars is highest in the leaves, somewhat lower in the root, and very low in the stem. According to lit from Dr. Trapp, the half life of TCE in plants is approximately 2 days. I am using a value of 15 days in the secondary growth unsaturated root zone.

Units: month

unsat_2d_G_uptake_coeff =
SMTH3(secondary_root_flow_weight*Sec_G_unsat_%_uptake*Sec_G_uptake_coeff_4,2)

DOCUMENT: This coefficient approximates the weighted flow in the unsaturated root xylem.

Units: % flow rate

unsat_FR_diff_rate = TCE_Conc_in_Unsat_FR_Rhizo*rhizo_diffusion_factor

DOCUMENT: This equation represents the rate of diffusion of TCE from the unsaturated fine root portion of the rhizosphere.

Units: mg TCE/month

unsat_FR_tiss_metab_rate =
(.693/unsat_RH_TCE_half_life)*Unsat_FR_Zone_Tissue*Seasonal_Fluctuation

DOCUMENT: This equation takes the form of the half-life equation - ln2/T half life * mass TCE in unsaturated fine roots.

Units: mg TCE/month

unsat_FR_uptake_coeff =
SMTH3(fine_root_flow_weight*RH_unsat_%_uptake*Unsat_FR_uptake_coeff_2,2)

DOCUMENT: This coefficient approximates the weighted flow in the unsaturated root hair zone vascular tissue.

Units: % flow rate

Unsat_FR_uptake_coeff_2 =
IF(Unsat_to_CF_FR_coeff=1)THEN(1)ELSE(IF(soil_horizon_ratio<1)THEN(Unsat_FR_uptake_coeff_1)ELSE(1))
unsat_RH_TCE_half_life = 15/30

DOCUMENT: According to Dr. Newman, 23 Jul 97, in a telephone conversation, metabolism in poplars is highest in the leaves, somewhat lower in the root, and very low in the stem. According to lit from Dr. Trapp, the half life of TCE in plants is approximately 2 days. I am using value of 15 days in the root hair zone.

Units: month

Unsat_to_CF_2d_G_root_coeff =
IF(depth_of_root<=unsaturated_soil_thickness)THEN(1)ELSE(1-(depth_of_root-unsaturated_soil_thickness)/(CF_soil_thickness*3))

DOCUMENT: I am assuming the secondary root growth volume will be primarily found in the unsaturated soil. This coefficient partitions the total root volume between the unsaturated and capillary fringe soil.

Units: % secondary root

Unsat_to_CF_2d_G_root_Vol_coeff =
unsat_2d_G_growth_coeff*Unsat_to_CF_2d_G_root_coeff

DOCUMENT: This converter represents the % of secondary growth root in the unsaturated zone with changing soil horizon profiles (changing depth of capillary fringe and unsaturated zone).

Units: % root hair in unsat zone

Unsat_to_CF_FR_coeff =
IF(depth_of_root<=unsaturated_soil_thickness)THEN(1)ELSE(1-(depth_of_root-unsaturated_soil_thickness)/(CF_soil_thickness*2))

DOCUMENT: Some authors state fine roots are primarily found in the top 1.5 feet of soil [Heilman, 1994:1191]. Researchers at Argon National Laboratory have found the same correlation, with fine roots decreasing in an inverse exponential rate with depth [Hinchman, 1997]. Dr. Gatliff, President of Applied Natural Sciences, stated in dry climates with little rainfall, the roots extend down into the capillary fringe with a mass of fine roots [Gatliff, 1997]. Since I am modeling a dry climate in Texas, I am assuming there will be a balance between the two during the growing season. This coefficient partitions the fine root volume between the unsaturated and capillary fringe soil.

Units: % unsaturated fine root volume

Unsat_to_CF_FR_Vol_coeff =
SMTH3(Unsat_FR_uptake_coeff_2*Unsat_to_CF_FR_coeff,1)

DOCUMENT: This converter represents the % of fine roots in the unsaturated zone with changing soil horizon profiles (changing depth of capillary fringe and unsaturated zone).

Units: % fine root in unsat zone

RH_unsat_%_uptake = GRAPH(Unsat_to_CF_FR_coeff)
(0.5, 0.15), (0.55, 0.159), (0.6, 0.171), (0.65, 0.188), (0.7, 0.218), (0.75, 0.273), (0.8, 0.405), (0.85, 0.707), (0.9, 0.911), (0.95, 0.975), (1.00, 1.00)

DOCUMENT: The ordinate of this graph is the ratio of unsaturated to CF fine roots. Using this input parameter the ratio of uptake in the fine root unsaturated zone and capillary fringe is calculated.

Units: % uptake in fine root unsat root

Sec_G_growth_coeff_2 = GRAPH(soil_horizon_ratio)
(1.00, 1.00), (2.90, 1.00), (4.80, 1.01), (6.70, 1.02), (8.60, 1.03), (10.5, 1.04), (12.4, 1.06), (14.3, 1.08), (16.2, 1.11), (18.1, 1.16), (20.0, 1.25)

DOCUMENT: This graph gives a representation of the unsaturated to capillary fringe soil depth ratio from 1 to 20. As the unsaturated thickness increases over the capillary fringe thickness, the ouput from this graph increases from 1 to 1.25. This factor is then multiplied by the growth coefficients to balance the growth between the two soil horizons.

Units: % growth in unsat secondary growth

Sec_G_unsat_%_uptake = GRAPH(Unsat_to_CF_2d_G_root_coeff)
(0.667, 0.154), (0.7, 0.163), (0.734, 0.193), (0.767, 0.244), (0.8, 0.35), (0.834, 0.473), (0.867, 0.66), (0.9, 0.856), (0.933, 0.949), (0.967, 0.983), (1.00, 1.00)

DOCUMENT: This abscissa of this graph is the ratio of unsaturated to CF secondary growth root and is used as an input parameter to find the ratio of uptake in the secondary growth unsaturated zone and capillary fringe.

Units: % uptake in sec growth unsat root

Sec_G_uptake_coeff_1 = GRAPH(soil_horizon_ratio)
(0.00, 0.00), (0.1, 0.2), (0.2, 0.37), (0.3, 0.51), (0.4, 0.65), (0.5, 0.76), (0.6, 0.85), (0.7, 0.905), (0.8, 0.95), (0.9, 0.98), (1, 1.00)

DOCUMENT: This graph represents the represents the change in root uptake with variation in the ratio of unsaturated soil depth to capillary fringe depth from 0 to 1. As the ratio increases from 0 to 1, the output goes from 0 to 1.

Units: % uptake in unsat secondary growth

Sec_G_uptake_coeff_2 = GRAPH(soil_horizon_ratio)
(1.00, 1.00), (3.11, 1.04), (5.22, 1.10), (7.33, 1.18), (9.44, 1.34), (11.6, 1.60), (13.7, 2.06), (15.8, 2.72), (17.9, 3.70), (20.0, 5.00)

DOCUMENT: This graph gives a representation of the unsaturated to capillary fringe soil depth ratio from 1 to 20. As the unsaturated thickness increases over the capillary fringe thickness, the output from this graph increases from 1 to 1.4. This factor is then multiplied by the uptake coefficients to balance the uptake between the two soil horizons.

Units: % uptake in unsat secondary growth

Unsat_FR_uptake_coeff_1 = GRAPH(soil_horizon_ratio)
(0.00, 0.00), (0.1, 0.195), (0.2, 0.365), (0.3, 0.52), (0.4, 0.65), (0.5, 0.755), (0.6, 0.85), (0.7, 0.91), (0.8, 0.95), (0.9, 0.985), (1, 1.00)

DOCUMENT: This graph gives output that varies from 0 to 1 as the soil horizon ratio (unsaturated/CF) varies from 0 to 1. The output is used to give a representation of the uptake weight as the unsaturated zone decreases to 0.

Units: NA

vertical_growth_of_root_over_time = GRAPH(TIME)
(0.00, 0.3), (3.00, 0.7), (6.00, 1.00), (9.00, 1.35), (12.0, 1.70), (15.0, 2.04), (18.0, 2.45), (21.0, 2.90), (24.0, 3.50), (27.0, 4.15), (30.0, 4.85), (33.0, 5.60), (36.0, 6.30), (39.0, 7.10), (42.0, 7.85), (45.0, 8.64), (48.0, 9.30), (51.0, 10.0), (54.0, 10.5), (57.0, 10.8), (60.0, 10.9)

DOCUMENT: This graph gives a representation of vertical root growth over time. One-year poplars have a roothing depth of 1.7 meters [Heilman, 1994:911]. Two-year poplars have a reported rooting depth of 3.35 to 4 meters [Tech Demo Plan, 1996:8-9; Simon, 1996:11]. I am assuming this value approaches a depth of 11 meters by the fifth year.

Units: meters

Stem

TCE_inStem_Xylem(t) = TCE_inStem_Xylem(t - dt) + (R_to_S_TCE_xyl_flow_2 - S_to_L_TCE_Xyl_Flow_2 - stem_xyl_flow_2 - stem_phl_xyl_flow_2) * dt
INIT TCE_inStem_Xylem = 0

DOCUMENT: This is the amount of TCE in the xylem of the stem.

Units: mg TCE

INFLOWS:
R_to_S_TCE_xyl_flow_2 (Not in a sector)

OUTFLOWS:
S_to_L_TCE_Xyl_Flow_2 (Not in a sector)

stem_xyl_flow_2 = xyl_stem_flow

DOCUMENT: This is an equilibrium flow equation, balancing the concentration of TCE between the stem xylem to the stem itself using a transfer rate coefficient between the two.

Units: mg TCE/month

stem_phl_xyl_flow_2 = stem_phl_xyl_flow

DOCUMENT: This is an equilibrium flow equation, balancing the concentration of TCE between the stem phloem to the stem xylem using a transfer rate coefficient between the two.

Units: mg TCE/month

TCE_in_Stem(t) = TCE_in_Stem(t - dt) + (stem_xyl_flow_2 - stem_metab_rate_2) * dt
INIT TCE_in_Stem = 0

DOCUMENT: This is the amount of TCE in the stem.

Units: mg TCE

INFLOWS:

stem_xyl_flow_2 = xyl_stem_flow

DOCUMENT: This is an equilibrium flow equation, balancing the concentration of TCE between the stem xylem to the stem itself using a transfer rate coefficient between the two.

Units: mg TCE/month

OUTFLOWS:

stem_metab_rate_2 = stem_metab_rate

DOCUMENT: This is the metabolic rate of TCE from the stem of a tree.

Units: mg TCE/month

TCE_in_Stem_Phloem(t) = TCE_in_Stem_Phloem(t - dt) + (L_to_S_TCE_Phl_Flow_2 + stem_phl_xyl_flow_2 - S_to_R_TCE_phl_flow_2) * dt
INIT TCE_in_Stem_Phloem = 0

DOCUMENT: This is the amount of TCE in the phloem of the stem.

Units: mg TCE

INFLOWS:

L_to_S_TCE_Phl_Flow_2 (Not in a sector)

stem_phl_xyl_flow_2 = stem_phl_xyl_flow

DOCUMENT: This is an equilibrium flow equation, balancing the concentration of TCE between the stem phloem to the stem xylem using the rate of transfer between the two.

Units: mg TCE/month

OUTFLOWS:
S_to_R_TCE_phl_flow_2 (Not in a sector)

Stem Equations

R_to_S_TCE_Xyl_Flow =
(Unsat_2d_G_Xylem/Root_Xyl_Vol)*(Xyl_Q_per_Leaf_Area)*Seasonal_Fluctuation*
Leaf_Area

DOCUMENT: This is the flow rate of the TCE in the xylem transpiration stream, from the root to the stem.

Units: mg TCE/month

stem_mass = stem_density*Stem_Volume

DOCUMENT: Stem mass is computed by multiplying the stem density (kg/cubic meter) by the stem volume (cubic meter), giving stem mass.

Units: kg stem

stem_metab_rate = (.693/TCE_stem_half_life)*TCE_in_Stem*Seasonal_Fluctuation

DOCUMENT: This equation takes the form of the half-life equation - ln2/T half life * mass TCE in stem.

Units: mg TCE/month

stem_phl_TCE_conc = TCE_in_Stem_Phloem/(Stem_Phl_Vol/10000)

DOCUMENT: This is the concentration of TCE in the phloem of the stem.

Units: mg TCE/month

stem_phl_xyl_flow = (stem_xyl_TCE_conc-
(stem_phl_TCE_conc*stem_part_coeff))*phl_xyl_trans_rate_coeff*Seasonal_Fluctuati
on

DOCUMENT: This is an equilibrium flow equation, balancing the concentration of TCE between the stem phloem to the stem xylem using a transfer rate coefficient between the two.

Units: mg TCE/month

stem_TCE_conc = TCE_in_Stem/Stem_Volume

DOCUMENT: This is the concentration of TCE in the stem.

Units: mg TCE/m3

stem_xyl_TCE_conc = TCE_inStem_Xylem/(Stem_Xyl_Vol/10000)

DOCUMENT: This is the concentration of TCE in the xylem of the stem.

Units: mg TCE/m3

S_to_R_TCE_Phl_Flow =
(TCE_in_Stem_Phloem/(Stem_Phl_Vol/10000))*(Phl_Q_per_Leaf_Area)*Seasonal_Fluctuation*Leaf_Area

DOCUMENT: This is the flow rate of the TCE in the phloem transpiration stream, from the stem to the root.

Units: mg TCE/month

TCE_stem_half_life = 30/30

DOCUMENT: According to Dr. Newman, 23 Jul 97, in a telephone conversation, metabolism in poplars is highest in the leaves, somewhat lower in the root, and very low in the stem. According to lit from Dr. Trapp, the half life of TCE in plants is approximately 2 days. I am using a value 30 days in the stem.

Units: month

xyl_stem_flow = (stem_xyl_TCE_conc-
(stem_TCE_conc*stem_part_coeff))*xyl_stem_trans_rate_coeff*Seasonal_Fluctuation

DOCUMENT: This is an equilibrium flow equation, balancing the concentration of TCE between the stem xylem to the stem itself using a transfer rate coefficient between them.

Units: mg TCE/month

Transpiration

Log_Kla = 4.1

DOCUMENT: This is the partition coefficient between the leaf and air. The value of 4.1 is from the doctoral disertation by Dr. Burken, pg 107.

Units: NA

TCE_Air_Conc = .0205

DOCUMENT: The Agency for Toxic Substances and Disease Registry reports mean TCE concentrations of 11-30 ppt in the northern hemisphere. This equates to .011-.030 milligrams/cubic meter, for an average of .0205.

Units: mg TCE/m3

TCE_Leaf_Conc = TCE_in_Leaf/(Leaf_Volume-(Leaf_Xyl_Vol+Leaf_Phl_Vol))

DOCUMENT: This gives the concentration of TCE in the leaves.

Units: mg TCE/cubic meter

transpiration_flow_rate = (TCE_Leaf_Conc-(TCE_Air_Conc*Log_Kla))*leaf_air_trans_rate_coeff*Seasonal_Fluctuation

DOCUMENT: This equilibrium flow equation allows biflow of TCE, depending on which is greater - the concentration of TCE in the leaf or air.

Units: mg TCE/month.

Unsaturated Rhizosphere and Root

TCE_in_2d_G_Unsat_Rhizo(t) = TCE_in_2d_G_Unsat_Rhizo(t - dt) +
(TCE_flow_into_unsat_2d_G_rhizo_2 - Unsat_2d_G_Rhizo_TCE_loss_rate -
cometab_2d_G_unsat_rhizo_2 - Unsat_2d_G_uptake) * dt
INIT TCE_in_2d_G_Unsat_Rhizo = 0

DOCUMENT: This is the approximation for the amount of TCE in the unsaturated portion of the rhizosphere.

Units: mg TCE

INFLOWS:

TCE_flow_into_unsat_2d_G_rhizo_2 = TCE_flow_into_unsat_2d_G_rhizo

DOCUMENT: This is the TCE flow into the unsaturated root hair zone of the rhizosphere.

Units: mg TCE/month

OUTFLOWS:

Unsat_2d_G_Rhizo_TCE_loss_rate =
Rhizo_TCE_loss_fluctuation*unsat_2d_G_diff_rate

DOCUMENT: This gives a representation of the loss of TCE from the rhizosphere during the tree's dormant months when active uptake is not taking place.

Units: mg TCE/month

cometab_2d_G_unsat_rhizo_2 = Cometab_2d_G_Unsat_Rhizo

DOCUMENT: This is the metabolism of TCE in the unsaturated 2d growth portion of the rhizosphere.

Units: mg TCE/month.

Unsat_2d_G_uptake = half_sat_eq_unsat_2d_G_soil

DOCUMENT: This is the uptake by the root in the unsaturated secondary root portion of the soil.

Units: mg TCE/month

TCE_in_FR_Zone_Unsat_Rhizo(t) = TCE_in_FR_Zone_Unsat_Rhizo(t - dt) + (TCE_flow_in_unsat_FR_rhizo_2 - Unsat_FR_uptake - Cometab_Fr_unsat_Rhizo_2 - unsat_FR_TCE_loss_rate) * dt
INIT TCE_in_FR_Zone_Unsat_Rhizo = 0

DOCUMENT: This is the approximation for the amount of TCE in the unsaturated zone of the rhizosphere surrounding the root hair zone.
Units: mg TCE

INFLOWS:

TCE_flow_in_unsat_FR_rhizo_2 = TCE_flow_into_unsat_FR_rhizo

DOCUMENT: This is the TCE flow into the fine root unsat zone of the rhizosphere.

Units: mg TCE/month

OUTLFOWS:

Unsat_FR_uptake = half_sat_eq_unsat_FR_soil

DOCUMENT: This is the TCE uptake by the root hair zone in the unsaturated soil.

Units: mg TCE/month

Cometab_Fr_unsat_Rhizo_2 = Cometab_FR_Unsat_Rhizo

DOCUMENT: This is the metabolism of TCE in the fine root unsat zone of the rhizosphere.

Units: mg TCE/month

unsat_FR_TCE_loss_rate = Rhizo_TCE_loss_fluctuation*unsat_FR_diff_rate

DOCUMENT: This gives a representation of the loss of TCE from the rhizosphere during the tree's dormant months when active uptake is not taking place.

Units: mg TCE/month

Unsat_2d_G_Phloem(t) = Unsat_2d_G_Phloem(t - dt) + (S_to_R_TCE_phl_flow_2 + Unsat_2d_G_uptake - R_to_R_TCE_phl_flow_2 - Unsat_phl_to_FR_phl_flow_2 - unsat_2d_G_phl_xyl_flow_2) * dt
INIT Unsat_2d_G_Phloem = 0

DOCUMENT: This is the amount of TCE in the phloem of the unsaturated root.

Units: mg TCE

INFLOWS:

S_to_R_TCE_phl_flow_2 (Not in a sector)

Unsat_2d_G_uptake = half_sat_eq_unsat_2d_G_soil

DOCUMENT: This is the uptake by the root in the unsaturated secondary root portion of the soil.

Units: mg TCE/month

OUTLFOWS:

R_to_R_TCE_phl_flow_2 = R_to_R_TCE_Phl_Flow

DOCUMENT: This is the flow rate of the TCE in the phloem transpiration stream, from the root in the unsaturated zone to the root in the capillary fringe.

Units: mg TCE/month

Unsat_phl_to_FR_phl_flow_2 = Unsat_phl_to_FR_phl_flow

DOCUMENT: This is the flow rate of the TCE in the phloem transpiration stream, from the secondary root in the unsaturated zone to the fine roots in the unsaturated zone.

Units: mg TCE/month

unsat_2d_G_phl_xyl_flow_2 = unsat_2d_G_phl_xyl_flow

DOCUMENT: This is an equilibrium flow equation, from the phloem to the xylem vascular elements.

Units: mg TCE/month

Unsat_2d_G_Root(t) = Unsat_2d_G_Root(t - dt) + (unsat_2d_G_root_xyl_flow_2 - unsat_2d_G_root_metab_rate_2) * dt
INIT Unsat_2d_G_Root = 0

DOCUMENT: This is the amount of TCE in the root in the unsaturated zone of the soil.

Units: mg TCE

INFLOWS:

unsat_2d_G_root_xyl_flow_2 = unsat_2d_G_root_xyl_flow

DOCUMENT: This is an equilibrium flow equation, balancing the concentration of TCE between the root xylem to the root in the unsaturated portion of the soil using a rate of transfer coefficient between the two.

Units: mg TCE/month

OUTFLOWS:

unsat_2d_G_root_metab_rate_2 = unsat_2d_G_root_metab_rate

DOCUMENT: This is the metabolic rate of TCE from the unsaturated root of a tree.

Units: mg TCE/month

Unsat_2d_G_Xylem(t) = Unsat_2d_G_Xylem(t - dt) + (R_to_R_TCE_xyl_flow_2 + unsat_FR_xyl_to_2d_G_xyl_flow_2 + unsat_2d_G_phl_xyl_flow_2 - R_to_S_TCE_xyl_flow_2 - unsat_2d_G_root_xyl_flow_2) * dt
INIT Unsat_2d_G_Xylem = 0

DOCUMENT: This is the amount of TCE in the xylem of the root in the unsaturated zone of the soil.

Units: mg TCE

INFLOWS:

R_to_R_TCE_xyl_flow_2 = R_to_R_TCE_Xyl_Flow

DOCUMENT: This is the flow rate of the TCE in the xylem transpiration stream, from the root in the capillary fringe to the root in the unsaturated zone.

Units: mg TCE/month

unsat_FR_xyl_to_2d_G_xyl_flow_2 = unsat_FR_xyl_to_2d_G_xyl_flow

DOCUMENT: This is the flow rate of the TCE in the xylem transpiration stream, from the root hair zone in the unsaturated soil to the secondary growth root in the unsaturated zone.

Units: mg TCE/month

unsat_2d_G_phl_xyl_flow_2 = unsat_2d_G_phl_xyl_flow

DOCUMENT: This is an equilibrium equation, balancing the concentration of TCE between the root phloem to the root xylem in the secondary growth root in the unsaturated soil.

Units: mg TCE/month

OUTFLOWS:

R_to_S_TCE_xyl_flow_2 (Not in a sector)

unsat_2d_G_root_xyl_flow_2 = unsat_2d_G_root_xyl_flow

DOCUMENT: This is an equilibrium flow equation, balancing the concentration of TCE between the root xylem to the root in the unsaturated portion of the soil using a transfer rate coefficient between the two.

Units: mg TCE/month

Unsat_FR_Zone_Phloem(t) = Unsat_FR_Zone_Phloem(t - dt) +
(Unsat_phl_to_FR_phl_flow_2 - unsat_FR_xyl_phl_flow_2 -
Unsat_FR_phl_tiss_flow_2) * dt
INIT Unsat_FR_Zone_Phloem = 0

DOCUMENT: This stock represents the amount of TCE in the unsaturated root hair zone phloem.

Units: mg TCE

INFLOWS:

Unsat_phl_to_FR_phl_flow_2 = Unsat_phl_to_FR_phl_flow

DOCUMENT: This is the flow rate of the TCE in the phloem transpiration stream, from the secondary root in the unsaturated zone to the fine roots in the unsaturated zone.

Units: mg TCE/month

OUTLFOWS:

unsat_FR_xyl_phl_flow_2 = Unsat_FR_xyl_phl_flow

DOCUMENT: This is an equilibrium flow equation, balancing the concentration of TCE between the unsaturated fine root phloem to the unsaturated fine root xylem using a transfer rate coefficient between the two.

Units: mg TCE/month

Unsat_FR_phl_tiss_flow_2 = Unsat_FR_phl_tiss_flow

DOCUMENT: This is the flow rate from the unsaturated zone fine root phloem to the unsaturated zone fine root tissue.

Units: mg TCE/month

Unsat_FR_Zone_Tissue(t) = Unsat_FR_Zone_Tissue(t - dt) + (Unsat_FR_uptake + Unsat_FR_phl_tiss_flow_2 - Unsat_FR_tiss_xyl_flow_2 - unsat_FR_tiss_metab_rate_2) * dt
INIT Unsat_FR_Zone_Tissue = 0

DOCUMENT: This stock represents the amount of TCE in the unsaturated root hair zone tissue.

Units: mg TCE

INFLOWS:

Unsat_FR_uptake = half_sat_eq_unsat_FR_soil

DOCUMENT: This is the TCE uptake by the root hair zone in the unsaturated soil.

Units: mg TCE/month

Unsat_FR_phl_tiss_flow_2 = Unsat_FR_phl_tiss_flow

DOCUMENT: This is the flow rate from the unsaturated zone fine root phloem to the unsaturated zone fine root tissue.

Units: mg TCE/month

OUTLFOWS:

Unsat_FR_tiss_xyl_flow_2 = Unsat_FR_tiss_xyl_flow

DOCUMENT: This is the flow rate of the TCE in the xylem transpiration stream, from the fine root tissue in the unsaturated zone to the fine root xylem in the unsaturated zone.

Units: mg TCE/month

unsat_FR_tiss_metab_rate_2 = unsat_FR_tiss_metab_rate

DOCUMENT: This is the metabolic rate of TCE from the unsaturated fine roots of a tree.

Units: mg TCE/month

Unsat_FR_Zone_Xylem(t) = Unsat_FR_Zone_Xylem(t - dt) +
(Unsat_FR_tiss_xyl_flow_2 + unsat_FR_xyl_phl_flow_2 -
unsat_FR_xyl_to_2d_G_xyl_flow_2) * dt
INIT Unsat_FR_Zone_Xylem = 0

DOCUMENT: This stock represents the amount of TCE in the unsaturated root hair zone xylem.

Units: mg TCE

INFLOWS:

Unsat_FR_tiss_xyl_flow_2 = Unsat_FR_tiss_xyl_flow

DOCUMENT: This is the flow rate of the TCE in the xylem transpiration stream, from the fine root tissue in the unsaturated zone to the fine root xylem in the unsaturated zone.

Units: mg TCE/month

unsat_FR_xyl_phl_flow_2 = Unsat_FR_xyl_phl_flow

DOCUMENT: This is an equilibrium flow equation, balancing the concentration of TCE between the unsaturated fine root phloem to the unsaturated fine root xylem using a transfer rate coefficient between the two.

Units: mg TCE/month

OUTFLOWS:

unsat_FR_xyl_to_2d_G_xyl_flow_2 = unsat_FR_xyl_to_2d_G_xyl_flow

DOCUMENT: This is the flow rate of the TCE in the xylem transpiration stream, from the root hair zone in the unsaturated soil to the secondary growth root in the unsaturated zone.

Units: mg TCE/month

Unsaturated Root Flows

unsat_2d_G_phl_xyl_flow = (Unsat_2d_G_Phloem/(Rt_2d_G_Phl_Vol*Unsat_to_CF_FR_Vol_coeff)*Sec_G_tiss_vol_coeff)*(Xyl_Q_per_Leaf_Area)*unsat_2d_G_uptake_coeff*Leaf_Area*Seasonal_Fluctuation

DOCUMENT: This is an approximation of the flow of TCE from the root phloem apoplast and symplast to the root xylem in the secondary growth root in the unsaturated zone.

Units: mg TCE/month

unsat_2d_G_root_xyl_flow = IF(unsaturated_soil_thickness=0)THEN(0)ELSE((unsat_root_xyl_2d_G_TCE_conc-(unsat_root_2d_G_TCE_conc*Sec_G_part_coeff))*unsat_2d_G_root_xyl_trans_rate_coeff*Seasonal_Fluctuation)

DOCUMENT: This is an equilibrium flow equation, balancing the concentration of TCE between the root xylem to the root in the unsaturated portion of the soil using a transfer rate coefficient between the two.

Units: mg TCE/month

Unsat_FR_phl_TCE_conc =
Unsat_FR_Zone_Phloem/(Fine_Root_Phl_Vol*Unsat_to_CF_FR_Vol_coeff)

DOCUMENT: This is the concentration of TCE in the phloem root hair zone in the unsaturated portion of the soil.

Units: mg TCE/m3

Unsat_FR_phl_tiss_flow =
(Unsat_FR_Zone_Phloem/(Fine_Root_Phl_Vol*Unsat_to_CF_FR_Vol_coeff))*(Phl_Q_per_Leaf_Area)*unsat_FR_uptake_coeff*Leaf_Area*Seasonal_Fluctuation

DOCUMENT: This is the flow rate from the unsaturated zone fine root phloem to the unsaturated zone fine root tissue.

Units: mg TCE/month

Unsat_FR_tiss_xyl_flow = (Unsat_FR_Zone_Tissue/(((Fine_Root_Volume-(Fine_Root_Phl_Vol+Fine_Root_Xyl_Vol))*Unsat_to_CF_FR_Vol_coeff)*FR_tiss_vol_coeff)*(Xyl_Q_per_Leaf_Area)*unsat_FR_uptake_coeff*Seasonal_Fluctuation*Leaf_Area)

DOCUMENT: This is the flow rate of the TCE in the xylem transpiration stream, from the fine root tissue in the unsaturated zone to the fine root xylem in the unsaturated zone.

Units: mg TCE/month

Unsat_FR_xyl_phl_flow = (Unsat_FR_phl_TCE_conc-(Unsat_FR_xyl_TCE_conc*fine_root_part_coeff))*phl_xyl_trans_rate_coeff*Seasonal_Fluctuation

DOCUMENT: This is an equilibrium flow equation, balancing the concentration of TCE between the unsaturated fine root phloem to the unsaturated fine root xylem using a transfer rate coefficient between the two.

Units: mg TCE/month

Unsat_FR_xyl_TCE_conc =
Unsat_FR_Zone_Xylem/(Fine_Root_Xyl_Vol*Unsat_to_CF_FR_Vol_coeff)

DOCUMENT: This is the concentration of TCE in the xylem root hair zone in the unsaturated portion of the soil.

Units: mg TCE/m3

unsat_FR_xyl_to_2d_G_xyl_flow =
(Unsat_FR_Zone_Xylem/(Fine_Root_Xyl_Vol*Unsat_to_CF_FR_Vol_coeff))*(Xyl_Q_per_Leaf_Area)*(unsat_FR_uptake_coeff)*Leaf_Area*Seasonal_Fluctuation

DOCUMENT: This is the flow rate of the TCE in the xylem transpiration stream, from the root hair zone in the unsaturated soil to the secondary growth root in the unsaturated zone.

Units: mg TCE/month

Unsat_phl_to_FR_phl_flow =
(Unsat_2d_G_Phloem/(Rt_2d_G_Phl_Vol*Unsat_to_CF_FR_Vol_coeff))*(Phl_Q_per_Leaf_Area)*unsat_FR_uptake_coeff*Leaf_Area*Seasonal_Fluctuation

DOCUMENT: This is the flow rate of the TCE in the phloem transpiration stream, from the secondary root in the unsaturated zone to the fine roots in the unsaturated zone.

Units: mg TCE/month

unsat_root_2d_G_TCE_conc = (Unsat_2d_G_Root)/((Root_Volume-(Root_Phl_Vol+Root_Xyl_Vol))*root_2d_G_to_FR_ratio*Unsat_to_CF_2d_G_root_Vol_coeff)

DOCUMENT: This is the concentration of TCE in the 2d root in the unsaturated portion of the soil.

Units: mg TCE/m3

unsat_root_xyl_2d_G_TCE_conc =
Unsat_2d_G_Xylem/(Rt_2d_G_Xyl_Vol*Unsat_to_CF_2d_G_root_Vol_coeff)

DOCUMENT: This is the concentration of TCE in the xylem of the root in the unsaturated portion of the soil.

Units: mg TCE/m3

Uptake Equations

half_sat_eq_CF_2d_G_soil =
((Vmax*TCE_Conc_in_CF_2d_G_Rhizo)/(Km+TCE_Conc_in_CF_2d_G_Rhizo))*tre
e_mass*Seasonal_Fluctuation

DOCUMENT: This is the uptake by the root in the capillary fringe secondary growth portion of the soil.

Units: mg TCE/month

half_sat_eq_CF_FR_soil =
((Vmax*TCE_Conc_in_CF_FR_Rhizo)/(Km+TCE_Conc_in_CF_FR_Rhizo))*tree_m
ass*Seasonal_Fluctuation

DOCUMENT: This is the uptake by the root in the capillary fringe fine root portion of the soil.

Units: mg TCE/month

half_sat_eq_unsat_2d_G_soil =
((Vmax*TCE_Conc_in_Unsat_2d_G_Rhizo)/((Km)+TCE_Conc_in_Unsat_2d_G_Rhi
zo))*tree_mass*Seasonal_Fluctuation

DOCUMENT: This is the uptake by the root in the unsaturated secondary root portion of the soil.

Units: mg TCE/month

half_sat_eq_unsat_FR_soil =
((Vmax*TCE_Conc_in_Unsat_FR_Rhizo)/((Km)+TCE_Conc_in_Unsat_FR_Rhizo))*
tree_mass*Seasonal_Fluctuation

DOCUMENT: This is the uptake by the root in the unsaturated fine root portion of the soil.

Units: mg TCE/month

Km = 75000

DOCUMENT: Through analysis of two experiments completed in peat soil, a saturable curve was fit. The resulting value for Km was 75000. I am assuming a Km value of 75,000.

Units: mg TCE/m3

Note: According to the USGS, the max amount of TCE that can dissolve in water is 1,100 mg/L or 1,100,000 mg/cubic meter.

rhizo_thickness = 1

DOCUMENT: This converter changes the thickness of the rhizosphere from the average to the known literature bounds of 2 to 5 mm.

Units: NA

TCE_Conc_in_CF_2d_G_Rhizo =
IF(Unsat_to_CF_2d_G_root_Vol_coeff=1)THEN(0)ELSE(TCE_in_2d_G_CF_Rhizo/(
(Sec_G_Rhizo_Volume*rhizo_thickness/10000)*(1-
Unsat_to_CF_2d_G_root_Vol_coeff)))

DOCUMENT: This is the concentration of TCE in the capillary fringe secondary growth portion of the root.

Units: mg TCE

TCE_Conc_in_CF_FR_Rhizo =
IF(Unsat_to_CF_FR_Vol_coeff=1)THEN(0)ELSE(TCE_in_FR_Zone_CF_Rhizo/((FR
_Rhizo_Volume*rhizo_thickness/10000)*(1-Unsat_to_CF_FR_Vol_coeff)))

DOCUMENT: This is the concentration of TCE in the capillary fringe fine root portion of the rhizosphere. It is found by dividing the amount of TCE in the Capillary Fringe of the Rhizosphere by the Rhizosphere Volume.

Units: mg TCE/m3

TCE_Conc_in_Unsat_2d_G_Rhizo =
(TCE_in_2d_G_Unsat_Rhizo)/((Sec_G_Rhizo_Volume*rhizo_thickness/1000)*Unsat_to_CF_2d_G_root_Vol_coeff)
TCE_Conc_in_Unsat_FR_Rhizo =
(TCE_in_FR_Zone_Unsat_Rhizo)/((FR_Rhizo_Volume*rhizo_thickness/10000)*Unsat_to_CF_FR_Vol_coeff)

DOCUMENT: This is the concentration of TCE in the unsaturated fine root portion of the rhizosphere. It is found by dividing the amount of TCE in the Unsaturated Rhizosphere by the Rhizosphere Volume.

Units: mg TCE/m3

Vmax = 20

DOCUMENT: Through analysis of two experiments completed in peat soil, a saturable curve was fit. The resulting value for Vmax was 19.44. This gave me an approximation for the Vmax value. I typically used a value of 20.

Units: mg TCE/kg plant/month

Parameters

CF_2d_G_root_xyl_trans_rate_coeff = 0.06
DOCUMENT: Since active vascular tissue in the secondary growth capillary fringe root is on the exterior surface I expect the rate of transfer to be low.

Units: m3/month

fine_root_density = 1000

DOCUMENT: A juvenile root has a density the same as water - 1000 kg/m3.

Units: kg/m3

fine_root_part_coeff = .923

DOCUMENT: The value I used for this parameter, .923, comes from an equation which takes the water content, lipid content, Kow raised to a root/stem correction factor, and density of CF root to water ratio into account.

Units: NA

FR_tiss_vol_coeff = .3

DOCUMENT: The flow through fine root tissue takes place through three routes; cell walls (apoplast), in the symplast, and through the vacuole [Weatherly, 1982:90]. The flow through the vacuole is considered insignificant in comparison to the first two [Weatherly, 1982:105]. The remaining symplast and apoplast are both considered likely pathways for movement of solutes around the root phloem of the secondary root into the adjacent xylem. According to Dr. Bleckmann, approximately 20-40% of the cell is made up of the apoplast and symplast. I am using this estimate to find the flow volume through the fine root tissue.

Units: % root hair tissue volume

leaf_air_trans_rate_coeff = 1

DOCUMENT: The boundary layer around a leaf is directly affected by the turbulence of the surrounding air, or mean wind speed. Stomata open more frequently during the peak summer months and during the heat of the day (unless there is a shortage of water, then a midday depression takes place) to maintain the humidity around the leaf to maintain the cooling effect. To a lesser extent, water is transpired throught the cuticle of leaves. Since 30% of leaf volume is air, and considering the rapid dispersion of solutions across the air layer, stomatal openings, and cuticle of a leaf, I am assuming the leaf air transfer rate will be very high.

Units: m3/month

leaf_density = 700

DOCUMENT: The leaf density is approximated as 700 kg/m3 [Nobel, pg 523].

Units: kg leaf/m3

leaf_part_coeff = .549

DOCUMENT: The value I used for this parameter, .549, comes from an equation which takes the water content, lipid content, Kow raised to a leaf correction factor, and density of leaf to water ratio into account.

Units: NA

Leaf_Vasc_ratio = .05

DOCUMENT: Since leaf structure does not change for a plant with age, that is, the cross-section shows the same physiology over time, I am assuming the leaf vascular volume will remain constant over the life of the tree. After talking to Dr. Bleckmann, I am assuming the leaf is made up of 5% of both xylem and phloem tissue [Bleckmann, 1997].

Units: m3

Phl_Q_per_Leaf_Area = .000162

DOCUMENT: This is the flow rate of the phloem (cubic centimeters/month) per leaf area (square meters). The peak value in the midsummer months is .000162 cubic meters/month*m2 of leaf.

Units: m3/month*m2 of leaf

phl_xyl_trans_rate_coeff = .001

DOCUMENT: This is the transfer rate coefficient between the xylem and phloem in the tree. I am assuming this rate will be relatively low, since partitioning is minimal between these two vascular members.

Units: m3/month

rhizo_diffusion_factor = .001

DOCUMENT: This is a soft parameter based solely on intuition of how fast the TCE will flow out from the rhizosphere during the dormant months.

Units: mg TCE/month

rhizo_TCE_half_life = 1.167

DOCUMENT: This is the half-life of TCE in soil with plants. The value is from data collected on rice, lotus, and vegetables in TCE contaminated soil. TCE half-life values in the literature vary from 10 days to 58 days in soil and ground water, depending on the substrate present [Anderson, 1991:10-13].

Units: month

root_2d_G_to_FR_ratio = .8

DOCUMENT: Field studies of Populus deltoides and P. trichocarpa show fine roots make up, on average, 6.8% of the root mass [Heilman, 1994:1188]. Other authors have found fine roots make up 40% of the total root in the second year [Friend and others, 1991:110]. In 4-year old trees, the fine roots make up 21-34% of the total root [Heilman, 1994:1191]. Actual amounts may be even higher due to the difficulty in detecting all fine roots. Based on the literature, I am assuming 20% of the root is fine root or root hairs and 80% is secondary root.

Units: % root volume

sec_growth_root_density = 750

DOCUMENT: I have read that a juvenile root has a density of 1000 kg/cubic meter, but I am assuming an older root will be somewhat less dense. Therefore, I am using a value of 750 kg/cubic meter.

Units: kg root/m3

Sec_G_part_coeff = .68

DOCUMENT: The value I used for this parameter, .68, comes from an equation which takes the water content, lipid content, Kow raised to a root/stem correction factor, and density of unsat root to water ratio into account.

Units: NA

Sec_G_tiss_vol_coeff = .3

DOCUMENT: The flow through root tissue takes place through three routes; cell walls (apoplast), in the symplast, and through the vacuole [Weatherly, 1982:90]. In the phloem the vacuole is not present; this is the route of phloem flow. The remaining symplast and apoplast are both considered likely pathways for movement of solutes around the root phloem of the secondary root into the adjacent xylem. According to Dr. Bleckmann, approximately 20-40% of the phloem cell is made up of the apoplast and symplast. I am using this estimate to find the flow volume through the phloem tissue.

Units: % phloem tissue volume

stem_density = 600

DOCUMENT: Conversations with various tree experts have indicated the stem density will be somewhat less than the root density.

Units: kg stem/m3

stem_part_coeff = .43

DOCUMENT: The value I used for this parameter, .43, comes from an equation which takes the water content, lipid content, Kow raised to a root/stem correction factor, and density of stem to water ratio into account.

Units: NA

TCE_in_GW = 605

DOCUMENT: The known TCE concentration at AF Plant 4 varies from 240 to 970 mg/m3 with an average of 605. The greenhouse tests at WSU were at 50,000 mg/m3.

Units: mgTCE/m3 or ppb

unsat_2d_G_root_xyl_trans_rate_coeff = .06

DOCUMENT: Since active vascular tissue in the secondary growth unsat root is on the exterior surface I expect the rate of partitioning to be low.

Units: m3/month

Xyl_Q_per_Leaf_Area = .019

DOCUMENT: This is the flow rate of the xylem (cubic meters/month) per leaf area (square meters). The peak value of a mature phreatophyte in the midsummer months varies from .0065 to .032 m3/m2 leaf-month for an average of .019 m3/m2 leaf-month.

Units: m3/m2 leaf*month

xyl_stem_trans_rate_coeff = .06

DOCUMENT: Since active vascular tissue in the stem is on the exterior surface and taking into consideration the storage and lipid content, I expect the transfer rate to be moderate to low in the stem.

Units: m3/month

Not in a Sector

L_to_S_TCE_Phl_Flow_2 = L_to_S_TCE_Phl_Flow

DOCUMENT: This is the flow rate of the TCE in the phloem transpiration stream, from the leaf to the stem.

Units: mg TCE/month

OUTFLOW FROM: TCE_in_Leaf_Phloem (IN SECTOR: Leaf)

INFLOW TO: TCE_in_Stem_Phloem (IN SECTOR: Stem)

R_to_S_TCE_xyl_flow_2 = R_to_S_TCE_Xyl_Flow

DOCUMENT: This is the flow rate of the TCE in the xylem transpiration stream, from the root to the stem.

Units: mg TCE/month

OUTFLOW FROM: Unsat_2d_G_Xylem (IN SECTOR: Unsat Rhizo/Root)

INFLOW TO: TCE_inStem_Xylem (IN SECTOR: Stem)

S_to_L_TCE_Xyl_Flow_2 = S_to_L_TCE_Xyl_Flow

DOCUMENT: This is the flow rate of the TCE in the xylem transpiration stream, from the stem to the leaf.

Units: mg TCE/month

OUTFLOW FROM: TCE_inStem_Xylem (IN SECTOR: Stem)

INFLOW TO: TCE_in_Leaf_Xylem (IN SECTOR: Leaf)

S_to_R_TCE_phl_flow_2 = S_to_R_TCE_Phl_Flow

DOCUMENT: This is the flow rate of the TCE in the phloem transpiration stream, from the stem to the root.

Units: mg TCE/month

OUTFLOW FROM: TCE_in_Stem_Phloem (IN SECTOR: Stem)

INFLOW TO: Unsat_2d_G_Phloem (IN SECTOR: Unsat Rhizo/Root)

Appendix 3 - Saturable Uptake Approximation

Estimating Half Saturation Data Points

Using data received from Dr. Lee Newman, a graph of V versus concentration was developed, establishing the saturable uptake equation. The information from Dr. Newman includes data from hydroponic studies, studies using peat for soil media, different types of lighting for these first two studies, and field control studies. Since the peat studies were ran at two concentrations, this information was used to establish the data points. The peat studies lasted for two weeks each, at concentrations of 5 ppm and 15 ppm. It was found in lab studies that approximately 70-90% of the TCE taken up by the plant is transpired, whereas in field studies, the amount transpired is 5-10%.

PEAT 1

At 5ppm (5000 mg/m3), transpiration values range from .013 - .023 µg TCE/gm leaf/hour, with leaf mass of 8.6 and 15.7 gm. Assumed averages of .018 µg TCE/gm leaf/hour and 12.15 grams leaf tissue were used.

$$.018 \frac{\mu gram TCE}{gram Leaf} \cdot 12.15 \frac{gram Leaf}{hour} \cdot 12 \frac{hour}{day} \cdot 30 \frac{day}{month}$$

$$Leaf1_{mass} := \frac{8.6 + 15.7}{2} \qquad Leaf1_{mass} = 12.15$$

$$Peat1 := .018 \cdot Leaf1_{mass} \cdot 12 \cdot 30 \qquad Peat1 = 78.732 \quad \mu g\ TCE/month$$

The result was divided by .8 to convert the transpiration mass of TCE to total mass of TCE taken up by the plant (According to Dr. Newman, 23 Jul 97 1800, 70 - 90% of TCE taken up by plants in their lab studies was transpired.)

At maturity, the model tree has a total plant volume of 7.25 m3, with leaves making up 1 m3 of the total. It is also known that leaf density is 700 kg/m3, the stem density is approximately 600 kg/m3, and the root density is approximately 750 kg/m3. Using the mature volumes and converting them to masses gives 15% of the plant mass as leaf mass. The leaf mass was divided by this figure to get an approximation of total plant mass for the uptake.

$Plant1_{fract} := .15$ $\quad Plant_{mass} := \frac{Leaf1_{mass}}{Plant1_{fract}}$

$V_{Peat1} := \frac{Peat1}{Plant_{mass}} \cdot \frac{1}{.8}$ $\quad V_{Peat1} = 1.215$ mg TCE/kg Plant/month

at a TCE soil water concentration of 5000 mg/m3.

PEAT 2

At 15ppm (15000 mg/m3), transpiration values range from .042 - .054 µg TCE/gm leaf/hour, with leaf masses of 9.5, 11.7, and 13.1 gm. Assumed averages of .048 µg TCE/gm leaf/hour and 11.433 grams leaf tissue were used.

$Leaf2_{mass} := \frac{9.5 + 11.7 + 13.1}{3}$

$.048 \frac{\mu gramTCE}{gramLeaf} \cdot 11.433 \frac{gramLeaf}{hour} \cdot 12 \frac{hour}{day} \cdot 30 \frac{day}{month}$ $\quad Leaf2_{mass} = 11.433$

$Peat2 := .048 Leaf2_{mass} \cdot 12 \cdot 30$ $\quad Peat2 = 197.568$ µg TCE/month

This result was divided by .8, to convert the transpiration mass of TCE to total mass of TCE taken up by the plant (According to Dr. Newman, 23 Jul 97 1800, 70 - 90% of TCE taken up by plants in their lab studies was transpired).

At maturity, the model tree has a total plant volume of 7.25 m3, with leaves making up 1 m3 of the total. It is also known that leaf density is 700 kg/m3, the stem density is approximately 600 kg/m3, and the root density is approximately 750 kg/m3. Using the mature volumes and converting them to masses gives 15% of the plant mass as leaf mass. The leaf mass was divided by this figure to get an approximation of total plant mass for the uptake.

$Plant2_{fract} := .15$ $\quad Plant_{mass} := \frac{Leaf2_{mass}}{Plant2_{fract}}$

$V_{Peat2} := \frac{Peat2}{Plant_{mass}} \cdot \frac{1}{.8}$ $\quad V_{Peat2} = 3.24$ mg TCE/kg Plant/month

at a TCE soil water concentration of 15000 mg/m3.

Curve Fitting - Establishing Vmax and Km

Now the experimental data is used from Dr. Newman's Peat tests at 5 and 15 ppm to correlate values of Vmax and Km using the half saturation equation. First, the half saturation equation is defined and its partial derivative with respect to Vmax and Km.

$$f(Vmax, Km, C) := \frac{Vmax \cdot C}{Km + C} \qquad \frac{d}{d\,Vmax} f(Vmax, Km, C) \rightarrow \blacksquare$$

$$\frac{d}{d\,Km} f(Vmax, Km, C) \rightarrow \blacksquare$$

Now a matrix consisting of the half saturation equation and its derivatives and the concentration and experimental lab data vectors are defined.

$$i := 1..3 \qquad X := 0, 100..500000$$

$$F(C, G) := \begin{bmatrix} \frac{G_1 \cdot C}{(G_2 + C)} \\ \frac{C}{(G_2 + C)} \\ -G_1 \cdot \frac{C}{(G_2 + C)^2} \end{bmatrix}$$

$$Conc := \begin{pmatrix} 0 \\ 5000 \\ 15000 \end{pmatrix} \qquad Rates := \begin{pmatrix} 0 \\ 1.215 \\ 3.24 \end{pmatrix}$$

$$V_{Peat1} = 1.215 \qquad V_{Peat2} = 3.24$$

Next, guesses for Vmax and Km are provided and the fitting function is defined. The fitting function uses a vector returned by Mathcad's genfit function. This vector contains the optimal values for Vmax and Km. This fitting function is plotted against the actual data points.

$$Guess := \begin{pmatrix} 20 \\ 75000 \end{pmatrix} \qquad bestfit := genfit(Conc, Rates, Guess, F)$$

$$fit(X) := F(X, bestfit)_1 \qquad V_{max} := bestfit_1 \quad K_m := bestfit_2 \qquad bestfit = \begin{pmatrix} 19.44 \\ 7.5 \cdot 10^4 \end{pmatrix}$$

$$V_{max} = 19.44 \quad \text{mg TCE/kg Plant/month}$$

$$K_m = 7.5 \cdot 10^4 \quad \text{mg TCE/m}^3$$

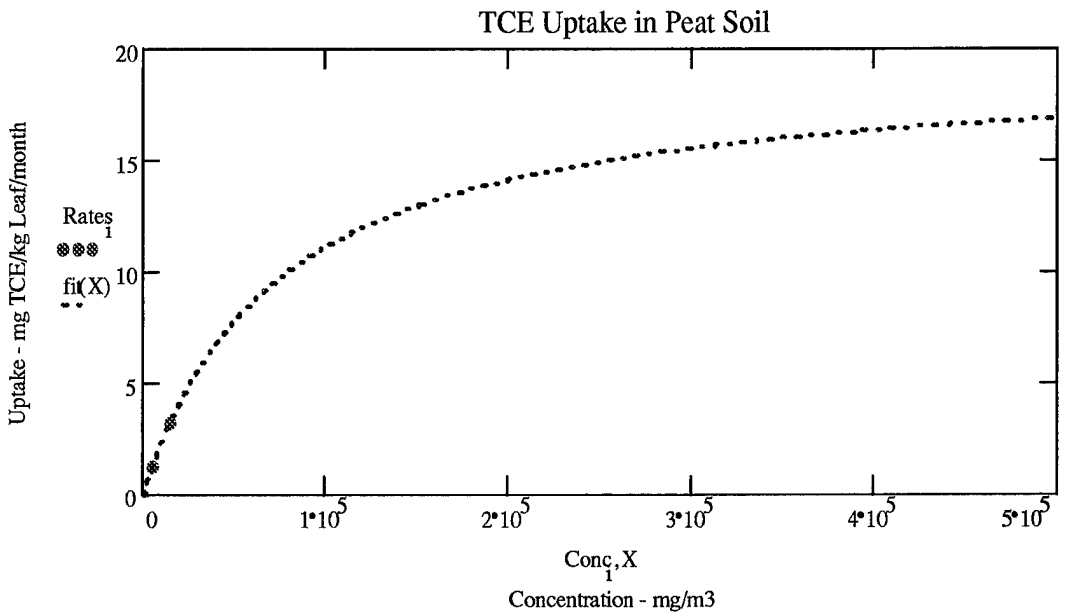
TCE Uptake in Peat Soil
Uptake - mg TCE/kg Leaf/month
Rates i
fi(X)
20
15
10
5
0
0
1•10^5
2•10^5
3•10^5
4•10^5
5•10^5
Conc i, X
Concentration - mg/m3

Appendix 4 - Rhizosphere Volume Approximation

Using information from the root volume, the surface area of the root or rhizoplane was established.

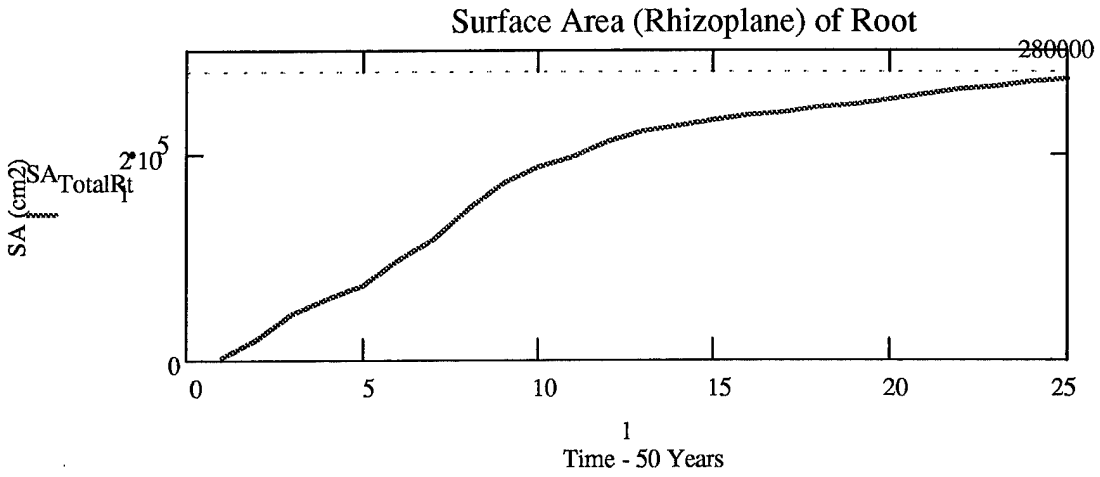

Different authors approximate the rhizosphere thickness as 2 mm to 5 mm. Using these parameters the following graphs are estimated for rhizosphere volume.

$Rhizo_{low} := .2$ $Rhizo_{high} := .5$ Values in centimeters.

$Vol1_{rhizo_1} := SA_{TotalRt_1} \cdot Rhizo_{low}$ $Vol2_{rhizo_1} := SA_{TotalRt_1} \cdot Rhizo_{high}$

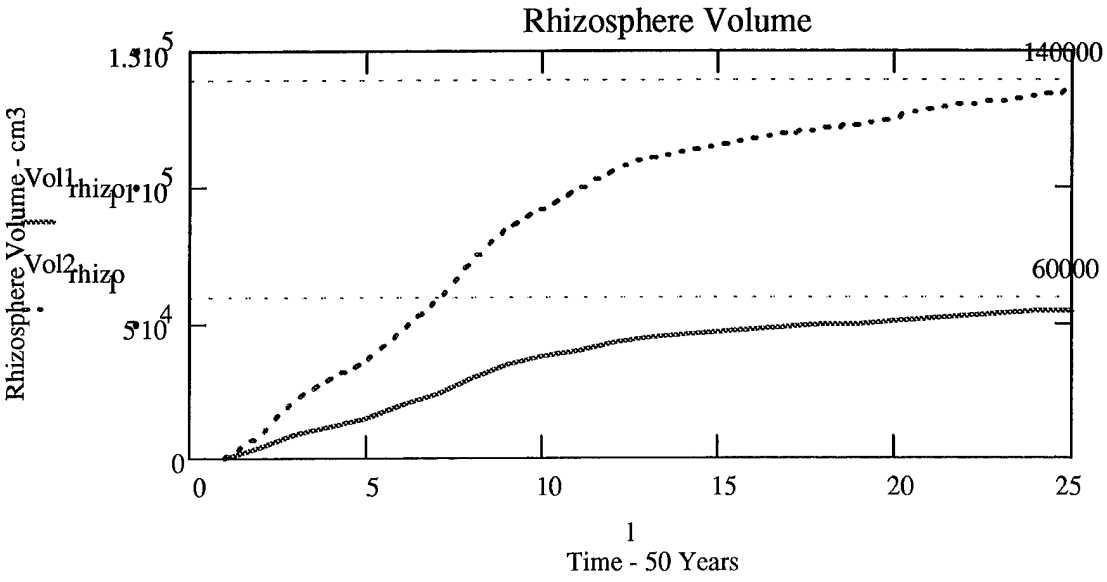

Now to calculate the volume of the rhizosphere in the secondary growth and fine root portion of the phreatophytic tree.

$Rhizo_{thick} := .35$

This is the average rhizosphere thickness.

$$RhizoVol1_1 := \frac{SA_{2droot_1}}{100} \cdot Rhizo_{thick} \qquad RhizoVol2_1 := SA_{finert_1} \cdot Rhizo_{thick}$$

Equation 1 is divided by 100 to get the two equations in the same units of m-cm2.

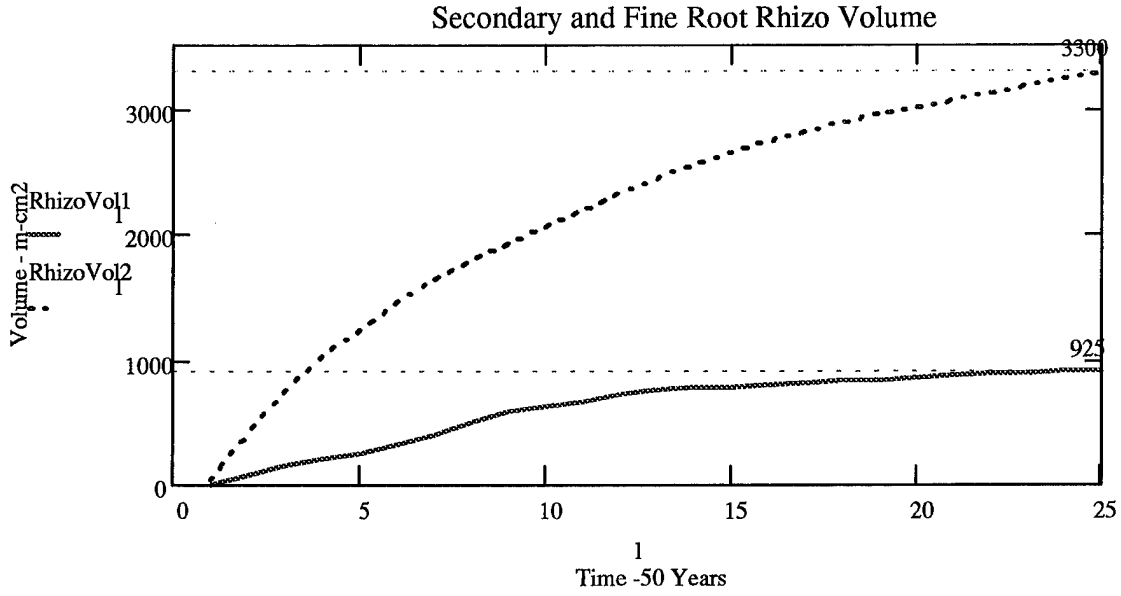

This gives an approximation of the volume of the secondary growth and root hair rhizosphere volumes over time. At maturity, the secondary root rhizosphere is 925 m-cm2 and the fine root rhizosphere is 3300 m-cm2.

Appendix 5 - Xylem and Phloem Flow Rates

Known values for xylem and phloem flows were converted to the correct units for the model. First, the xylem flow rate was calculated.

$$2\text{to}10 \cdot \frac{\mu gm\text{transpirate}}{cm^2 \cdot sec}$$

McFarlane; Crank et al. Transpiration flow rate for xylem.

$$10 \cdot \frac{\mu gm}{cm^2 \cdot sec} \cdot \frac{gm}{10^6 \cdot \mu gm} \cdot \frac{kg}{1000\,gm} \cdot \frac{m^3}{1000\,kg} \cdot 100^2 \cdot \frac{cm^2}{m^2} \cdot 60 \cdot \frac{sec}{min} \cdot 60 \cdot \frac{min}{hr} \cdot 3 \cdot \frac{hr}{day} \cdot 30 \cdot \frac{day}{month}$$

$$\text{Trans}_{\text{xyllow}} := \frac{2}{10^6 \cdot 10001000} \cdot 100^2 \cdot 60 \cdot 60 \cdot 3 \cdot 30$$

$$\text{Trans}_{\text{xyllow}} = 0.00648 \quad m^3\ H_2O/m^2\ \text{leaf/month}$$

$$\text{Trans}_{\text{xylup}} := \frac{10}{10^6 \cdot 10001000} \cdot 100^2 \cdot 60 \cdot 60 \cdot 3 \cdot 30$$

$$\text{Trans}_{\text{xylup}} = 0.0324 \quad m^3\ H_2O/m^2\ \text{leaf/month}$$

A value of 3 hr/day was used since this is the max rate per day and would at least triple the average daily rate.
According to Nobel, a leaf is generally 4-10 cells thick (pg 3), and each cell is 50 μm thick. Coupling this with the fact at canopy closure a tree has 1 cubic meter of leaves, an approximation for the foliage area at canopy closure is - 1 m^3 total leaf volume * 500 μm.

$$\text{Leaf}_{\text{Vol}} := .9 \qquad \text{Leaf}_{\text{Thick}} := \frac{500}{10001000}$$

$$\text{Leaf}_{\text{Area}} := \frac{\text{Leaf}_{\text{Vol}}}{\text{Leaf}_{\text{Thick}}} \qquad \text{Leaf}_{\text{Area}} = 1800$$

According to Mr. Harvey, the total leaf area at canopy closure is 2000 m3, so this checks.

$\text{Trans}_{xyllow} := \text{Trans}_{xyllow} \cdot \text{Leaf Area}$ $\text{Trans}_{xyllow} = 11.664$ $m^3\ H_2O/\text{month}$

$\text{Trans}_{xylup} := \text{Trans}_{xylup} \cdot \text{Leaf Area}$ $\text{Trans}_{xylup} = 58.32$ $m^3\ H_2O/\text{month}$

The average value (.019) comes out very close to the known value of 300-400 GPD (1.135-1.51 m^3/d or 34.05-45.3 m^3/month). Using a value of .019 m^3/month-m^2 leaf results in a transpiration rate of 38.9 m^3/month.

Next, the phloem flow rate was calculated.

$$.05 \cdot \frac{\mu gm\,transpirate}{cm^2 \cdot sec}$$

McFarlane; Crank et al. Transpiration flow rate for phloem.

$$.05 \cdot \frac{\mu gm}{cm^2 \cdot sec} \cdot \frac{gm}{10^6 \cdot \mu gm} \cdot \frac{kg}{1000\,gm} \cdot \frac{m^3}{1000\,kg} \cdot 100^2 \cdot \frac{cm^2}{m^2} \cdot 60 \cdot \frac{sec}{min} \cdot 60 \cdot \frac{min}{hr} \cdot 3 \cdot \frac{hr}{day} \cdot 30 \cdot \frac{day}{month}$$

$$\text{Trans}_{phloem} := \frac{.05}{10^6 \cdot 1000\,1000} \cdot 100^2 \cdot 60 \cdot 60 \cdot 3 \cdot 30$$

$\text{Trans}_{phloem} = 1.62 \cdot 10^{-4}\ m^3\ H_2O/m^2$ leaf-month

$\text{Trans}_{phl} := \text{Trans}_{phloem} \cdot 1800$

$\text{Trans}_{phl} = 0.292 m^3\ H_2O/\text{month}$

Appendix 6 - Leaf, Stem, and Root Growth Volumes

The following statistical phreatophyte growth data was used in five different equations to approximate the leaf, stem, and root growth volumes over a 50 year time period.

$i := 1..12$

dbh is in cm and H is in m.

dbh and H are average values taken off a graph by Tingle and van Laar.

$$dbh := \begin{bmatrix} 5 \\ 10 \\ 16 \\ 26 \\ 38 \\ 44 \\ 50 \\ 52 \\ 54 \\ 56 \\ 58 \\ 60 \end{bmatrix} \qquad H := \begin{bmatrix} 3 \\ 5 \\ 11 \\ 21 \\ 26 \\ 31 \\ 33.5 \\ 38 \\ 39.25 \\ 40.5 \\ 41.75 \\ 43 \end{bmatrix}$$

LEAF VOLUME

Equation from Alan Ek for *Populus tristis* #1, converted from lbs to kg to cubic meters.

$$leaves_i := .2243 \cdot \left(\frac{dbh_i}{2.54}\right)^{2.0892} \cdot \left[\left(H_i\right) \cdot 3.28083\right]^{-.17178}$$

2.54 cm / inch

$$leaves2_i := \left[\frac{.2243 \left(\frac{dbh_i}{2.54}\right)^{2.0892} \cdot \left[\left(H_i\right) \cdot 3.28083\right]^{-.17178}}{2.20462}\right]$$

3.28083 ft / m, 2.20462 lb / kg

Density of a leaf - 700 kg/m^3. Values are in dry weight; leaves are ~95% water by weight (Dickmann - slightly <100%), so divide the outcome of leaves3 by .05 to get the total weight.

$$leaves3_i := \left[\frac{.2243 \cdot \left(\frac{dbh_i}{2.54} \right)^{2.0892} \cdot \left[\left(H_i \right) \cdot 3.28083 \right]^{-.17178}}{2.20462 \cdot 700 \cdot .05} \right]$$

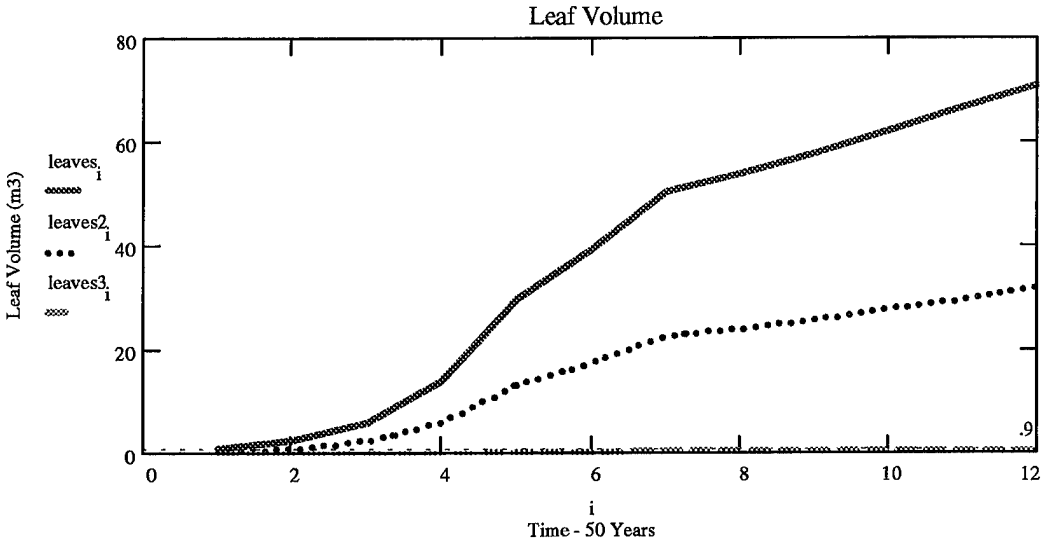

STEM VOLUME

Three separate equations were found which approximated stem growth volume over time. Each equation is as follows:

Equation from Krinard, converted from cubic feet to cubic meters.

$$stem_i := \frac{.1856 + .002074 \left[\left(\frac{dbh}{2.54} \right)_i \right]^2 \cdot \left(H_i \cdot 3.28083 \right)}{35.147}$$

2.54 cm / inch, 3.28083 ft / m,35.147 ft^3 / m^3

Equation from Tritton, converted from kgs to cubic meters.

$$stem2_i := \frac{.00246 \left(dbh_i \right)^{1.84763} \cdot \left(H_i \right)^{1.7235}}{600}$$

Assume ~ 600 kg / 1 m^3, (1000 kg/m^3 for water)

Equation from Tingle, converted from cubic feet to cubic meters.

$$stem3_i := \frac{.00231 \cdot \left(\frac{dbh_i}{2.54}\right)^{1.77593} \cdot \left(H_i \cdot 3.28083\right)^{1.11983}}{35.147}$$

35.147 ft^3 / m^3

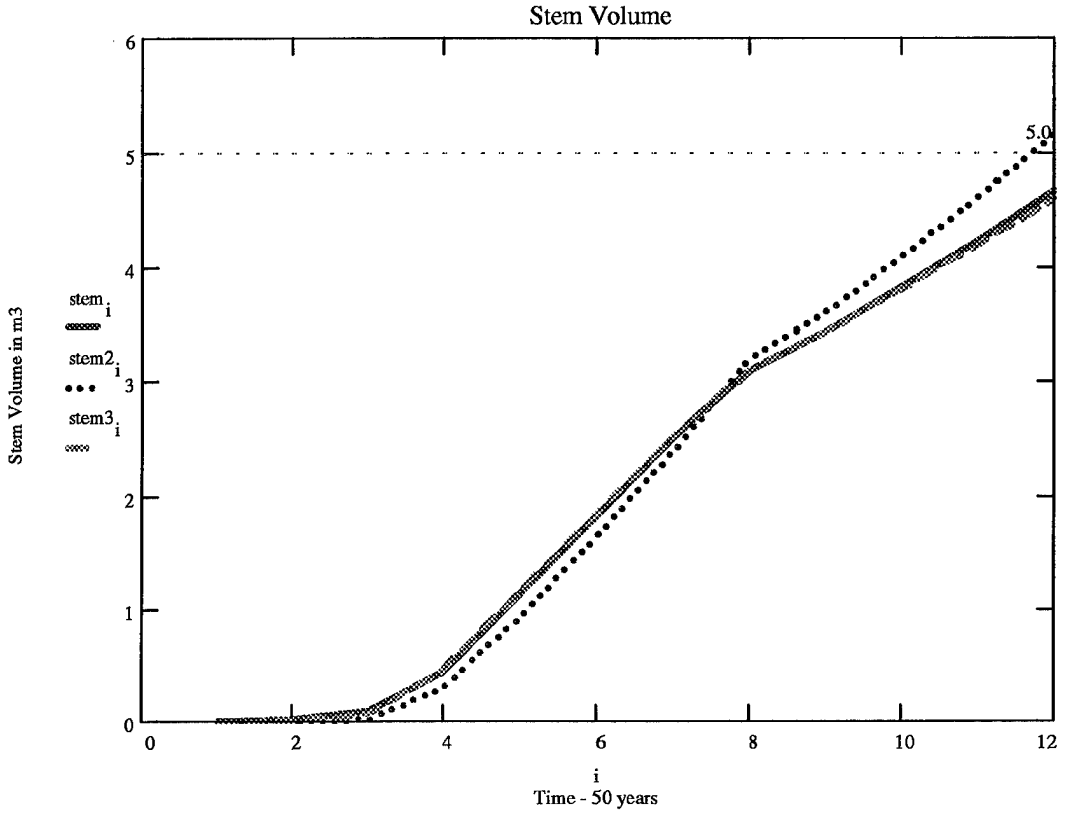

These equations give a good estimation of stem volume. Graph by Tingle and van Laar show a max volume of approximately 4.75 m^3 for a tree 35 meters in height and 60 dbh.

ROOT

Equation from Francis. This equation only takes into consideration the stump-taproot which makes up 6.8% of the total tree biomass. The close laterals make up 8.2%, the close fine roots .7%, and the extended roots 11.6% of the total tree biomass. The equation was then converted from lb dry weight to lb wet weight to kg to m^3.

$$root_i := \left[\frac{-17.386 + 1.328 \cdot \left[\left(\frac{dbh}{2.54} \right)_i \right]^{1.7}}{.125 \cdot 2.20462 \cdot (750 \cdot .93 + 1000 \cdot .07)} \right]$$

80-<100% water by weight, so divide by ~.125. From e-mail from Hendricks and Dickmann.

2.20462 lb / kg
750 kg / 1 m^3, and 1000 kg/m^3 for suberized and fine roots, respectively.

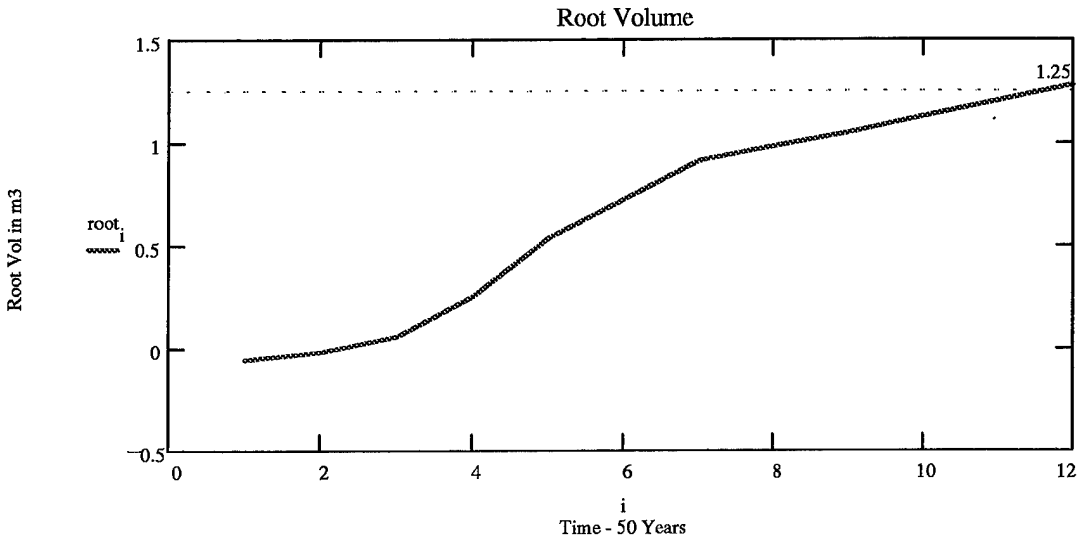

The leaf, stem, and root volume equations were then combined into one graph for assessment.

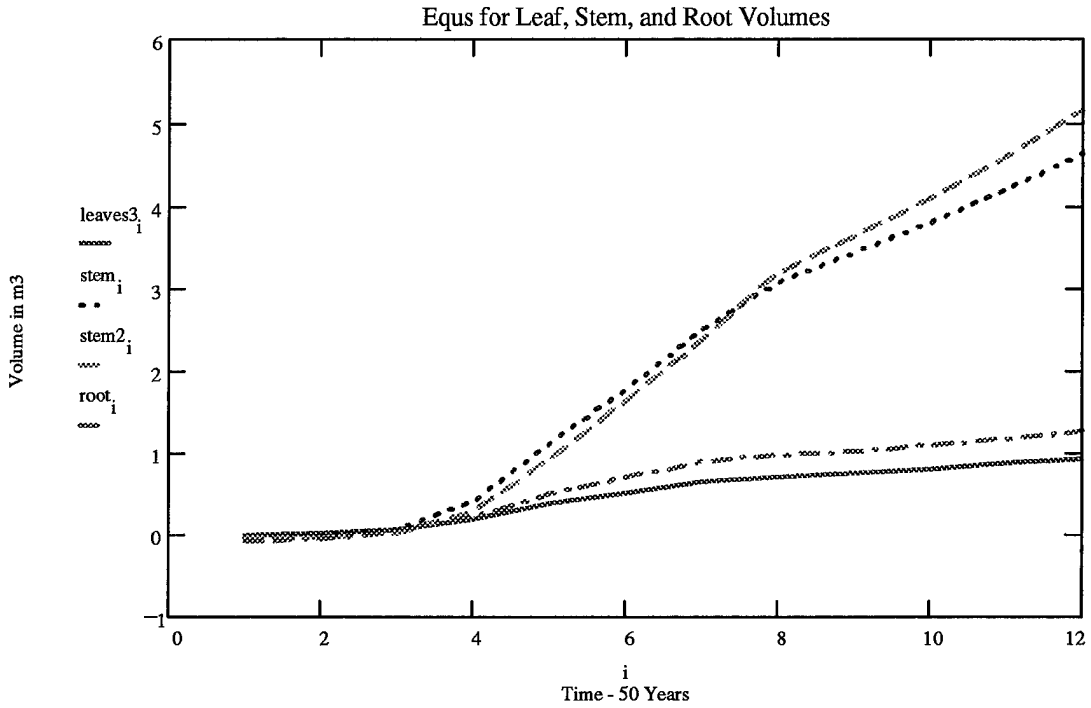

This is the behavior I am expecting in my growth over time for each of the respective compartments. Roots make up 19-37% of the total plant volume, with an average of 27% (root to above ground biomass) [Francis, 1985:3]. The higher value is typically seen in younger trees, and as the tree ages, the ratio decreases to the lower value. Ceuleman found *Populus deltoides* clone root to shoot (root to stem) ratios at .27 for the first year and .20 for the second year [Ceulemans, 1990:99]. Other authors state the root to shoot ratio (root to stem) varies from .34 to .42 [Heilman, 1994:1188]. By the sixth year in Populus deltoides, the root to shoot ratio is .25, approaching a constant ratio [Dickmann and Pregitzer, 1992:103]. Assuming a mature stem volume of 5, mature root volume of 1.25, and a mature leaf volume of 1, the root to shoot ratio is .25, so I am in the ballpark. Field studies of 2-year old Populus deltoides and P. trichocarpa show fine roots make up, on average, 6.8% of the root mass [Heilman, 1994:1188]. Most forest stands of mixed tree species report a value of 5% [Santantonio, 1989]. Other authors have found fine roots make up 40% of the total root in the second year [Friend and others, 1991:110] and 21-34% of the total root in 4-year old trees [Heilman 1994:1191]. Actual values of fine root hairs may be even higher, due to the difficulty in removing them from soil material. In a phreatophyte, where greater ground water uptake takes place, higher values are expected. The majority of these roots are typically found in the top .5 m of soil [Heilman, 1994:1191]. It should be noted this was when the plants were surface watered which may have affected their results.

Appendix 7 - Root Vascular Volumes

Root Xylem and Phloem Approximation

Here a relationship is established between the approximated root growth volume graph and the phloem and xylem root volumes. First an approximated run was made of diameters (cm) over a 50 year time frame for a tree taproot based off of stem growth characteristics in Appendix 6. Also the depth of the tree root (meters) with growth was approximated. This is the value of H. A ground water depth of 5 meters was assumed, which the tree will reach in the 4th year. Nobel states a single vascular xylem element is 20 μm (ranges from 8 to 500 μm [pg 507], but in a tree the average is 100 μm [pg 511]. Phloem elements are approximately 12 μm [pg 517]. Since they occur in bundles, a value of .2 cm for the phloem and .4 cm for the xylem was assumed [Bleckmann]. Both values were assumed as constant.

From Francis, the stump-taproot makes up approximately 25%, close laterals 30%, close fine roots 2.5%, and extended roots 42.5% of the total root. Since the stump is not considered in this analysis, Francis' taproot value was decreased to 15% and the amount of fine roots was increased to the average literature value of 20%. The final values used in this analysis were; 15% taproot, 25% close laterals, 20% fine roots, and 40% extended secondary roots. At maturity this means there is - .1875 m3 taproot, .3125 m3 close laterals, .25 m2 fine roots, and .50 m3 extended secondary roots.

$$D := \begin{bmatrix} 3.75 \\ 5 \\ 7.5 \\ 10 \\ 12 \\ 16 \\ 19.5 \\ 24.5 \\ 28.5 \\ 31 \\ 33 \\ 35.5 \\ 37 \\ 37.8 \\ 38.5 \\ 39.3 \\ 40 \\ 40.6 \\ 41 \\ 41.9 \\ 42.75 \\ 43.4 \\ 44 \\ 44.6 \\ 45 \end{bmatrix} \quad H := \begin{bmatrix} .3 \\ 3.3 \\ 5 \\ 5 \\ 5 \\ 5 \\ 5 \\ 5 \\ 5 \\ 5 \\ 5 \\ 5 \\ 5 \\ 5 \\ 5 \\ 5 \\ 5 \\ 5 \\ 5 \\ 5 \\ 5 \\ 5 \\ 5 \\ 5 \end{bmatrix} \quad Rt_{fine} := \begin{bmatrix} 1000 \\ 8000 \\ 14000 \\ 19000 \\ 23000 \\ 27000 \\ 30000 \\ 33000 \\ 35333 \\ 37667 \\ 40000 \\ 42667 \\ 44667 \\ 46667 \\ 48333 \\ 50000 \\ 51500 \\ 53000 \\ 54000 \\ 55000 \\ 56000 \\ 57000 \\ 58000 \\ 59000 \\ 60000 \end{bmatrix}$$

It was assumed that the taproot diameter is approximately 3/4 the stem diemater - these were the values used for D. It was also assumed that the close roots and extended roots are 1/10 & 1/5 the diameter of the taproot. Extended roots grow further horizontally than the taproot does vertically; some authors estimate this growth as several times the taproot length while others have found a linear relationship between extended root growth and tree height [Faulkner, Hansen]. The value of H was multiplied by 2 to estimate this growth. The close laterals were divided by 2 to approximate their shorter length.

The equations for volume of the taproot, close laterals, and extended root take the form of a long cone, which approximates a root growing into the soil horizon. Fine roots take on the form of a tube, so an equation of a cylinder was used.

The fine root volume parameters are estimations from literature and from discussions with plant experts. A fine root has a radius of 500μm and an approximate length of a few centimeters.

ORIGIN≡1 $1 := 1..25$ $D_{fine} := 1$ $L_{fine} := .05$

$Phl_t := .2$ $Xyl_t := .4$ $Rt_{taproot} := 1$ $Rt_{closelat} := 225$ $Rt_{extlat} := 25$

$$V_{taproot_1} := \frac{\pi}{3} \cdot \left(\frac{D_1}{2}\right)^2 \cdot H_1 \cdot Rt_{taproot} \qquad V_{fine_1} := \pi \cdot \left(\frac{D_{fine}}{2}\right)^2 \cdot L_{fine} \cdot Rt_{fine_1}$$

$$V_{closelat_1} := \frac{\pi}{3} \cdot \left(\frac{D_1}{2 \cdot 10}\right)^2 \cdot \frac{H_1}{2} \cdot Rt_{closelat} \qquad V_{extlat_1} := \frac{\pi}{3} \cdot \left(\frac{D_1}{2 \cdot 5}\right)^2 \cdot H_1 \cdot 2 \cdot Rt_{extlat}$$

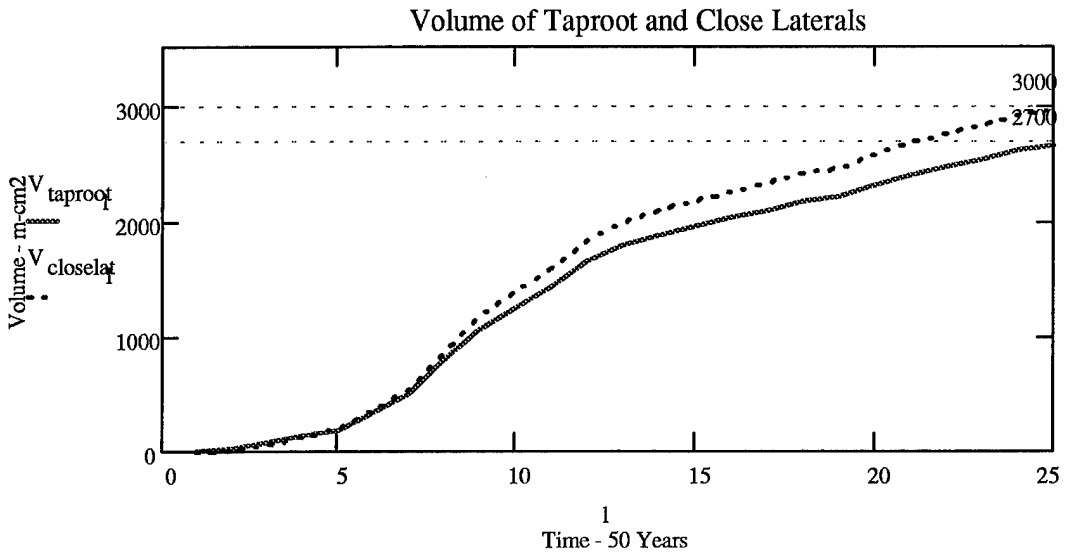

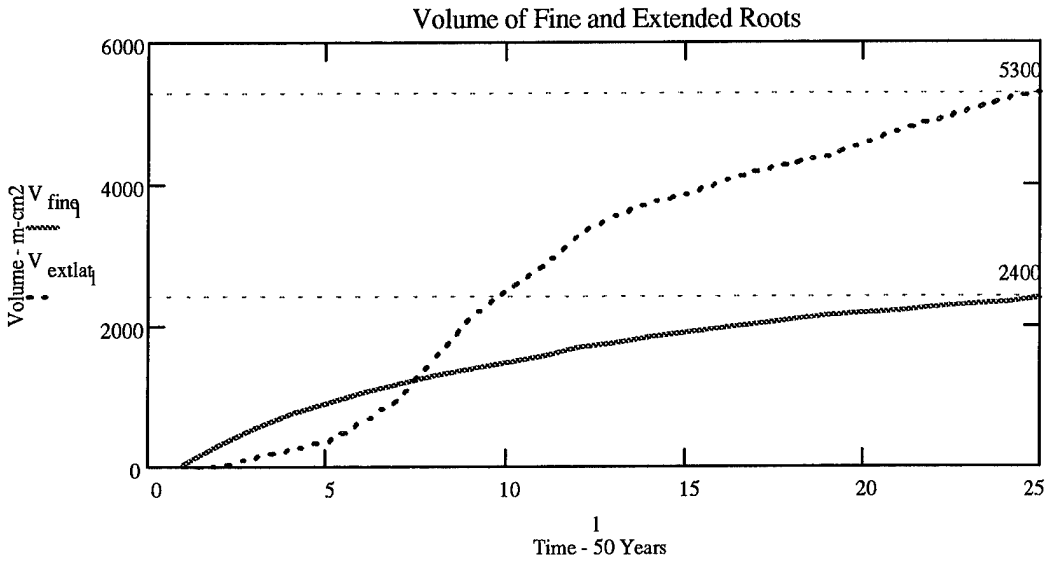

Now to check the various % of root volumes against the total volume to see how close it is to the expected mature value of 1.25 m3 or 125000 m-cm2.

$V_{taproot} := 2700$ $V_{closelat} := 3000$ $V_{fine} := 2400$ $V_{extlat} := 5300$

$V_T := V_{taproot} + V_{closelat} + V_{fine} + V_{extlat}$ $V_T = 13400$

$\frac{V_{taproot}}{V_T} = 0.201$ $\frac{V_{closelat}}{V_T} = 0.224$ $\frac{V_{fine}}{V_T} = 0.179$ $\frac{V_{extlat}}{V_T} = 0.396$

These values come out close to the expected percentages of 15%, 25%, 20%, and 40%. Now to calculate the volumes and surface areas of the various root compartments over time.

$$V_{2drt_l} := \frac{\pi}{3} \cdot \left(\frac{D_l}{2}\right)^2 \cdot H_l \cdot Rt_{taproot} + \frac{\pi}{3} \cdot \left(\frac{D_l}{2 \cdot 10}\right)^2 \cdot \frac{H_l}{2} \cdot Rt_{closelat} + \frac{\pi}{3} \cdot \left(\frac{D_l}{2 \cdot 5}\right)^2 \cdot H_l \cdot 2 \cdot Rt_{extlat}$$

$$V_{finert_l} := \pi \cdot \left(\frac{D_{fine}}{2}\right)^2 \cdot L_{fine} \cdot Rt_{fine_l} \qquad V_{Total_l} := V_{2drt_l} + V_{finert_l}$$

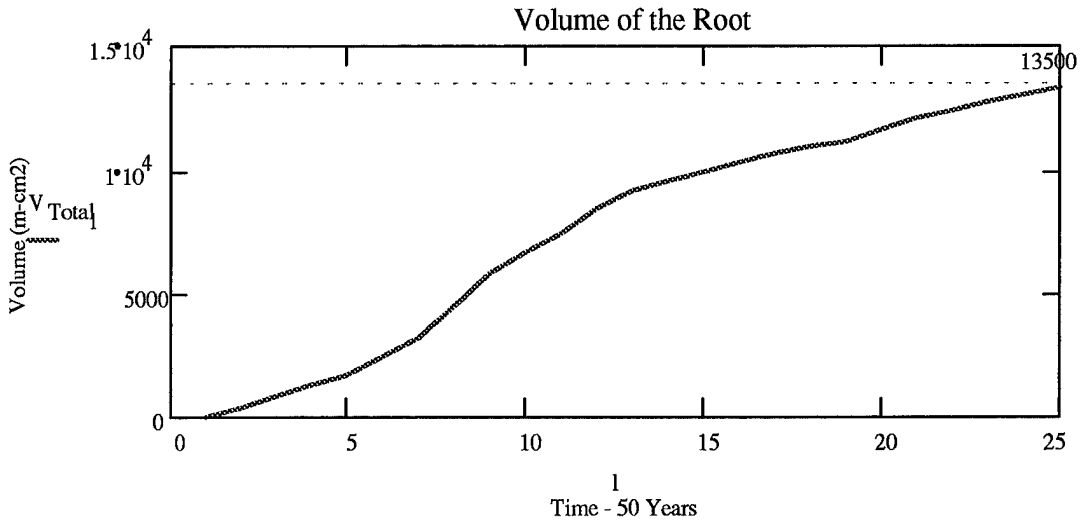

This gives a close approximation for the root volume of 12,500 m-cm2 or 125 m3, which corresponds with the graph of root volume found using known equations.

Next, an approximation of the secondary root surface area over time. These are equations to calculate the surface are of a right angle cone (not including the base) [Lindeburg].

$$SA_{taproot_l} := \frac{\pi}{3} \cdot \frac{D_l}{2} \cdot \left[\left(\frac{D_l}{2} \right)^2 + \left(H_l \cdot 100 \right)^2 \right]^{\frac{1}{2}} \cdot Rt_{taproot}$$

$$SA_{close_l} := \frac{\pi}{3} \cdot \frac{D_l}{20} \cdot \left[\left(\frac{D_l}{20} \right)^2 + \left(\frac{H_l}{2} \cdot 100 \right)^2 \right]^{\frac{1}{2}} \cdot Rt_{closelat}$$

$$SA_{ext_l} := \frac{\pi}{3} \cdot \frac{D_l}{10} \cdot \left[\left(\frac{D_l}{10} \right)^2 + \left(H_l \cdot 200 \right)^2 \right]^{\frac{1}{2}} \cdot Rt_{extlat}$$

$$SA_{2droot_l} := SA_{taproot_l} + SA_{ext_l} + SA_{close_l}$$

This is the total surface area of the secondary root.

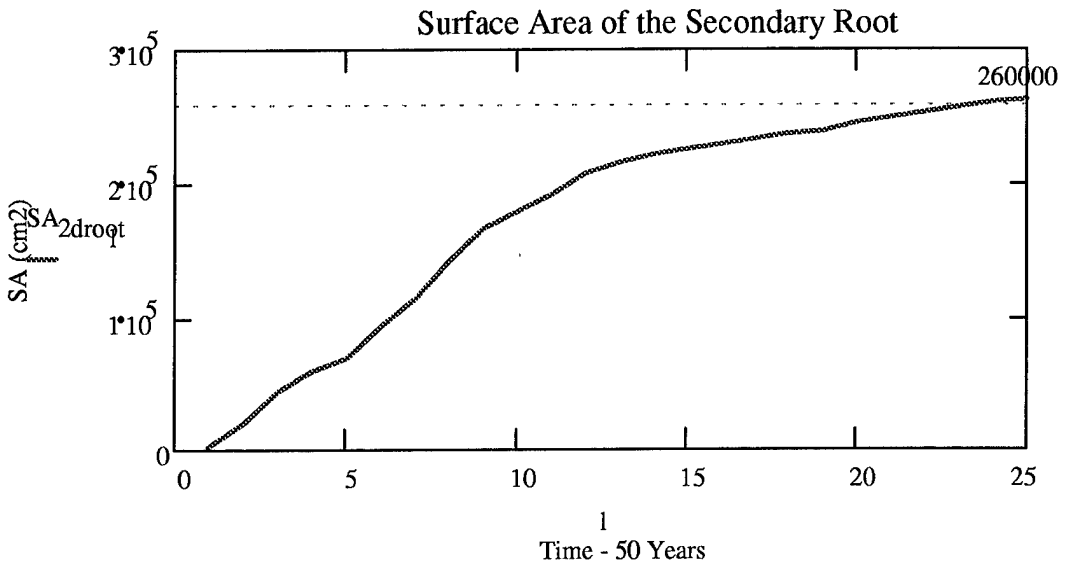

Now the surface area of the fine roots and total surface area are calculated.

$SA_{finert_l} := \pi \cdot D_{fine} \cdot L_{fine} \cdot Rt_{fine_l}$ $SA_{TotalRt_l} := SA_{2droot_l} + SA_{finert_l}$

The total surface area of the root is used in Appendix 4 to find the rhizosphere volume.

Next, the vascular volume in the secondary root is calculated. Knowing the vascular volume occurs on the exterior surface in the secondary root, the approximated values of .2 and .4 cm are used for the phloem and xylem, respectively.

$VolPhl_l := SA_{2droot_l} \cdot Phl_t$ $VolXyl_l := SA_{2droot_l} \cdot Xyl_t$

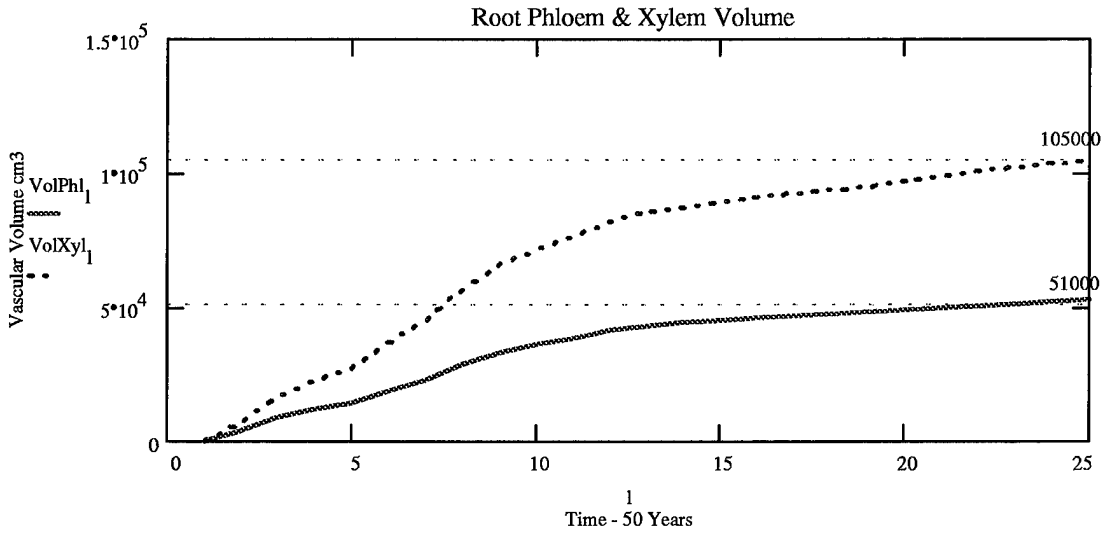

This means, at maturity, the total vascular volume is approximately .15 m3 when the total root secondary root volume is 1.00 m3 or 15% of the secondary root is vascular tissue. Values of .1 m3 and .05 m3 will be used for the total xylem and phloem volumes at maturity.

Now to find the volume of the root hair vascular tissue. Vascular tissue in the root hair zone is towards the interior, unlike in the secondary root and stem, where the vascular tissue is found on the surface. Because of this, the root hair vascular tissue approximation is made differently. By looking at diagrams showing cross-sections of the root hair zone, approximations of 10-30% of the root hair as vascular tissue were made. Xylem makes up 2/3 of this total. An average value of 20% of the root hair as vascular tissue was used.

$Vasc\% := .2 \qquad Xyl\% := .667 \qquad Phl\% := .333$

$$V_{fine_l} := \frac{\pi}{3} \cdot \frac{\left(\frac{D_l}{2}\right)^2}{16} \cdot \left(\frac{H_l}{100}\right) \cdot Rt_{fine}$$

$$Vol_{finexyl_l} := V_{finert_l} \cdot Vasc\% \cdot Xyl\% \qquad Vol_{finephl_l} := V_{finert_l} \cdot Vasc\% \cdot Phl\%$$

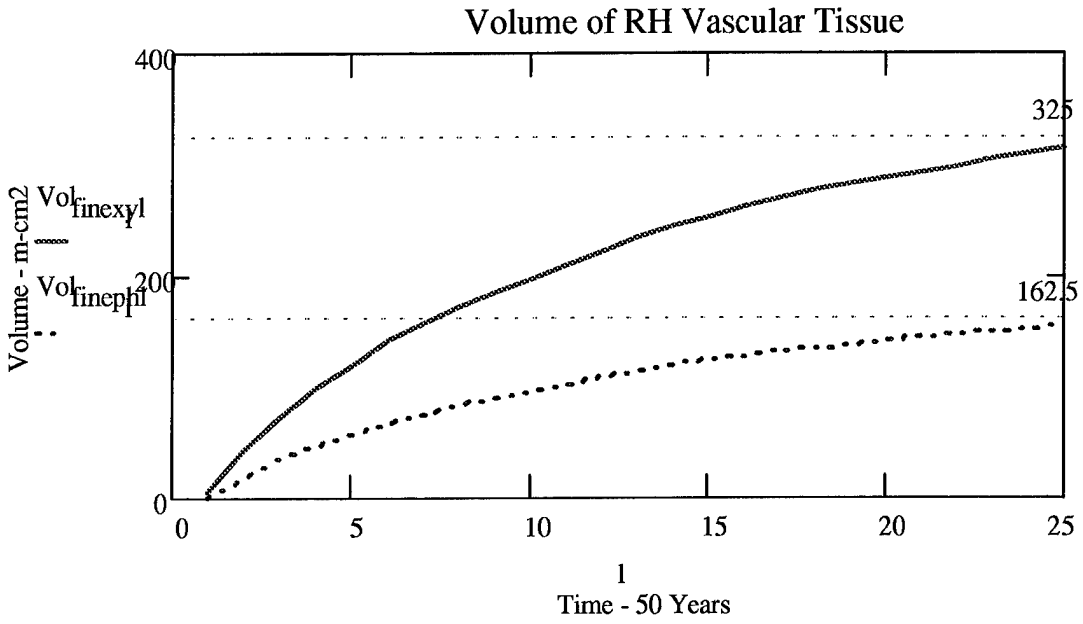

The xylem and phloem root hair vascular tissue is .0325 and .0625 m3 at maturity. The root hair volume is .25 m3 at maturity, so this gives a value of 19.5% of the root hair as vascular tissue.

Next, the total vascular volumes were calculated.

$VolPhl_I := SA_{2droot_I} \cdot Phl_t$ $VolXyl_I := SA_{2droot_I} \cdot Xyl_t$

$Vol_{finexyl_I} := V_{finert_I} \cdot Vasc\% \cdot Xyl\%$ $Vol_{finephl_I} := V_{finert_I} \cdot Vasc\% \cdot Phl\%$

$Vol_{TotalXyl_I} := \frac{VolXyl_I}{100} + Vol_{finexyl_I}$ $Vol_{TotalPhl_I} := \frac{VolPhl_I}{100} + Vol_{finephl_I}$

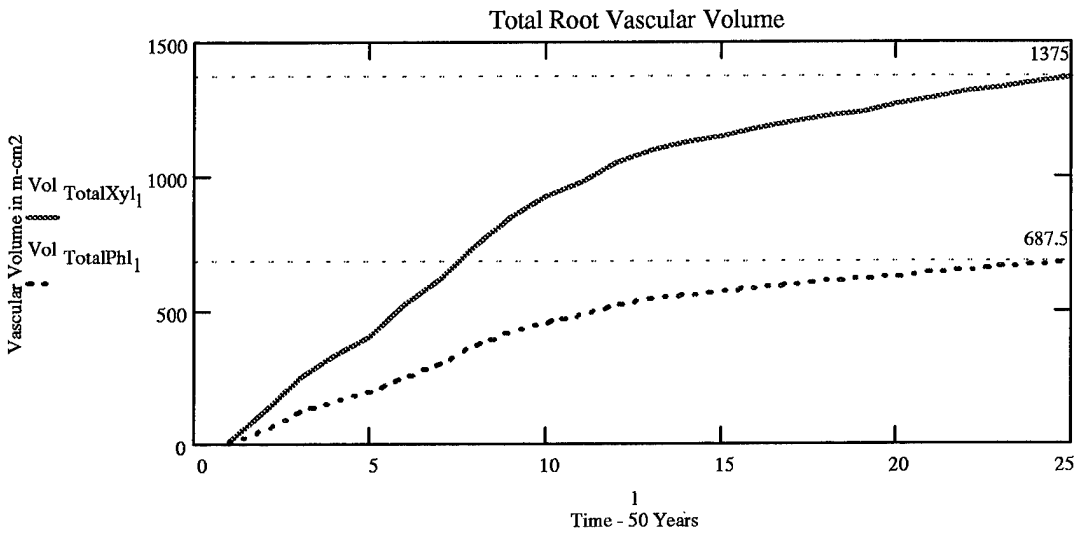

The total vascular volume is .20625 m3 or 16.5% of the mature root is vascular tissue.

Appendix 8 - Stem Vascular Volumes

Stem Xylem and Phloem Approximation

The stem xylem and phloem will grow in a similar fashion to the root xylem and phloem, but with a larger increment.

Here a relationship between the approximated root growth volume graph and the phloem and xylem root volumes was developed. First, an approximated run of diameters (cm) over a 50 year time frame for a tree stem was made. Next, an approximation was made of the growth in meters as a tree ages (from table by Tingle and van Laar). This is the value of H. Nobel states a single vascular element is 20 μm, and since they occur in bundles it was assumed a value of .2 cm for the phloem and .4 for the xylem. Both values were assumed constant. The volume and surface area equations assume the main stem is a cylinder with $Branch_{number}$ = 75 branches 1/5 the main stem diameter and 1/10 the height.

ORIGIN≡1 $l := 1..25$ $Phl_t := .2$ $Xyl_t := .4$ $Brch_{nbr} := 75$

$$D_s := \begin{bmatrix} 4 \\ 9.5 \\ 14.5 \\ 19 \\ 22.5 \\ 26 \\ 29 \\ 32 \\ 34.5 \\ 37 \\ 39.5 \\ 42 \\ 44 \\ 46 \\ 47.5 \\ 49 \\ 50 \\ 51 \\ 52 \\ 53 \\ 54 \\ 55 \\ 56 \\ 57 \\ 58 \end{bmatrix} \qquad H_s := \begin{bmatrix} 3 \\ 4 \\ 5 \\ 8.5 \\ 11 \\ 17 \\ 21 \\ 24 \\ 26 \\ 29 \\ 31 \\ 32.125 \\ 33.5 \\ 34.25 \\ 35 \\ 37 \\ 38 \\ 38.7 \\ 39.25 \\ 39.9 \\ 40.5 \\ 41.2 \\ 41.75 \\ 42.5 \\ 43 \end{bmatrix}$$

$$V_l := \frac{\pi}{3}\cdot\left(\frac{D_{s_l}}{2}\right)^2 \cdot H_{s_l} + \frac{\pi}{3}\cdot\left(\frac{D_{s_l}}{2.5}\right)^2 \cdot \frac{H_{s_l}}{10}\cdot Brch_{nbr} \qquad SA_l := \frac{\pi}{3}\cdot D_{s_l}\cdot H_{s_l} + \frac{\pi}{3}\cdot\frac{D_{s_l}}{5}\cdot\frac{H_{s_l}}{10}\cdot Brch_{nbr}$$

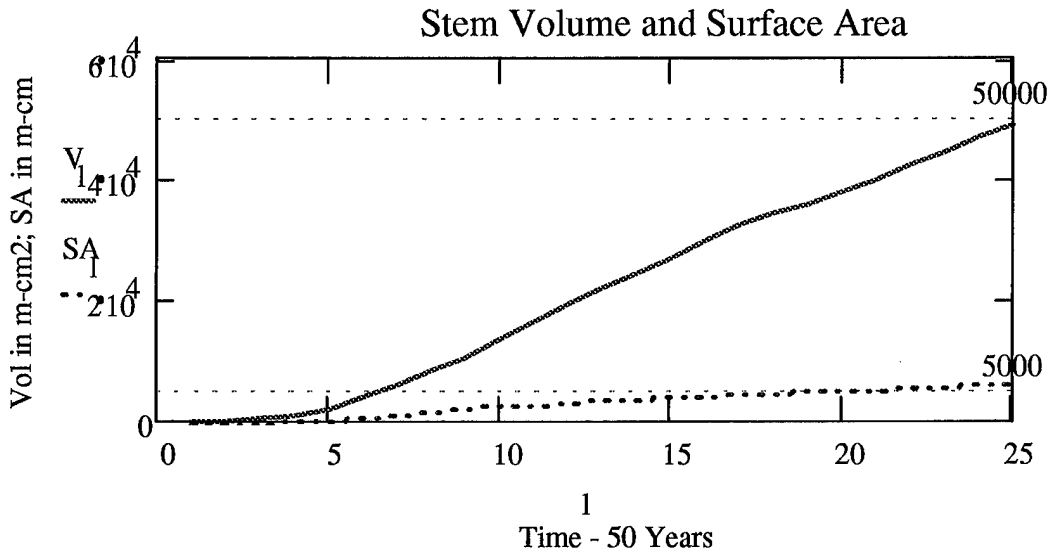

Now the stem surface area is multiplied by an approximate vascular thickness to find the vascular volume.

$$VolPhl_l := SA_l \cdot Phl_t \qquad VolXyl_l := SA_l \cdot Xyl_t$$

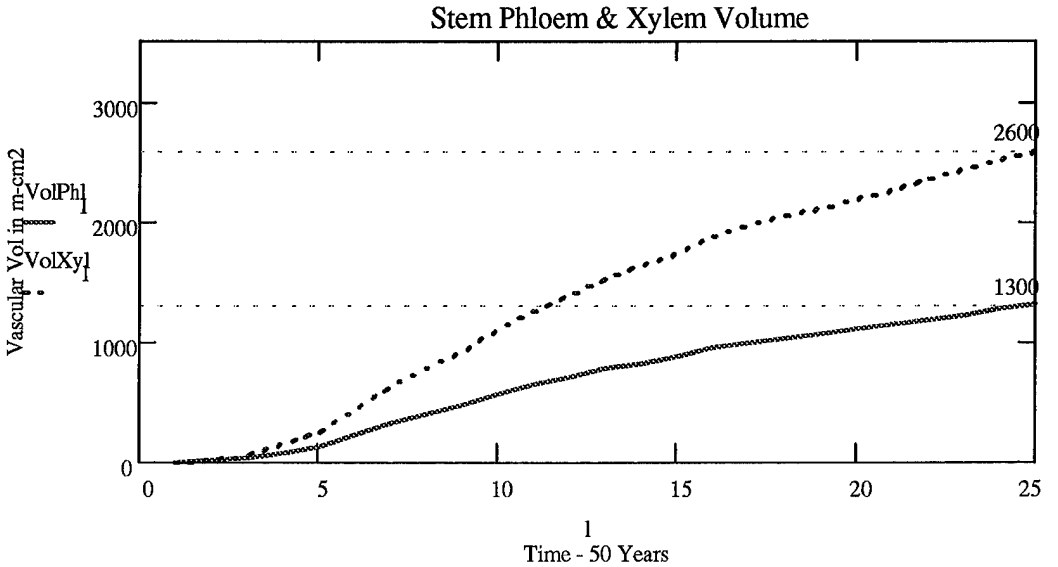

This gives a total stem vascular volume of .39 m3 or 7.8% of the mature stem is vascular tissue.

Appendix 9 - Partition Coefficients

This Appendix derives the partition coefficients between plant parts and vascular tissue. These equations were adapted from work by Trapp and McFarlane to estimate the partitioning between plant tissue and a contaminated solution.

LEAF FLUX COEFFICIENT

Density of xylem fluid is expected to be slightly higher than water (kg/m^3) (Blekmann, 23 Sep).

$\rho_x := 1050$

$K_{ow} := 2.355$

$W_l := .80$ Water content in the leaf. Value used by Trapp. Approximation by Hendrick (70-90%), Dickmann approximation (100% or less).

$L_l := .01$ Lipid content in the leaf (Trapp and McFarlane)

$b_l := .97$ Cuticle coefficient (Trapp and McFarlane)

$\rho_l := 700$ Density of leaf (kg/m^3) (Nobel, pg 423).

$$K_{lx} := \left(W_l + L_l \cdot K_{ow}^{\,b_l}\right) \cdot \frac{\rho_l}{\rho_x} \qquad K_{lx} = 0.549$$

STEM FLUX COEFFICIENT

$W_s := .60$ Water content in the stem. Approximation from e-mail by Hendricks (50-60%) and Dickmann (80-90% in sapwood, less in heartwood).

$L_s := .08$ Lipid content in the stem (6-10% of softwood xylem cells are storage parenchyma) (Gartner)

$b_s := .75$ Stem coefficient (Trapp and McFarlane)

$\rho_s := 600$ Density of stem (kg/m^3) (Approximation from water content)

$$K_{sx} := \left(W_s + L_s \cdot K_{ow}^{\ b_s}\right) \cdot \frac{\rho_s}{\rho_x} \qquad K_{sx} = 0.43$$

MATURE ROOT FLUX COEFFICIENT

$W_r := .80$ Water content in the root. Approximation from e-mail by Hendrick (higher than stem value of 50-60%) & Dickmann (20-30% higher than stem).

$L_r := .08$ Lipid content in the root (Approximation)

$b_r := .75$ Root coefficient (Trapp and McFarlane)

$\rho_r := 750$ Density of root (kg/m^3) (based on water content)

$$K_{rx} := \left(W_r + L_r \cdot K_{ow}^{\ b_r}\right) \cdot \frac{\rho_r}{\rho_x} \qquad K_{rx} = 0.68$$

JUVENILE ROOT FLUX COEFFICIENT

$W_r := .95$ Water content in the root. Approximation from e-mail by Hendrick (higher than stem value of 50-60%) & Dickmann (20-30% higher than stem).

$L_r := .01$ Lipid content in the root (Approximation)

$b_r := .75$ Root coefficient (Trapp and McFarlane)

$\rho_r := 1000$ Density of young root (kg/m^3) (Source unknown)

$$K_{rx} := \left(W_r + L_r \cdot K_{ow}^{\ b_r}\right) \cdot \frac{\rho_r}{\rho_x} \qquad K_{rx} = 0.923$$

BIBLIOGRAPHY

Agency for Toxic Substances and Disease Registry (ATSDR). Toxicological Profile for Trichloroethylene. ATSDR/TP-88/24. Syracuse: Syracuse Research Corporation, 1989.

Alexander, Donald. "Growth and Yield of Cottonwood Plantations Prediction and Realization," Symposium on Eastern Cottonwood and Related Species. LSU: Baton Rouge, LA, 1976.

Altman, P. L. and Dittmer, D. S. Environmental Biology. Federation of American Societies for Experimental Biology, Bethesda, Maryland. 1966.

American Conference of Governmental Industrial Hygienists (ACGIH). Documentation of the Threshold Limit Values and Biological Exposure Indices. Cincinnati, OH: American Conference of Governmental Industrial Hygienists, Inc., 1986.

Anderson, Todd, Guthrie, E., and Walton, B. "Bioremediation in the Rhizosphere," Environmental Science and Technology, 27(13): (1993).

Anderson, Todd and Walton, Barbara. "Comparative Fate of [^{14}C]Trichloroethylene in the Root Zone of Plants from a Former Solvent Disposal Site," Environmental Toxicology and Chemistry, 14(12): 2041-2047 (1995).

Anderson, Todd. Comparative Plant Uptake and Microbial Degradation of TCE in the Rhizosphere of Five Plant Species: Implications for Bioremediation of Contaminated Surface Soils. Ph.D. dissertation. University of Tennessee, Knoxville TN, 1991 (9221728).

Arciero, David, Vannelli, Todd, Logan, Myke, and Hooper, Alan B. "Degradation of TCE by the Ammonia-Oxidizing Bacterium *Nitrosomonas europaea*," Biochemical and Biophysical Research Communications, 159(2): 640-643 (1989).

Atlas, Ronald and Bartha, Richard. Microbial Ecology: Fundamentals and Applications, 3rd Edition. Redwood City, CA: The Benjamin/Cummings Publishing Co., Inc., 1992.

Augustin, Roy-Alan. Analysis of the Potential for the Plant Uptake of Trichloroethylene and an Assessment of the Relative Risk from Different Crop Types. Air Force Institute of Technology (AU), Wright-Patterson AFB OH, July 1994 (AFIT/GEE/ENV/94S-01).

Barber, Stanley and Claassen, Norbert. "A Mathematical Model to Simulate Metal Uptake by Plants Growing in Soil," Fifteenth Annual Hanford Life Science Symposium. 358-364. Richland, WA: Batelle, Pacific Northwest Laboratories, September 1975.

Bazin, M. J., Markham, P., Scott, E. M., and Lynch, J. M. "Population Dynamics and Rhizosphere Interactions," in The Rhizosphere. New York: John Wiley and Sons, 1990.

Biernacki, M.; Doust, J. L.; and Doust, L. D. "Effects of Trichloroethylene, Plant Sex and Site of Origin on Modular Demography in *Vallisneria americana*," Journal of Applied Ecology, 32: 761-777 (1995).

Black, Harvey. "Absorbing Possibilities," Environmental Heath Perspectives,103(12): 1106-1108 (December 1995).

Bleckmann, Charles. Professor, Department of Engineering and Environmental Management, Air Force Institute of Technology, Personal Interview, 4 Sep 1997.

Bouwer, Edward J., Rittmann, Bruce E., and McCarty Perry L. "Anaerobic Degradation of Halogenated 1- and 2-Carbon Organic Compounds," Environmental Science and Technology, 15: 596-599 (1981).

Bowen, Glynn and Rovira, Albert. "The Rhizosphere: The Hidden Half of the Hidden Half," in Plant Roots: The Hidden Half. New York: Marcel-Dekker, Inc., 1991.

Briggs, Geoffrey G., Bromilow, Richard H., and Evans, Avis A. "Relationships Between Lipophilicity and Root Uptake and Translocation of Non-ionized Chemicals by Barley," Pesticide Science, 13: 495-504 (1982).

Brouwer, R. "Water Absorption by the Roots of *Vicia faba* at Various Transpiration Strengths - Causal Relation Between Suction Tension, Resistance and Uptake," Proceedings of the Koninklijke Nederlandse Akademie van Wetenschappen (Biological and Medical Sciences -Series C) Conference. C56:129-136 (1953).

Brouwer, R. "Water Absorption by the Roots of *Vicia faba* at Various Transpiration Strengths - Changes in Water Conductivity Artificially Obtained," Proceedings of the Koninklijke Nederlandse Akademie van Wetenschappen (Biological and Medical Sciences -Series C) Conference. C57:68-80 (1954).

Bruckner, James V., Davis, Barbara D., and Blancato, Jerry N. "Metabolism, Toxicity, and Carcinogenicity of Trichloroethylene," Critical Reviews in Toxicology, 20(1): 31-50 (1989).

Burken, Joel and Schnoor, Jerald L. "Phytoremediation Gets to the Root of Soil Contamination," The Hazardous Waste Consultant. 1.22-1.24 (May/June 1996).

Burken, Joel and Schnoor, Jerald. "Phytoremediation: Plant Uptake of Atrazine and Role of Root Exudates," Journal of Environmental Engineering: 958-963 (Nov 1996).

Burken, Joel. Uptake and Fate of Organic Contaminants by Hybrid Poplar Trees. Ph.D. Dissertation. University of Iowa, Iowa, Dec 1996.

Burken, Joel and Schnoor, Jerald. "Uptake and Metabolism of Atrazine by Poplar Trees," Environmental Science and Technology, 31: 1399-1406 (1997).

Burken, Joel. Assistant Professor of Civil Engineering, Environmental Engineering Program. University of Missouri-Rolla, Rolla, MO. Personal Interview. 19 Jun 1997.

Campbell, R. "The Structure and Dynamics of Microbial Populations in Soil," Microbial Ecology, 5: 63-91 (1997).

Campbell, R. Plant Microbiology. Baltimore, Maryland: Edward Arnold Publishers, Ltd., 1985.

Campbell, R. "Anatomy and Community Structure of the Rhizosphere," in The Rhizosphere. New York: John Wiley and Sons, 1990.

Cermak, J., Demi, M., and Penka, M. "A New Method of Sap Flow Rate Determination in Trees," Biologia Plantarum, 15(3): 171-178 (1973).

Ceulamans, Reinhart and Saugler, Bernhard. Physiology of Trees. New York: John Wiley and Sons, 1991.

Chappell, Jonathan. Phytoremediation of TCE Using *Populus*. Prepared for the U.S. EPA Technology Innovation Office under a National Network of Environmental Management Studies Fellowship. August 22, 1997.

Clarkson, David T. "Root Structure and Site of Ion Uptake," in Plant Roots: The Hidden Half. New York: Marcel-Dekker, Inc., 1991.

Code of Federal Regulations (CFRs), Parts 100 to 149. A Codification of Documents of General Applicability and Future Effect. Office of the Federal Register National Archives and Records Administration, July 1, 1994.

Cohrssen, John and Covello, Vincent. Risk Analysis: A Guide to Principles and Methods for Analyzing Health and Environmental Risks. Springfield, VA: United States Council on Environmental Quality, 1989.

Crank, J., McFarlane, N. R., Newby, J. C., Paterson, G. D., and Pedley, J. B. Diffusion Processes in Environmental Systems. London, England: Macmillan Press Ltd., 1981.

Creech, J. L. and Johnson, N. M. "Angiocarcinoma of the Liver in the Manufacture of Polyvinyl Chloride," Journal of Occupational Medicine, 16: 150 (1974).

Cunningham, Scott D., Berti, William R., and hang, Jianwei W. "Phytoremediation of Soils Contaminated with Organic Pollutants," Advances in Agronomy. New York: Academic Press, 1996.

Cunningham, Scott D. and Berti, William R. "Remediation of Contaminated Soils with green Plants: An Overview," In Vitro Cellular and Developmental Biology: 207-212 (Oct 1993).

Curl, E. and Truelove, B. The Rhizosphere. New York: Springer-Verlag, 1986.

Cutler, D. F. Root Identification Manual of Trees and Shrubs. London, England: Chapman and Hall, Ltd., 1987.

Davis, L. C., Erickson, L. E., Lee, E., Shimp, J. F., and Tracy, J. C. "Modeling the Effects of Plants on the bioremediation of Contaminated Soils and Ground Water," Environmental Progress, 12(1): 67-75 (Feb 1993).

Dickmann, Donald I. and Stuart, Katherine W. The Culture of Poplars in North America. Ann Harbor, Michigan: McNaughton and Gunn, Inc., 1983.

Dickmann, Donald I. and Pregitzer, Kurt S. "The Structure and Dynamics of Woody Plant Root Systems," in Ecophysiology of Short Rotation Forest Crops. New York: Elsevier Applied Science, 1992.

Dickmann, Donald I. Department of Forestry, Michigan State University, East Lansing, MI. E-mail. 8 Jul 1997.

Drew, M. C. "Root Function, Development, Growth, and Mineral Nutrition," in The Rhizosphere. New York: John Wiley and Sons, 1990.

Duba, A. G., Jackson, K. J., Jovanovich, M. C., Knopp, R. B., and Taylor R. T. "TCE Remediation Using In Situ, Resting-State Bioaugmentation," Environmental Science and Technology, 30: 1982-1989 (1996).

Ek, Alan R. and Dawson, David. "Actual and Projected Growth Yields of *Populus tristis* #1 Under Intensive Culture," Canada Journal of Forestry Resources, 6: 132-144 (1976).

Ensley, B. D. "Biochemical Diversity of Trichloroethylene Metabolism," Annual Review of Microbiology, 45: 283-299 (1991).

Erickson, Larry E., Shimp, J. F., Tracy, J. C., Lee, E., Davis, L. C., Huang, W., and Schnoor, J. L. "Concepts Involved in Developing Soil and Groundwater Remediation Strategies Using Plants," Proceedings of the Conference on Hazardous Waste Research. 629-647. Manhattan, KS: KSU Engineering Extension, May 1991.

Ewers, Jens, Freier-Schroder, Doris, and Knackmus, Hans-Joachim. "Selection of Trichloroethylene (TCE) Degrading Bacteria that Resist Inactivation by TCE," Archives of Microbiology, 154: 410-413 (1990).

Ferro, Ari. President and Technical Director, Phytokinetics. North Logan, Utah. Personal Interview. 17 Jun 1997.

Fitter, A. H. "Characteristics and Functions of Root Systems," in Plant Roots: The Hidden Half. New York: Marcel-Dekker, Inc., 1991.

Fogel, R. "Root System Demography and Production in Forest Ecosystems," in Plant Root Growth. Boston, MA: Blackwell Scientific Publications, 1991.

Folsom, B. R., Chapman, P. J., and Pritchard, P. H. "Phenol Trichloroethylene Degradation by Pseudomonas Cepacia G4 Kinetics and Interactions Between Substrates," Applied Environmental Microbiology, 56: 1279-1285 (1990).

Foote, Knowlton and Schaedle, Michail. "Diurnal and Seasonal Patterns of Photosynthesis and Respiration by Stems of *Populus tremuloides* Michx," Plant Physiology, 58: 651-655 (1976).

Forrester, Jay and Senge, Peter. "Tests for Building Confidence in System Dynamics Models," in Studies in Management Science, Vol. 14. New York: North-Holland Publishing Company, 1980.

Foster, R. C. "Ultrastructure of the Root-Soil Interface," American Phytopathological Society. St. Paul, MN: 1983.

Fox, Brian G., Borneman, James G., Wackett, Lawrence P., and Lipscomb, John D. "Haloalkane Oxidation by the Soluble Methane Monooxygenase from Methylosinus Trichosporidium OB3b: Mechanistic and Environmental Implications," Biochemistry, 29: 6419-6427 (1990).

Francis, John. U. S. Department of Agriculture. The Roots of Plantation Cottonwood: Their Characteristics and Properties. Forest Service, SO-314. Washington: Government Printing Office, Aug 1985.

Fried, Maurice and Broeshart, Hans. The Soil Plant System. New York: Academic Press, Incorporated, 1967.

Friend, Alexander L., Scarascia-Mugnozza, Giuseppe, Isebrands, J. G., and Heilman, Paul E. "Quantification of Two-Year Old Hybrid Poplar Root Systems: Morphology, Biomass, and 14C Distribution," Tree Physiology, 8: 109-119 (1991).

Fuller, M. E., Mu, D. Y., and Scow, K. M. "Biodegradation of Trichloroethylene and Toluene by Indigenous Microbial Populations in Vadose Sediments," Microbial Ecology, 29: 311-325, 1995.

Gartner, Barbara L. "Patterns of Xylem Variation within a Tree and Their Hydraulic and Mechanical Consequences," in Plants and Stems, Physiology and Functional Morphology. San Diego, CA: Academic Press, 1995.

Gatliff, Edward G. President, Applied Natural Sciences, Fairfield, OH. Telephone interview. 24 Aug 1997.

Gatliff, Edward G. President, Applied Natural Sciences, Fairfield, OH. Telephone interview. 14 Oct 1997.

Gordon, Milton, Choe, Nami, Duffy, Jim, Ekuan, Gordon, Heilman, Paul, Muiznieks, Indulis, Newman, Lee, Rusjaz, Marty, Shurtleff, Brook B., Strand, Stuart, and Wilmoth, Jodi. "Phytoremediation of Trichloroethylene with Hybrid Poplars," In Review for Publication, 1997.

Gordon, Milton. Professor, Department of Biochemistry. University of Washington, School of Medicine, Seattle, WA. Personal Interview. 18 Jun 1997.

Green, Trevor. "Chloroethylenes: A Mechanistic Approach to Human Risk Evaluation," Annual Review of Pharmacological Toxicology, 30: 73-89 (1990).

Gurdarshan, S. Brar. President, EarthCare, Inc., Hanover, NH. "Challenges of Phytoremediation Application in the Field - Strategies for Success and Learned Lessons." Presentation at the IBC Second Annual International Conference on Phytoremediation. DoubleTree Guest Suites Hotel, Seattle, WA. June 18-19, 1997.

Harvey, Greg. ASC Environmental Management Directorate Restoration Division, Special Project Head, WPAFB, OH. Personal Interview. 10 Apr 1997.

Harvey, Greg. ASC Environmental Management Directorate Restoration Division, Special Project Head, WPAFB, OH. Personal Interview. 12 Jul 1997.

Harvey, Greg and Eberts, Sandra. ASC Environmental Management Directorate Restoration Division, Special Project Head, WPAFB, OH. "Plant Enhanced Bioremediation," ESTCP in Progress Review. 16 September, 1997.

Heilman, Paul E., Ekuan, Gordon, and Fogle, Diane B. "Above- and Below-Ground Biomass and Fine roots of 4-Year Old Hybrids of *Populus trichocarpa x Populus deltoides* and Parental Species in Short-Rotation Culture," Canadian Journal of Forestry, 24 (6): 1186-1192 (1994).

Heilman, Paul E., Ekuan, Gordon, and Fogle, Diane B. "First-Order Development from Cuttings of *Populus trichocarpa* x *P. deltoides* hybrids," Tree Physiology, 14: 911-920 (1994).

Hendrick, Ronald. D. B. Warnell School of Forest Resources, University of Georgia, Athens, GA. E-mail. 10 Jul 1997.

Hendrick, Ronald. D. B. Warnell School of Forest Resources, University of Georgia, Athens, GA. E-mail. 11 Sep 1997.

Henschler, D. "Science, Occupational Exposure Limits and Regulations: A Case Study on Organochlorine Solvents," American Industrial Hygiene Association Journal, 51: 523-530 (1990).

Hinchman, Ray R., Negri, Cristina M., and Gatliff, Edward G. Phytoremediation: Using Green Plants to Clean Up Contaminated Soil, Ground Water, and Wastewater. U.S. Department of Energy: Argonne National Lab, 1996.

Hinchman, Ray. Energy Systems Division, Argonne National Laboratory, Argonne, IL. Telephone interview. 22 Aug 1997.

Hinckley, T. M., Brooks, J. R., Cermak, J., Ceulemans, R., Kucera, J., Meinzer, F. C., and Roberts, D. A. "Water Flux in Hybrid Poplar Stand," Tree Physiology, 14: 1005-1018 (1994).

Hofer, Rose-Marie. "Root Hairs," in Plant Roots: The Hidden Half. New York: Marcel-Dekker, Inc., 1991.

Hopkins, W. Introduction to Plant Physiology. New York: John Wiley and Sons, 1995.

Host, George, Rauscher, H. Michael, Isebrands, J. G., Dickmann, Donald I., Dickson, Richard E., Crow, Thomas R., and Michael, D. A. U. S. Department of Agriculture. The Microcomputer Scientific Software Series 6 - The ECOPHYS User's Manual. Forest Service, NC-141. Washington: Government Printing Office, 1990.

Howes, M. C. "Living Plant Cells Released from the Root Cap: A Regulator of Microbial Populations in the Rhizosphere?," in The Rhizosphere and Plant Growth. Boston, MA: Kluwer Academic Pubs, 1991.

Http: sunsite.unc.edu/. "Botany," 1-21, December 1996

Hutchinson, G. L. and Mosier, A. R.. "Nitrous Oxide Emissions from an Irrigated Corn Field," Science, 205: 1125-1126 (1979).

Jachetta, John J., Appleby, Arnold P., and Boersma, Larry. "Apoplastic and Symplastic Pathways of Atrazine and Glyphospate Transport in Shoots of Seedling Sunflower," Plant Physiology, 82: 1000-1007 (1986).

Joshi, P. C. and Pande, D. C. "A Note on Growth Performance of *Populus ciliata*," Symposium Proceedings: Silviculture Management and Utilization of Poplars. 103-105. Oct 15-18, 1979.

Katznelson, H. "The Rhizosphere Effect of Mangels on Certain Groups of Micro-organisms," Soil Science, 62: 343-354 (1946).

Katznelson, H. "Nature and Importance of the Rhizosphere," Ecology of Soil-Borne Plant Pathogens. Berkeley: University of California Press, 1965.

Kolek, J. and Kozinka, V. Physiology of the Plant Root System. Boston, MA: Kluwer Academic Pubs, 1992.

Krinard, Roger M. and Kennedy, Jr., A. E.. U. S. Department of Agriculture. Growth and Yields of 5-year-old Planted Hardwoods on Sharkey Clay Soil. Southern Forest Experiment Station, SO-271. Washington: Government Printing Office, 1981.

Krinard, Roger M. and Kennedy, Jr., A. E. U. S. Department of Agriculture. Ten-year Growth of Five Planted Hardwood Species with Mechanical Weed Control on Sharkey Clay Soil. Southern Forest Experiment Station, SO-303. Washington: Government Printing Office, Dec, 1983.

Krinard, Roger M. and Johnson, Robert L. U. S. Department of agriculture. Cottonwood Plantation Growth Through 20 Years. Southern Forest Experiment Station, SO-212. Washington: Government Printing Office, Dec, 1984.

Krinard, Roger M. and Burkardt, E. C. "Growth Through 13 Years of Two Pruned Cottonwood Plantations Spaced for Sawtimber Production," Southern Journal of Applied Forestry, 8(4): 221-223 (1984).

Krinard, Roger M. U. S. Department of Agriculture. Cottonwood Development Through 19 Years in a Neider's Design. Southern Forest Experiment Station, SO-322. Washington: Government Printing Office, Dec, 1985.

Krinard, Roger M. U. S. Department of Agriculture. Volume Equations for Plantation Cottonwood Trees (*Populus deltoides*). Southern Forest Experiment Station, SO-347. Washington: Government Printing Office, June, 1988.

Lenhard, R. J., Oostrom, M., Simmons, C. S., and White, M. D. "Investigation of Density-Dependent Gas Advection of Trichloroethylene: Experiment and a Model Validation Exercise," Journal of Contaminant Hydrology, 19: 47-67 (1995).

Licht, Lou. President, Ecolotree. University of Iowa, Iowa City, IA. Personal Interview. 17 Jun 1997.

Linderman, R. G. "Mycorrhizal Interactions in the Rhizosphere," in The Rhizosphere and Plant Growth. Boston, MA: Kluwer Academic Pubs, 1991.

Lindstrom, F. T., Boersma, L., and McFarlane, C. "Mathematical Model of Plant Uptake and Translocation of Organic Chemicals: Development of the Model," Journal of Environmental Quality, 20 129-136 (1991).

Lynch, J. M. and Whipps, J. M. "Substrate Flow in the Rhizosphere," in The Rhizosphere and Plant Growth. Boston, MA: Kluwer Academic Pubs, 1991.

Mackay, D. M. and Cherry, J. A. "Ground Water Contamination: Pump-and-Treat Remediation," Environmental Science and Technology, 23: 630-636 (1989).

Maisenhelder, L. C. "Eastern Cottonwood Selections Outgrow Hybrids on Southern Sites," Journal of Forestry, 68(5): 300-301 (May 1970).

Masters, Gilbert M. Introduction to Environmental Engineering and Science. Englewood Cliffs, NJ: Prentice Hall, 1991.

Matso, Kelle. "Mother Nature's Pump and Treat," Civil Engineering: 44-46 (Oct 1995).

McCarthy, Kathleen A. and Johnson, Richard L. "Transport of Volatile Organic Compounds Across the Capillary Fringe," Water Resources Research, 29(6): 1675-1683, (June 1993).

McFarlane, Craig. Diffusion Processes in Environmental Systems. London: Macmillan Press, Ltd., 1981.

McFarlane, Craig and Trapp, Stefan. "A Model of Organic Chemical Uptake by Plants from Soil and the Atmosphere," Environmental Science and Technology, 28: 2259-2266 (1994).

Meinzer, Oscar E. Plants as Indicators of Ground Water. U.S. Geological Survey. Washington: Government Printing Office, 1927.

Minnesota Valley Testing Laboratory (MVTL). Project Number: AFP4-PEBS, Lab Number: 196001-463, Work Order Number: 11-0088, Date Reported: 3/01/96. New Ulm, MN (507) 354-8517.

Moreshet, Samuel and Huck, Morris. "Dynamics of Water Permeability," in Plant Roots: The Hidden Half. New York: Marcel-Dekker, Inc., 1991.

Mu, Der Yi and Scow, Kate M. "Effect of Trichloroethylene (TCE) and Toluene Concentrations on TCE and Toluene Biodegradation and the Population Density of TCE and Toluene Degraders in Soil," Applied and Environmental Microbiology: 2661-2665 (Jul 1994).

Narayanan, M., Russell, N. K., Davis, L, C., and Erickson, L. E. "Experimental and Modeling Studies of the Fate of Trichloroethylene in a Chamber with Alfalfa Plants," Water Resource Research: 1996.

Narayanan, M. "Progress in Remediation Studies," Unpublished Article.

Nelson, David R., Kamataki, Tetsuya, Waxman, David J., Guengerich, F. Peter, Estabrook, Ronald W., Feyereisen, Rene, Gonzalez, Frank J., Coon, Minor J., Gunsalus, Irwin C., Gotoh, Osamu, Okuda, Kyuichiro, and Nebert, Daniel W. "The P-450 Superfamily: Update on New Sequences, Gene Mapping, Accession Numbers, Early Trivial Names of Enzymes, and Nomenclature," DNA Cell Biology, 12: 1-51, (1993).

Newman, E. and Watson, A. "Microbial Abundance in the Rhizosphere: A Computer Model," Plant and Soil, 48: 17-56 (1977).

Newman, E. J. "Patterns of Distribution of Bacteria on Root Surfaces," Soil Biology and Biochemistry, 6: 205-209 (1974).

Newman, E. J. "The Rhizosphere: Carbon Sources and Microbial Populations," in Ecological Interactions in Soil. Boston, MA: Blackwell Scientific Pubs, 1985.

Newman, Lee A., Strand, Stuart E., Choe, Nami, Duffy, James, Ekuan, Gordon, Ruszaj, Martin, Shurtleff, Brook B., Wilmoth, Jodi, Heilman, Paul, and Gordon, Milton P. "Uptake and Biotransformation of TCE by Hybrid Poplars," Environmental Science and Technology, 31(4): 1062-1067 (1997).

Newman, Lee. Professor, University of Washington, Seattle, WA. Telephone Interview. 18 Jun 1997.

Newman, Lee. Professor, University of Washington, Seattle, WA. Telephone Interview. 23 Jul 1997.

Newman, Lee. Professor, University of Washington, Seattle, WA. E-mail. 24 Jul 1997.

Nichols, W. D. "Groundwater Discharge by Phreatophyte Shrubs in the Great Basin," Water Resources Research, 30(12): 3265-3274 (1994).

Nissen, Per. "Uptake Mechanisms," in Plant Roots: The Hidden Half. New York: Marcel-Dekker, Inc., 1991.

Nobel, Park S. Physicochemical and Environmental Plant Physiology. New York: Academic Press, 1991.

Nyer, Evan K. and Gatliff, Edward G. "Phytoremediation," Ground Water Monitoring and Remediation: 58-62 (Winter 1996).

Oertli, J. J. and Eth. "Transport of Water in the Rhizosphere and in Roots," in Plant Roots: The Hidden Half. New York: Marcel-Dekker, Inc., 1991.

Paterson, Sally, Mackay, Donald, and McFarlane, Craig. "Uptake of Organic Chemicals by Plants: A Review of Processes, Correlations, and Models," Chemosphere, 21(3): 297-331 (1990).

Parke, J. L. "Root colonization by Indigenous and Introduced Microorganisms," in The Rhizosphere and Plant Growth. Boston, MA: Kluwer Academic Pubs, 1991.

Peake, Michael B. Modeling Plant Uptake of Metal in Constructed Wetlands Supported by Experimentally Derived Uptake Rates. MS thesis, AFIT/GEE/ENV/96D-15. School of Engineering, Air Force Institute of Technology (AU), Wright-Patterson AFB OH, December 1996.

Plaa, G. L. "Toxic Responses of the Liver," in Casarett and Doull's Toxicology: The Basic Science of Poisons. New York: Macmillan Publishing Co., 1986.

Polder, Marieke, Hulzebos, Etje M., and Jager, D. Tjalling. "Validation of Models on Uptake of Organic Chemicals by Plant Roots," Environmental Toxicology and Chemistry, 14(9): 1615-1623 (1995).

Randers, Jφrgen. "Guidelines for Model Conceptualization," in Modelling for Management, Vol. II. Brookfield, VT: Dartmouth Publishing Company, 1996.

Read, D. J. "Mycorrhizal Mycelia and Nutrient Cycling in Plant Communities," in Ecological Interactions in Soil. Boston, MA: Blackwell Scientific Pubs, 1985.

Reid, C. P. P. "Mycorrhizaes," in The Rhizosphere. New York: John Wiley and Sons, 1990.

Rovira, A. D., Foster, R. C., and Martin, J. K. "Note on Technology: Origin, Nature, and Nomenclature of the Organic Materials in the Rhizosphere," The Rhizosphere. John Wiley and Sons: Academic Press, 1979.

Russell, M., Colglazier, E. W., and English, M. R. Hazardous Waste Remediation: The Task Ahead. Knoxville: Waste Management Research and Education Institute, University of Tennessee, 1991.

Ryan, Michael and Yoder, Barbara. "Hydraulic Limits to Tree Height and Tree Growth," BioScience, 47(4): 235-242 (April 1997).

Sandermann, Jr. "Plant Metabolism of Xenobiotics," Trends in Biochemical Sciences, 17: 1-3 (Feb 1992).

Salisbury, Frank and Ross, Cleon. Plant Physiology, 4th Edition. Belmont, CA: Wadsworth Publishing Company, 1991.

Santantonio, D. "Dry-Matter Partitioning and Fine-Root Production in Forests - New Approaches to a Difficult Problem," in Biomass Production by Fast-Growing Trees. Dordrecht, Netherlands: Kluwer Academic Publishers, 1989.

Sauter, Jorg J. and van Cleve, Barbara. "Storage, Mobilization, and Interrelations of Starch, Sugars, Protein, and Fat in the Ray Storage Tissue of Poplar Trees," Trees, 8: 297-304 (1994).

Schaumberg, Frank. "Banning Trichloroethylene: Responsible Reaction or Overkill?," Environmental Science and Technology, 24(1): 17-22 (1990).

Schmidt. "Methods for Microbial Autecology in the Soil Rhizosphere," in The Rhizosphere. Boston, MA: Kluwer Academic Publishers, 1991.

Schnabel, William E., Dietz, Annette C., Burken,Joel G., Schnoor, Jerald L., and Alvarez, Pedro J. "Uptake and Transformation of Trichloroethylene by Edible Garden Plants," Water Resources, 31(4): 816 (1997).

Schnoor, Jerald L., Licht, Louis A., McCutcheon, Wolfe, N. Lee, and Carreira, Laura H. "Phytoremediation of Organic & Nutrient Contaminants," Environmental Science and Technology, 29(7): 318A-323A (1995).

Schroll, R., Bierling, B., Cao, G., Dorfler,U., Lahaniati, M., Langenbach, T., Scheunert, I., and Winkler, R. "Uptake Pathways of Organic Chemicals from Soil by Agricultural Plants," Chemosphere, 28(2): 297-303 (1994).

Schultz, R. C., Isebrands, J. G., and Kormanik, P. P. Mycorrhizae of Poplars. Journal Paper # J-10984 of the Iowa Agricultural and Home Economic Experiment Station, Ames, Iowa, 1983.

Science Applications International Corporation (SAIC). Soils Test Report. Phone - (201) 489-5200. Hackensack, NJ: 1996.

Sharma, K. C. and Kashyap, S. D. "Diameter Growth Rate in *Populus ciliata*," Symposium Proceedings: Silviculture, Management, and Utilization of Poplars. 101-102. Oct 15-18 1979.

Sheikh, Mahmood Iqbal. "Comparison of Six Poplar Clones for Growth and Survival," The Pakistan Journal of Forestry: 101-108 (April 1977).

Sheikh, Mahmood Iqbal. "Growth Pattern of Poplar Clones," The Pakistan Journal of Forestry: 217-220 (October 1983).

Shimp, J. F., Tracy, J. C., Davis, L. C., Lee, E., Huang, W., and Erickson, L. E. "Beneficial Effects of Plants in the Remediation of Soil and Ground Water Contaminated with Organic Materials," Environmental Science and Technology, 23(1): 41-77 (1993).

Sievers, Andreas and Hensel, W.. "Root Cap Structure and Function," in Plant Roots: The Hidden Half. New York: Marcel-Dekker, Inc., 1991.

Simon, Miklos. Some Phenological Observations About Deep-Bored Poplar Plants. Translated by Wright Lab Technical Library. 1-14 (Sep 1996).

Steinberg, Alfred A. and DeSesso, John M. "Have Animal Data Been Used Inappropriately to Estimate Risks to Humans from Environmental Trichloroethylene?," Regulatory Toxicology and Pharmacology, 18: 137-153 (1993).

Steinberg, Susan, van Bavel, Cornelius H. M., and McFarland, Marshall J. "A Gauge to Measure Mass Flow Rate of Sap in Stems and Trunks of Woody Plants," Journal of the American Society of Horticultural Science, 114(3): 466-472 (1989).

Stomp, A. M., Han, K. H., and Gordon, M. P. "Genetic Improvement of Tree Species for Remediation of Hazardous Wastes," In Vitro Cellular Development Biology, 29: 227-232 (1993).

Strand, Stuart E., Newman, Lee, Ruszaj, Martiin, Wilmoth, Jodi, Shurtleff, Brook, Brandt, Michael, Choe, Nami, Ekuan, Gordon, Duffy James, Massman, Joel W., Heilman, Paul E. and Gordon, Milton P. "Removal of TCE from Aquifers Using Trees," Innovative Technology for Site Remediation and Hazardous Waste Management. New York: ASCE, 1995.

Stringer, W., Shain, L., and Wittwer, R. F. "Growth and Survival of Eastern Cottonwood in Kentucky," Southern Journal of Applied Forestry, 2(2): 73-76 (1987).

Sutton, R. F. and Tinus, R. W. Root and Root System Terminology. Washington, D. C.: Society of American Foresters, 1983.

Technology Demonstration Plan. Phytoremediation of Shallow Trichloroethylene (TCE) Contaminated Groundwater. Aug 1996.

Tingle, A. C. and van Laar, A. "Revised Volume and Utilization Tables for *Populus deltoides*," South African Forest Journal, 100: 14-21 (Mar 1977).

Tracy, John C. "Solute Movement through Root-Soil Environment," Journal of Irrigation and Drainage Engineering, 115(4): 608-625 (August 1989).

Trapp, Stefan and Matthies, Michael. "Generic One-Compartment Model for Uptake of Organic Chemicals by Foliar Vegetation," Environmental Science and Technology, 29(9): 2333-2338 (1995).

Trapp, Stefan, McFarlane, Craig, and Matthies, Michael. "Model for Uptake of Xenobiotics into Plants: Validation with Bromacil Experiments," Environmental Toxicology and Chemistry, 13(3): 413-422 (1994).

Trapp, Stefan, Matthies, Michael, Scheunert, Irene, and Topp, Eva M. "Modeling the Bioconcentration of Organic Chemicals in Plants," Environmental Science and Technology, 24(8): 1246-1252 (1990).

Trapp, Stefan and Matthies, Michael. "Modeling Volatilization of PCDD/F from Soil and Uptake into Vegetation," Environmental Science and Technology, 31: 71-74 (1997).

Trapp, Stefan and McFarlane, J. Craig. Plant Contamination: Modeling and Simulation of Organic Chemical Processes. Ann Arbor, MI: Lewis Publishers, 1995.

Travis, C. C. and Doty, C. B. "Can Contaminated Aquifers at Superfund Sites be Remediated," Environmental Science and Technology, 24. 1464-1466 (1990).

Tritton, Louse M. and Hornbeck, James W. U. S. Department of Agriculture. Biomass Equations for Major Tree Species of the Northeast. Northern Forest Experiment Station, NE-69. Washington: Government Printing Office, 1982.

U. S. Department of Agriculture. How a Tree Grows. Forest Service, FS-32. Washington: Government Printing Office, 1982.

U. S. Department of Energy. Summary Report of a Workshop on Phytoremediation Research Needs. EM-0224. Washington: Government Printing Office, 1994.

U. S. Environmental Protection Agency (USEPA). Addendum to the Health Assessment Document for Trichloroethylene: Updated Carcinogenicity Assessment for Trichloroethylene. Review Draft. National Technical Information Service: Springfield, VA: 1987.

U. S. Environmental Protection Agency (USEPA). Contaminants and Remedial Options at Solvent-Contaminated Sites. EPA Office of Research and Development. EPA/600-R-94/203. November 1994.

U. S. Environmental Protection Agency (USEPA). Health Assessment Document for Trichloroethylene. Final Report. PB 85-249696. National Technical Information Service: Springfield, VA: 1985.

U. S. Environmental Protection Agency (USEPA). Toxicology Handbook. Rockville, MD: Government Institutes , Inc.. Sep 1986.

U. S. Environmental Protection Agency (USEPA). 1991 Toxics Release Inventory. EPA 745/R-93/003. Office of Pollution Prevention and Toxics, 1993.

U. S. Geological Survey (USGS). Hydrogeology at Air Force Plant 4 and Vicinity and Water Quality of the Paluxy Aquifer, Fort Worth, Texas. Water-Resource Investigations Report 96-4091. Austin, TX. 1996.

Verschueren, Karel. Handbook of Environmental Data on Organic Chemicals, 3rd Edition. New York: International Thomson Pub. Co., 1996.

Vogel, T. and McCarty, P. "Biotransformation of Tetrachloroethylene to Trichloroethylene, Dichloroethylene, Vinyl Chloride, and Carbon Dioxide Under Methanogenic Conditions," Applied Environmental Microbiology, 49: 1080-1083, (1985).

Vogel, Timothy M., Criddle, Craig S., McCarty, Perry L. "Transformations of Halogenated Aliphatic Compounds," Environmental Science and Technology, 21: 722-736 (1987).

Wackett, Lawrence P., Brusseau, Gregory A., Householder, Steven R., and Hanson, Richard S. "Survey of Microbial oxygenases: Trichloroethylene Degradation by Propane-Oxidizing Bacteria," Applied Environmental Microbiology, 55: 2960-2964 (1989).

Waldon, Hollis B., Jenkins, Michael B., Virginia, Ross A., and Harding, Ethelynda E. "Characteristics of Woodland Rhizobial Populations from Surface and Deep-Soil Environments of the Sonoran Desert," Applied Environmental Microbiology, 55: 3058-3064 (1989).

Walker, N. A. and Smith, S. E. "The Quantitative Study of Mycorrhizal Infection," New Phytology, 96: 55-69 (1984).

Walton, B. T. and Anderson, T. A. "Microbial Degradation of Trichloroethylene in the Rhizosphere: Potential Application to Biological Remediation of Waste Sites," Applied and Environmental Microbiology: 1012-1016 (Apr 1990).

Watanabe, Myrna. "Phytoremediation on the Brink of Commercialization," Environmental Science and Technology, 31(4): 182a-186a (1997).

Weatherly, P. E. "Water Uptake and Flow in Roots," in Physiology Plant Ecology II, Encyclopedia of Plant Physiology, Water Relations & Carbon Assimilation, Vol. 12B. New York: Springer-Verlag, 1982.

Westrick, J. J., Mello, J. W., and Thomas, R. F. "The Ground Water Supply Survey," Journal of American Water Works Association, 75: 52-59 (1984).

Whipps, J. M. "Carbon Economy," in The Rhizosphere. New York: John Wiley and Sons, 1990.

Whipps, J. M. and Lynch, J. M. "Energy Losses by the Plant in Rhizodeposition," in Plant Products and the New Technology. Oxford, England: Oxford University Press, 1985.

Wild, Alan. Russell's Soil Conditions and Plant Growth, 11th Edition. New York: John Wiley and Sons, 1988.

Williams, G. M. and Weisburg, J. H. "Chemical Carcinogens," in Casarett and Doull's Toxicology: The Basic Science of Poisons. New York: Macmillan Pub. Co., 1986.

Windholz, M. (Editor). The Merck Index, 10th Edition. Rahway, NJ: Merck and Co., Inc., 1983.

Yagi, O., Uchiyama, H., and Iwasaki, K. "Biodegradation Rate of Chloroethylene in Soil Environment," Water Science Technology, 25(11): 419-424 (1992).

Zobel, Richard W. "Root Growth and Development," in The Rhizosphere and Plant Growth. Boston, MA: Kluwer Academic Publishers, 1991.

Vita

Doug Wise was born on [redacted] in [redacted]. He graduated from Montana State University in 1988 with a Bachelor of Science Degree in Civil Engineering and was commissioned as a Second Lieutenant in the United States Air Force. His first assignment was to the 820th RED HORSE Squadron at Nellis AFB, Las Vegas, NV as a project engineer. In this position he traveled extensively to bases throughout the west completing a myriad of construction projects at military installations. He was also deployed to Honduras as a Supply-Liaison Officer, to Saudi Arabia and Iraq during Desert Shield/Storm as a project engineer and demolition expert, and to Cairo West, Egypt in support of Operation Restore Hope. In 1993, Capt Wise PCS'd to the 2d CES at Barksdale AFB where he served in positions of increasing responsibility, including the Chief of Construction Management, Chief of Programs, and Chief of Maintenance Engineering. During his time at Barksdale AFB he was also deployed to Guantanamo Bay, Cuba in support of Operation Sea Signal as the Joint Task Force Planning Engineer. In 1996, he was selected for the Graduate Environmental Engineering and Management (GEEM) program in the School of Engineering, Air Force Institute of Technology, Wright-Patterson AFB, Ohio where he commenced studies in June 1996. Upon graduation, Capt Wise will PCA to the AFMC/CE where he will perform duties in the Environmental Flight.

Permanent Address: [redacted]

REPORT DOCUMENTATION PAGE

Form Approved
OMB No. 0704-0188

1. AGENCY USE ONLY *(Leave blank)*	2. REPORT DATE	3. REPORT TYPE AND DATES COVERED
	December 1997	Master's Thesis

4. TITLE AND SUBTITLE
MODELING THE UPTAKE AND TRANSPIRATION OF TCE BY PHREATOPHYTIC TREES

5. FUNDING NUMBERS

6. AUTHOR(S)
Douglas P. Wise, Captain, USAF

7. PERFORMING ORGANIZATION NAME(S) AND ADDRESS(ES)
Air Force Institute of Technology, WPAFB OH 45433-6583

8. PERFORMING ORGANIZATION REPORT NUMBER
AFIT/GEE/ENV/97D-22

9. SPONSORING/MONITORING AGENCY NAME(S) AND ADDRESS(ES)

10. SPONSORING/MONITORING AGENCY REPORT NUMBER

11. SUPPLEMENTARY NOTES

12a. DISTRIBUTION AVAILABILITY STATEMENT
Approved for public release; distribution unlimited

12b. DISTRIBUTION CODE

13. ABSTRACT *(Maximum 200 words)*

Phytoremediation is a recent addition to the numerous methods used today to remediate ground water contaminants. It is proving more effective and efficient compared to existing remediation techniques. The use of phreatophytes, or water seeking trees, has great potential for phytoremediation. These trees are fast growing, long lived, grow their roots down to the ground water table, transpire large amounts of water, and are proven to actively remove contaminants from the soil horizon. The purpose of this research is to develop quantitative concepts for understanding the dynamics of TCE uptake and transpiration by phreatophytic trees over a short rotation woody crop time frame. This will be done by constructing a system dynamics model of this process and running it over a wide range of conditions. This researech will offer managers a tool to simulate long-term uptake and transpiration of TCE at potential sites. The results of this study indicate that TCE is actively removed from the soil horizon by phreatophytic trees and a significant proportiion of this TCE is then tranpsired. Changes in soil horizon parameters, xylem flow rates, and variables in the uptake equation greatly influence TCE uptake rates as well as transpiration. Also, parameters used in equations representing flows in and out of the leaf greatly influence transpiration. Better understanding of these processes is essential for managers to accurately predict the amount of TCE removed and transpired during potential phytoremediation projects.

14. SUBJECT TERMS
Trichloroethylene,Phreatophyte, Uptake, Translocation, Storage, Metabolism, Cometabolism, Transpiration, and Rhizosphere

15. NUMBER OF PAGES
318

16. PRICE CODE

17. SECURITY CLASSIFICATION OF REPORT	18. SECURITY CLASSIFICATION OF THIS PAGE	19. SECURITY CLASSIFICATION OF ABSTRACT	20. LIMITATION OF ABSTRACT
Unclassified	Unclassified	Unclassified	UL